Fabíola Maria Tavares Alves da Costa Moutinho

PhD Thesis

Surface-immobilized Antimicrobial Peptides (AMPs) for prevention of implant-related Osteomyelitis

Dissertação submetida à Faculdade de Engenharia da Universidade do Porto para obtenção do grau de Doutor em Engenharia Biomédica

Faculdade de Engenharia

Universidade do Porto

2015

This thesis was supervised by:

Doctor M. Cristina L. Martins

INEB – Instituto de Engenharia Biomédica, Universidade do Porto

ICBAS – Instituto de Ciências Biomédicas Abel Salazar, Universidade do Porto

I3S - Instituto de Investigação e Inovação em Saúde, Universidade do Porto

The research described in this thesis was conducted at:

INEB – Instituto de Engenharia Biomédica, Universidade do Porto

The research described in this thesis was financially supported by:

FEDER funds through the *Programa Operacional Factores de Competitividade* (COMPETE) and by Portuguese funds through FCT (*Fundação para a Ciência e a Tecnologia*) in the framework of the projects PTDC/CTM/101484/2008: CHITOSAMP - CHITOSan-AntiMicrobial Peptide-based biomaterials for the treatment of osteomyelitis, Pest-C/SAU/LA0002/2013, Pest-C/QUI/UI0081/2013 and the PhD grant SFRH/BD/72471/2010.

“ Segue o teu Destino,

rega as tuas plantas, ama as tuas rosas.

O resto é a sombra de árvores alheias.”

Fernando Pessoa

…to Miguel

…à minha mãe Arlete

Acknowledgments

Esta tese é o culminar de um periodo muito feliz da minha vida, em que aprendi e evolui muito, graças à paciência, generosidade e carinho de muitas pessoas.

“Aqueles que passam por nós, não vão sós, não nos deixam sós. Deixam um pouco de si, levam um pouco de nós”.

A. Saint-Exupéry

Assim, a todos os que passaram por mim, o meu Muito Obrigada! Tenho o coração mais cheio e rico por todos vós!

À minha mãe científica, Cristina Martins, deixo aqui uma pequena homenagem. A minha gratidão perdurará, juntamente com todos os seus ensinamentos. Muito Obrigada… pela oportunidade de ser sua aluna, pelo acompanhamento constante, por me ensinar a relativizar, por me ensinar a rir de mim mesma, por me mostrar que afinal o copo está sempre meio cheio, por me revelar que o futuro só pode ter um sentimento: confiança. Consigo, cresci imenso durante estes anos, quer científica, quer pessoalmente. O seu exemplo será bússola ao longo minha carreira profissional. A si desejo-lhe tudo de melhor! Que o futuro lhe recompense verdadeiramente por todo o trabalho e dedicação!

À professor Paula Gomes o meu sentido agradecimento. Obrigada por me fazer sentir tão benvinda, pela paciência e amabilidade com que tirou todas as minhas dúvidas, pela disponibilidade para discutir e corrigir trabalhos, pela ginástica na produção de “só mais umas miligramas de péptido”. Um beijinho muito especial também para Sílvia Maia e Mariana Barbosa por trabalharem tão arduamente para me entregar péptidos atempadamente.

Às minhas colegas “de carteira”, Joana Gomes e Daniela Sousa, o meu muito obrigado! Joaninha, foste uma luz ao fundo do tunel, que nunca me deixou desanimar! Obrigada pela ajuda, pelo ombro amigo, pelas gargalhadas que partilhámos! Querida Daniela, não poderia ter tido uma melhor professora nas

culturas celulares! A tua calma e simplicidade transmite uma tranquilidade que faz com que todo o processo só possa correr bem! E por falar em correr, muito obrigada pelas dicas de running, pela motivação, por esta amizade linda… Obrigada!

Não poderia ter tido melhor instituição de acolhimento para realizar o trabalho experimental. O INEB é realmente um instituto que sabe receber pessoas, é uma família unida, onde o apoio nunca falta. O meu muito obrigada a este instituto que me garantiu e providenciou todas as condições necessárias para que o meu trabalho se desenrolasse e evoluísse de forma positiva. Nesta grande família, não poderia deixar de agradecer à equipa administrativa: Ana Paula Filipe (por me receberes de forma tão calorosa, por fazeres "desaparecer" problemas e por encontrares sempre um jeitinho de melhorar tudo), Vírginia Fonseca (pela ajuda e disponibilidade em todas as minhas "questões financeiras"), Dulce Novo (querida Dulce muito obrigada pela compreensão, pela paciência, por tanto tempo dedicado em PADs e orçamentos e encomendas e um sem fim de questões… obrigada pelas conversas sobre filhotes, e pausas para o lanche mais animadas), Daniela Azevedo (pelas respostas e soluções, e simpatia constante), Gabriela Afonso (pela ajuda, pela simpatia… e claro por me teres aberto as portas do Cake Design!). Igualmente o meu Obrigada muito sentido à equipa técnica: Manuela Brás (querida Manuela, muito obrigada pela disponibilidade, pela dedicação e bondade que dedicas a este teu mundo. Muito obrigada pelo teu exemplo, pelas horas gastas em análise de AFM e por me ajudares a compreender o que estava a obter), Ricardo Vidal (querido Ricardo, és verdadeiramente um profissional que serve de exemplo a todos. Perdi conta ao número de vezes que vieste em meu Socorro… ao número de perguntas repetidas que te fiz… à quantidade de vezes que te pedi ajuda fora de horas… a tua generosidade não tem fim… a tua "boa cara" em todos os momentos inspira-nos a tentar ser e saber fazer melhor. Foste um farol no meio de experiências complicadas… por tudo isto, e pelas conversas e gargalhadas na cantina… o meu muito obrigada!), Eliana Vale (querida Eliana, que bom foi ter a oportunidade de conhecer-te, também tu demonstras como deve ser o amor e dedicação ao trabalho… muito obrigada por todo o acompanhamento no "submundo" (-1)… por garantires que tudo estava a funcionar e a funcionar bem, por verificares e voltares a

verificar… pela qualidade com que tive oportunidade de trabalhar! Obrigada pela companhia, pelas conversas, pela disponibilidade), Susana Carrilho (pelo apoio e muitas conversas "vegetarianas"), Dalila Pedro (pela amizade, pelo ouvido atento, pela disponibilidade, pela meiguice, pela companhia e riso) e – não menos importante – D. Rosa (muito Obrigada por tratar tão bem do nosso laboratório! Por tantos vidros lavados, por tantas pontas e eppendorfs autoclavados, por tanta arrumação e organização… pelos "Bons Dias" logo pela manhã, tão cheios de vitalidade!).

Aos Seniores do INEB, Professor Mário Barbosa (Caríssimo Professor, muito muito obrigada pelas lições, pela motivação, por insistir que devemos pensar sempre para além da "nossa caixinha", por me inspirar: "Podemos desistir do Plano, mas nunca devemos desitir do Sonho", por me ajudar a acreditar e a perseguir o sonho), Professor Fernando Jorge Monteiro (caríssimo Professor, muito obrigada pelo seu acolhimento, pela forma generosa com que nos dá atenção, por nos fazer sentir importantes, pelo carinho e simpatia), Meriem Lamghari (muito obrigada pelas dúvidas esclarecidas, pelo apoio, pelas correções do artigo, pelo sorriso caloroso), Cristina Barrias, Perpétua Pinto-do-Ó, Ana Paula Pêgo, Pedro Granja, Isabel Amaral, Susana Santos, Susana Sousa, Cristina Ribeiro (muito obrigada pelo apoio, pela companhia em congressos, pelo acolhimento, por criarem este ambiente familiar onde nos sentimos em casa!).

O meu agradecimento muito especial à minha equipa (que foi tendo vários nomes ao longo dos anos, mas que para mim será sempre: Bioengineered Surfaces). Todos os seus membros (passados e presentes) foram fundamentais para que existisse sempre bom ambiente, para que eu encontrasse equilíbrio nesta viagem por vezes atribulada que é a investigação. Assim, obrigada Inês Gonçalves (por me atazanares a cabeça de cada vez que tropeçava em experiências mal conseguidas. Prá frente é o caminho!;)), Sidónio Freitas (querido Sidónio, o teu apoio foi fundamental, creio que te importunei para aprender a trabalhar em todos os equipamentos de análise de superfície! Adorei as nossas discussões – quase filosóficas – sobre químicas de funcionalização… Obrigada pelo ombro amigo, pelo convívio, pelas gargalhadas partilhadas…), Catarina Baptista e Frederico Nogueira (colegas de aulas e cúmplices

no laboratório), Paula Parreira (por tantas dúvidas tiradas online… que os States ainda ficam longe!), Mariana Fernandes (pela companhia no laboratório, pela ajuda na purificação de quitosano, pelo exemplo da tua elegante forma de ser), Cláudia Monteiro (a tua chegada foi tão desejada! Foi uma promessa cumprida… muito obrigada pelo apoio, carinho e disponibilidade…pela Amizade!), Catarina Seabra (obrigada pelo miminho extra, pela compreensão e companhia no laboratório), Vanessa Graça (pela companhia na câmara, por tantos frascos lavados, pelas gargalhadas e pela tua constante boa disposição), Helena Felgueiras (pela alegria contagiante), Maura (a italiana mais portuguesa do INEB, de sorriso rasgado e piada pronta) e um beijinho especial aos benjamins da equipa (Patrícia Henriques, Ricardo Carvalho, Bernardo Antunes, Lia Costa e Susana Neto).

À minha equipa do coração, aquela que nos escolhe e que nós escolhemos e que participam de mãos dadas em todos os momentos bons e maus, o meu reconhecimento emocionado: Obrigada Nilza Ribeiro (tenho a certeza que a nossa cumplicidade perdurará mesmo que o destino nos separe por algum tempo, pelo obrigada pela mão, ombro, ouvido e coração aberto, obrigada pela tua franqueza, pela tua honestidade, por tudo), Obrigada Daniela Rocha (por me inspirares a ver sempre o melhor das pessoas, por me introduzires no mundo do craft, pela amizade bonita que temos), Obrigada Catarina Almeida (pelos conselhos sábios, pelo exemplo de humildade, pelo apoio, pelo convívio, pela alegria), Obrigada Joana Antunes (pelo mimo, pelos ensinamentos de spincoating, pelo carinho, por nunca te esqueceres de mim mesmo estando longe), Obrigada Maria Molinos (pela pessoa bonita que és, é tão bom conviver contigo!), Obrigada Joana Maciel (companheira de aventuras repetidas, musa inspiradora! Obrigada pelo mimo!), Obrigada Daniela Sousa (pela disponibilidade, pela compreensão, por ouvires, pelas gargalhadas e boa disposição), Obrigada Sílvia Bidarra (tão bom ter conterrâneas por perto, poder discutir parentalidade para além de ciência!;)), Obrigada Cláudia e Pedro (por ouvirem e aturarem de forma bem disposta as minhas idiossincracias, e entusiasmos excessivos).

Ao gang da Cantina (Sidónio Freitas, Ricardo Vidal, Catarina Almeida, Joana Antunes, Nilza Ribeiro, Daniel Vasconcelos, Sílvia Bidarra, Christiane Salgado, Maria Molinos, Maria Lázaro, Joana Caldeira, Carla Gomes, Dalila Pedro,….) e às animadoras oficiais

do INEB (Estrela Neto, Catarina Pereira, Daniela Vasconcelos, Filipa Lourenço, Ana Luisa Torres,…) às Pós-Doc intrepidas (Raquel Gonçalves, Vicky Leiro, Juliana Alves, Inês Alencastre, Diana Nascimento, Tatiana Resende) e a toda a restante família inebiana… o meu sentido Obrigado, pelo bom ambiente, por assistirem ao meu caminho, por questionarem, por sugerirem, por rirem comigo, por terem estado aí.

Não poderia igualmente deixar de agradecer ao CEMUP, esse centro de excelência, pela ajuda, pela partilha de conhecimento e por todas as análises de superfície de XPS e SEM. Assim, o meu muito obrigada ao Eng. Carlos Sá, à Liliana Alves e Daniela Silva.

Por último, e não menos importante, agradeço à minha Família. Aos meus pais (Arlete e Aparício), por me terem ensinado desde cedo os valores do trabalho e a importância da educação. Pelo amor dedicado, pelo exemplo e por todos os sacrifícios feitos em nome da minha felicidade. Aos meus irmãos (Alice, Pedro, Paulo e Sara) pelo companheirismo e por estarem sempre à distância de um telefonema a qualquer hora do dia. Um agradecimento muito especial aos meus Sogros (Celeste e Ilídio) pela forma generosa com que alargaram a família para me receber, por cuidarem tão bem de mim, e dos meus filhos. Esta tese nunca teria sido possível sem o vosso apoio constante e desprendido… muito obrigada! Aos meus cunhados (Paulinha e Sérgio) por estarem presentes e disponíveis a cada imprevisto, pela força e pela confiança que me transmitiram e por serem tão bons amigos quanto tios (que sorte os meus miúdos têm!).

Ao Diogo e à Sofia, por obrigarem a mamã a crescer, a redescobrir o Mundo e a saber com muita facilidade o que é realmente importante. Vocês enchem-me a Alma.

A ti Miguel faltam-me palavras para te agradecer. Obrigada por te manteres aí ao longo destes anos… por seres o meu porto seguro, por me transmitires confiança, por acreditares em mim e nas minhas capacidades, por não duvidares do futuro, por me incluires nos teus sonhos e desafios, por fazeres de mim uma melhor pessoa.

Abstract

Implant-related osteomyelitis infection is a clinical situation that has been growing with the increase of life expectancy. Despite state of the art surgical rooms and sterilization procedures, infection remains a serious problem without significant improvement in the last decades. Moreover, the increasing antibiotic-resistance phenomena have prompted the search for new alternatives.

Antimicrobial peptides (AMPs) are a promising class of antimicrobial compounds, having as main advantages: broad-spectrum of activity, fast killing at low titers, target specificity and most importantly, do not have the tendency to promote bacterial resistance development. However, AMPs application have some challenges, namely short half-life due to protease digestion or peptide aggregation, which leads to the application of high concentrations that may be associated with toxicity. To overcome these drawbacks, AMPs covalent immobilization on biomaterials surface has been proposed. So, the aim of the present work was to develop an AMP based coating for orthopedic applications.

hLF1-11 (GRRRRSVQWCA) and Dhvar5 (LLLFLLKKRKKRKY) are short AMPs with a head-to-tail amphipathicity and a broad spectrum of activity, including *Staphylococcus aureus*, which is the most prevalent species in implant-related infections. These two AMPs were immobilized onto chitosan, a natural polymer commonly explored for biomedical applications that was previously described to have antimicrobial and osteoconductive properties. However, since the immobilization strategy could affect AMP antimicrobial activity, different parameters were investigated namely, AMP immobilization process (covalent versus physical binding), AMP orientation (coupled from N- versus C-terminal) and AMP exposure from the surface (using different spacers with different lengths and flexibilities).

Antimicrobial studies using *S. aureus* demonstrated that the surface antimicrobial effect of both AMPs tested is higher when peptides are covalently immobilized onto chitosan than when they are only physically adsorbed.

hLF1-11 covalent immobilization was performed directly through the establishment of a disulfide bridge between a C-terminal cysteine residue of the peptide and N-acetyl cysteine (NAC) functionalized chitosan film. To evaluate the effect of a spacer,

chitosan film was functionalized with a SH-terminated polyethylene glycol (PEG) instead of NAC. hLF1–11 increased bacterial adhesion to chitosan films. However, results demonstrated that immobilized hLF1–11 maintain bactericidal activity against *S. aureus*, particularly with the use of a spacer.

Dhvar5 was synthesized with an SH-terminated spacer at the N- or C-terminal to evaluate the effect of peptide orientation. Spacers of different chain lengths and flexibilities were also used to explore the effect of peptide exposure. Again, disulfide bridge chemistry was used to immobilize the modified Dhvar5 to NAC-functionalized chitosan films. Antimicrobial studies demonstrated that increased spacer length is more beneficial than extended flexibility. Interestingly, only when immobilized through the N-terminal (exposing its cationic end), Dhvar5 was able to improve chitosan antimicrobial effect by decreasing bacterial colonization in opposition to Dhvar5 immobilized through its C-terminal (exposing its hydrophobic end) that has a detrimental effect on bacterial adhesion.

As NAC-functionalized chitosan control film also revealed high antiadherence properties, further development of this coating was performed. Results showed that NAC-functionalized chitosan is a promising material as it avoids bacterial adhesion, impairs biofilm formation, while allowing osteoblast adhesion and proliferation.

The knowledge obtained with this work can be further applied in the development of alternative and effective antimicrobial coatings for orthopedic implants.

Resumo

A infeção associada a implantes ósseoas representa uma situação clínica cuja prevalência tem crescido com o aumento de esperança média de vida. Apesar das avançadas salas de operação e dos optimizados processos de esterilização, a incidência de infeção continua como um problema relevante, que não tem sido significantivamente melhorado nas últimas décadas. Igualmente preocupante, tem sido o agravamento do fenómeno de resistência aos antibióticos, o que tem impulsionado a investigação na busca de novas alternativas.

Os péptidos antimicrobianos (PA) são uma classe promissora de compostos antimicrobianos, apresentando como principais vantagens: um alargado espectro de actividade, rápida actuação mesmo a baixas concentrações, elevada especificidade e, o mais importante, não têm tendência para promover o aparecimento de resistência em bactérias. No entanto, a aplicação de PA envolve alguns desafios, nomeadamente o curto tempo de semi-vida devido a digestão peptídica ou agregação de péptidos, o que conduz à aplicação de concentrações superiores de PA, que podem estar associadas ao aparecimento de toxicidade. A imobilização covalente de PA a biomateriais tem sido proposta como resposta a estes obstáculos. Desta forma, o objectivo principal do presente trabalho foi desenvolver um revestimento para próteses ortopédicas baseado em PA imobilizados.

O hLF1-11 (GRRRRSVQWCA) e o Dhvar5 (LLLFLLKKRKKRKY) são dois PA curtos, que apresentam anfipaticidade dependente da sequência e possuem um espectro de ação alargado, que inclui *Staphylococcus aureus*, a espécie mais prevalente em infeções associadas a implantes. Estes dois PA foram imobilizados em quitosano, um polímero natural frequentemente explorado para aplicações biomédicas, previamente descrito como possuidor de propriedades antimicrobianas e osteocondutoras. Contudo, uma vez que estratégia de imobilização covalente pode afetar negativamente a actividade antimicrobiana dos PA, diferentes parametros de imobilização foram avaliados, nomeadamente tipo de imobilização (covalente versus adsorção), orientação do PA (ligação através do terminal amino ou carboxílico) e exposição de PA (utilização de espaçadores com diferentes comprimentos e flexibilidades).

Os ensaios antimicrobianos com *S. aureus* demonstraram que o efeito antimicrobiano das superficies modificadas com cada PA, é maior quando os péptidos estão imobilizados covalentemente, do que quando a imobilização é feita por adsorção.

A imobilização covalente de hLF1-11 foi realizada de forma directa através do estabelecimento de uma ponte dissulfureto entre a cisteína do terminal carboxilico do peptido e N-acetilcisteina (NAC) previamente ligado ao filme de quitosano. Para avaliar o efeito de um espaçador, filmes de quitosano foram igualmente funcionalizados com polietilenoglicol com um grupo sulfidrilo no terminal. Em ambos os casos, hLF1-11 promoveu o aumento de adesão bacteriana aos filmes de quitosano. No entanto, resultados demonstraram que hLF1-11 manteve actividade bactericida, particularmente na presença de um espaçador.

O péptido Dhvar5 foi sintetizado com espaçadores (terminados em –SH) adicionados ao terminal amino ou ao terminal carboxílico, de forma a avaliar o efeito da orientação do péptido na actividade antimicrobiana. Espaçadores com diferentes comprimento e flexibilidades foram igualmente aplicados para avaliar o efeito da exposição do péptido. O estabelecimento da ponte disulfureto permitiu a ligação entre peptido e filme de quitosano funcionalizado com NAC. Ensaios antimicrobianos demonstraram que o aumento do comprimento do espaçador é mais importante que uma maior flexibilidade. Particularmente interessante é o facto de a orientação do péptido ter um impacto muito grande na actividade antimicrobiana, já que uma imobilização através do terminal amino (expondo a ponta catiónica do peptido) diminui consideravelmente a adesão bacteriana, enquanto que a imobilização pelo terminal carboxílico (expondo a ponta hidrofobica do peptido) tem um efeito negativo na adesão bacteriana.

Como o filme de quitosano funcionalizado com NAC apresentou excelentes propriedades antiadesivas, prosseguiu-se com a optimização deste revestimento. Os resultados mostraram que o quitosano funcionalizado com NAC é um material promissor na medida que evita adesão bacteriana, dificulta a formação de biofilme, e simultaneamente permite a adesão e proliferação de osteoblastos. O conhecimento obtido com este trabalho apresentado, pode ser aplicado no

desenvolvimento de novos revestimentos antimicrobianos para implantes ortopédicos.

Publications

The work performed in the frame of this Thesis resulted in the following international scientific publications:

F. Costa, I. F. Carvalho, R. C. Montelaro, P. Gomes, M. C. L. Martins. Antimicrobial Peptides (AMPs) covalently immobilized onto biomaterials surfaces. Acta Biomaterialia, 2011 Apr7(4):1431

F. Costa, S. Maia, J. Gomes, P. Gomes, M. C. L. Martins. Characterization of hLF1-11 immobilization onto chitosan ultrathin films, and its effects on antimicrobial activity. Acta Biomaterialia, 2014 March10(8): 3513

F. Costa, S. Maia, P. Gomes, M. C. L. Martins. Dhvar5 antimicrobial peptide (AMP) chemoselective covalent immobilization results on higher antiadherence effect than simple physical adsorption. Biomaterials, 2015 52:531

F. Costa, S. Maia, D. M. Sousa, M. Lamghari, P. Gomes, M. C. L. Martins. N-acetyl cysteine-immobilized coating avoids bacteria adhesion/biofilm formation without impairing osteoblast adhesion and proliferation. Biomaterials, Submitted at 17.07.2015 (Under review)

Abbreviations List

A
ABA - 4-aminobutanoic acids
AFM - Atomic force microscopy
AGE – Allyl Glycidil Ether
AHA- 6-aminohexanoic acids
AMP/AMPs – Antimicrobial peptide
APMA - N-(3-aminopropyl)methacrylamide hydrochloride
APTES – 3-aminopropyltriethoxysilane
ATRP – Atom Transfer Radical Polimerization

B
BTCPS - 11-(2-bromo-2- methyl)propionyloxyundecenyltrichlorosilane

C
Ca–P - Calcium phosphate
CFU - colony forming units
Ch – chitosan film
Chit_b- chitosan film incubated with reaction buffer (MES buffer)
Chit_NAC – chitosan film functionalized with N-acetyl cysteine
Chit_NAC_hLF1-11 – chitosan film with hLF1-11 immobilized through N-acetyl cysteine
Chit_Sp – chitosan film functionalized with O-(2-Carboxyethyl)-O´-(2-mercaptoethyl)heptaethylene glycol spacer
Chit_Sp_hLF1-11 – chitosan film with hLF1-11 immobilized through O-(2-Carboxyethyl)-O´-(2-mercaptoethyl)heptaethylene glycol spacer
CPTES - (3-chloropropyl)triethoxysilane
CuAAC – CuI-catalyzed azide-alkyne cycloaddition

D
DAPI - 4’,6- diamidino-2-phenylindole
DD – Degree od Deacetylation
DMA - N,N-dimethylacrylamide
DMSO - dimethyl sulfoxide

E
EDC - 1-ethyl-3-(3-dimethylaminopropyl)carbodiimidehydrochloride

F
FBGC – Foreign Body Giant Cells
Fmoc – 9-fluorenylmethoxycarbonyl

G
GG- dipeptide GlyGly

H
hLF1–11 – human Lactoferrin 11-mer from 1 to 11 amino acid residue
HOEGMA – Hydroxyl-terminated oligo(ethylene glycol) methacrylate
HPLC- High Performance Liquid

I
IM – Inner membrane
IRRAS - Infrared reflection absorption spectroscopy

L
LbL – Layer by Layer
LC-ESI/IT MS- Liquid Chromatography-Electrospray Ionization/Ion Trap Mass Spectrometry
LPS – Lipopolysaccharide
LTA – Lipoteichoic Acid

M
MEO_2MA – 2-(2-methoxyethoxy)ethylmethacrylate
MES – (N-morpholino) ethanesulfonic acid
MHB – Mueller Hinton Broth
MIC - Minimal inhibitory concentration
MPA – 3-mercaptopropionic acid
MRSA – Methicillin-resistant *Staphylococcus aureus*
MSCRAMM – Microbial surface components recognizing adhesive matrix molecules
MLT – Maltose transporter
Mw – Molecular Weight
MWNTs – Multi-Walled Carbon nanotubes

N
NAC – N-acetyl Cysteine
NHS - N-hydroxysulfosuccimide

O
OCA - Optical contact angle
OEG – Oligo-(ethylene glycol)
OM – Outer membrane

P
PDITC – p-Phenylene diisothiocyanate
PDLLA – Poly(D,L-lactide)
PDMA – Poly(N,N-dimethylacrylamide)
PDMS – Polydimethylsiloxane
PEGDA – Poly(ethylene glycol) diacrylate
PHEMA – Poly(hydroxyethylmethacrylate
PHQ - 9,10-phenanthrenequinone
PIA – exopolysaccharide intercellular adhesin
PEG – Polyethylene glycol

P (continuation)
PLGA – Poly(lactide-co-glycolide)
PNG - Peptidoglican
PMMA - poly(methylmethacrylate)
PS – Polystyrene
PTMD – Pentaerythritol tetrakis(3-mercaptoprionate)
PVC – Polyvinyl Chloride

Q
QS – Quorum-sensing
QSAR – Quantitative structure-activity relationship modelling

R
RIP – RNAIII-inhibiting peptide
Rq - root mean square roughness

S
SAMs – Self-assembled monolayers
SPPS – Solid-phase peptide synthesis
Sp - O-(2-Carboxyethyl)-O´-(2-mercaptoethyl)heptaethylene glycol spacer

T
TSA - tryptic soya agar
TSB - tryptic soya broth

X
XPS - X-ray photoelectron spectroscopy

Aim and Structure of the Thesis

Osteomyelitis in general, and orthopedic implant infection-related in particular, are clinical situations that have been growing in the last decades [1]. With increasing life expectancy, increasingly more patients suffer from osteoarthritis and therefore need joint replacement [2]. Despite all sterilization and surgical good practices, infection still remains as one of the major issues to be solved. Current applied treatment generically consists on the combination of debridment, implant removal and long antibiotherapy, which not always is sufficient for patient recovery [2-4]. This represents huge psychological, and physical burden for patients, implying in most cases lost of function. Also, the economical effort is tremendous, as these revision processes are many fold more expensive than the original implant introduction procedure [2]. As the current antiobiotics pipeline have not produced clear replacement for the conventional antibiotics applied today, development of new fighting strategies are mandatory. Antimicrobial peptides (AMPs) are a promising class of antimicrobial compounds, as they have broad spectrum of activity, promote fast killing at low titers, have target specificity and most importantly do not have the tendency to promote resistance development [5-8]. Some of the challenges associated with AMPs application include relatively short half-life due to a rapid protease digestion, or to peptide aggregation, which oblige the application of higher concentrations that may be associated with toxicity [9, 10]. AMPs covalent immobilization appears as a strategy to overcome the drawbacks stated above [11].

Therefore, the ultimate goal of the work described in this thesis is to develop an antimicrobial implant coating for orthopedic applications that do not impair bone cells adhesion and proliferation. Strategy is based on covalent immobilization of AMPs (hLF1-11 and Dhvar5) onto a polymeric coating that was previously described to have some antimicrobial and osteoconductive properties, chitosan.

To that end, the following tasks were proposed:

a) Production and characterization of AMP-functionalized chitosan coatings, using different immobilization parameters: orientation, spacer insertion, spacer length and spacer flexibility;
b) Assessment of the implication of the different immobilization parameters on the antimicrobial activity of the coatings;
c) Assessment of the biological effect of the most antimicrobial surface on mammalian cells namely in osteoblasts;
d) Translational assays for *in vivo* studies.

This thesis is divided in eight chapters with the following contents. **Chapter I** reviews the pathology, etiologic agents, current treatment protocols as well as the different research lines involved in orthopedic implant-related infection. **Chapter II** is an adaptation/actualization of the review paper published in 2011, ("Covalent immobilization of antimicrobial peptides (AMPs) onto biomaterial surfaces" of Acta Biomaterialia 2011 7: 1431–1440), and gives an overview on the most important features of AMPs, their putative mode of action and also the impact of covalent immobilization of AMPs onto surfaces through different chemical coupling strategies, length of spacers, and peptide orientation and concentration.

Since, during this work chitosan was used as an implant coating, **Chapter III** gives an overview of the implication of different chitosan characteristics on the biological activity when used in film form. **Chapter IV** presents a brief review of the most important surface characterization techniques used in the work developed during this thesis.

hLF1-11 is a short AMP with broad antimicrobial activity, already tested on an *in vivo* chronic osteomyelitis model. Therefore, the effect of covalent immobilization of hLF1-11 through direct and spacer-mediated coupling on its antimicrobial properties is described in **Chapter V**. Dhvar5 is also a broad spectrum AMP with reported membrane-related antimicrobial activity, which is an essential feature for the production of contact-killing surfaces. Further immobilization parameters where assessed including peptide orientation, spacer length and spacer flexibility. **Chapter**

VI revises the implication of such parameters on the antimicrobial activity of the immobilized peptide.

As the N-acetylcysteine-functionalized chitosan film proved to have strong antiadherence effect, this surface was further optimized and tested for its antiadherence and antibiofilm activity as well as effect towards osteoblast cells. **Chapter VII** focus in such findings.

In **Chapter VIII** the overall results presented in this thesis are analyzed considering each chapter and integrating the whole results, highlighting the most striking findings. Also, future prospects on the translational assays for *in vivo* testing are discussed in this chapter.

[1] Zimmerli W, Moser C. Pathogenesis and treatment concepts of orthopaedic biofilm infections. FEMS immunology and medical microbiology. 2012;65:158-68.

[2] Zimmerli W. Clinical presentation and treatment of orthopaedic implant-associated infection. Journal of internal medicine. 2014;276:111-9.

[3] Toms AD, Davidson D, Masri BA, Duncan CP. The management of peri-prosthetic infection in total joint arthroplasty. The Journal of bone and joint surgery British volume. 2006;88:149-55.

[4] Darouiche RO. Treatment of infections associated with surgical implants. The New England journal of medicine. 2004;350:1422-9.

[5] Zasloff M. Antimicrobial peptides of multicellular organisms. Nature. 2002;415:389-95.

[6] Reddy KV, Yedery RD, Aranha C. Antimicrobial peptides: premises and promises. International journal of antimicrobial agents. 2004;24:536-47.

[7] van't Hof W, Veerman EC, Helmerhorst EJ, Amerongen AV. Antimicrobial peptides: properties and applicability. Biological chemistry. 2001;382:597-619.

[8] Wang G, Mishra B, Lau K, Lushnikova T, Golla R, Wang X. Antimicrobial peptides in 2014. Pharmaceuticals. 2015;8:123-50.

[9] Haynie SL, Crum GA, Doele BA. Antimicrobial activities of amphiphilic peptides covalently bonded to a water-insoluble resin. Antimicrobial agents and chemotherapy. 1995;39:301-7.

[10] Willcox MD, Hume EB, Aliwarga Y, Kumar N, Cole N. A novel cationic-peptide coating for the prevention of microbial colonization on contact lenses. Journal of applied microbiology. 2008;105:1817-25.

[11] Costa F, Carvalho IF, Montelaro RC, Gomes P, Martins MC. Covalent immobilization of antimicrobial peptides (AMPs) onto biomaterial surfaces. Acta biomaterialia. 2011;7:1431-40.

Table of Contents

CHAPTER I

Orthopedic implant-related infection

1. Osteomyelitis

Osteomyelitis is a pathology defined as an infection and inflammation at the bone level, that is frequently associated with implant introduction, such as hip or knee replacement, fracture fixation or ligament and tendon reconstruction [1-3]. Indeed, it has been shown that the risk of infection increased more than 100 000-fold by the presence of a foreign body [4].

The number of such surgeries has been augmenting in last years (see table 1).

Table 1. Epidemiological data regarding both hip replacements and total knee arthroplasties in Europe (particularly in Finland) [5] and in USA [6].

Country	**Finland**		**USA**	
Study period	**1995**	**2009**	**1990**	**2007**
Hip replacement	5000	9200	100 000	200 000
Fold increase	**~2**		**~2**	
Total Knee arthroplaties	3000	9100	110 000	550 000
Fold increase	**~3**		**~5**	

The risk of infection varies depending on the surgical procedure in question. Published infection rates of about 5% have been reported for internal fracture fixation devices [7]. Increased infection rates have been reported within certain high-risk groups: for example, the infection rate in patients with open fractures may exceed 30% [8], in comparison with 0.5-2% for equivalent closed fractures [8]. Although the infection rate for primary joint replacement is approximately 1-4% [9-11], this value may increase up to 40% in revision of failed prosthetic joints [8].

Despite the low rates, infection represents the most serious cause of implant failure, as no improvement on treatment rates has been seen in the last decades [3]. Early detection of infection is of paramount importance, as a delayed treatment may result in multiple surgeries with device removal, and worst prognosis [12]. However, infection diagnosis in its earlier stages can be difficult, as a result of unspecific symptoms and frequently unreliable blood biomarkers [13, 14]. According to the origin, bone implant-associated infections and osteomyelitis, can be divided into

different types of the condition: 1) osteomyelitis from hematogenous spread of infection, 2) osteomyelitis secondary to a contiguous focus of infection, 3) osteomyelitis associated with vascular insufficiency and 4) osteomyelitis from iatrogenic inoculation during surgery or trauma [12].

Implant surface susceptibility to infection is dependent on the immune system performance and on the activity and virulence of the involved microorganisms [15, 16]. Immune system performance can be compromised by direct surgical trauma, implant presence, low availability of blood vessels in the implant vicinity and inflammatory escalation, with lower level of phagocytosis [17]. Indeed, when an implanted material comes in contact with blood, a conditioning layer of host proteins (fibronectin, vitronectin, fibrinogen, albumin and immunoglobulins) instantaneously adsorbs to the material surface [18]. At the same time, inflammatory cells begin to arrive to the injured tissue (Figure 1). Acute inflammation lasts from minutes to days, and is dominated by neutrophils. Given that implanted biomaterials are usually much larger than the leukocytes themselves, frustrated phagocytosis replaces the normal phagocytic response, where leukocyte products (e.g., lysosomal proteases and oxygen free radicals) are released in an attempt to degrade the foreign body. Neutrophils are usually cleared from the implant site within a day or two, and are replaced by monocytes, macrophages, and lymphocytes. As activated monocytes/macrophages initiate the healing response at the implant site, endothelial cells and fibroblasts begin to proliferate, giving rise to granulation tissue. This chronic inflammation is followed by the foreign body reaction, which consists of varying proportions of granulation tissue components and the formation of foreign body giant cells (FBGC). FBGC are multinucleated cells resulting from the fusion of macrophages [19].

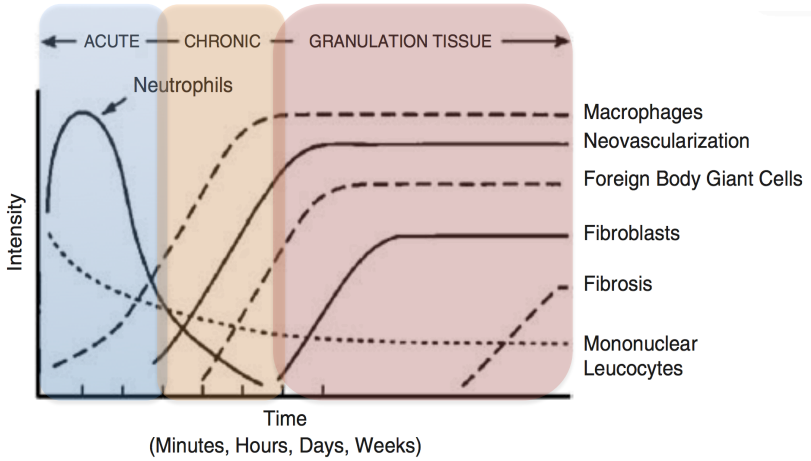

Figure 1. The general timeline of the cellular response against implanted biomaterials. Adapted from [20].

Therefore, tissue degradation and osteolysis (in bone tissues) are not a direct effect caused by the infection *per se*. The tissue damage is rather dependent on the pro-inflammatory microenvironment generated by frustrated phagocytosis of neutrophils accumulated at implant surface, resulting on release of proinflammatory mediators and tissue-destroying substances, which also promotes bone resorption by osteoclasts [21]. The activity and virulence of microorganisms are correlated with their capacity for biofilm formation [22]. Biofilm establishment results from a specific sequence of events: (i) microbial adherence supported by non-specific interactions between bacteria and the surface, mediated by physiochemical forces, such as Van der Waals forces, hydrophobic interactions and ionic interactions [23] and specific interactions mediated by the already mentioned conditioning film, which provide specific binding sites for bacterial surface proteins: MSCRAMMs – microbial surface components recognizing adhesive matrix molecules, (ii) microcolony formation and proliferation, (iii) matrix production, biofilm maturation and, finally (iv) cell detachment with propagation of infection [15-17, 21]. Therefore, biofilms may represent reservoirs for the development of pathogenic infections [15-17, 21]. Biofilms can colonize almost every kind of material (metals, ceramics and polymers) and therefore medical devices [24] as well as the surface of dead bone and living tissue [25, 26]. Biofilms are a differentiated, high-density population of microorganisms that are surrounded by a three-dimensional, well-organized exopolymeric matrix (slime) composed of polysaccharides, proteins, nucleic acids

and lipids produced simultaneously by the microorganisms in the biofilm [27] and by proximal host cells [27]. This biofilm matrix is characterized by its resistance to stressful environmental conditions [24]. There are a variety of potential mechanisms implicated in biofilm resistance to antimicrobial agents, which are summarized at Figure 2.

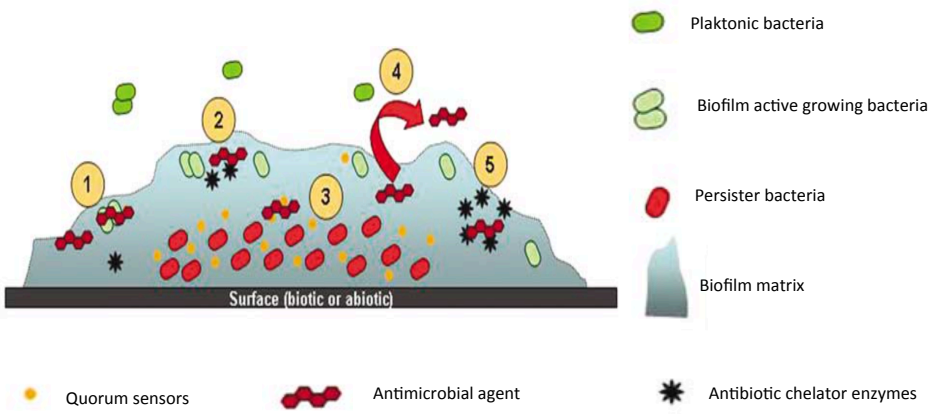

Figure 2. Some proposed-biofilm associated resistance mechanisms: (1) Antimicrobial agents may fail to penetrate beyond the surface layers of the biofilm. Outer layers of biofilm cells absorb damage. Antimicrobial agents action may be impaired in areas of waste accumulation or altered environment (pH, pCO2, pO2, etc). (2) Antimicrobial agents may be trapped and destroyed by enzymes in the biofilm matrix. (3) Altered growth rate inside the biofilm. Antimicrobial agents may not be active against nongrowing microorganisms (persister cells). (4) Expression of biofilm-specific resistance genes (e.g., efflux pumps). (5) Stress response to hostile environmental conditions (e.g., leading to an overexpression of antimicrobial agent-destroying enzymes). Adapted from [28].

Although frequently proposed as first line of resistance, the restrictive penetration of antimicrobial agents and immune cells into the biofilm matrix, may not be a real factor as showed by some reports [29-31]. Indeed, one important factor may be the metabolic state of the bacteria within the biofilm. Implant-adherent bacteria are in stationary phase of growth because oxygen and glucose are limited in biofilms [32]. This allows for the establishment of a community in a dormancy state that is less susceptible to antibiotics (persister cells), increasing the odds of late future reinfection [12, 33]. Also, biofilm-protected bacteria can release enzymes, (e.g. β-lactamases) capable of destroying antimicrobial agents [34]. Furthermore, the biofilm structure facilitates horizontal gene transfer between resistant and non-resistant microbial strains [24], which is aggravated by the elevated mutation rate promoted by inflammation [35]. Bacterial communication in biofilms, also known as quorum sensing (QS), is crucial for survival of biofilm bacteria. Bacterial functions

under QS control include surface attachment, extracellular polymer production, biosurfactant synthesis, sporulation, bioluminescence and the secretion of nutrient sequestering compounds and virulence factors [36]. The overall result is an antibiotic resistance that is typically 10–1000 higher in biofilms than in the planktonic form of the same bacterial species [24, 37]. Moreover recent research data have demonstrated that sub-therapeutic doses of both classical and recent antibiotics may induce specific gene expression, resulting in the paradoxical effect of exarcebating biofilm formation [37-41].

Regarding the etiologic agent of orthopedic implant-related infection, epidemiological data concerning nearly 800 orthopedic clinical isolates, exclusively from implant-related infections, reveal that about 16% of infections are polymicrobial. A very large proportion is caused by Staphylococci (~4 out of 5), particularly *Staphylococcus aureus* and *S. epidermidis* that account together for 2 out of 3 infection isolates [14]. Of greatest concern, is the fact that the majority of these strains no longer respond to penicillin drugs such as cephalosporins, and a lower number is resistant to methicillin/oxacillin. This Methicillin/oxacillin resistance represents major threat as these strains are not sensible to any of the numerous β-lactam drugs, and frequently exhibit multiresistance to several drugs of different antibiotic classes such as aminoglycosides, macrolides, lincosamides, tetraciclines, trimethoprim and sulfonamides [14]. Other species involved in implant-related infections are depicted on Figure 3.

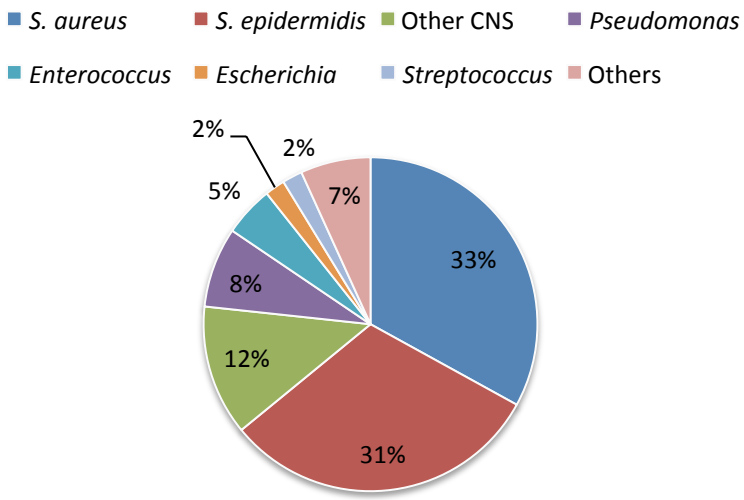

Figure 3. Frequency of main pathogenic species among orthopedic clinical isolates of implant-related infections. (CNS: Coagulase-negative Staphylococci.) Adapted from [14].

2. Current treatment protocols

Current treatment of implant-related infections requires the optimal surgical procedure combined with long-term antimicrobial therapy. Options include (i) debridement plus retention of the prosthesis, (ii) One-stage replacement, which includes the removal and implantation of a new prosthesis during the same surgical procedure, (iii) Two-stage replacement, which includes removal of the prosthesis with implantation of a new prosthesis during a later surgical procedure [1, 3]. In this case antibiotic-loaded filler may be placed in the area where the infected bone was removed [42]. Procedure choice depends on multiple factors concerning both host conditions and pathogen susceptibility. Trampuz & Zimmerli [43], proposed a modified treatment algorithm depicted in Figure 4.

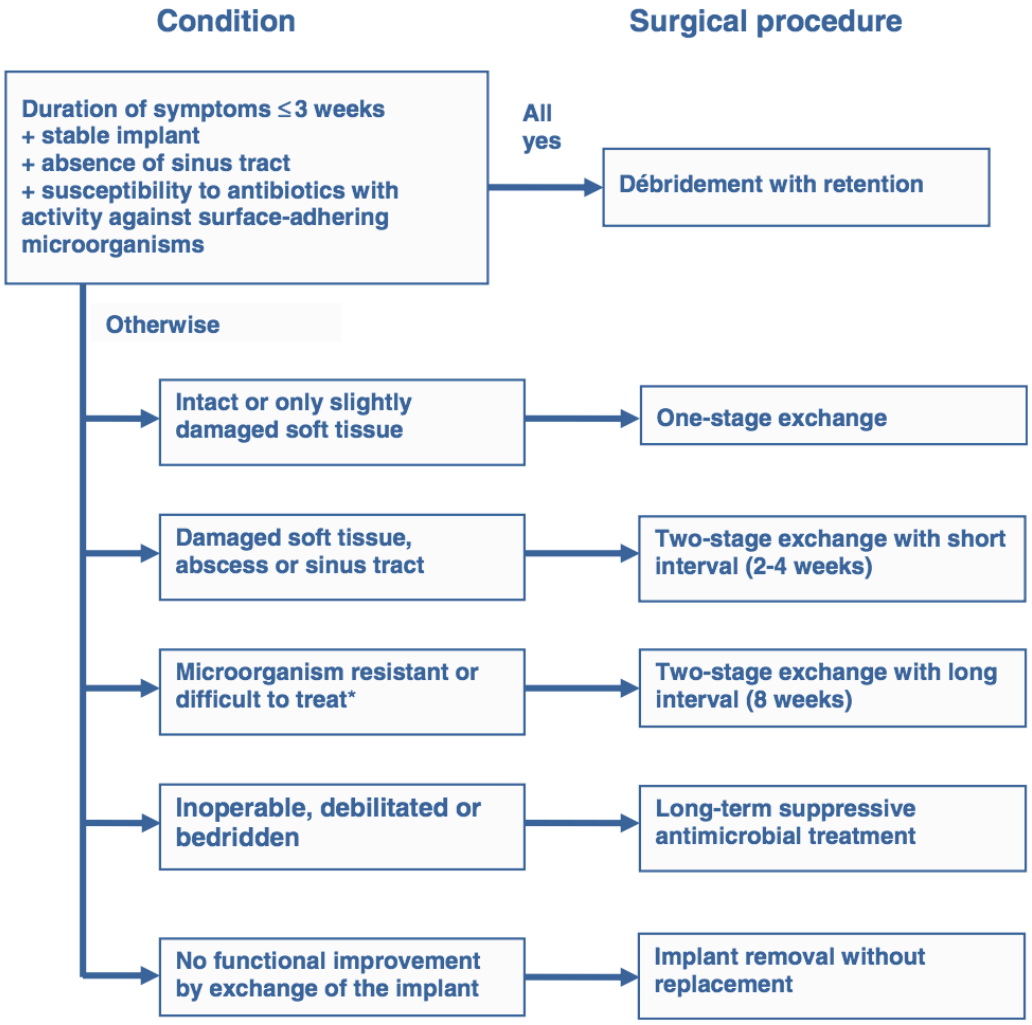

Figure 4. Surgical treatment algorithm for prosthetic joint infections. *Difficult-to-treat microorganisms include microorganism resistant to antibiotics with good oral bioavailability, rifampin-resistant *Staphylococci*, *Enterococci*, quinolone-resistant gram-negative *bacilli* and fungi. Adapted from [43].

In all cases, a long-term antimicrobial therapy is mandatory, which may span from 4 to 12 weeks [1, 2]. Good practice includes initial intravenous antibiotherapy, followed by oral route, in order to have a faster lowering of the bacteria load at the infection site [2]. Frequently, therapy includes a cocktail of different classical antibiotics in order to avoid resistance emergence [1]. However, one of the problems associated to systemic delivery of antibiotics is that insufficient concentrations are reached at vascular compromised locations, such as a fracture site or other compromised tissues [12]. Increasing the dose of systemic delivery antibiotics is not the answer, as this approach is often accompanied by systemic renal and liver

toxicity. Therefore, a common protocol is to combine the systemic therapy with local delivery of antibiotics [44]. Presently, the aminoglycosides gentamicin and tobramycin, and the glycopeptide vancomycin are the most commonly used antibiotics in local delivery vehicles [12]. Table 2 summarizes some of the most used prophylactic delivery systems and its major drawbacks.

Table 2. Most frequently used antibiotic local delivery systems in clinical settings, and its major drawbacks.

Local delivery system	Antibiotic	Drawbacks
PMMA bone cement	Gentamicin Tobramycin	- Heat generated during cement polymerization can promote tissue necrosis [45]; - Rapidly reducing local antibiotic levels [46]; - Permanent presence of a foreign body, which may be colonized by bacteria; - Low-inhibitory antibiotics levels over an extended period of time can induce bacterial resistance [47];
PMMA Beads	Gentamicin	- non-degradable, additional risk for acquiring new intraoperative infection - incomplete release
Sponge-like collagen	Gentamicin	- biodegradable, however, the mismatch between the rate of antibiotic release and the rate of collagen degradation may allow bacteria attachment via MSCRAMMs
PDLLA intramedullary nail coating	Gentamicin	- synthetic biodegradable implant, however, the acidic degradation products of PDLLA might evoke inflammatory foreign body reaction [48]

PMMA – poly(-methylmethacrylate); PDLLA – poly(D,L-lactide)

Although aminoglycosides are the most widely used in clinical settings, they do not represent the ideal candidate for such applications. Indeed, they are associated with local cytotoxicity, and bone regeneration impairment, particularly gentamicin [49]. Also, aminoglycosides have reduced activity at: low pH, low oxygen-containing environment, in the presence of calcium and magnesium ions, and in the case of

hyperosmolarity [50, 51]. Moreover, gentamicin has already a high level of resistant strains [52]. However, in opposition to most antibiotics, gentamicin is not heat labile, which explains its wide application on bone cements.

Therefore, better solutions are needed, as a number of clinical situations remains without answer, or with a significant lost of function, representing a high humane and also economical burden as infection costs treatment are many fold higher than the primary implantation of the device [11, 53, 54].

3. Current research strategies

Research community pursues the endeavor of finding new, more efficient solutions for both prevention and treatment of implant-related infections. Because the implant is an ideal surface for biofilm formation, and the current prosthetic bulk materials have already reached best achievable biomechanical performances, the most convenient way to interfere with the early phases of microbial adhesion is a modification of the surface of the device through a coating, as reviewed in references: [12, 55-59]. To this end two classical approaches have been addressed: (i) anti-adhesive (non-fouling) or bacteria-repellent surfaces [60-64] and (ii) anti-infective surfaces (either by drug-delivery, or by contact-killing [65-67]) as depicted on Figure 5.

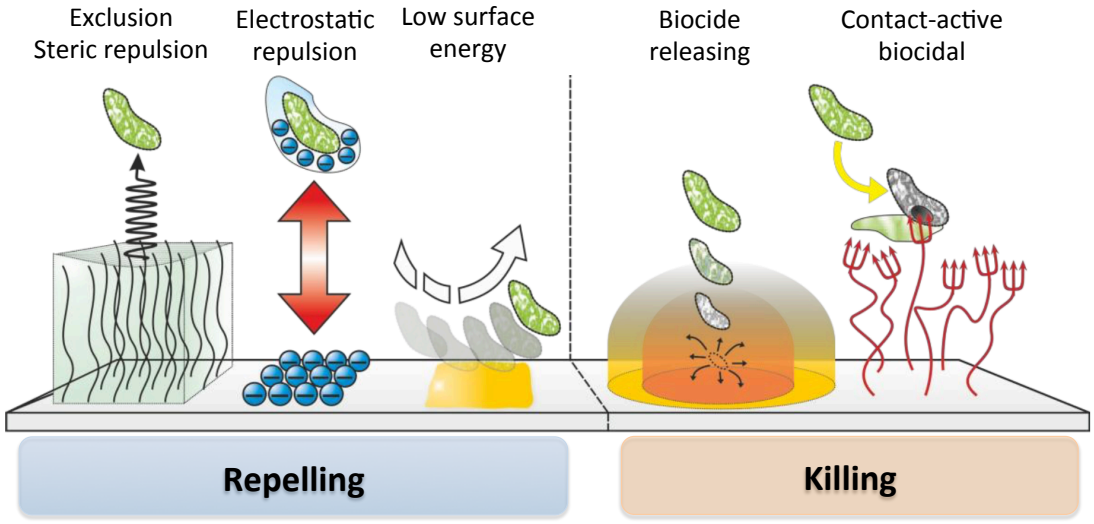

Figure 5. General principles of antimicrobial surfaces. Adapted from [68].

3.1 Anti-adhesive (non-fouling) or bacteria-repellent surfaces

The physicochemical properties of the implant surface, such as surface roughness, energy and potential, are fundamental issues in the initial adhesion and subsequent growth of bacteria. Non-fouling surfaces combine one or more approaches in order to influence the amount and/or conformation of adsorbed proteins, preventing bacterial adhesion and biofilm formation. Some examples are UV radiation of titanium surfaces to augment wettability [69], passivating proteins (e.g., albumin)[70], use of anti-adherent agents bearing negative charges [71], polymer coatings such as poly(ethylene glycol) (PEG), poly(hydroxyethylmethacrylate) (PHEMA) [72, 73], poly(methacrylic acid) [74], poly-urethanes [75], or even bioactive polymers such as chitosan, which possess the ability to inhibit bacterial adhesion and/or to kill adherent bacteria [67]. Recently, self-defensive coatings have been development by using thermoresponsive polymeric brushes [76] or even pH responsive layer-by-layer polymeric coatings [77]. Other approach is the immobilization of antibacterial enzymes such as DNase I [56] and dispersin B [78] responsible for disruption of the extracellular polymeric substances.

One of the major concerns of anti-adhesive surfaces is that by avoiding protein adsorption and bacterial adhesion, cell adhesion may also be prevented, thus impairing full integration of the implanted biomaterial.

3.2 Anti-infective surfaces

3.2.1 Drug release systems

Surfaces combined with antibiotics or other biocidal substances have the advantage of delivering drugs directly to the implant site, resulting in locally high drug doses without exceeding the systemic toxicity level of the drug, thus preventing harmful side effects [66]. Several antimicrobial surfaces have been described in the literature, including non-antibiotic antimicrobial agents such as silver, salicylic acid, chlorhexidine and nitric oxide [66, 79-81]. However, many of these compounds are associated with anaphylaxis, cytotoxicity or low efficiency [79, 80]. Also, QS

inhibitors have been proposed for its antimicrobial activity. Early interference with QS may prevent implant-associated infection, as this communication system allows bacteria to detect their local population density and to coordinate their gene expression [82]. The major problem associated with these compounds application is their possible cytotoxic and mutagenic effects [2]. The QS inhibitor RNAIII-inhibiting peptide (RIP) has been evaluated *in vitro* and *in vivo*. In a rat model, RIP coating to bone cement beads prevented *S. aureus* infection [83]. However, therapeutic efficacy of this concept has not yet been shown clinically.

These limiting aspects prompt the use of true antibiotics such as vancomycin, tobramycin, cefalozin, teicoplanin, carbenicillin, amoxicillin, penicillin, ampicillin and gentamicin [66, 84-87], with the above mentioned resistance challenge. The release strategy offers the potential for extended activity, but has to date failed to achieve delivery of a sustained and effective dosage over a relatively prolonged period of time, which may result sub-inhibitory levels that may induce resistance development [12].

3.2.2 Covalently immobilized drugs

To address the resistance induction by sub-inhibitory antibiotic levels issue, there has been an increased interest in covalent attachment of drugs to the implant surface. The advantages of covalent attachment of the drug to the implant surface are long-lasting antimicrobial activity, low incidence of side effects and non-accumulation in tissues (brain, liver and spleen) [79]. For example, vancomycin has been successfully attached to titanium and proven to be bactericidal to *S. aureus* and *S. epidermidis* [16, 79, 87]. In addition, Aumsuwan *et al*. [87] reported the covalent attachment of penicillin and ampicillin to expanded polytetrafluoroethylene. When these drugs were immobilized through a PEG-spacer, the surfaces displayed high antimicrobial efficiency among their spectrum of activity, indicating that antibiotic mobility is essential to activity. However, the effectiveness of coatings with classical antibiotics is strongly dependent on the spectrum of activity of the chosen drug, and the possibility of development of antimicrobial resistance in a relatively short time

period [88]. Therefore, alternative answers must be developed. There is a clear need for a broad-spectrum antimicrobial that prevents colonization of biomaterials, minimizes the development of bacterial resistance, displays long-term stability, even through the sterilization process, and has a low cytotoxic profile. Antimicrobial peptides have the potential to meet these criteria [89-93] and therefore represent a promise for the new generation of antimicrobial surfaces.

3.3 Alternative strategies to coatings

Innovative alternative measures to antimicrobial coatings have been proposed such as vaccination against biofilms [94], and the application of a cathodic current directly to the bulk titanium implant material [95].

Whether vaccination against staphylococcal infection is a promising means to control staphylococcal diseases is controversial. The crucial problem for vaccine development is the identification of a relevant antigen that is present in the planktonic and biofilm state of most clinical strains [94]. However, many antisera that have been raised for example to exopolysaccharide intercellular adhesin (PIA) [96] and several surface proteins, such as fibronectin-binding protein [97], have proven effective in animal infection models. Nevertheless, many of these vaccines still need to be tested for their usefulness against biofilm-associated infections [21].

The application of a constant cathodic voltage of 1.8V to commercially pure Ti for 1h was able to significantly reduce Methicillin-resitant *Staphylococcus aureus* (MRSA) viability both *in vitro* and *in vivo* [95]. However, such strategy was not yet applied to titanium alloys, more frequently used as orthopedic implant material.

[1] Toms AD, Davidson D, Masri BA, Duncan CP. The management of peri-prosthetic infection in total joint arthroplasty. The Journal of bone and joint surgery British volume. 2006;88:149-55.

[2] Zimmerli W, Moser C. Pathogenesis and treatment concepts of orthopaedic biofilm infections. FEMS immunology and medical microbiology. 2012;65:158-68.

[3] Zimmerli W. Clinical presentation and treatment of orthopaedic implant-associated infection. Journal of internal medicine. 2014;276:111-9.

[4] Zimmerli W, Waldvogel FA, Vaudaux P, Nydegger UE. Pathogenesis of foreign body infection: description and characteristics of an animal model. The Journal of infectious diseases. 1982;146:487-97.

[5] Jamsen E, Virta LJ, Hakala M, Kauppi MJ, Malmivaara A, Lehto MU. The decline in joint replacement surgery in rheumatoid arthritis is associated with a concomitant increase in the intensity of anti-rheumatic therapy: a nationwide register-based study from 1995 through 2010. Acta orthopaedica. 2013;84:331-7.

[6] Del Pozo JL, Patel R. Clinical practice. Infection associated with prosthetic joints. The New England journal of medicine. 2009;361:787-94.

[7] Trampuz A, Zimmerli W. Diagnosis and treatment of infections associated with fracture-fixation devices. Injury. 2006;37 Suppl 2:S59-66.

[8] Trampuz A, Widmer AF. Infections associated with orthopedic implants. Current opinion in infectious diseases. 2006;19:349-56.

[9] Greene LR. Guide to the elimination of orthopedic surgery surgical site infections: an executive summary of the Association for Professionals in Infection Control and Epidemiology elimination guide. American journal of infection control. 2012;40:384-6.

[10] Laffer RR, Graber P, Ochsner PE, Zimmerli W. Outcome of prosthetic knee-associated infection: evaluation of 40 consecutive episodes at a single centre. Clinical microbiology and infection: the official publication of the European Society of Clinical Microbiology and Infectious Diseases. 2006;12:433-9.

[11] Darouiche RO. Treatment of infections associated with surgical implants. The New England journal of medicine. 2004;350:1422-9.

[12] ter Boo GJ, Grijpma DW, Moriarty TF, Richards RG, Eglin D. Antimicrobial delivery systems for local infection prophylaxis in orthopedic- and trauma surgery. Biomaterials. 2015;52:113-25.

[13] Pull ter Gunne AF, Mohamed AS, Skolasky RL, van Laarhoven CJ, Cohen DB. The presentation, incidence, etiology, and treatment of surgical site infections after spinal surgery. Spine. 2010;35:1323-8.

[14] Campoccia D, Montanaro L, Arciola CR. The significance of infection related to orthopedic devices and issues of antibiotic resistance. Biomaterials. 2006;27:2331-9.

[15] Vila J, Soriano A, Mensa J. Molecular basis of microbial adherence to prosthetic materials. Role of biofilms in prosthesis-associated infection. Enfermedades infecciosas y microbiologia clinica. 2008;26:48-54.

[16] Subramani K, Jung RE, Molenberg A, Hammerle CH. Biofilm on dental implants: a review of the literature. The International journal of oral & maxillofacial implants. 2009;24:616-26.

[17] da Silva Domingues JF, Roest S, Wang Y, van der Mei HC, Libera M, van Kooten TG, et al. Macrophage phagocytic activity toward adhering staphylococci on cationic and patterned hydrogel coatings versus common biomaterials. Acta biomaterialia. 2015;18:1-8.

[18] Wilson CJ, Clegg RE, Leavesley DI, Pearcy MJ. Mediation of biomaterial-cell interactions by adsorbed proteins: A review. Tissue Eng. 2005;11:1-18.

[19] Bryers JD, Giachelli CM, Ratner BD. Engineering biomaterials to integrate and heal: the biocompatibility paradigm shifts. Biotechnology and bioengineering. 2012;109:1898-911.

[20] Anderson JM. Inflammation, wound healing, and foreign-body response. In: D. RB, editor. Biomaterials Science: Elsevier Academic Press; 2004. p. 309.

[21] Arciola CR, Campoccia D, Speziale P, Montanaro L, Costerton JW. Biofilm formation in Staphylococcus implant infections. A review of molecular mechanisms and implications for biofilm-resistant materials. Biomaterials. 2012;33:5967-82.

[22] Aslam S, Darouiche RO. Role of antibiofilm-antimicrobial agents in controlling device-related infections. The International journal of artificial organs. 2011;34:752-8.

[23] Donlan RM. Biofilm formation: a clinically relevant microbiological process. Clinical infectious diseases: an official publication of the Infectious Diseases Society of America. 2001;33:1387-92.

[24] de Carvalho CC. Biofilms: recent developments on an old battle. Recent patents on biotechnology. 2007;1:49-57.

[25] Donlan RM. Biofilms and device-associated infections. Emerging infectious diseases. 2001;7:277-81.

[26] Donlan RM. Biofilms: microbial life on surfaces. Emerging infectious diseases. 2002;8:881-90.

[27] Costerton JW, Stewart PS, Greenberg EP. Bacterial biofilms: a common cause of persistent infections. Science. 1999;284:1318-22.

[28] del Pozo JL, Patel R. The challenge of treating biofilm-associated bacterial infections. Clinical pharmacology and therapeutics. 2007;82:204-9.

[29] Vrany JD, Stewart PS, Suci PA. Comparison of recalcitrance to ciprofloxacin and levofloxacin exhibited by *Pseudomonas aeruginosa* biofilms displaying rapid-transport characteristics. Antimicrobial agents and chemotherapy. 1997;41:1352-8.

[30] Stone G, Wood P, Dixon L, Keyhan M, Matin A. Tetracycline rapidly reaches all the constituent cells of uropathogenic *Escherichia coli* biofilms. Antimicrobial agents and chemotherapy. 2002;46:2458-61.

[31] Darouiche RO, Dhir A, Miller AJ, Landon GC, Raad, II, Musher DM. Vancomycin penetration into biofilm covering infected prostheses and effect on bacteria. The Journal of infectious diseases. 1994;170:720-3.

[32] Anderl JN, Zahller J, Roe F, Stewart PS. Role of nutrient limitation and stationary-phase existence in *Klebsiella pneumoniae* biofilm resistance to ampicillin and ciprofloxacin. Antimicrobial agents and chemotherapy. 2003;47:1251-6.

[33] Williamson KS, Richards LA, Perez-Osorio AC, Pitts B, McInnerney K, Stewart PS, *et al.* Heterogeneity in Pseudomonas aeruginosa biofilms includes expression of ribosome hibernation factors in the antibiotic-tolerant subpopulation and hypoxia-induced stress response in the metabolically active population. Journal of bacteriology. 2012;194:2062-73.

[34] Anderl JN, Franklin MJ, Stewart PS. Role of antibiotic penetration limitation in *Klebsiella pneumoniae* biofilm resistance to ampicillin and ciprofloxacin. Antimicrobial agents and chemotherapy. 2000;44:1818-24.

[35] Hoiby N, Bjarnsholt T, Givskov M, Molin S, Ciofu O. Antibiotic resistance of bacterial biofilms. International journal of antimicrobial agents. 2010;35:322-32.

[36] Nadell CD, Xavier JB, Levin SA, Foster KR. The evolution of quorum sensing in bacterial biofilms. PLoS biology. 2008;6:e14.

[37] Lewis K. Riddle of biofilm resistance. Antimicrobial agents and chemotherapy. 2001;45:999-1007.

[38] Gooderham WJ, Bains M, McPhee JB, Wiegand I, Hancock RE. Induction by cationic antimicrobial peptides and involvement in intrinsic polymyxin and antimicrobial peptide resistance, biofilm formation, and swarming motility of PsrA in *Pseudomonas aeruginosa*. Journal of bacteriology. 2008;190:5624-34.

[39] Hoffman LR, D'Argenio DA, MacCoss MJ, Zhang Z, Jones RA, Miller SI. Aminoglycoside antibiotics induce bacterial biofilm formation. Nature. 2005;436:1171-5.

[40] Ahmed NA, Petersen FC, Scheie AA. AI-2/LuxS is involved in increased biofilm formation by *Streptococcus intermedius* in the presence of antibiotics. Antimicrobial agents and chemotherapy. 2009;53:4258-63.

[41] Bagge N, Schuster M, Hentzer M, Ciofu O, Givskov M, Greenberg EP, *et al. Pseudomonas aeruginosa* biofilms exposed to imipenem exhibit changes in global gene expression and beta-lactamase and alginate production. Antimicrobial agents and chemotherapy. 2004;48:1175-87.

[42] Peng KT, Chen CF, Chu IM, Li YM, Hsu WH, Hsu RW, *et al*. Treatment of osteomyelitis with teicoplanin-encapsulated biodegradable thermosensitive hydrogel nanoparticles. Biomaterials. 2010;31:5227-36.

[43] Trampuz A, Zimmerli W. Prosthetic joint infections: update in diagnosis and treatment. Swiss medical weekly. 2005;135:243-51.

[44] Engesaeter LB, Lie SA, Espehaug B, Furnes O, Vollset SE, Havelin LI. Antibiotic prophylaxis in total hip arthroplasty: effects of antibiotic prophylaxis systemically and in bone cement on the revision rate of 22,170 primary hip replacements followed 0-14 years in the Norwegian Arthroplasty Register. Acta orthopaedica Scandinavica. 2003;74:644-51.

[45] Kuehn KD, Ege W, Gopp U. Acrylic bone cements: composition and properties. The Orthopedic clinics of North America. 2005;36:17-28.

[46] Frutos Cabanillas P, Diez Pena E, Barrales-Rienda JM, Frutos G. Validation and in vitro characterization of antibiotic-loaded bone cement release. International journal of pharmaceutics. 2000;209:15-26.

[47] Weber FA, Lautenbach EE. Revision of infected total hip arthroplasty. Clinical orthopaedics and related research. 1986:108-15.

[48] Fuchs T, Stange R, Schmidmaier G, Raschke MJ. The use of gentamicin-coated nails in the tibia: preliminary results of a prospective study. Archives of orthopaedic and trauma surgery. 2011;131:1419-25.

[49] Rathbone CR, Cross JD, Brown KV, Murray CK, Wenke JC. Effect of various concentrations of antibiotics on osteogenic cell viability and activity. Journal of orthopaedic research : official publication of the Orthopaedic Research Society. 2011;29:1070-4.

[50] Baudoux P, Bles N, Lemaire S, Mingeot-Leclercq MP, Tulkens PM, Van Bambeke F. Combined effect of pH and concentration on the activities of gentamicin and oxacillin against *Staphylococcus aureus* in pharmacodynamic models of extracellular and intracellular infections. The Journal of antimicrobial chemotherapy. 2007;59:246-53.

[51] Schlessinger D. Failure of aminoglycoside antibiotics to kill anaerobic, low-pH, and resistant cultures. Clinical microbiology reviews. 1988;1:54-9.

[52] Hope PG, Kristinsson KG, Norman P, Elson RA. Deep infection of cemented total hip arthroplasties caused by coagulase-negative *Staphylococci*. The Journal of bone and joint surgery British volume. 1989;71:851-5.

[53] Bryers JD. Medical biofilms. Biotechnology and bioengineering. 2008;100:1-18.

[54] Gottenbos B, Busscher HJ, Van Der Mei HC, Nieuwenhuis P. Pathogenesis and prevention of biomaterial centered infections. Journal of materials science Materials in medicine. 2002;13:717-22.

[55] Gallo J, Holinka M, Moucha CS. Antibacterial Surface Treatment for Orthopaedic Implants. International Journal of Molecular Sciences. 2014;15:13849-80.

[56] Swartjes JJ, Sharma PK, van Kooten TG, van der Mei HC, Mahmoudi M, Busscher HJ, *et al*. Current Developments in Antimicrobial Surface Coatings for Biomedical Applications. Current medicinal chemistry. 2015;22:2116-29.

[57] Salwiczek M, Qu Y, Gardiner J, Strugnell RA, Lithgow T, McLean KM, *et al.* Emerging rules for effective antimicrobial coatings. Trends in biotechnology. 2014;32:82-90.

[58] Brooks BD, Brooks AE. Therapeutic strategies to combat antibiotic resistance. Advanced drug delivery reviews. 2014;78:14-27.

[59] Harding JL, Reynolds MM. Combating medical device fouling. Trends in biotechnology. 2014;32:140-6.

[60] Glinel K, Jonas AM, Jouenne T, Leprince J, Galas L, Huck WT. Antibacterial and antifouling polymer brushes incorporating antimicrobial peptide. Bioconjug Chem. 2009;20:71-7.

[61] Goncalves IC, Martins MC, Barbosa MA, Naeemi E, Ratner BD. Selective protein adsorption modulates platelet adhesion and activation to oligo(ethylene glycol)-terminated self-assembled monolayers with C18 ligands. J Biomed Mater Res A. 2009;89:642-53.

[62] Harris LG, Tosatti S, Wieland M, Textor M, Richards RG. *Staphylococcus aureus* adhesion to titanium oxide surfaces coated with non-functionalized and peptide-functionalized poly(L-lysine)-grafted-poly(ethylene glycol) copolymers. Biomaterials. 2004;25:4135-48.

[63] Chen SF, Jiang SY. A new avenue to nonfouling materials. Advanced materials. 2008;20:335-338.

[64] Banerjee I, Pangule RC, Kane RS. Antifouling coatings: recent developments in the design of surfaces that prevent fouling by proteins, bacteria, and marine organisms. Advanced materials. 2011;23:690-718.

[65] Zilberman M, Elsner JJ. Antibiotic-eluting medical devices for various applications. Journal of controlled release : official journal of the Controlled Release Society. 2008;130:202-15.

[66] Hetrick EM, Schoenfisch MH. Reducing implant-related infections: active release strategies. Chemical Society reviews. 2006;35:780-9.

[67] Tiller JC, Liao CJ, Lewis K, Klibanov AM. Designing surfaces that kill bacteria on contact. Proceedings of the National Academy of Sciences of the United States of America. 2001;98:5981-5.

[68] Siedenbiedel F, Tiller JC. Antimicrobial Polymers in Solution and on Surfaces: Overview and Functional Principles. Polymers. 2012;4:46-71.

[69] Gallardo-Moreno AM, Pacha-Olivenza MA, Saldana L, Perez-Giraldo C, Bruque JM, Vilaboa N, *et al*. *In vitro* biocompatibility and bacterial adhesion of physico-chemically modified Ti6Al4V surface by means of UV irradiation. Acta biomaterialia. 2009;5:181-92.

[70] An YH, Bradley J, Powers DL, Friedman RJ. The prevention of prosthetic infection using a cross-linked albumin coating in a rabbit model. The Journal of bone and joint surgery British volume. 1997;79:816-9.

[71] Jansen B, Kohnen W. Prevention of biofilm formation by polymer modification. Journal of industrial microbiology. 1995;15:391-6.

[72] Harbers GM, Emoto K, Greef C, Metzger SW, Woodward HN, Mascali JJ, *et al*. A functionalized poly(ethylene glycol)-based bioassay surface chemistry that facilitates bio-immobilization and inhibits non-specific protein, bacterial, and mammalian cell adhesion. Chemistry of materials: a publication of the American Chemical Society. 2007;19:4405-14.

[73] Martins MC, Wang D, Ji J, Feng L, Barbosa MA. Albumin and fibrinogen adsorption on cibacron blue F3G-A immobilised onto PU-PHEMA (polyurethane-poly(hydroxyethylmethacrylate)) surfaces. Journal of biomaterials science Polymer edition. 2003;14:439-55.

[74] Zhang F, Zhang Z, Zhu X, Kang ET, Neoh KG. Silk-functionalized titanium surfaces for enhancing osteoblast functions and reducing bacterial adhesion. Biomaterials. 2008;29:4751-9.

[75] Flemming RG, Capelli CC, Cooper SL, Proctor RA. Bacterial colonization of functionalized polyurethanes. Biomaterials. 2000;21:273-81.

[76] Laloyaux X, Fautre E, Blin T, Purohit V, Leprince J, Jouenne T, *et al*. Temperature-responsive polymer brushes switching from bactericidal to cell-repellent. Advanced materials. 2010;22:5024-8.

[77] Lu Y, Wu Y, Liang J, Libera MR, Sukhishvili SA. Self-defensive antibacterial layer-by-layer hydrogel coatings with pH-triggered hydrophobicity. Biomaterials. 2015;45:64-71.

[78] Kaplan JB, Ragunath C, Velliyagounder K, Fine DH, Ramasubbu N. Enzymatic detachment of *Staphylococcus epidermidis* biofilms. Antimicrobial agents and chemotherapy. 2004;48:2633-6.

[79] Zhao L, Chu PK, Zhang Y, Wu Z. Antibacterial coatings on titanium implants. J Biomed Mater Res B Appl Biomater. 2009;91:470-80.

[80] Monteiro DR, Gorup LF, Takamiya AS, Ruvollo-Filho AC, de Camargo ER, Barbosa DB. The growing importance of materials that prevent microbial adhesion: antimicrobial effect of medical devices containing silver. International journal of antimicrobial agents. 2009;34:103-10.

[81] Chernousova S, Epple M. Silver as antibacterial agent: ion, nanoparticle, and metal. Angewandte Chemie. 2013;52:1636-53.

[82] Costerton JW, Montanaro L, Arciola CR. Bacterial communications in implant infections: a target for an intelligence war. The International journal of artificial organs. 2007;30:757-63.

[83] Anguita-Alonso P, Giacometti A, Cirioni O, Ghiselli R, Orlando F, Saba V, *et al*. RNAIII-inhibiting-peptide-loaded polymethylmethacrylate prevents *in vivo* *Staphylococcus aureus* biofilm formation. Antimicrobial agents and chemotherapy. 2007;51:2594-6.

[84] Aumsuwan N, Danyus RC, Heinhorst S, Urban MW. Attachment of ampicillin to expanded poly(tetrafluoroethylene): surface reactions leading to inhibition of microbial growth. Biomacromolecules. 2008;9:1712-8.

[85] Faber C, Stallmann HP, Lyaruu DM, Joosten U, von Eiff C, van Nieuw Amerongen A, *et al*. Comparable efficacies of the antimicrobial peptide human lactoferrin 1-11 and gentamicin in a chronic methicillin-resistant *Staphylococcus aureus* osteomyelitis model. Antimicrobial agents and chemotherapy. 2005;49:2438-44.

[86] Cevher E, Orhan Z, Mulazimoglu L, Sensoy D, Alper M, Yildiz A, et al. Characterization of biodegradable chitosan microspheres containing vancomycin and treatment of experimental osteomyelitis caused by methicillin-resistant *Staphylococcus aureus* with prepared microspheres. International journal of pharmaceutics. 2006;317:127-35.

[87] Aumsuwan N, Heinhorst S, Urban MW. Antibacterial surfaces on expanded polytetrafluoroethylene; penicillin attachment. Biomacromolecules. 2007;8:713-8.

[88] Palumbi SR. Humans as the world's greatest evolutionary force. Science. 2001;293:1786-90.

[89] Gordon YJ, Romanowski EG, McDermott AM. A review of antimicrobial peptides and their therapeutic potential as anti-infective drugs. Current eye research. 2005;30:505-15.

[90] Perron GG, Zasloff M, Bell G. Experimental evolution of resistance to an antimicrobial peptide. Proceedings Biological sciences / The Royal Society. 2006;273:251-6.

[91] Reddy KV, Yedery RD, Aranha C. Antimicrobial peptides: premises and promises. International journal of antimicrobial agents. 2004;24:536-47.

[92] van 't Hof W, Veerman EC, Helmerhorst EJ, Amerongen AV. Antimicrobial peptides: properties and applicability. Biological chemistry. 2001;382:597-619.

[93] Wang G, Mishra B, Lau K, Lushnikova T, Golla R, Wang X. Antimicrobial peptides in 2014. Pharmaceuticals. 2015;8:123-50.

[94] Harro JM, Peters BM, O'May GA, Archer N, Kerns P, Prabhakara R, *et al*. Vaccine development in *Staphylococcus aureus*: taking the biofilm phenotype into consideration. FEMS immunology and medical microbiology. 2010;59:306-23.

[95] Ehrensberger MT, Tobias ME, Nodzo SR, Hansen LA, Luke-Marshall NR, Cole RF, *et al*. Cathodic voltage-controlled electrical stimulation of titanium implants as treatment for methicillin-resistant *Staphylococcus aureus* periprosthetic infections. Biomaterials. 2015;41:97-105.

[96] Kelly-Quintos C, Cavacini LA, Posner MR, Goldmann D, Pier GB. Characterization of the opsonic and protective activity against *Staphylococcus aureus* of fully human monoclonal antibodies specific for the bacterial surface polysaccharide poly-N-acetylglucosamine. Infection and immunity. 2006;74:2742-50.

[97] Rennermalm A, Li YH, Bohaufs L, Jarstrand C, Brauner A, Brennan FR, *et al*. Antibodies against a truncated Staphylococcus aureus fibronectin-binding protein protect against dissemination of infection in the rat. Vaccine. 2001;19:3376-83.

CHAPTER II

Covalent immobilization of antimicrobial peptides (AMPs) onto biomaterial surfaces

---

This chapter was produced by adapting and updating data from the following review (the original paper is presented in Appendix 1):

Fabíola Costa [a,b], Isabel F. Carvalho [c], Ronald C. Montelaro [d], Paula Gomes [e], M. Cristina L. Martins [a,f]

Acta Biomaterialia 2011 7: 1431-1440

[a] INEB – Instituto de Engenharia Biomédica, Universidade do Porto, Rua do Campo Alegre, 823, 4150-180 Porto, Portugal

[b] Universidade do Porto, Faculdade de Engenharia, Porto, Portugal

[c] IBMC – Instituto Biologia Celular e Molecular, Universidade do Porto, Rua do Campo Alegre 823, 4150-180 Porto, Portugal

[d] Microbiology and Molecular Genetics, University of Pittsburgh School of Medicine, Pittsburgh, PA, USA

[e] Universidade do Porto, CIQ-UP – Departamento de Química e Bioquímica, Faculdade de Ciências, Porto, Portugal

[f] Universidade do Porto, Instituto de Ciências Biomédicas Abel Salazar, Porto, Portugal

1. Antimicrobial peptides, new therapeutic solution?

In the last decades, resistance to new antibiotics has appeared in microbial populations within a few years of the introduction of a new therapeutic drug, as depicted in Figure 1 [1].

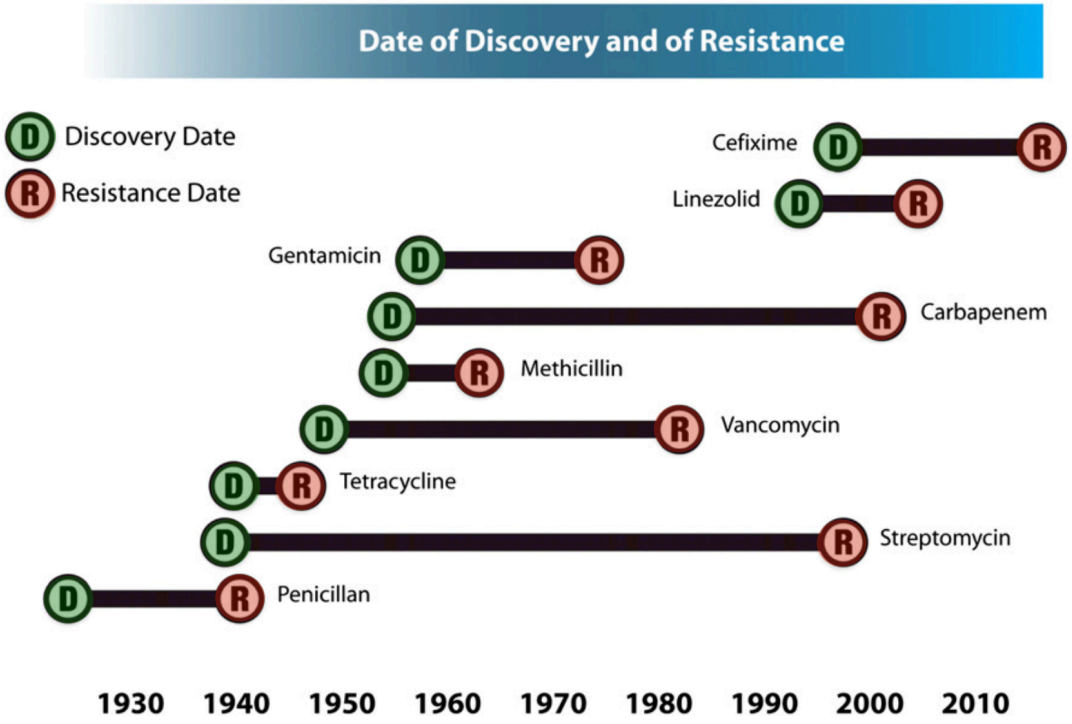

Figure 1. Date of discovery and of resistance of classical antibiotics. At most there is roughly 60 years between antibiotic discovery to the first incidence of resistance to that same antibiotic. Adapted from [1].

The decline in the effectiveness of current therapies has led to a search for new kinds of agents, including antibiotics based on antimicrobial peptides (AMPs), which are part of the innate immune system of all multicellular organisms [2-6]. So far, more than 2400 AMPs have been reported in the antimicrobial peptide database (http://aps.unmc.edu/AP/main.php), which have been isolated from a wide variety of animals, plants, bacteria, fungi and viruses [6]. The AMPs comprise a chemically and structurally heterogeneous family. Nevertheless, three characteristics are shared by almost all known AMPs: (i) small size (10 to 100 amino acids), (ii) highly cationic character, though with large variations in the net positive charge (+2 - +9);

(iii) tendency to adopt amphipathic structures, i.e. structures with separate hydrophobic and hydrophilic domains, in non-polar media [7]. These peptides offer several attractive advantages as therapeutic drugs: they exhibit bactericidal, fungicidal, viricidal, tumoricidal, endotoxin neutralization and immunomodulatory properties, they act at a very low concentration, and they are less likely to promote bacterial resistance [4, 6-8]. Unlike conventional antibiotics such as penicillin, which microbes readily deceive, acquisition of resistance by a sensitive microbial strain against AMPs is less probable. Indeed, it takes 30 passages for *Pseudomonas aeruginosa* in subminimal inhibitory concentration peptide to increase its resistance by two- to fourfold [9], whereas under the same conditions, resistance to gentamicin can increase by 190-fold [10].

2. AMPs mechanism of action

The exact mechanism of action of AMPs is still not fully understood. However, it is widely assumed that the principal target of AMPs is the plasma membrane. As this structure is vital for all cells, membrane destabilization may cause cell death [11]. Therefore, the low cytotoxicity towards mammalian cells may be explained by membrane composition. Bacterial membranes are organized in such a way that lipids with negatively charged phospholipid headgroups heavily occupy the outermost leaflet of the bilayer. In contrast, the outer leaflet of the membranes of plants and animals is composed principally of lipids with no net charge. Here most of the lipids with negatively charged headgroups are segregated into the inner leaflet, facing the cytoplasm [12] (Figure 2).

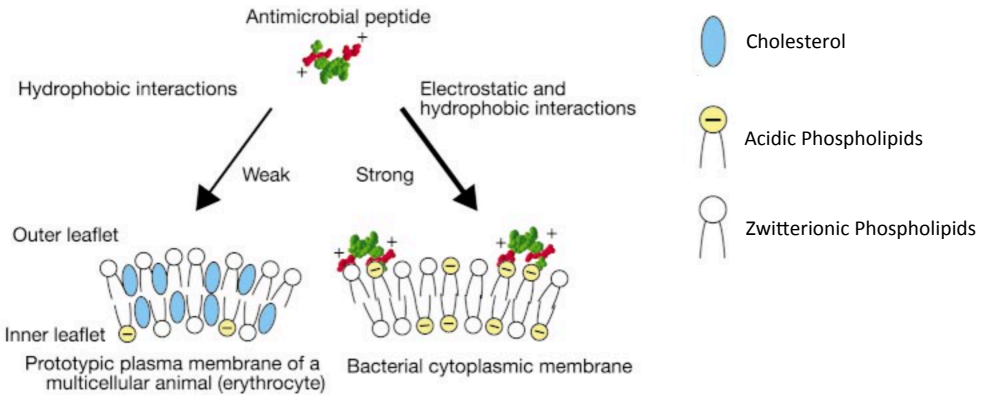

Figure 2. The membrane target specificity of antimicrobial peptides. Adapted from [12].

There is a consensus regarding the initial steps of AMPs interaction with bacterial membranes, which includes the following: (i) cationic, *i.e.* positively charged, peptides are electrostatically attracted to the negatively charged microbial cell membranes, then (ii) AMPs adopts an amphipathic structure upon binding to the phospholipid membrane, adapting to the specific conditions at the membrane–water interface. This interaction is generally believed to lead to a lethal increase in the permeability of the cell membrane [5]. The most cited models to explain AMPs membrane interaction are: barrel stave pore model, toroidal pore model and carpet model (Figure 3). In the barrel stave pore model, peptides interact laterally with one another to form a specific structure enclosing a water-filled channel, much like a protein ion channel. In the toroidal pore, specific peptide–peptide interactions are not present but, instead, peptides affect the local curvature of the membrane cooperatively such that a peptide–lipid toroid of high curvature forms. In the carpet model, antimicrobial peptides accumulate on the membrane surface with an orientation that is parallel to the membrane. When peptide concentration has reached a critical level (i.e., a peptide-rich ‘‘carpet’’ has formed on the membrane surface), permeabilization occurs via global bilayer destabilization.

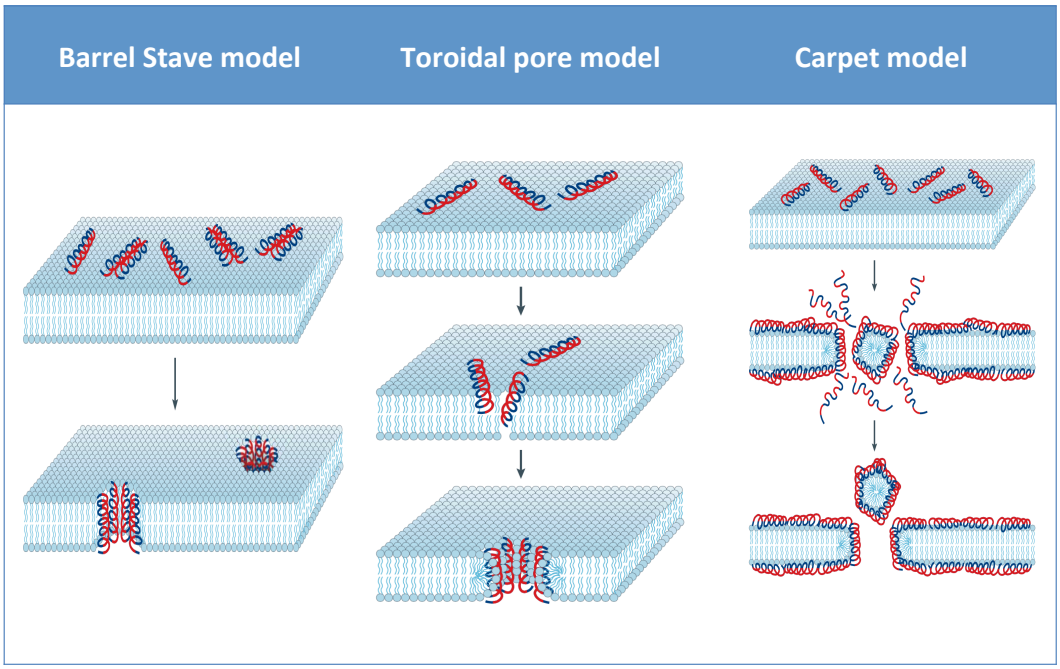

Figure 3. Firstly proposed models for the mechanism of action of membrane-active antimicrobial peptides (AMPs). Adapted from [13].

How this interaction ends in fatal outcome still remains to be determined. Many hypotheses have been proposed meanwhile, based on the understanding of different known AMPs. Figure 4 summarizes some of these hypotheses.

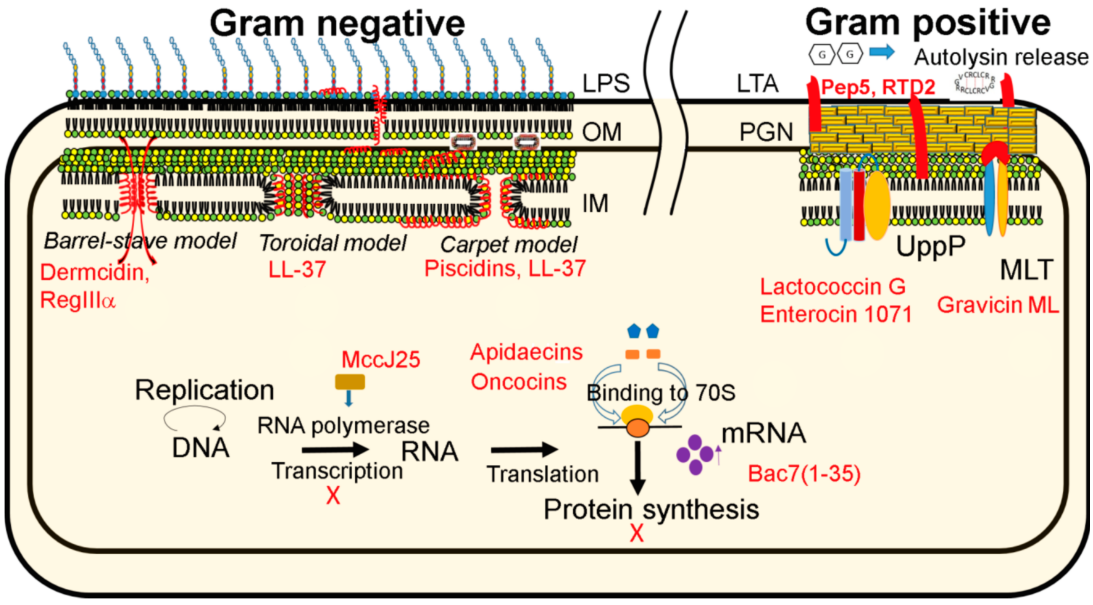

Figure 4. Current proposed mechanisms of action of antimicrobial peptides (AMPs, in red). Each model has a studied AMP presented in red. Adapted from [6]. Abbreviations used in the figure: OM, outer membrane; IM, inner membrane; PGN, peptidoglycan; LTA, lipoteichoic acid; LPS, lipopolysaccharide, MLT, maltose transporter.

New proposed putative mechanism of action include: a) cell wall synthesis inhibition (ligation to UppP enzyme or to maltose ABC receptors) as observed for the AMPs, Lactococcin G and Enterocin 1071 or Gravicin ML; b) Autolysin release by membrane interaction by the AMPs, RTD2 and lantibiotic Pep5; c) RNA polymerase inhibition by the AMP, MccJ25 and binding to ribosomal proteins promoting protein synthesis inhibition by the AMPs, apidaecins, oncocins and Bac7; d) interaction with nucleic acids by the AMP, Buforin II, between others [6, 14]. Furthermore, some cationic peptides bind to lipopolysaccharide (LPS) and lipoteichoic acid (LTA) with high affinity (competitively displacing membrane-stabilizing bivalent cations Ca^{2+} or Mg^{2+}), disrupting these sites and leading to enhanced uptake of cationic peptides across the outer membrane (self-promoted uptake process). This property is responsible for a two additional advantages: anti-endotoxin activity, in contrast to other antibiotics, which induce endotoxinaemia, and ‘‘enhancer’’ activity (i.e. synergy with classical antibiotics) [5, 15, 16].

Nevertheless, it is well established that the first principal target of AMPs is the plasma membrane. This fact may explain why AMPs are not prone to promote resistance, as a microorganism would have to redesign its membrane, changing the composition and/or organization of its lipids, which represent an expensive solution for most microbial species.

Still, some resistance mechanisms have been reported in Gram-positive and Gram-negative bacteria. For instance, some Gram-positive bacteria (e.g. *S. epidermidis, S. aureus*) can express an AMP sensor system that has been proposed to regulate selected resistance genes when the bacteria come into contact with AMPs [17-19]. These resistance genes include dlt-operon, which is responsible for D-alanylation of teichoic acid; mprF, which mediates the incorporation of lysyl-phosphatidylglycerol in the cytoplasmic membrane (both of these genes decrease the negative net charge of the cell envelope); and the vraFG genes of a transport system [17, 18, 20-22]. Other reported resistance mechanisms include protease inhibitors, such *S. aureus* IsdA surface protein [23], and biofilm stabilizers such PIA [24]. Nevertheless, bacterial resistance mechanisms to AMPs differ with regard to efficiency, specificity and distribution among species [17], and natural AMPs have evolved to avoid some of these resistance mechanisms. Moreover, synthetic AMPs can be rationally

engineered (*de novo* AMPs) to circumvent specific bacterial resistance mechanisms based on the specific application (target bacteria, environment, etc.), as well as enhanced activity and very low cytotoxic properties [25]. These *de novo* AMPs are distinct from those in nature, with simpler but rationally engineered composition, obtained by varying the amino acid content and sequence and overall peptide length. New tools such as robotics and machine learning are being developed to facilitate rational design of peptides, minimizing the number and amount of peptides synthesized and tested. These novel peptides are then tested *in vitro* to identify those with enhanced antimicrobial activity, which go on to become templates for the synthesis of new libraries. One example is quantitative structure-activity relationship modeling (QSAR) analysis. Cherkasov *et al.* used the bovine cathelicidin bactenecin as the initial template to iteratively generate two large 9-amino acid peptide libraries with enhanced biological activity [26]. Another example is designing shorter AMPs, derived from a highly effective and broad-spectrum synthetic AMP, MSI-78 (22 residues), by truncating this peptide at the N- and/or C-termini while spanning its entire sequence with 1 amino acid shifts [27, 28].

Finally, although the commercial development of AMPs has been limited, several peptides have shown outstanding *in vitro* activities against multi-resistant pathogens and have entered Phase III clinical trials (e.g., pexiganan and omiganan). To date, however, none has been approved or commercialized for clinical use [29]. Nisin is still the only commercialized AMP that has been approved as a food additive in the United States and Europe (food additive E234)[30].

The toxicity associated with some AMPs is usually related to the high concentrations used to compensate for the relatively short half-life of AMPs due to a rapid protease digestion [31], or to peptide aggregation [32]. Moreover, the broad-spectrum antimicrobials also carry the risk of eradicating the natural flora, thereby providing a niche for opportunistic pathogens such as fungi to invade [8]. These characteristics have limited the use of AMPs in applications that require systemic distribution of the antimicrobial. However, AMPs are designed to work at local surfaces in most of their natural applications. Thus, stable immobilization of AMPs onto a biomaterial could be the pathway to overcome these difficulties [33].

3. Immobilization of an antimicrobial peptide

AMPs immobilization represents a way of developing a local therapy. Immobilization can be performed both through physical adsorption and covalent tethering.

3.1 AMPs immobilization through physical methods

One of the easiest methods for AMP immobilization is by simple physical adsorption. Bower *et al.,* assessed the effect of Nisin adsorbed onto Polyvinyl Chloride (PVC) suction catheter tubing [34]. After, both *in vitro* and *in vivo* studies the material revealed to have activity but not in a sustained manner (only until 5h after application). On the other hand, Gopinath *et al*., tested pexiganan incorporated onto collagen, both *in vitro* and *in vivo* on a rat wound infection model [35]. Again, activity was sustained for a short period of time (72h). Among the physical immobilization methods, layer-by-layer (LbL) has been the most explored technique to immobilize AMPs on surfaces. In this approach, which is based on the alternate adsorption of polycations and polyanions on a solid substratum, AMPs can be simply embedded in the multilayer architecture to prepare functional films [36]. The number of layers (thickness) of the LbL coatings, determine the amount of AMPs bound to the surface. For instance, Etienne *et al.*, incorporated the peptide defensin into polyelectrolyte multilayer films, promoting a 98% growth inhibition of *Escherichia coli* at the surface when 10 antimicrobial peptide layers were inserted in the film architecture [37]. This approach is, however, restricted to the use of highly charged and water-soluble AMPs, which are not so frequently encountered. And as stressed out by Alves *et al*.,[38] the electrostatic interactions between the peptides and the polyelectrolyte matrix may denature the peptide or reduce its motility, which therefore compromises its antimicrobial activity. Other approach used non-water-soluble AMP, gramicidin A conjugated with a non-denaturing amphiphilic polysaccharide (hydrophobically modified carboxymethylpullulan) to obtain a negatively charged complex that was LbL assembled with cationic poly(L-lysine) to form biofunctionalized films. These films exhibited a strong antibacterial activity against *Enterococcus faecalis* [39]. Again, the number of layers controlled the effectiveness

of the antibacterial activity. Nevertheless, the lacking of a sustained release of the AMPs is still a drawback of such system.

Shukla *et al*., proposed controlling AMP release by using hydrolytically degradable LbL assembled films [40]. The AMP Ponericin G1 was successful incorporated into polyelectrolyte assemblies based on a hydrolytically degradable cationic poly(β-amino ester) and an anionic polyanion such as alginic acid. The films obtained were able to inhibit *S. aureus* attachment over 10 days owing to the degradation of poly(β-amino ester). Moreover, release profiles could be controlled by changing the film microstructure [40].

Although the physical entrapment of AMPs into polymer layers has been successfully explored to prepare antibacterial coatings, there are some drawbacks associated with these strategies that limit their application into biomaterial implants or medical devices. The gradually decreasing level of released peptide may lead to sub-inhibitory concentrations in the surrounding bulk, which may provide conditions for development of microbial resistance. Another concern inherent to physical immobilization strategies is related to the long-term stability of these assemblies, which are still largely not reported.

3.2 AMPs chemical covalent immobilization

Covalent immobilization of AMP can increase their long-term stability while decreasing their toxicity, as compared to incorporation approaches on leach- or release-based systems [32, 33, 41, 42]. Furthermore, the proper orientation of the peptide may result in enhanced activity [43]. Table 3 summarizes the different covalent immobilization strategies reported to date.

Ref.	AMP	Substrate	AMP Immobilization strategy	Microorganisms assessed
[31]	Magainin 2 and Related synthetic amphiphilic peptides	Polyamide resin (pepsin K)	Directly synthesized on polyamide resin, after immobilization through their C-terminal amino acids. • AMP orientation was controlled • Short spacer, with two- or six-carbon chains, was used • Stability to heat was studied • no AMP release was observed	*E. coli* ATCC 35695; and ATCC 25922, *S. aureus* ATCC 25923 and ATCC 6538, *Klebsiella pneumoniae* ATCC 4352, *Bacillus subtilis* ATCC 6051, *Candida albicans* ATCC 10231, *Aspergillus niger* ATCC 6275, and *P. aeruginosa* ATCC 27853.
[44]	Magainin I	Non-fouling copolymer brushes based on different percentages of: 2-(2-methoxyethoxy)ethyl methacrylate (MEO_2MA) / hydroxyl-terminated oligo(ethylene glycol) methacrylate (HOEGMA)	Immobilized by the carboxy-terminated amino acid of the peptide. The process consisted of a previous incorporation of a cysteine residue on the C-terminal of Magainin, to be reacted with the polymeric brushes via (N-(*p*-maleimidophenyl)isocyanate). • AMP orientation was controlled • Brushes were used as spacers • Different AMPs densities was tested	*Listeria ivanovii*, *Bacillus cereus*
[45]	Magainin I	Mixed OH/COOH-terminated self-assembled monolayers (SAMs)	Immobilization by the free AMP amines after activation of the COOH groups of the SAM with NHS/EDC. • AMP orientation was not controlled • No spacers • no AMP release was observed	*L. ivanovii*, *E. faecalis* and *S. aureus*
[42]	Magainin-derived MK5E and KLAL	PEGylated TentaGel S, HypoGel 400 and HypoGel 200 resin beads	*C*-terminally immobilized peptides were achieved by standard solid-phase peptide synthesis and Fmoc (9-fluorenylmethoxycarbonyl)-chemistry. *N*-terminal and side-chain immobilization were achieved by thioalkylation and oxime formation • AMP orientation was controlled • Different AMPs densities were tested • effect of PEGylated spacers was tested • the hemolytic effect was assayed	*E. coli* strain DH5α, *B. subtilis* strain DSM 347
[32]	Melimine	Commercial contact lenses (etafilcon A)	Immobilization by the free AMP amines using 1-ethyl-3-(3-dimethylaminopropyl)carbodiimide. • AMP orientation was not controlled • No spacers	*P. aeruginosa* 6294, *P. aeruginosa* ATCC 15442, *S. aureus* Saur31, *S. aureus* CK5, *Streptococcus pneumoniae* 010

Ref.	AMP	Substrate	AMP Immobilization strategy	Microorganisms assessed
[46]	Melimine	Glass coverslips	Immobilization by the free AMP amines using two different strategies: a. using 1-ethyl-3-(3-dimethylaminopropyl) carbodiimide after previous activation of the OH groups of the glass substrate with 4-azidobenzoic acid and irradiation with UV-light (320nm) b. after activation of the OH groups of the glass substrate with 4-fluoro-3-nitrophenyl azide and irradiation with UV-light (320nm) • AMP orientation was not controlled • No spacers • Different AMPs densities were tested	*S. aureus* strain 38, *P. aeruginosa* PA01
[43]	Cathelin LL37	Silanized titanium surfaces: a. Using glycidyloxypropyl triethoxysilane (epoxy silane) b. 3-aminopropyl triethoxysilane (amino silane)	a. Random immobilization: Immobilization by the free AMP amines with and without PEGylated spacer onto epoxy-silanized Ti. b. Controlled immobilization: Immobilized by the carboxy-terminated amino acid of LL37 (Cys residue), after the treatment of the amino-silanized Ti with: (i) N-maleimidopropionic acid succinimide ester (ii) R-N-hydroxysuccinimidyl-ö-maleimidyl-PEG (NHS-PEG-Mal) • Effect of AMP orientation was tested • Effect of PEGylated spacers was tested • Different AMPs densities were tested	*E. coli* strain K12
[47]	E14LKK	Oxidized polyethylene films	Immobilization by the terminal AMP amine (using protected E14LKK side chains amines) with and without PEGylated spacer onto ox-PE using 1-ethyl-3-(3-aminopropyl)-carbodiimide. • AMP orientation was controlled • Effect of PEGylated spacers was tested	*E. coli* ATCC 25922
[16]	FKVKFKVKFK	PEG-PS Resin beads	Peptide-resin conjugates were synthesized by using Fmoc (9-fluorenylmethoxycarbonyl)-chemistry. To investigate the effect of the resin on the activity, the β-sheet peptide was conjugated with 4-Methylbenzhydrylamine hydrochloride (MBHA)-resin	*S. aureus* ATCC 6538, *Micrococcus luteus* ATCC 9341, *P. aeruginosa* ATCC9027, *E. coli* ATCC 25922

Ref.	AMP	Substrate	AMP Immobilization strategy	Microorganisms assessed
[48]	6K8L	PEG-PS Resin beads	The peptide was synthesized by solid-phase peptide synthesis on a PEG-modified polystyrene resin (PEG-PS) using Fmoc-chemistry. The antimicrobial activity of the peptide-resin conjugate was evaluated against different microorganisms.	*B. subtilis* (wild-type PB2, 168 Marburg strain27), *E. coli* O157 : H7 ATCC 33150, *Kluyveromyces marxianus, L. monocytogenes* ATCC 689426, *P. fluorescence, Salmonella typhimurium* H 3380 phage type DT 104, *Serratia liquefasciens* and *S. aureus* ATCC 13566.
[49]	122 variant peptides of 2 starting sequences: Bac2A and Indolicidin	Cellulose bifunctional resin TGS (1–6-dichloro-1-Beta-dideoxy-Beta-fructofuranos M-chloro-4-deoxy-galactopyranoside) NH2/RAM (p-[(R,S)-a-[1-(9H-fluren-9- yl)-methoxyformamido]-2,4-dimethoxybenzyl]-phenoxyacetic acid) Microtiter plate	Peptides were: (i) directly synthesized on a cellulose support using a cellulose-amino-hydroxypropyl ether linker chemistry or; (ii) directly synthesized onto a bifunctional resin or; (iii) directly bound to the microtiter plate via biotin–streptavidin interaction. • AMP orientation was controlled • No spacers	*Mini-Tn5-luxfliC::lux CDABE strain H1001 of P. aeruginosa PAO1, S. aureus ATCC 25923, C. albicans (lab isolate).*
[50]	Tet-213	Poly (N,N-dimethyacrylamide) (PDMA) brush coated Ti	Synthesis of peptide immobilized polymer layers involves i) surface immobilization of atom transfer radical polymerization (ATRP) initiator, ii) ATRP of DMA and APMA from the surface, and iii) maleimide functionalization of copolymer brushes followed by peptide conjugation • AMP orientation controlled (Cys added C-terminal) • Spacer obtained by brush strategy • Anti-biofilm assessment • *In vitro* cytotoxicity testing (MG-63 Osteoblast-like cells) • In vivo testing (Rat)	*P. aeruginosa* PA01 expressing a luciferase gene cassette (luxCDABE)
[51]	IG-25	oligo-(ethylene glycol) (OEG) terminated silicon surfaces	CuI-catalyzed azide–alkyne cycloaddition (CuAAC) of an azide modified AMP onto oligo-(ethylene glycol) (OEG) terminated silicon surfaces • AMP orientation controlled (C-terminal azide-IG-25) • Different AMP densities tested • *In vitro* cytotoxicity testing (NIH3T3 fibroblast cells)	*P. aeruginosa* PA01

Ref.	AMP	Substrate	AMP Immobilization strategy	Microorganisms assessed
[52]	Nisin	multi-walled carbon nanotubes (MWNTs)	MWNTs were first modified with COOH groups by using concentrated H_2SO_4 and HNO_3. The modified MWNTs were grafted with PEG1000 (Mw≈1000) as a spacer via esterification reaction. MWNT–PEG was linked with nisin using hexamethylene diisocyanate as a coupling agent and dibutyltin dilaurate as a catalyst. • Anti-biofilm assessment	*E. coli* (ATCC 8739), *P. aeruginosa* (ATCC 9027), *S. aureus* (ATCC 6538) and *B. subtilis* (ATCC 6051)
[53]	SESBV and VEGF	Titanium discs	Acid-treated titanium substrates were immersed in dopamine and then incubated with the peptide solutions • AMP randomnly immobilized • No spacer • *In vitro* cytotoxicity testing (corneal fibroblasts)	*Bacillus cereus (ATCC 14579), E. coli (ATCC 35218)*
[54]	Chrysophsin-1 and cys-chrysophin-1	Silicon dioxide and gold crystals	APTS silanization followed by succinimidyl-[(N-maleimidopropionamido)-dodecaethyleneglycol] functionalization with subsequent incubation with cys-peptide • N-terminal orientation • Compared with adsorbed peptide • Assessment of peptide leaching	*E. coli HB101 (ATCC 33694)*
[55]	melimine	Glass coverslips	Maleimide-functionalized glass was then treated with crosslinker or 4-azidobenzoic acid and irradiation with UV-light (320nm) Three different orientations were investigated by adding a cysteine residue to the N-, C-terminus or at a central point (position 13) in the peptide. • No spacer included • AMP orientation studied	*S. aureus strain 38 or P. aeruginosa PAO1*
[56]	Magainin I	Titanium coupons	Catecol (3,4-Dihydroxyphenylacetic acid) titanium functionalization was followed by PEG (O,O'-bis(2-aminoethyl)poly(ethylene glycol), Mw 3000) tethering by carbodiimide chemistry, followed by AMP tethering again through carbodiimide chemistry • Anti-biofilm assessment	*L. ivanovii* Li4pVS2

Ref.	AMP	Substrate	AMP Immobilization strategy	Microorganisms assessed
[57]	IG-25	fluorous slide, or Fluoroperm 60 contact lens	The fluorous surfaces were dip-coated with fluorous-tagged oligo(ethylene) chain terminated with an alkynyl group. N-terminal azide-IG-25 was immobilized through click-chemistry. Other surface was obtained by covalent immobilization of IG-25 free amines through carbodiimide chemistry • AMP orientation was assessed (N-terminal vs random immobilization)	*P. aeruginosa* PAO1
[58]	CWR11	PDMS	Allyl Glycidyl Ether (AGE) polymer brush synthesis on PDMS slides performed by continuos plasma activation and UV treatment. Then the surface were functionalized with Maleimide-PEG-amine and finally the peptide was tethered • Random immobilization • Stability testing • Anti-biofilm testing • *In vitro* cytotoxicity testing with human red blood ceels and smooth muscle cells CC-2571	*E. coli (ATCC 8739), S. aureus (ATCC 6538) and P. aeruginosa (ATCC 9027 ; PAO1, green fluorescence protein (GFP)-expressing strain*
[59]	melimine	etafilcon A lenses	Immobilization by the free amines after activation of the COOH of the contact lenses with NHS/EDC • Random AMP orientation • Different AMP densities tested • Heat stability and hypertonic solution testing • *In vitro* cytotoxicity (murine L929 cells) • Compared against a surface with physically adsorbed AMP	*P. aeruginosa* 6294, *S. aureus* 31, *P. aeruginosa* ATCC 9027, *S. aureus* ATCC 6538, *Serratia marcescens* ATCC 13880, *C. albicans* ATCC 10231, *Fusarium solani* ATCC 36031, *Acanthamoeba castellanii* ATCC 50370, *P. aeruginosa* 31, *P. aeruginosa* 34, *P. aeruginosa* 35, *P. aeruginosa* 37, *P. aeruginosa* 142, *S. aureus* 60, *S. aureus* 61, *S. aureus*, 62 *S. aureus* 110, *S. aureus* 103.
[60]	GL13K	Commercially pure (cp) grade 2 titanium	titanium samples were silanized with CPTES and then incubated with AMP (random immobilization by AMP free amines) • compared against a non-AMP • compared with physically asorbed surface • Surface stability testing (ultrasonication in deionized water for 2 h, and after 5 and 8 days of immersion in PBS) • Anti-biofilm assessment • *In vitro* cytotoxicity testing (Human gingival fibroblasts (HGF) and MC3T3-E1 murine osteo- blasts (OB))	*Porphyromonas gingivalis* ATCC 33277

Ref.	AMP	Substrate	AMP Immobilization strategy	Microorganisms assessed
[61]	inverso- CysHHC10 (H-ckrwwkwirw-NH2, all D-enantiomer)	poly(ethylene terephthalate) surface	Pentaerythritol tetrakis(3-mercaptopropionate) (PTMP) crosslinker + poly(ethylene glycol) diacrylate (PEGDA) spacer + AMP is mixed with poly(ethylene terephthalate) surface and UV irradiated to promote a thiol-ene click • AMP orientation controlled by Cys at C-terminal • Different AMP densities tested • Surface stability and activity was assessed using different pH and plasma proteins presence	*S. aureus* (ATCC 49230), *S. epidermidis* (ATCC 35984).
[62]	hLF1-11	Commercially pure (cp) grade 2 titanium	titanium samples were silanized with either APTES or CPTES and then mixed with pre-prepared AMP : hLf1-11, + 3 units of 6-aminohexanoic acid (AHA) as a spacer and 3-mercaptopropionic acid (MPA) as the anchoring moiety (MPA-AHA-AHA-AHA-GRRRRSVQWCA-NH_2) • AMP orientation controlled (C-terminal) • Different AMP densities tested • *In vitro* Cytotoxicity (Human foreskin fibroblasts)	*Streptococcus sanguinis* (CECT 480, Colección Española de Cultivos Tipo (CECT), Spain) and *Lactobacillus salivarius* (CCUG 17826, Culture Collection University of Goteborg (CCUG), Sweden)
[63]	RK1 (RWKRWWRRKK) and RK2 (RKKRWWRRKK)	silicone surfaces	Allyl glycidyl ether (AGE) was synthesized on the surface of PDMS by plasma ultraviolet (UV) induced surface grafting polymerization. AMPs immobilization was performed via reaction between the amine or amide groups of the AMPs and the epoxy groups on the AGE-grafted surfaces. • No AMP orientation controlled • Anti-biofilm assessment • *In vitro* cytotoxicity testing (smooth muscle cells)	*E. coli* (ATCC 8739), *S. aureus* (ATCC 6538) and *C. albicans* (ATCC 10231).
[64]	Temporin-SHa (FLSGIVGMLGKLFamide), temporin-SHa-COOH (FLSGIVGMLGKLFCOOH), [$A^{2,6,9}$]temporin-SHa (FASGIAGMAGKLFamide) and [$A^{2,6,9}$]temporin-SHa-COOH (FASGIAGMAGKLFCOOH)	SAMs of Mercaptoundecanoic acid, 11-mercaptoundecylamine, 6-mercapto-1-hexanol on Gold surface	Immobilization by the free AMP amines through carbodiimide chemistry • Random immobilization and C-terminal immobilization	*L. ivanovii*

Ref.	AMP	Substrate	AMP Immobilization strategy	Microorganisms assessed
[65]	CysLasioglossin- III	commercial silicone catheter	Silicone catheter was fisrtly UV-treated with allyl glycidyl ether (AGE). AGE-functionalized catheter surfaces were then reacted with ethylene-diamine. Then the surface is further reacted with NHS–PEG12–maleimide. Finally, this surface is incubated with the AMP • C-terminal immobilization • Anti-biofilm assessment • *In vitro* cytotoxicity testing (human red blood cells and THP-1 cells)	*E. coli* (ATCC8739), *P. aeruginosa* (ATCC9027), *S. aureus* (ATCC6538) and *E. faecalis* (ATCC29212).
[66]	buforin II, LL-37, BMAP-27, protamine	Commercial preactivated reactive surfaces with epoxy, aldehyde, NHS, and PDITC functionalities (PolyAn).	AMP free amines were immobilized onto the preactivated surfaces • Release Control measurements • *In vitro* cytotoxicity testing (histiocytic lymphoma model cell line U937)	*E. coli* Dh5α
[67]	SESB2V	Ti substrates	Ti substrates were firstly incubated with dopamine solution and then with AMP solution • *In vivo* testing with a rabbit keratitis model	*S. aureus* (ATCC 29213) and *P. aeruginosa* (ATCC 9027)
[68]	Tet-213	silicon surface	CuAAC click-chemistry to the N-terminal azide OEG-Tet-213 • *In vitro* cytotoxicity testing (rat bone mesenchymal stem cells)	*S. aureus* and *E. coli*
[69]	GL13K	commercially pure Titanium Grade II	titanium samples were silanized with CPTES and then incubated with AMP • Random AMP immobilization • Proteolytic degradation assay • Drip Flow Bioreactor Culture in comparison with simple adhesion assays	*Streptococcus gordonii* ML-5
[70]	Magainin II	poly(lactide-co-glycolide) (PLGA) and PLGA/gelatin electrospun fibrous membranes.	Free AMP amine immobilized by carbodiimide chemistry • Random AMP immobilization	*E. coli* and *S. aureus*
[71]	LeucocinA	Gold substrates	N-immobilization : SAMs of 11-mercaptoundecenoic acid and 3-mercapto-1-propanol were activited with carbodiimide chemistry and finally incubated with peptide ; For C-immobilization, the gold surface were first treated with cysteamine hydrochloride and 3-mercapto-1-propanol, and peptide was immobilized by carbodiimide chemistry • Controlled immobilization (N and C-terminal)	*L. monocytogenes (ATCC 43256), L. monocytogenes (ATCC 19116, Carnobacterium divergens LV13, S. aureus (ATCC 13565), E. faecalis (ATCC 19533)*

Ref.	AMP	Substrate	AMP Immobilization strategy	Microorganisms assessed
[72]	hLF1-11	Chitosan films	Dissulfide bridge establishment between Ct- Cys residue and the N-acetylcysteine functionalized chitosan film (chitosan functionalization obtained through carbodiimide chemistry) • C-terminal immobilization • Effect of PEGylated spacer was tested	*S. aureus (ATCC 33591) (MRSA)*
[73]	Dhvar5	Chitosan films	Dissulfide bridge establishment between the introduced Cys residue at a terminal and the N-acetylcysteine functionalized chitosan film (chitosan functionalization obtained through carbodiimide chesmistry) • C- and N-terminal immobilization • Effect of different spacers length • Effect of different flexibilities of spacers with similar lenght	*S. aureus (ATCC 33591) (MRSA)*
[74]	HHC36 (KRWWKWWRR) and RGD	titanium surfaces	Click-chemistry between AMPs with N-terminal integration of azido-PEG12-acid or azido-PEG24-acid and surface with silanization through alkynyl-PEG-triethoxysilane • Different AMP densities tested • *In vitro* cytotoxicity testing (rat bone mesenchymal stem cells)	*S. aureus, E. coli*
[75]	hLF1-11	Commercially pure (cp) grade 2 titanium	Comparison between 3 strategies : by silanization, by ATRP and APTES as an initiator, by ATRP and BTCPS as a initiator, using the above modified AMP : MPA-AHA-AHA-AHA-GRRRRSVQWCA-NH_2 • AMP orientation controlled (C-terminal) • Surface stability testing (ultrasonication for 2h in PBS) • Anti-biofilm assessment • *In vitro* cytotoxicity testing (Human foreskin fibroblasts)	*S. sanguinis* and *L. salivarius*
[76]	hLF1-11	Commercially pure (cp) grade 2 titanium	Comparison between different strategies : silanization – CPTES followed by meleimide crosslinker and peptide ;-APTES followed by DMA-APMA copolymer followed by iodoacetyl crosslinker and peptide ;-BPTCS followed by by DMA-APMA copolymer followed by iodoacetyl crosslinker and peptide • Controlled orientation • In vitro cytotoxicity human foreskin fibroblasts • Antibiofilm testing (comparison between single-species and multispecies biofilm)	*S. sanguinis* and *L. salivarius*

In the current chapter, an overview of the AMP surface covalent immobilization strategies known at the time this thesis was started is discussed (see published review at Appendix I). Studies published after 2011 were included at the blue zone of Table 3 and are discussed within subsequent chapters.

As summarized in Table 3, the various studies regarding immobilized AMPs differ in important aspects, including the immobilization method applied, the peptide sequence, mode of action of the AMPs used, and the bacteria tested. These experimental variations make it difficult to achieve a straightforward comparison. Nevertheless, important lessons can be derived from these diverse studies.

In 1995, Haynie *et al.* [31] demonstrated that some AMPs (natural occurring magainin 2 and several idealized synthetic amphipathic peptides) immobilized onto a polyamide resin (pepsin K) retained lethal activity against several Gram-positive and Gram-negative bacteria. As already mentioned, these results demonstrated that the interaction of magainin with the outer membrane of the bacteria is sufficient for their lethal activity, since the potential peptide penetration depth is very low due to the short spacer (short 2 or 6 carbon chain linkers) used.

Willcox *et al.* [32] compared the antimicrobial activity of the synthetic peptide melimine that was adsorbed or covalently immobilized onto commercial contact lenses (Etafilcon A). Covalent immobilization was performed directly through the free peptide amines (the N-terminal amino acid or the lysine side chain) without a specific control on the orientation of the peptide onto the surface. An apparent increase in efficacy was observed when the peptide was covalently attached to the surface, which was ascribed to a possibly higher relative surface availability of the peptide, in contrast to the adsorption process where peptide aggregation could produce uneven peptide distribution.

The effect of α-helix secondary structure of immobilized AMP was also studied by Haynie *et al*. [31]. They demonstrated that only those immobilized peptides still retaining their ability to form amphipathic α-helices had antibacterial activity. Likewise, in the work of Cho *et al.* [16], the secondary β-sheet structure was essential for antibacterial activity. Thus, these studies indicate that the biocidal activity of immobilized AMPs is dependent on the presence of a well-established secondary structure.

Other important activity-modulating parameters include the length, flexibility and kind of spacer between the active sequences and the solid matrices [31, 42, 43], the AMP surface density [42, 44, 45], and orientation after immobilization [31, 32, 42-48]. These parameters are discussed below.

3.2.1 Solid supports and chemical coupling strategies

A wide variety of solid supports has been assessed for production of surfaces with immobilized AMPs, including polymeric brushes and resins [16, 31, 42, 44, 47-49], metal (e.g. silanized titanium) [43], glass coverslips [46], model surfaces (e.g. self-assembled monolayers) [45], microtitre plates [49] and even commercial contact lenses [32].

As shown in Table 3, the chemical strategies behind covalent immobilization of peptides differ depending on the sequence, orientation and position of the specific AMP, the presence/absence of a spacer, or the spacer properties such as length and flexibility.

Peptide immobilization may be carried out in a relatively random manner, e.g. through formation of amide bonds between amine groups from the pre-synthesized peptide and surface carboxyls (or the other way around, i.e. carboxyls from the peptide reacting with surface amines), as in Refs. [16, 25, 32] (Table 3). Alternatively, peptide immobilization can be controlled through peptide construction (or immobilization) on the surface by chemo-selective formation of a peptide–surface covalent bond, enabling tethering in a predictable and defined fashion.

Controlled immobilization is obviously preferred over random tethering, as the former can be designed (i) to maintain peptide structural motifs known to be relevant for activity, and (ii) to allow exposure and flexibility that more closely mimic the behaviour of soluble AMPs. Uncontrolled immobilization can be especially detrimental when involving peptide amine groups, as these amine groups are normally provided by lysines which are key amino acids in the majority of cationic amphipathic AMPs [2, 77-79].

The best way to control orientation of immobilized peptides is to synthesize them directly onto the solid support (e.g. polyamide resins, PEG-modified polystyrene

resins, cellulose), as done in Refs. [77, 80, 81] (Table 3). To this end, standard solid-phase peptide synthesis (SPPS) methods may be used, such as the well-established Fmoc/tBu strategy [82]. In this strategy selectively protected amino acids are incorporated stepwise into the growing peptide chain that is built from its C- to its N-terminal residue. Once the peptide sequence is assembled, convenient treatment to cleave off the amino acid side-chain-protecting groups is performed.

An alternative to building the peptide directly onto the surface is to pre-synthesize a peptide chain with a specific building block incorporated in a selected position. This peptide chain can subsequently be chemoselectively attached to an adequately functionalized surface. The most common approaches involve incorporation of an additional cysteine into the peptide chain (e.g. [44]) or exploiting a cysteine already available in the native sequence (if not crucial for AMP activity), taking advantage of chemical reactions specific to the thiol group. These reactions may include, as depicted in Figure 5, (i) disulfide bond formation between peptide and surface thiols, as well as specific reactions of the peptide Cys thiol with (ii) surface-bound maleimide groups [43, 44], or (iii) surface-bound epoxides (though these are generally reactive towards any nucleophiles, including lysine amines, and hence are not truly chemoselective).

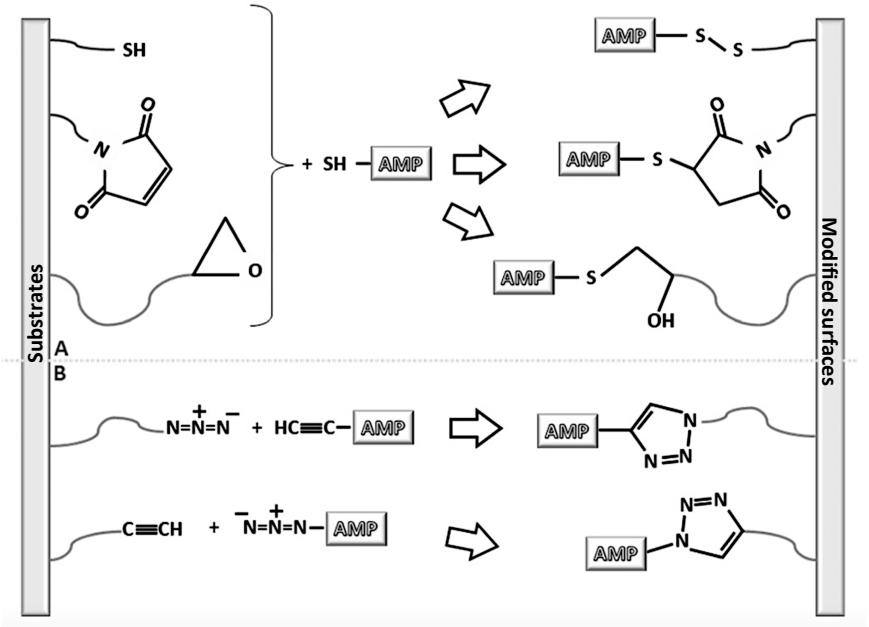

Figure 5. Examples of chemical strategies for controlled covalent attachment of AMPs on surfaces: (A) use of thiol-bearing peptides (Cys usually as thiol donor) for covalent immobilization onto thiol-, maleimide- or epoxide-modified surfaces; (B) use of the Huisgen 1,3-dipolar cycloaddition for immobilization of either alkyne-bearing peptides onto azide-modified surfaces or azide-bearing peptides onto alkyne-modified surfaces [33].

Other chemoselective approaches not involving Cys or other thiol donors have been proposed more recently, namely those involving Huisgen 1,3-dipolar cycloadditions, the so-called click-reactions [83]. Here, the peptide can bear an additional azide (e.g. from incorporation of 6-azidohexanoic acid) or an alkyne donor (e.g. from incorporation of propynoic acid) to be ‘‘clicked on’’ surface-bound alkyne or azide groups, respectively.

Both epoxide and click-based approaches have been used to immobilize peptides and proteins onto surfaces (e.g. [84-86]), but examples of their application to AMP tethering are still scarce.

Irrespective of alternatives available for peptide tethering onto surfaces, careful comparative investigation of different strategies must be carried out, in which the influence of peptide-surface spacers, coupling chemistries and support materials on antimicrobial activity should be thoroughly analyzed. Only Hilpert *et al*. [49] have assessed the effect of different support materials on the antimicrobial activity, and

found that, at least for their specific systems, the supports did not affect the activity of the tested peptides.

3.2.2 Influence of the spacer

Although some studies demonstrated that immobilized AMPs have antimicrobial activity without incorporation of a spacer [32, 45, 46, 49], most protocols presented a spacer attachment step [16, 31, 42-44, 47, 48], particularly with a PEG spacer with a Molecular weight (Mw) ranging from 3000 to 5400 [16, 42, 43, 47, 48]. The utilization of PEG as a spacer presents several advantages. This polymer can create non-adhesive surfaces due to its non-fouling characteristics, thus preventing non-specific peptide binding to the surface and shielding the peptides from the hydrophobic nature of a particular biomaterial [16, 47]. Studies comparing AMP immobilization with and without PEGylated spacers demonstrated that some immobilized AMPs are only bactericidal when a PEGylated spacer was used [16, 42, 43, 47]. For example, Gabriel *et al.* [87] demonstrated that the LL37 peptide bound to titanium through a PEGylated spacer was capable of killing *E. coli* on contact. In marked contrast, LL37 peptide attached directly to the titanium surface displayed no antibacterial activity. The authors suggest that the use of a long, flexible PEG spacer provided a parallel peptide orientation and lateral mobility that were required for bactericidal activity. Bagheri *et al.* [42] also analyzed the influence of PEGylated spacer length (3000, 400 and 200 Da) on bactericidal activity of an amphipathic model KLAL peptide and magainin-derived MK5E. They demonstrated that the antimicrobial activity of these peptides distinctly decreased with reduction in the spacer length, suggesting that the increased flexibility associated with longer spacers maximizes the antimicrobial activity of immobilized peptides [69].

However, these results contradict those of Haynie *et al.* [31] whose experiments indicated no difference in bactericidal activity whether peptides were conjugated to the support with a two-carbon or a six-carbon chain linker [31]. In addition, Hilpert *et al.* [49] reported that short 9-mers covalently linked without spacer have bactericidal activity. They suggested an electrostatic interference and destabilization rather than a penetrating mechanism.

Comparison of these studies is difficult, since AMPs, support materials, coupling chemistry and peptide orientations differ from study to study. However, one can speculate that the requirement for a spacer is directly associated with the mode of action of the specific AMP.

3.2.3 Peptide concentration

Peptide surface concentration depends on the immobilization strategy used, as limited accessibility of the peptide reactive groups and different coupling procedures can affect the efficiency of peptide immobilization. Most studies indicate that peptide concentrations, albeit important, do not appear to be the most critical parameter for antimicrobial activity [42, 43, 46, 88]. Gabriel *et al.* [43] observed that the bactericidal activity of LL37 immobilized onto titanium surfaces was independent of the peptide concentration. Glinel *et al.* [44] demonstrated that the biocidal activity of magainin I was not substantially reduced as the concentration of immobilized peptide was reduced. Bagheri *et al.* [42] reported a study aimed to determine the effect on bactericidal activity of different surface peptide densities and spacer lengths. These studies demonstrated that an increase in the loading capacity of the resin was not sufficient to compensate for the decrease in activity due to reduction of the spacer length. Based on these observations, they concluded that spacer length has a more profound impact on activity than peptide concentration. Further, the maximum peptide loading concentration was obtained with the C-terminal coupling strategy, which correlated with higher Minimal Inhibitory Concentration (MICs), suggesting that immobilization orientation can compensate for low peptide loading [42].

Despite these reports, which strongly support the concept that peptide surface loading levels are not a key factor in the antimicrobial activity of immobilized AMP, other studies have provided evidence that the effects of peptide surface concentration cannot be disregarded. For instance, Chen *et al.* [46] evaluated the effect of melimine concentration after immobilization by two different bifunctional azides (4-fluoro-3-nitrophenyl azide and 4-azidobenzoic acid) as crosslinking reagents. In this study, the higher concentration of the peptide via 4-azidobenzoic acid immobilization correlated with a more profound antibacterial activity. Humblot

et al. [45] correlated low peptide concentrations with bacteriostatic rather than bacteriocidal effect of immobilized magainin I, explaining that the low peptide concentration precludes the possibility of multiple peptide entries into the cell membrane. In addition, Hilpert *et al.* [49] studied the effect of immobilized peptide density on antimicrobial activity by utilizing different concentrations of biotinylated peptide solutions with streptavidin-coated plates. Antimicrobial activity was clearly concentration dependent, decreasing sigmoidally as a function of decreasing peptide concentration.

3.2.4 Peptide orientation after immobilization

Different strategies for surface binding of peptides have been conducted on different chain positions, such as C-terminal, N-terminal and/or N-side-chain peptide attachment. As a result, different peptide orientations and flexibility were obtained, which could be correlated with differential antimicrobial activities. The chain position was determined based upon (i) previous knowledge of peptide robustness to changes in given positions, i.e. on its ability to retain or lose antimicrobial activity upon deletion of N-terminal or C-terminal amino acids or amino acid segments; (ii) the availability of functional groups suitable for a particular coupling chemistry; or (iii) the promotion of parallel alignment of peptide chains [16, 31, 43, 45]. The studies of Gabriel *et al.* [43] and Steven *et al.* [47] compared the antimicrobial efficiency of N-terminally and N-side-chain immobilized peptides. They performed site-specific activation and coupling by blocking the undesired functional groups. Even though the experimental AMPs were different in the respective studies, only N-terminally attached peptides displayed antimicrobial activity. Gabriel *et al.* [43] concluded that only N-terminal conjugation allowed the appropriate parallel orientation of the peptide helices, which is required for interaction among the peptide molecules and between the peptides and the lipid double layer during membrane pore formation. These results are supported by the reported key role of basic lysine side-chains (and of those from other basic amino acids, as arginine or histidine) in the bioactivity of cationic AMP [2, 77-79], which could explain the deleterious effect of AMP immobilization through Lys ε-amino groups towards

antimicrobial activity. The possibility of C-terminal peptide immobilization should be considered as this orientation may achieve similar specific activity as N-terminal conjugation. Bagheri *et al.* [42] compared the activity profile of C-terminal, N-terminal and N-side-chain immobilized AMP sequences. Slightly different results were obtained depending on the specific peptide sequence and bacteria tested. C-terminally attached AMPs displayed higher MICs, compared to N-terminal and N-side-chain immobilization. The N-immobilization orientations presented similar results, suggesting that the blockage of the cationic Lys side chains was of minor importance to the overall antimicrobial activity. However, it is possible that the observed reactivity pattern may be specific to the systems used by these authors, where the AMP orientation appeared to be less relevant when peptides were immobilized using long and flexible spacers [42]. Hilpert *et al.* [49] used a different strategy to screen the efficiency of immobilized AMPs. They rearranged the sequence of a known active peptide and C-terminally immobilized the different variants. They concluded that the placement of cationic residues close to the linker site correlated with increased antimicrobial activity as compared with peptides with cationic residues localized to the N-terminus or within the middle portion of the peptide. The positioning of hydrophobic residues proximal to the N-terminus was critical to the activity of their immobilized AMPs.

3.2.5. Activity efficiency of immobilized AMPs

Only a few studies have described an experimental comparison of soluble and immobilized AMPs [16, 31, 42, 49]. However, a straightforward comparison between MICs of soluble and immobilized AMPs is very difficult because precise quantification of immobilized AMP can be problematic. In most cases the immobilized AMPs displayed an increase in their MIC value compared to the soluble peptide. In studies by Haynie *et al.* [31] the immobilized AMPs presented a 50-fold higher MIC compared to soluble peptides. These investigators suggested that the coupling chemistry may have resulted in more covalently bound peptide in the resin interior than on the surface, which could explain the higher concentration needed for activity. Cho *et al.* [16] found an extensive variation range in the observed MIC

values which were augmented 8- or 64-fold depending on the bacteria evaluated (*E. coli*, *Micrococcus luteus* and *S. aureus* more sensitive; *P. aeruginosa* less susceptible). In the Bagheri *et al.* [42] studies, the active concentrations increased about 100-fold from the micromolar MICs of the soluble peptides to the milimolar range of the immobilized-AMPs. All these studies reported MIC increases that varied with peptide and bacteria specificity.

However, Hilpert *et al.* [49] compared soluble MICs and inhibition of luminescence by immobilized AMPs. No correlation of antimicrobial activity was observed between soluble and immobilized AMPs, as inactive soluble AMPs presented activity when immobilized, and some active soluble AMPs lost activity when immobilized.

3.2.6 Cytotoxicity

KLAL and MK5E are examples of immobilized AMPs for which haemolytic activity has been assessed. The KLAL- and MK5E-soluble haemolytic concentrations (EC25) were at least 16-fold higher than the respective MIC. Moreover, the haemolytic activity levels of the immobilized-peptide beads and the bare beads were indistinguishable from each other. This observation leads to the conclusion that both immobilized peptides at their MICs are inactive toward red blood cells [42]. Hilpert *et al.* [49] assessed cytotoxicity of a battery of immobilized peptides through human red blood cell haemolysis. They reported that the immobilization of AMPs had a reduced haemolytic activity when compared with the soluble counterpart. Thus, these initial studies indicate that peptide immobilization does not enhance the haemolytic properties of the peptides, and may actually reduce potential haemolysis when compared to soluble peptides.

3.2.7 Long-term stability

In order to check the activity persistence of immobilized peptides, investigators have subjected the modified surfaces to various harsh procedures, such as washing operations, heat treatments, pH variations and long-term activity assessment [31, 32, 45, 48]. In the washing influence study, two different AMP-modified resin beads were extensively washed without loss of antimicrobial activity [31, 48]. The heat

stability experiment was conducted to evaluate whether exposure of AMP to autoclaving (121 °C for 20 min) or to a dry oven (200 °C for 30 min) would alter the ability of the peptide to inhibit bacterial growth. The bactericidal efficacy of the heat-treated 6K8L was maintained under both heating conditions [48]. In addition, the antimicrobial efficacy of melimine was maintained during autoclaving [32]. Cole *et al.* [89] verified that the levels of melimine in lenses after removal, cleaning and sterilization did not differ from those determined before 24 h of use. The effect of pH on the modified surface was assessed. The peptide 6K8L immobilized on PEG-poly(styrene) resin beads retained its antimicrobial activity over a pH range of 3.5–7 in citrate buffer, although bacterial killing was significantly greater at pH 3.5 than at pH 7 [48], possibly due to the higher positive charge at the lower pH. Humblot *et al.* [45] assayed the stability of antimicrobial activity of immobilized peptide at various times over a 6-month period. Samples were cleaned, dried and stored at 4 °C, between each antibacterial activity assay. The results showed that the peptide remained active over the 6-month period, even though the activity of the immobilized peptide was reduced at the 6-month time point.

All these studies, although limited, point to remarkably high long-term stability and resistance of immobilized AMP to environmental conditions.

[1] Brooks BD, Brooks AE. Therapeutic strategies to combat antibiotic resistance. Advanced drug delivery reviews. 2014;78:14-27.

[2] Gordon YJ, Romanowski EG, McDermott AM. A review of antimicrobial peptides and their therapeutic potential as anti-infective drugs. Current eye research. 2005;30:505-15.

[3] Perron GG, Zasloff M, Bell G. Experimental evolution of resistance to an antimicrobial peptide. Proceedings Biological sciences / The Royal Society. 2006;273:251-6.

[4] Reddy KV, Yedery RD, Aranha C. Antimicrobial peptides: premises and promises. International journal of antimicrobial agents. 2004;24:536-47.

[5] van't Hof W, Veerman EC, Helmerhorst EJ, Amerongen AV. Antimicrobial peptides: properties and applicability. Biological chemistry. 2001;382:597-619.

[6] Wang G, Mishra B, Lau K, Lushnikova T, Golla R, Wang X. Antimicrobial peptides in 2014. Pharmaceuticals. 2015;8:123-50.

[7] Jenssen H, Hamill P, Hancock RE. Peptide antimicrobial agents. Clinical microbiology reviews. 2006;19:491-511.

[8] Afacan NJ, Yeung AT, Pena OM, Hancock RE. Therapeutic potential of host defense peptides in antibiotic-resistant infections. Current pharmaceutical design. 2012;18:807-19.

[9] Zhang L, Parente J, Harris SM, Woods DE, Hancock RE, Falla TJ. Antimicrobial peptide therapeutics for cystic fibrosis. Antimicrobial agents and chemotherapy. 2005;49:2921-7.

[10] Steinberg DA, Hurst MA, Fujii CA, Kung AH, Ho JF, Cheng FC, *et al*. Protegrin-1: a broad-spectrum, rapidly microbicidal peptide with *in vivo* activity. Antimicrobial agents and chemotherapy. 1997;41:1738-42.

[11] Wimley WC, Hristova K. Antimicrobial peptides: successes, challenges and unanswered questions. The Journal of membrane biology. 2011;239:27-34.

[12] Zasloff M. Antimicrobial peptides of multicellular organisms. Nature. 2002;415:389-95.

[13] Brogden KA. Antimicrobial peptides: pore formers or metabolic inhibitors in bacteria? Nature reviews Microbiology. 2005;3:238-50.

[14] Lopez-Abarrategui C, Figueroa-Espi V, Reyes-Acosta O, Reguera E, Otero-Gonzalez AJ. Magnetic nanoparticles: new players in antimicrobial peptide therapeutics. Current protein & peptide science. 2013;14:595-606.

[15] Hancock RE. Peptide antibiotics. Lancet. 1997;349:418-22.

[16] Cho WM, Joshi BP, Cho H, Lee KH. Design and synthesis of novel antibacterial peptide-resin conjugates. Bioorganic & medicinal chemistry letters. 2007;17:5772-6.

[17] Li M, Cha DJ, Lai Y, Villaruz AE, Sturdevant DE, Otto M. The antimicrobial peptide-sensing system aps of *Staphylococcus aureus*. Molecular microbiology. 2007;66:1136-47.

[18] Li M, Lai Y, Villaruz AE, Cha DJ, Sturdevant DE, Otto M. Gram-positive three-component antimicrobial peptide-sensing system. Proceedings of the National Academy of Sciences of the United States of America. 2007;104:9469-74.

[19] Otto M. Bacterial sensing of antimicrobial peptides. Contributions to microbiology. 2009;16:136-49.

[20] Peschel A, Collins LV. Staphylococcal resistance to antimicrobial peptides of mammalian and bacterial origin. Peptides. 2001;22:1651-9.

[21] Peschel A, Jack RW, Otto M, Collins LV, Staubitz P, Nicholson G, *et al. Staphylococcus aureus* resistance to human defensins and evasion of neutrophil killing via the novel virulence factor MprF is based on modification of membrane lipids with l-lysine. The Journal of experimental medicine. 2001;193:1067-76.

[22] Cao M, Helmann JD. The Bacillus subtilis extracytoplasmic-function sigmaX factor regulates modification of the cell envelope and resistance to cationic antimicrobial peptides. Journal of bacteriology. 2004;186:1136-46.

[23] Clarke SR, Foster SJ. IsdA protects *Staphylococcus aureus* against the bactericidal protease activity of apolactoferrin. Infection and immunity. 2008;76:1518-26.

[24] Vuong C, Voyich JM, Fischer ER, Braughton KR, Whitney AR, DeLeo FR, et al. Polysaccharide intercellular adhesin (PIA) protects Staphylococcus epidermidis against major components of the human innate immune system. Cellular microbiology. 2004;6:269-75.

[25] Statz AR, Park JP, Chongsiriwatana NP, Barron AE, Messersmith PB. Surface-immobilised antimicrobial peptoids. Biofouling. 2008;24:439-48.

[26] Cherkasov A, Hilpert K, Jenssen H, Fjell CD, Waldbrook M, Mullaly SC, *et al.* Use of artificial intelligence in the design of small peptide antibiotics effective against a broad spectrum of highly antibiotic-resistant superbugs. ACS chemical biology. 2009;4:65-74.

[27] Monteiro C, Pinheiro M, Fernandes M, Maia S, Seabra CL, Ferreira-da-Silva F, *et al.* A 17-mer Membrane-Active MSI-78 Derivative with Improved Selectivity toward Bacterial Cells. Molecular pharmaceutics. 2015.

[28] Monteiro C, Fernandes M, Pinheiro M, Maia S, Seabra CL, Ferreira-da-Silva F, *et al.* Antimicrobial properties of membrane-active dodecapeptides derived from MSI-78. Biochimica et biophysica acta. 2015;1848:1139-46.

[29] Kang SJ, Park SJ, Mishig-Ochir T, Lee BJ. Antimicrobial peptides: therapeutic potentials. Expert review of anti-infective therapy. 2014;12:1477-86.

[30] Espitia PJP, Soares NDF, Coimbra JSD, de Andrade NJ, Cruz RS, Medeiros EAA. Bioactive Peptides: Synthesis, Properties, and Applications in the Packaging and Preservation of Food. Comprehensive Reviews in Food Science and Food Safety. 2012;11:187-204.

[31] Haynie SL, Crum GA, Doele BA. Antimicrobial activities of amphiphilic peptides covalently bonded to a water-insoluble resin. Antimicrobial agents and chemotherapy. 1995;39:301-7.

[32] Willcox MD, Hume EB, Aliwarga Y, Kumar N, Cole N. A novel cationic-peptide coating for the prevention of microbial colonization on contact lenses. Journal of applied microbiology. 2008;105:1817-25.

[33] Costa F, Carvalho IF, Montelaro RC, Gomes P, Martins MC. Covalent immobilization of antimicrobial peptides (AMPs) onto biomaterial surfaces. Acta biomaterialia. 2011;7:1431-40.

[34] Bower CK, Parker JE, Higgins AZ, Oest ME, Wilson JT, Valentine BA, *et al.* Protein antimicrobial barriers to bacterial adhesion: *in vitro* and *in vivo* evaluation of nisin-treated implantable materials. Colloid Surface B. 2002;25:81-90.

[35] Gopinath D, Kumar MS, Selvaraj D, Jayakumar R. Pexiganan-incorporated collagen matrices for infected wound-healing processes in rat. Journal of Biomedical Materials Research Part A. 2005;73A:320-31.

[36] Ariga K, Hill JP, Ji Q. Layer-by-layer assembly as a versatile bottom-up nanofabrication technique for exploratory research and realistic application. Physical chemistry chemical physics. 2007;9:2319-40.

[37] Etienne O, Picart C, Taddei C, Haikel Y, Dimarcq JL, Schaaf P, *et al.* Multilayer polyelectrolyte films functionalized by insertion of defensin: a new approach to protection of implants from bacterial colonization. Antimicrobial agents and chemotherapy. 2004;48:3662-9.

[38] Alves D, Olivia Pereira M. Mini-review: Antimicrobial peptides and enzymes as promising candidates to functionalize biomaterial surfaces. Biofouling. 2014;30:483-99.

[39] Guyomard A, De E, Jouenne T, Malandain JJ, Muller G, Glinel K. Incorporation of a hydrophobic antibacterial peptide into amphiphilic polyelectrolyte multilayers: A

bioinspired approach to prepare biocidal thin coatings. Advanced Functional Materials. 2008;18:758-65.

[40] Shukla A, Fleming KE, Chuang HF, Chau TM, Loose CR, Stephanopoulos GN, *et al*. Controlling the release of peptide antimicrobial agents from surfaces. Biomaterials. 2010;31:2348-57.

[41] Faber C, Stallmann HP, Lyaruu DM, Joosten U, von Eiff C, van Nieuw Amerongen A, *et al*. Comparable efficacies of the antimicrobial peptide human lactoferrin 1-11 and gentamicin in a chronic methicillin-resistant *Staphylococcus aureus* osteomyelitis model. Antimicrobial agents and chemotherapy. 2005;49:2438-44.

[42] Bagheri M, Beyermann M, Dathe M. Immobilization reduces the activity of surface-bound cationic antimicrobial peptides with no influence upon the activity spectrum. Antimicrobial agents and chemotherapy. 2009;53:1132-41.

[43] Gabriel M, Nazmi K, Veerman EC, Nieuw Amerongen AV, Zentner A. Preparation of LL-37-grafted titanium surfaces with bactericidal activity. Bioconjugate Chemistry. 2006;17:548-50.

[44] Glinel K, Jonas AM, Jouenne T, Leprince J, Galas L, Huck WT. Antibacterial and antifouling polymer brushes incorporating antimicrobial peptide. Bioconjugate Chemistry. 2009;20:71-7.

[45] Humblot V, Yala JF, Thebault P, Boukerma K, Hequet A, Berjeaud JM, *et al.* The antibacterial activity of Magainin I immobilized onto mixed thiols Self-Assembled Monolayers. Biomaterials. 2009;30:3503-12.

[46] Chen R, Cole N, Willcox MD, Park J, Rasul R, Carter E, *et al*. Synthesis, characterization and *in vitro* activity of a surface-attached antimicrobial cationic peptide. Biofouling. 2009;25:517-24.

[47] Steven MD, Hotchkiss JH. Covalent Immobilization of an Antimicrobial Peptide on Poly(ethylene) FilmJournal of Applied Polymer Science. 2008;110:2665-70.

[48] Appendini P, Hotchkiss JH. Surface modification of poly(styrene) by the attachment of an antimicrobial peptide. Journal of Applied Polymer Science. 2001;81:609-16.

[49] Hilpert K, Elliott M, Jenssen H, Kindrachuk J, Fjell CD, Korner J, *et al.* Screening and Characterization of Surface-Tethered Cationic Peptides for Antimicrobial Activity. Chemistry & Biology. 2009;16:58-69.

[50] Gao G, Lange D, Hilpert K, Kindrachuk J, Zou Y, Cheng JT, *et al*. The biocompatibility and biofilm resistance of implant coatings based on hydrophilic polymer brushes conjugated with antimicrobial peptides. Biomaterials. 2011;32:3899-909.

[51] Li Y, Santos CM, Kumar A, Zhao M, Lopez AI, Qin G, *et al.* "Click" immobilization on alkylated silicon substrates: model for the study of surface bound antimicrobial peptides. Chemistry. 2011;17:2656-65.

[52] Qi X, Poernomo G, Wang K, Chen Y, Chan-Park MB, Xu R, *et al.* Covalent immobilization of nisin on multi-walled carbon nanotubes: superior antimicrobial and anti-biofilm properties. Nanoscale. 2011;3:1874-80.

[53] Tan XW, Lakshminarayanan R, Liu SP, Goh E, Tan D, Beuerman RW, *et al.* Dual functionalization of titanium with vascular endothelial growth factor and beta-defensin analog for potential application in keratoprosthesis. Journal of Biomedical Materials Research Part B: Applied Biomaterials. 2012;100:2090-100.

[54] Ivanov IE, Morrison AE, Cobb JE, Fahey CA, Camesano TA. Creating antibacterial surfaces with the peptide chrysophsin-1. ACS applied materials & interfaces. 2012;4:5891-7.

[55] Chen RX, Willcox MDP, Cole N, Ho KKK, Rasul R, Denman JA, *et al.* Characterization of chemoselective surface attachment of the cationic peptide melimine and its effects on antimicrobial activity. Acta biomaterialia. 2012;8:4371-9.

[56] Peyre J, Humblot V, Methivier C, Berjeaud JM, Pradier CM. Co-grafting of amino-poly(ethylene glycol) and Magainin I on a TiO2 surface: tests of antifouling and antibacterial activities. The journal of physical chemistry B. 2012;116:13839-47.

[57] Santos CM, Kumar A, Kolar SS, Contreras-Caceres R, McDermott A, Cai C. Immobilization of antimicrobial peptide IG-25 onto fluoropolymers via fluorous interactions and click chemistry. ACS applied materials & interfaces. 2013;5:12789-93.

[58] Lim K, Chua RR, Saravanan R, Basu A, Mishra B, Tambyah PA, *et al.* Immobilization studies of an engineered arginine-tryptophan-rich peptide on a silicone surface with antimicrobial and antibiofilm activity. ACS applied materials & interfaces. 2013;5:6412-22.

[59] Dutta D, Cole N, Kumar N, Willcox MD. Broad spectrum antimicrobial activity of melimine covalently bound to contact lenses. Investigative ophthalmology & visual science. 2013;54:175-82.

[60] Holmberg KV, Abdolhosseini M, Li Y, Chen X, Gorr SU, Aparicio C. Bio-inspired stable antimicrobial peptide coatings for dental applications. Acta biomaterialia. 2013;9:8224-31.

[61] Cleophas RT, Sjollema J, Busscher HJ, Kruijtzer JA, Liskamp RM. Characterization and activity of an immobilized antimicrobial peptide containing bactericidal PEG-hydrogel. Biomacromolecules. 2014;15:3390-5.

[62] Godoy-Gallardo M, Mas-Moruno C, Fernandez-Calderon MC, Perez-Giraldo C, Manero JM, Albericio F, *et al.* Covalent immobilization of hLf1-11 peptide on a titanium surface reduces bacterial adhesion and biofilm formation. Acta biomaterialia. 2014;10:3522-34.

[63] Li X, Li P, Saravanan R, Basu A, Mishra B, Lim SH, *et al.* Antimicrobial functionalization of silicone surfaces with engineered short peptides having broad spectrum antimicrobial and salt-resistant properties. Acta biomaterialia. 2014;10:258-66.

[64] Lombana A, Raja Z, Casale S, Pradier CM, Foulon T, Ladram A, *et al.* Temporin-SHa peptides grafted on gold surfaces display antibacterial activity. Journal of peptide science: an official publication of the European Peptide Society. 2014;20:563-9.

[65] Mishra B, Basu A., Yuan Chua R.R., Saravanan R., Tambyah P.A., Ho B., Chang M.W., Jan Leong S.S. Site specific immobilization of a potent antimicrobial peptide onto silicone catheters: evaluation against urinary tract infection pathogens. Journal of Materials Chemistry B. 2014:1706-16.

[66] Rapsch K, Bier FF, Tadros M, von Nickisch-Rosenegk M. Identification of antimicrobial peptides and immobilization strategy suitable for a covalent surface coating with biocompatible properties. Bioconjugate Chemistry. 2014;25:308-19.

[67] Tan XW, Goh TW, Saraswathi P, Nyein CL, Setiawan M, Riau A, *et al.* Effectiveness of antimicrobial peptide immobilization for preventing perioperative cornea implant-associated bacterial infection. Antimicrobial agents and chemotherapy. 2014;58:5229-38.

[68] Wang L, Chen J, Shi L, Shi Z, Ren L, Wang Y. The promotion of antimicrobial activity on silicon substrates using a "click" immobilized short peptide. Chemical communications. 2014;50:975-7.

[69] Chen X, Hirt H, Li Y, Gorr SU, Aparicio C. Antimicrobial GL13K peptide coatings killed and ruptured the wall of *Streptococcus gordonii* and prevented formation and growth of biofilms. PloS one. 2014;9:e111579.

[70] Yuksel E, Karakecili A. Antibacterial activity on electrospun poly(lactide-co-glycolide) based membranes via Magainin II grafting. Materials science & engineering C, Materials for biological applications. 2014;45:510-8.

[71] Etayash H, Norman L, Thundat T, Stiles M, Kaur K. Surface-conjugated antimicrobial peptide leucocin a displays high binding to pathogenic gram-positive bacteria. ACS applied materials & interfaces. 2014;6:1131-8.

[72] Costa F, Maia S, Gomes J, Gomes P, Martins MC. Characterization of hLF1-11 immobilization onto chitosan ultrathin films, and its effects on antimicrobial activity. Acta biomaterialia. 2014;10:3513-21.

[73] Costa FM, Maia SR, Gomes PA, Martins MC. Dhvar5 antimicrobial peptide (AMP) chemoselective covalent immobilization results on higher antiadherence effect than simple physical adsorption. Biomaterials. 2015;52:531-8.

[74] Lin W, Junjian, C., Chenzhi, C., Lin, S., Sa, L., Li, R., Yingjun, W. Multi-biofunctionalization of a titanium surface with a mixture of peptides to achieve excellent antimicrobial activity and biocompatibilty. Journal of Materials Chemistry B. 2015:30-3.

[75] Godoy-Gallardo M, Mas-Moruno C, Yu K, Manero JM, Gil FJ, Kizhakkedathu JN, et al. Antibacterial properties of hLf1-11 peptide onto titanium surfaces: a comparison study between silanization and surface initiated polymerization. Biomacromolecules. 2015;16:483-96.

[76] Godoy-Gallardo M, Wang Z, Shen Y, Manero JM, Gil FJ, Rodriguez D, et al. Antibacterial coatings on titanium surfaces: a comparison study between in vitro single-species and multispecies biofilm. ACS applied materials & interfaces. 2015;7:5992-6001.

[77] Andreu D, Rivas L. Animal antimicrobial peptides: an overview. Biopolymers. 1998;47:415-33.

[78] Rivas L, Luque-Ortega JR, Andreu D. Amphibian antimicrobial peptides and Protozoa: lessons from parasites. Biochimica et biophysica acta. 2009;1788:1570-81.

[79] Guani-Guerra E, Santos-Mendoza T, Lugo-Reyes SO, Teran LM. Antimicrobial peptides: general overview and clinical implications in human health and disease. Clinical immunology. 2010;135:1-11.

[80] Jansen B, Kohnen W. Prevention of biofilm formation by polymer modification. Journal of industrial microbiology. 1995;15:391-6.

[81] Cevher E, Orhan Z, Mulazimoglu L, Sensoy D, Alper M, Yildiz A, *et al.* Characterization of biodegradable chitosan microspheres containing vancomycin and treatment of experimental osteomyelitis caused by methicillin-resistant *Staphylococcus aureus* with prepared microspheres. International journal of pharmaceutics. 2006;317:127-35.

[82] Fields GB, Noble RL. Solid phase peptide synthesis utilizing 9-fluorenylmethoxycarbonyl amino acids. International Journal of Peptide and Protein Research. 1990;35:161-214.

[83] Rostovtsev VV, Green LG, Fokin VV, Sharpless KB. A stepwise huisgen cycloaddition process: copper(I)-catalyzed regioselective "ligation" of azides and terminal alkynes. Angewandte Chemie. 2002;41:2596-9.

[84] Lee MR, Shin I. Fabrication of chemical microarrays by efficient immobilization of hydrazide-linked substances on epoxide-coated glass surfaces. Angewandte Chemie. 2005;44:2881-4.

[85] Abad JM, Velez M, Santamaria C, Guisan JM, Matheus PR, Vazquez L, *et al*. Immobilization of peroxidase glycoprotein on gold electrodes modified with mixed epoxy-boronic Acid monolayers. Journal of the American Chemical Society. 2002;124:12845-53.

[86] Hudalla GA, Murphy WL. Immobilization of peptides with distinct biological activities onto stem cell culture substrates using orthogonal chemistries. Langmuir. 2010;26:6449-56.

[87] Gallardo-Moreno AM, Pacha-Olivenza MA, Saldana L, Perez-Giraldo C, Bruque JM, Vilaboa N, *et al. In vitro* biocompatibility and bacterial adhesion of physico-chemically modified Ti6Al4V surface by means of UV irradiation. Acta biomaterialia. 2009;5:181-92.

[88] Glinel K, Thebault P, Humblot V, Pradier CM, Jouenne T. Antibacterial surfaces developed from bio-inspired approaches. Acta biomaterialia. 2012;8:1670-84.

[89] Cole N, Hume EB, Vijay AK, Sankaridurg P, Kumar N, Willcox MD. *In vivo* performance of melimine as an antimicrobial coating for contact lenses in models of CLARE and CLPU. Investigative ophthalmology & visual science. 2010;51:390-5.

CHAPTER III

Chitosan film – potential implant coating?

1. Chitosan: wide family of polysaccharides

Chitosan is obtained from chitin, which is the second most abundant polysaccharide in nature after cellulose with a worldwide production of 10^{10}–10^{12} tons per year [1]. It generally comes from crustacean shells, insects, mollusks or fungi [2]. Chitosan is obtained by chitin deacetylation in the presence of alkaline agents, which originates a copolymer of glucosamine and N-acetylglucosamine units as depicted in Figure 1. The fraction of glucosamine to N-acetyl glucosamine units in the chain is referred to as the degree of deacetylation (DD) [2], which is therefore related with the number of free primary amine groups (-NH_2).

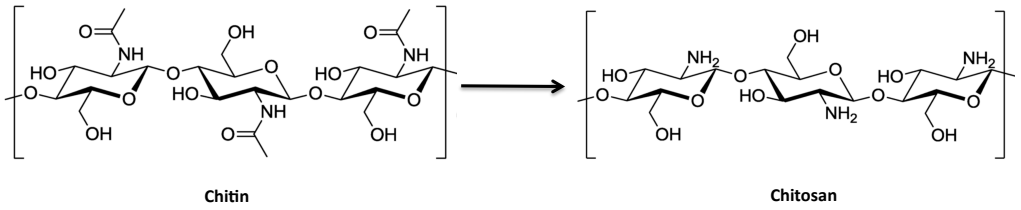

Figure 1. Chitosan derivation from chitin

The term “chitosan” does not refer to a single well-defined structure, since chitosans can differ in Mw, DD, and sequence (i.e., whether the acetylated residues are distributed along the backbone in a random or blocky manner), which directly affect the chemical and biological properties of the polymer [3].

The amine groups present in chitosan structure are responsible for its charge, reactivity and physical behaviour [4] as depicted on Figure 2.

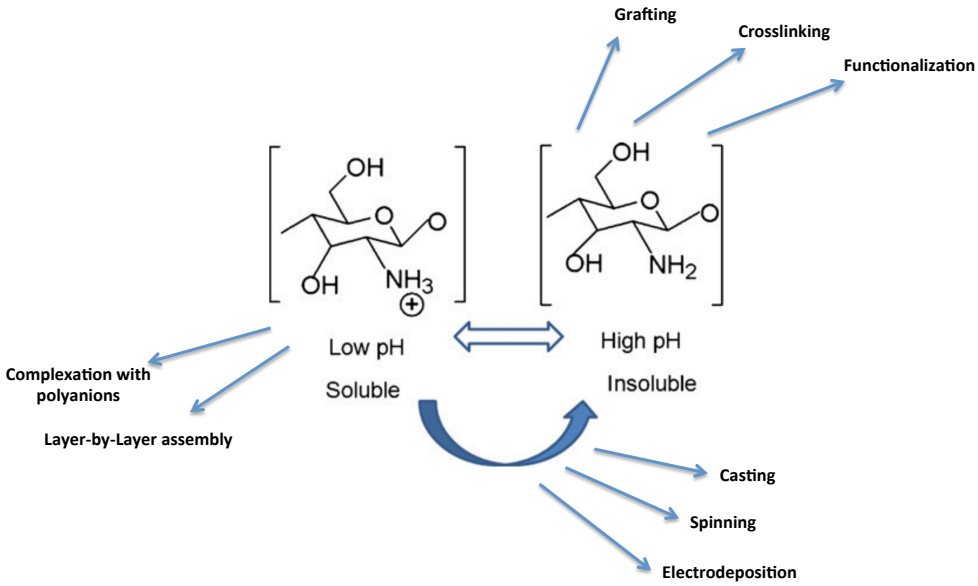

Figure 2. The soluble–insoluble transition of chitosan occurs with a pH shift at its pKa, having profound implications in its solubility and processability. Adapted from [3].

At pH below its pKa (between 6 and 6.5), these amines become positively charged allowing chitosan to be soluble under mildly acidic aqueous conditions. For pH above its pKa, chitosan becomes insoluble due to the amine deprotonation [4]. As the pKa value is highly dependent on the degree of N-deacetylation, the solubility of chitosan is dependent on the DD and the method of deacetylation used [2]. This soluble-insoluble transition allows the use of several processing techniques as summarized in Figure 2.

Although chitosan have been researched for a number of biomedical applications, including wound dressing [5], orthopaedic tissue engineering [6], drug delivery carrier [7] and haemodialysis [8], this chapter will focus on its application as a coating for orthopaedic implants, exploring its antimicrobial [9-12] and osteogenic [13-19] properties.

Chitosan films can be easily produced, due to its solubility under mildly acidic aqueous conditions, which allows for spincoating or casting [20] into membranes and films that can be converted into insoluble networks by neutralization. These films have been reported to have a broad spectrum of activity (e.g. *S. epidermidis*, *S. aureus*, *Klebsiella pneumoniae*, *P. aeruginosa* and *C. albicans*), acting also as anti-biofilm agent [9-12].

2. Chitosan films

2.1 Antimicrobial activity

2.1.1 Mechanism of action

The exact mechanism of antimicrobial action of chitosan is still imperfectly known, but different mechanisms have been proposed [21-23]. The physical state of chitosan has a huge impact in the morphology and interaction of molecules, which in turn is responsible for the antimicrobial activity. In the solid state molecules are tightly packed together, and as a result, Mw does not seem to have high impact in antimicrobial activity [24]. Compared with soluble chitosan, rather than the extending conformation with thorough contact with solution, solid chitosan (fibers, films, microspheres and nanoparticles) only touch solution through the surface. Therefore, from the literature proposed mechanisms of action, only the following could also putatively explain the antimicrobial activity of chitosan in film form. The first mechanism consists on the electrostatic interaction between chitosan positively charged amino groups and negatively charged microbial cell membranes [25]. This electrostatic interaction results in two-fold interference: i) by promoting changes in the properties of membrane wall permeability, thus provoking internal osmotic imbalances and consequently inhibiting the growth of microorganisms, and ii) by the hydrolysis of the peptidoglycans in the microorganism wall, leading to the leakage of intracellular electrolytes such as potassium ions and other low molecular weight proteinaceous constituents (e.g. proteins, nucleic acids, glucose, and lactate dehydrogenase) [23, 26, 27].

Secondly, chitosan also acts as a chelating agent (including Ni^{2+}, Zn^{2+}, Co^{2+}, Fe^{2+}, Mg^{2+} and Cu^{2+}) that selectively binds trace metals [28] and thereby inhibits the production of bacterial toxins and microbial growth [21, 22](see Figure 3).

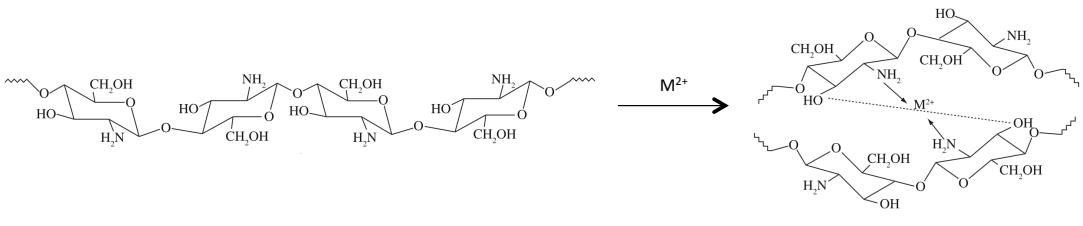

Figure 3. Metal-chitosan complexation model according to [29].

In general, chelating mechanism is more efficient at high pH, where positive ions are bounded to chitosan, since the amine groups are unprotonated and the electron pair on the amine nitrogen is available for donation to metal ions. A model proposed based on the system chitosan-Cu relates the pH dependence on the proportion of available sites for interacting in polysaccharide backbone [30]. At pH<6 the complexation involves only one amine group and three hydroxyls or H_2O molecules, while at pH>6.7 is likely to have two amines involved in the complex formation. For higher pHs, i.e., 7-9, the deprotonation of hydroxyl groups are considered to occur and the predominant complexation is ruled by two amines and two hydroxyl groups dissociated [30].

2.1.2 Parameters influencing chitosan films antimicrobial activity

There are a few parameters that may influence the antimicrobial activity of chitosan films, both intrinsic as DD and extrinsic as ionic strength, the already mentioned pH or even the fabrication procedure of chitosan films [21, 23, 24].

The most important intrinsic pre-requisite for antimicrobial activity of chitosan films is the polycationic structure. Accordingly, chitosan with higher DD shows a stronger inhibitory effect than chitosan with lower DD, meaning the higher the cationic profile, the stronger the electrostatic interactions with bacteria [31].

Regarding external factors, altering the ionic strength in a medium may disturb the inhibitory activity of chitosan, as the increase of metal ions, especially divalent ions, could attenuate the effective chelating capacity of chitosan [23, 32]. Also, aspects relating to the fabrication procedure of the chitosan films can influence its antimicrobial performance. These include existence of i) crosslinking, ii) film thickness, iii) film neutralization and iv) film sterilization.

Crosslinking effect

In order to improve the film stability it is possible to perform a crosslinking step. Indeed it has been reported that the use of a low degree of crosslinking (either by glutaraldehyde or by aglycone geniposidic acid) will not alter their antimicrobial capability [33]. On the other hand, high degrees of crosslinking may result on lower amount of free amines, i.e. cationic profile of chitosan, which may impair its antimicrobial activity.

Film thickness

Film thickness may have a huge impact on the activity. This can be related with the way the polymer chains are packed together. Thicker films have a larger number of chains that can establish a higher number of inter- and intra-molecular hydrogen bonds. The hydroxyl groups (a primary hydroxyl in C6 and a secondary hydroxyl in C3) and the highly reactive amino group in C2 are responsible for the formation of such bonds, resulting in the formation of different polymorphic forms, whose properties may vary considerably. The higher the number of amines occupied in the establishment of such bonds, the lower the positively charges available for bacterial membrane interactions [34]. Therefore, thinner films are more probable to have better antimicrobial performance.

Film neutralization

Also, film neutralization may influence the biological effect of chitosan. He *et al*., [35] reported that the use of different solutions at the neutralization step would affect surface chemistry, swelling ratio, nanotopography and mechanical properties of chitosan films. Although, the effect on the chitosan antimicrobial activity was not tested, these modifications had profound impact on the human microvascular endothelial cells behavior. Therefore, it is expected that would influence the antimicrobial behavior as well.

Film sterilization

Film sterilization procedure is another issue that can influence the antimicrobial activity of chitosan films. It has been reported that autoclaving chitosan cast film can abolish its anti-biofilm properties towards S*. epidermidis* [9]. Autoclaving the cast film results in polymer crosslinking and chain breakage, which may interfere with the antimicrobial properties of the positively charged amine groups [9]. It is also known that ethylene oxide gas sterilization induces crosslinking of the chitosan materials [36, 37]. However, the way this influences antimicrobial activity was not tested [36, 37].

2.2 Chitosan films for orthopaedic coatings

A wide number of studies have assessed chitosan suitability as an orthopaedic coating [2, 6, 15, 17, 18, 36, 38-43]. Indeed, a number of different procedures have been tested to produce such coating, namely chitosan cast onto a surface [18, 44], chitosan immobilization onto titanium through silane-glutaraldehyde chemistry [15, 17], or through dopamine linkage [42, 45], or even in combined strategies through LbL deposition with negatively charged polymers [43, 46, 47], or sol-gel deposition [41].

In fact there are a number of advantages in using chitosan as a coating for orthopedic applications, besides the aforementioned antimicrobial properties, such as i) osteoconductivity [13-15, 18], ii) wound healing stimulation for rapid fixation in bone [15] and iii) it is biodegraded in simple sugars and oligosaccharides [19].

Osteoconductivity

One essential feature of a coating for orthopaedic implants is its compatibility in allowing bone cell adhesion, spreading and proliferation resuming in osteointegration of the implant. The most important feature of chitosan related to the attachment and growth of cells is probably the cationic nature of the amine groups. Therefore degree of cell attachment has been reported to be related with the percent of deacetylation, with results indicating that cells were more readily attached to more highly deacetylated chitosans [18, 36, 48]. It has been suggested that as the level of deacetylation increases, the positive charge density of chitosan is also increased, enhancing the attraction for negatively charged cells [18]. Moreover, it was also demonstrated that the higher level of amine groups is responsible for a higher amount of protein adsorption, particularly, fibronectin a serum protein rich in RGD sequences, which in turn may explain the higher levels of cell adhesion. Other study reported that chitosan supports the initial attachment and spreading of osteoblasts preferentially over fibroblasts [44], which is particularly important to reduce the foreign body reaction.

The ability of chitosan films to support cell adhesion has also been related to film properties such as surface roughness, hydrophilicity, swelling, adhesion molecule

adsorption capacity and other factors apart from those mentioned that could be involved in the film-cell recognition [16, 47, 49, 50].

Wound healing stimulation

The enhanced wound healing and osteoconductive properties of chitosan are attributed to its structural similarity to extracellular proteoglycans such as hyaluronic acid, which electrostatically bind, protect and retain growth factors at the healing site, and guide organization and biomineralization of collagen fibers in regenerating tissues [36, 51].

Chitosan Biodegradation

The degradation of chitosan films has been reported to be associated with DD [36]. An *in vivo* study demonstrated that highly deacetylated chitosan presented the lowest degradation rate (possibly by enzymatic hydrolysis)[19]. The limited degradation of highly deacetylated forms of chitosan resulted in minor foreign-body tissue reactions in animal models, purportedly due to minimal accumulation of degradation products [17, 19].

In conclusion, chitosan gathers a number of characteristics, which are tunable in order to achieve a very promising candidate material for orthopaedic coatings.

[1] Kumar MNVR. A review of chitin and chitosan applications. Reactive and Functional Polymers. 2000;46:1-27.

[2] Dash M, Chiellini F, Ottenbrite RM, Chiellini E. Chitosan-A versatile semi-synthetic polymer in biomedical applications. Progress in Polymer Science. 2011;36:981-1014.

[3] Yi HM, Wu LQ, Bentley WE, Ghodssi R, Rubloff GW, Culver JN, *et al.* Biofabrication with chitosan. Biomacromolecules. 2005;6:2881-94.

[4] Sorlier P, Denuziere A, Viton C, Domard A. Relation between the degree of acetylation and the electrostatic properties of chitin and chitosan. Biomacromolecules. 2001;2:765-72.

[5] Azuma K, Izumi R, Osaki T, Ifuku S, Morimoto M, Saimoto H, *et al*. Chitin, chitosan, and its derivatives for wound healing: old and new materials. Journal of functional biomaterials. 2015;6:104-42.

[6] Di Martino A, Sittinger M, Risbud MV. Chitosan: a versatile biopolymer for orthopaedic tissue-engineering. Biomaterials. 2005;26:5983-90.

[7] Duttagupta DS, Jadhav VM, Kadam VJ. Chitosan: A Propitious Biopolymer for Drug Delivery. Current drug delivery. 2015.

[8] Yu JG, Yu LY, Jiang XY, Chen XQ, Tao LJ, Jiao FP. Hemodialysis membranes for acute and chronic renal insufficiency. Current neurovascular research. 2013;10:263-8.

[9] Carlson RP, Taffs R, Davison WM, Stewart PS. Anti-biofilm properties of chitosan-coated surfaces. Journal of biomaterials science Polymer edition. 2008;19:1035-46.

[10] Asadinezhad A, Novak I, Lehocky M, Bilek F, Vesel A, Junkar I, *et al*. Polysaccharides coatings on medical-grade PVC: a probe into surface characteristics and the extent of bacterial adhesion. Molecules. 2010;15:1007-27.

[11] Harris LG, Mead L, Muller-Oberlander E, Richards RG. Bacteria and cell cytocompatibility studies on coated medical grade titanium surfaces. Journal of Biomedical Materials Research Part A. 2006;78A:50-8.

[12] Smith JK, Bumgardner JD, Courtney HS, Smeltzer MS, Haggard WO. Antibiotic-loaded chitosan film for infection prevention: A preliminary *in vitro* characterization. Journal of Biomedical Materials Research Part B. 2010;94B:203-11.

[13] Moutzouri AG, Athanassiou GM. Attachment, spreading, and adhesion strength of human bone marrow cells on chitosan. Annals of biomedical engineering. 2011;39:730-41.

[14] Kawai T, Yamada T, Yasukawa A, Koyama Y, Muneta T, Takakuda K. Biological fixation of fibrous materials to bone using chitin/chitosan as a bone formation accelerator. Journal of Biomedical Materials Research Part B Applied Biomaterials. 2009;88:264-70.

[15] Bumgardner JD, Chesnutt BM, Yuan Y, Yang Y, Appleford M, Oh S, *et al.* The integration of chitosan-coated titanium in bone: an in vivo study in rabbits. Implant dentistry. 2007;16:66-79.

[16] Bumgardner JD, Wiser R, Elder SH, Jouett R, Yang Y, Ong JL. Contact angle, protein adsorption and osteoblast precursor cell attachment to chitosan coatings bonded to titanium Journal of biomaterials science Polymer edition. 2003;14:1401-9.

[17] Bumgardner JD, Wiser R, Gerard PD, Bergin P, Chestnutt B, Marin M, *et al.* Chitosan: potential use as a bioactive coating for orthopaedic and craniofacial/dental implants. Journal of biomaterials science Polymer edition. 2003;14:423-38.

[18] Lieder R, Darai M, Thor MB, Ng CH, Einarsson JM, Gudmundsson S, *et al. In vitro* bioactivity of different degree of deacetylation chitosan, a potential coating material for titanium implants. Journal of Biomedical Materials Research Part A. 2012;100:3392-9.

[19] Tomihata K, Ikada Y. In vitro and in vivo degradation of films of chitin and its deacetylated derivatives. Biomaterials. 1997;18:567-75.

[20] Park SY, Marsh KS, Rhim JW. Characteristics of different molecular weight chitosan films affected by the type of organic solventsJournal of Food Science. 2002;67:194-7.

[21] Rabea EI, Badawy ME, Stevens CV, Smagghe G, Steurbaut W. Chitosan as antimicrobial agent: applications and mode of action. Biomacromolecules. 2003;4:1457-65.

[22] Dutta PK, Tripathi S, Mehrotra GK, Dutta J. Perspectives for chitosan based antimicrobial films in food applications. Food chemistry. 2009;114:1173-82.

[23] Goy RC, de Britto D, Assis OBG. A Review of the Antimicrobial Activity of Chitosan. Polimeros. 2009;19:241-7.

[24] Kong M, Chen XG, Xing K, Park HJ. Antimicrobial properties of chitosan and mode of action: a state of the art review. International journal of food microbiology. 2010;144:51-63.

[25] Kong M, Chen XG, Liu CS, Liu CG, Meng XH, Yu LJ. Antibacterial mechanism of chitosan microspheres in a solid dispersing system against *E. coli.* Colloid Surface B. 2008;65:197-202.

[26] Papineau AM, Hoover DG, Knorr D, Farkas DF. Antimicrobial Effect of Water-Soluble Chitosans with High Hydrostatic-Pressure. Food Biotechnology. 1991;5:45-57.

[27] Sudarshan NR, Hoover DG, Knorr D. Antibacterial Action of Chitosan. Food Biotechnology. 1992;6:257-72.

[28] Kurita K. Chemistry and application of chitin and chitosan. Polymer Degradation and Stability. 1998;59:117-20.

[29] Wang XH, Du YM, Fan LH, Liu H, Hu Y. Chitosan-metal complexes as antimicrobial agent: Synthesis, characterization and structure-activity study. Polymer Bulletin. 2005;55:105-13.

[30] Guibal E. Interactions of metal ions with chitosan-based sorbents: a review. Separation and Purification Technology. 2004;38:43-74.

[31] Takahashia T, Imai M, Suzuki I, Sawai J. Growth inhibitory effect on bacteria of chitosan membranes regulated with deacetylation degree. Biochemical Engineering Journal. 2008;40:485-91.

[32] Chung YC, Wang HL, Chen YM, Li SL. Effect of abiotic factors on the antibacterial activity of chitosan against waterborne pathogens. Bioresource technology. 2003;88:179-84.

[33] Mi FL, Huang CT, Liang HF, Chen MC, Chiu YL, Chen CH, *et al*. Physicochemical, antimicrobial, and cytotoxic characteristics of a chitosan film cross-linked by a naturally occurring cross-linking agent, aglycone geniposidic acid. Journal of agricultural and food chemistry. 2006;54:3290-6.

[34] Madeleine-Perdrillat C, Karbowiak T, Raya J, Gougeon R, Bodart PR, Debeaufort F. Water-induced local ordering of chitosan polymer chains in thin layer films. Carbohydrate Polymers. 2015;118:107-14.

[35] He Q, Ao Q, Gong YD, Zhang XF. Preparation of chitosan films using different neutralizing solutions to improve endothelial cell compatibilityJournal of Materials Science: Materials in Medicine. 2011;22:2791-802.

[36] Yuan Y, Chesnutt BM, Wright L, Haggard WO, Bumgardner JD. Mechanical property, degradation rate, and bone cell growth of chitosan coated titanium influenced by degree of deacetylation of chitosan. Journal of Biomedical Materials Research Part B: Applied Biomaterials. 2008;86:245-52.

[37] Franca R, Mbeh DA, Samani TD, Le Tien C, Mateescu MA, Yahia L, *et al.* The effect of ethylene oxide sterilization on the surface chemistry and *in vitro*

cytotoxicity of several kinds of chitosan. Journal of Biomedical Materials Research Part B. 2013;101:1444-55.

[38] Martin HJ, Schulz KH, Bumgardner JD, Walters KB. XPS study on the use of 3-aminopropyltriethoxysilane to bond chitosan to a titanium surface. Langmuir. 2007;23:6645-51.

[39] Swanson TE, Cheng X, Friedrich C. Development of chitosan-vancomycin antimicrobial coatings on titanium implants. Journal of Biomedical Materials Research Part A. 2011;97:167-76.

[40] Kung S, Devlin H, Fu E, Ho KY, Liang SY, Hsieh YD. The osteoinductive effect of chitosan-collagen composites around pure titanium implant surfaces in rats. Journal of periodontal research. 2011;46:126-33.

[41] Jun SH, Lee EJ, Yook SW, Kim HE, Kim HW, Koh YH. A bioactive coating of a silica xerogel/chitosan hybrid on titanium by a room temperature sol-gel process. Acta biomaterialia. 2010;6:302-7.

[42] Lim TY, Wang W, Shi ZL, Poh CK, Neoh KG. Human bone marrow-derived mesenchymal stem cells and osteoblast differentiation on titanium with surface-grafted chitosan and immobilized bone morphogenetic protein-2. Journal of Materials Science: Materials in Medicine. 2009;20:1-10.

[43] Cai KY, Rechtenbach A, Hao JY, Bossert J, Jandt KD. Polysaccharide-protein surface modification of titanium via a layer-by-layer technique: Characterization and cell behaviour aspects. Biomaterials. 2005;26:5960-71.

[44] Fakhry A, Schneider GB, Zaharias R, Senel S. Chitosan supports the initial attachment and spreading of osteoblasts preferentially over fibroblasts. Biomaterials. 2004;25:2075-9.

[45] Shi Z, Neoh KG, Kang ET, Poh C, Wang W. Bacterial adhesion and osteoblast function on titanium with surface-grafted chitosan and immobilized RGD peptide. Journal of Biomedical Materials Research Part A. 2008;86:865-72.

[46] Chua PH, Neoh KG, Kang ET, Wang W. Surface functionalization of titanium with hyaluronic acid/chitosan polyelectrolyte multilayers and RGD for promoting osteoblast functions and inhibiting bacterial adhesion. Biomaterials. 2008;29:1412-21.

[47] Park JH, Olivares-Navarrete R, Wasilewski CE, Boyan BD, Tannenbaum R, Schwartz Z. Use of polyelectrolyte thin films to modulate osteoblast response to microstructured titanium surfaces. Biomaterials. 2012;33:5267-77.

[48] Prasitsilp M, Jenwithisuk R, Kongsuwan K, Damrongchai N, Watts P. Cellular responses to chitosan in vitro: The importance of deacetylation. Journal of Materials Science: Materials in Medicine. 2000;11:773-8.

[49] Amaral IF, Lamghari M, Sousa SR, Sampaio P, Barbosa MA. Rat bone marrow stromal cell osteogenic differentiation and fibronectin adsorption on chitosan membranes: the effect of the degree of acetylation. Journal of Biomedical Materials Research Part A. 2005;75:387-97.

[50] Amaral IF, Cordeiro AL, Sampaio P, Barbosa MA. Attachment, spreading and short-term proliferation of human osteoblastic cells cultured on chitosan films with different degrees of acetylation. Journal of biomaterials science Polymer edition. 2007;18:469-85.

[51] Ponsonnet L, Reybier K, Jaffrezic N, Comte V, Lagneau C, Lissac M, *et al.* Relationship between surface properties (roughness, wettability) of titanium and titanium alloys and cell behaviour. Materials Science and Engineering C2003;23:551-60.

[52] Hallab NJ, Bundy KJ, O'Connor K, Moses RL, Jacobs JJ. Evaluation of metallic and polymeric biomaterial surface energy and surface roughness characteristics for directed cell adhesion. Tissue Engineering. 2001;7:55-71.

[53] Madihally SV, Matthew HW. Porous chitosan scaffolds for tissue engineering. Biomaterials. 1999;20:1133-42.

CHAPTER IV

Surface characterization techniques

There are many techniques available for materials surface characterization. During the work developed in this thesis several characterization techniques were used, such as: Contact angle goniometry, Ellipsometry, Infrared Reflection-Absorption Spectroscopy (IRRAS), X-ray photoelectron spectroscopy (XPS) and Atomic Force Microscopy (AFM). A briefly explanation of their basic principles of action and applications in the scope of this thesis is given.

1. Contact angle goniometry

Contact angle measurements provide information about the wettability of a surface and allow the determination of the surface free energy that is directly proportional to the tendency of molecules to adsorb onto a material surface. This technique is very usefull to detect surface modifications (such as AMP immobilization), surface contamination and to predict future biological interactions with materials surface [1-11]. It measures the contact angle between the liquid/vapor interface and the liquid/solid interface (solid surface) – (Figure 1)

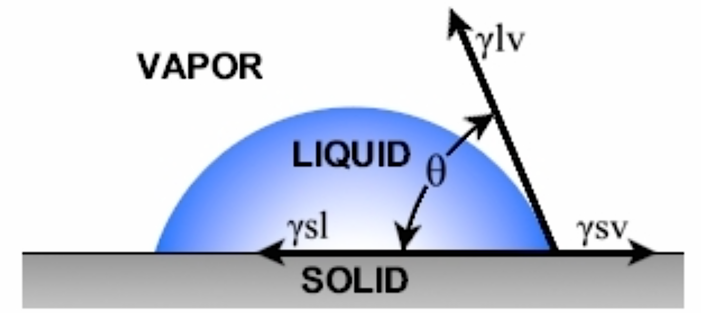

Figure 1. Scheme of liquid contact angle in a surface. γ_{sv}-solid surface free energy, γ_{sl}-solid/liquid interfacial tension, and γ_{lv}-liquid/vapor surface tension . Adapted from [12].

The phenomenon of the contact angle between a liquid and a solid surface can be explained as a balance between the force of attraction of the liquid molecules to each other (the cohesive force) and the attraction of the liquid molecules to the molecules of the surface (the adhesive force) [13, 14]. When a drop of liquid is placed on a surface, it spreads to reach equilibrium between cohesive and adhesive

forces with minimum energy. This equilibrium between forces is described by the Young equation:

$\gamma_{sv} = \gamma_{sl} + \gamma_{lv}.\cos\theta$,

where γ_{sv} is the solid surface free energy, γ_{sl} is the solid/liquid interfacial tension, γ_{lv} is the liquid/vapor surface tension and θ is the contact angle [13, 14]. Since Young equation contains two unknowns variables (γ_{sl} and γ_{lv}), surface energy (γ_{sv}) need to be calculated using more than one contact angle obtained with liquids with different surface tensions [13].

The static sessile drop technique is the simplest method to measure the contact angle. It is usually established that a contact angle less than 90° (low contact angle) indicates that the liquid spreads over a large area of the surface, enabling the wetting of the surface. A contact angle higher than 90° (high contact angle) means that the liquid minimizes the contact with the surface, which is unfavorable for the wetting of the surface [14].

This technique is one of the most sensitive of all surface analytical techniques because only the top nanometer of a surface influences wettability [2, 3]. Therefore it can be used to detect surface modification, namely detection of AMP immobilization [4-11].

2. Ellipsometry

Ellipsometry is a non-destructive optical method that measures the change in state of polarization of the light upon reflection from a surface. This technique is very useful for the determination of the thickness of a thin film deposited onto a reflective substrate, since the state of reflected polarized light depends on the thickness and the refractive index of the coating [15, 16].

When light reflects from a surface both p- and s- components of the incident polarized light (p-parallel and s-perpendicular to the plan of incidence) will be changed from linear to elliptical. This is schematically demonstrated in Figure 2.

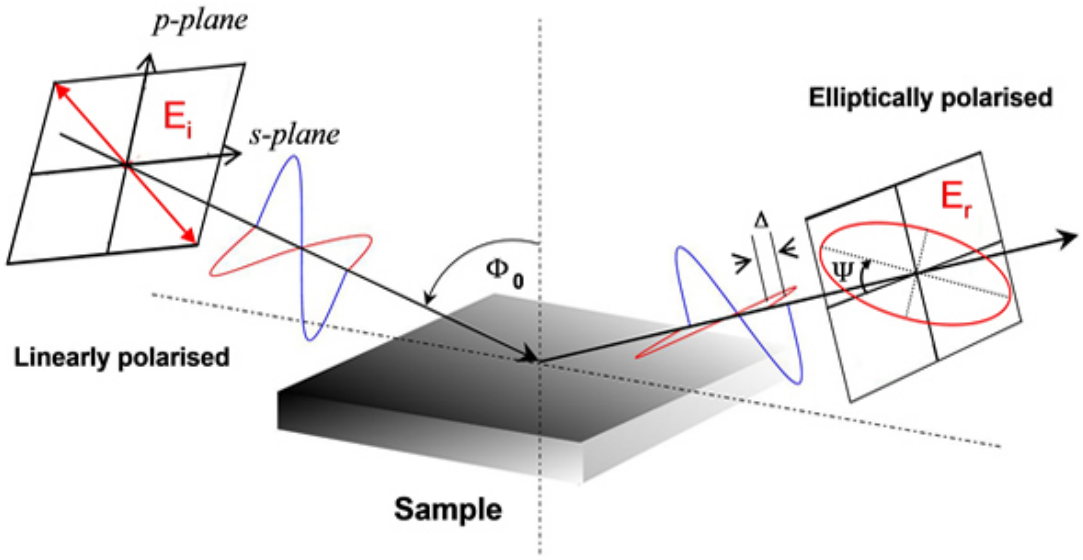

Figure 2. Schematic representation of light's polarization due to optical components and it is elliptical polarised upon reflection with asymmetric intensity difference (tan Ψ) and phase difference (Δ). Reproduced from [17].

The change of polarization is characterized by the amplitude ratio (Ep/Es), and the phase difference (δp-δs) of the two components (p- and s-) of the electric vector E. The change of polarization due to reflection at an interface is defined by two ellipsometric angles Ψ and Δ:

$$Tan\,\Psi = \frac{E_p^r/E_s^r}{E_p^i/E_s^i}$$

and

$$\Delta = (\delta_p{}^r - \delta_s{}^r) - (\delta_p{}^i - \delta_s{}^i)$$

where Tan Ψ is the change in the amplitude ratio due to reflection and Δ is the change in the phase difference of both p- and s- components of the polarized light before (i) and after its reflection from a surface (r). These two angles are related with the optical characteristics of the surface, namely to its refractive index (n) and extinction coefficient (k) and also the thickness of a thin film deposited onto a reflective surface [15, 16].

This technique can be very useful to determine surface modification of thin films (<100 nm), particularly when a thickness change is expected, such in the case of AMP immobilization.

3. Fourier-Transform Infrared reflection-absorption spectroscopy (IRRAS)

Infrared spectroscopy provides information about chemical bonds and chemical functional groups present in the sample. IRRAS is a specific adaptation of infrared spectroscopy for characterization of thin films deposited on reflective surfaces. The infrared beam emitted induces molecular vibrations at specific frequencies matching the fundamental vibrations modes of a molecule. Absorption only occurs for those vibrations that induce oscillating dipoles perpendicular to the surface [3]. Experimentally, the infrared beam emitted is polarized through a polarizer. The polarized light incises into the sample at 80° grazing angle that is nearly parallel to the surface increasing the sensitivity to the upper surface layers of the thin films. Afterwards, the detector senses the reflected beam (see Figure 3).

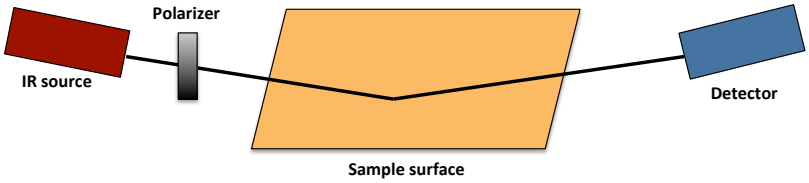

Figure 3. Scheme of IRRAS. Polarized Infrared is incident in to sample at 80° grazing angle and reflected to the detector. Adapted from [18].

The reflected frequencies are compared with the incident frequencies giving the frequencies absorbed by the film on the surface. The obtained spectra present the absorption bands corresponding to the frequencies at which radiation is absorbed. These absorbed frequencies correspond to specific molecular vibrations of specific chemical bonds and chemical functional groups.

This technique is therefore used to detect thin films deposited onto a reflective surface, the introduction/remotion of new functional groups (e.g., functionalization

of a chitosan thin film), the increase/decrease of specific functional groups due to the immobilization of other compounds (e.g., AMP immobilization, chitosan deacetylation.

4. X-ray photoelectron spectroscopy (XPS)

X-ray photoelectron spectroscopy is a semi-quantitative spectroscopic technique based on the photoelectric effect that allow the measure of the elemental composition, empirical formula, chemical state and electronic state of the elements that exist within a material [2, 3, 19].

XPS measures the kinetic energy (K_e) and the number of electrons that escape from the top (until 10 nm) of the material being irradiated with a X-ray beam in ultra-high vacuum (to assure that no other specimens are present in the chamber). A scheme of a X-ray photoelectron spectroscopy system is depicted in Figure 4.

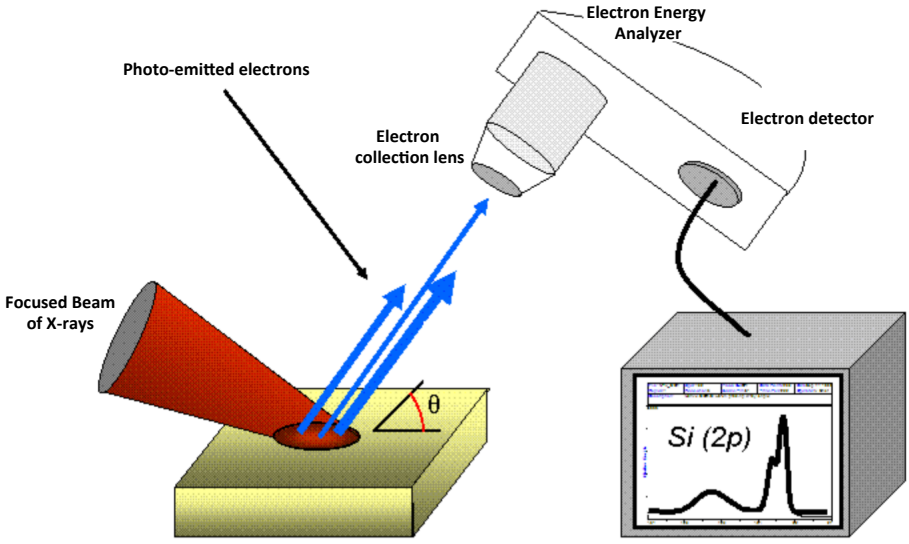

Figure 4. Scheme of an X-ray photoelectron spectroscopy system: x-ray source, sample, electrostatic analyzer and electron detector. Adapted from [20].

The binding energy of an electron to an atom (B_e) is determined from the photoelectric relationship:

$B_e = h\nu - K_e$,

Where $h\nu$ is the known energy of the incident X-ray beam and K_e is the kinetic energy of the emitted electron measured by the X-ray spectrometer. Since B_e is

specific of each chemical element, XPS provides identification of all elements (with the exceptions of H and He) that exist in or on the surface of the material. Furthermore, since B_e is determined by the local chemical environment and type of atom, peak shifts can be used to obtain information about the chemical bond state of atom, e.g. if it is bond to other more electronegative atom. [2, 3, 19]. Therefore, this technique can be extremely valorous in detecting surface chemical modifications, as it can detect the introduction of new elements to the surface, as well as, clarifying changes on the chemical bonds established by particular elements. Its semi-quantitative character, also helps understanding the different amounts of a particular element in the different samples, allowing an estimation of the amount of tethered AMP.

5. Atomic Force Microscopy

Atomic force microscopy (AFM) is a three-dimensional topographic technique with a high atomic resolution to measure surface roughness. AFM is a near-field technique based on the interaction between a sharp tip and the atoms of the sample surface. Atomic resolution of samples is attained in AFM by monitoring small forces applied over a surface using a sharp probe mounted on a flexible cantilever, which acts as a spring. The movements of the flexible cantilever can be monitored by changes in laser deflection off of a reflective surface on the backside of the cantilever. A photodiode detector detects the changes in deflection of the laser [21]. Figure 5 depicts a schematic representantion of an AFM.

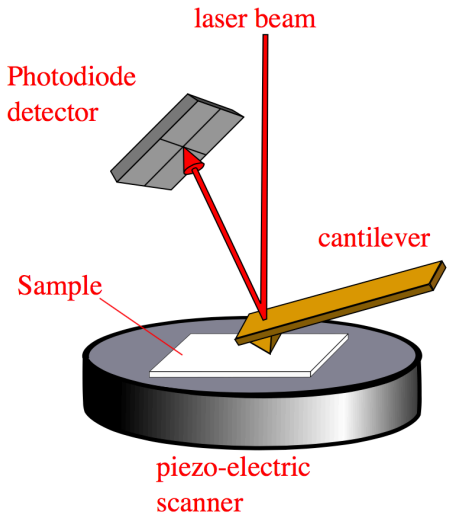

Figure 5. Schematic representation of an AFM. Reproduced from [22].

Several imaging modes are available in AFM that provide information about the surface properties of materials as experienced by the touch of the AFM probe. The most frequently used AFM imaging modes in biology include contact mode and tapping or intermittent contact mode (reviewed in [23-25]). Therefore, AFM is particularly important to disclose topographical appearance of surfaces, whose roughness changes may be related to surface modification. Moreover, as it has a very high spatial resolution (up to sub-nanometer), it provides the ability to map the distribution of single molecules [26, 27].

[1] Goncalves IC, Martins MC, Barbosa MA, Naeemi E, Ratner BD. Selective protein adsorption modulates platelet adhesion and activation to oligo(ethylene glycol)-terminated self-assembled monolayers with C18 ligands. Journal of Biomedical Materials Research Part A. 2009;89:642-53.

[2] Bain CD, Whitesides GM. A Study by Contact-Angle of the Acid-Base Behavior of Monolayers Containing Omega-Mercaptocarboxylic Acids Adsorbed on Gold - an Example of Reactive Spreading. Langmuir. 1989;5:1370-8.

[3] Hook AL, Anderson DG, Langer R, Williams P, Davies MC, Alexander MR. High throughput methods applied in biomaterial development and discovery. Biomaterials. 2010;31:187-98.

[4] Godoy-Gallardo M, Mas-Moruno C, Fernandez-Calderon MC, Perez-Giraldo C, Manero JM, Albericio F, *et al.* Covalent immobilization of hLf1-11 peptide on a titanium surface reduces bacterial adhesion and biofilm formation. Acta biomaterialia. 2014;10:3522-34.

[5] Godoy-Gallardo M, Mas-Moruno C, Yu K, Manero JM, Gil FJ, Kizhakkedathu JN, *et al.* Antibacterial properties of hLf1-11 peptide onto titanium surfaces: a comparison study between silanization and surface initiated polymerization. Biomacromolecules. 2015;16:483-96.

[6] Godoy-Gallardo M, Wang Z, Shen Y, Manero JM, Gil FJ, Rodriguez D, *et al.* Antibacterial coatings on titanium surfaces: a comparison study between *in vitro* single-species and multispecies biofilm. ACS applied materials & interfaces. 2015;7:5992-6001.

[7] Li Y, Santos CM, Kumar A, Zhao M, Lopez AI, Qin G, *et al.* "Click" immobilization on alkylated silicon substrates: model for the study of surface bound antimicrobial peptides. Chemistry. 2011;17:2656-65.

[8] Lim K, Chua RR, Saravanan R, Basu A, Mishra B, Tambyah PA, *et al.* Immobilization studies of an engineered arginine-tryptophan-rich peptide on a silicone surface with antimicrobial and antibiofilm activity. ACS applied materials & interfaces. 2013;5:6412-22.

[9] Li X, Li P, Saravanan R, Basu A, Mishra B, Lim SH, *et al.* Antimicrobial functionalization of silicone surfaces with engineered short peptides having broad spectrum antimicrobial and salt-resistant properties. Acta biomaterialia. 2014;10:258-66.

[10] Chen X, Hirt H, Li Y, Gorr SU, Aparicio C. Antimicrobial GL13K peptide coatings killed and ruptured the wall of Streptococcus gordonii and prevented formation and growth of biofilms. PloS one. 2014;9:e111579.

[11] Holmberg KV, Abdolhosseini M, Li Y, Chen X, Gorr SU, Aparicio C. Bio-inspired stable antimicrobial peptide coatings for dental applications. Acta biomaterialia. 2013;9:8224-31.

[12] http://www.ramehart.com/contactangle.htm. Accessed July 2015.

[13] Ratner BD HA, Schoen FJ, Lemons JL. Biomaterials science - an introduction to materials in medicine: ed. San Diego, CA, USA; 2004.

[14] Dee KC PD, Bizios R. An Introduction To Tissue-Biomaterial Interactions2002.

[15] Tompkins HG IE. Handbook of Ellipsometry: Norwich, NY William Andrews Publications; 2005.

[16] Tompkins HG MW. Spectroscopic Ellipsometry and Reflectometry: A User's Guide: John Wiley & Sons Inc; 1999.

[17] https://http://www.tcd.ie/Physics/Surfaces/images/elli_dia.JPG. Accessed in July 2015.

[18] Chechik V SC. Gold-thiol self-assembled monolayers. In: Patai S RZ, editors, editor. The chemistry of organic derivatives of gold and silver. New York: John Wiley & Sons, Ltd; 1999. p. 551-640.

[19] Kingshott P, Andersson G, McArthur SL, Griesser HJ. Surface modification and chemical surface analysis of biomaterials. Curr Opin Chem Biol. 2011;15:667-76.

[20] https://en.wikipedia.org/wiki/X-ray_photoelectron_spectroscopy#/media/File: System2.gif. Accessed in July 2015.

[21] Liu SY, Wang YF. Application of AFM in Microbiology: A Review. Scanning. 2010;32:61-73.

[22] Roduit C. AFM Figures. Creative Commons Attribution; 2010.

[23] Alonso JL, Goldmann WH. Feeling the forces: atomic force microscopy in cell biology. Life sciences. 2003;72:2553-60.

[24] Hansma HG, Hoh JH. Biomolecular imaging with the atomic force microscope. Annual review of biophysics and biomolecular structure. 1994;23:115-39.

[25] Frederix PT, Hoogenboom BW, Fotiadis D, Muller DJ, Engel A. Atomic force microscopy of biological samples. Materials Research Society Bulletin. 2004;29:449-55.

[26] Dufrene YF. AFM for nanoscale microbe analysis. The Analyst. 2008;133:297-301.

[27] Engel A, Muller DJ. Observing single biomolecules at work with the atomic force microscope. Nature structural biology. 2000;7:715-8.

CHAPTER V

Characterization of hLF1-11 immobilization onto ultrathin films, and its effects on antimicrobial activity

---

Fabíola Costa [a,b], Sílvia Maia [c], Joana Gomes [a], Paula Gomes [c], M. Cristina L. Martins [a,d]

Acta Biomaterialia 2014 10: 3513-3521

[a] INEB – Instituto de Engenharia Biomédica, Universidade do Porto, Rua do Campo Alegre, 823, 4150-180 Porto, Portugal

[b] Universidade do Porto, Faculdade de Engenharia, Porto, Portugal

[c] Universidade do Porto, CIQ-UP – Departamento de Química e Bioquímica, Faculdade de Ciências, Porto, Portugal

[d] Universidade do Porto, Instituto de Ciências Biomédicas Abel Salazar, Porto, Portugal

1. Abstract

hLF1–11 (GRRRRSVQWCA) is an antimicrobial peptide (AMP) with high activity against methicillin-resistant *Staphylococcus aureus* (MRSA), the most prevalent species in implant-associated infection. In this work, the effect of the surface immobilization on hLF1–11 antimicrobial activity was studied. Immobilization was performed onto chitosan thin films as a model for an implant coating due to its reported osteogenic and antibacterial properties. Chitosan thin films were produced by spin-coating on gold surfaces. hLF1–11 was immobilized onto these films by its C-terminal cysteine in an orientation that exposes the antimicrobial activity-related arginine-rich portion of the peptide. Two levels of exposure (with and without a polyethylene glycol (PEG) spacer) were analyzed. Covalent immobilization was further compared with the AMP physical adsorption onto chitosan films. Surfaces were characterized using ellipsometry, contact angle measurements, atomic force microscopy, infrared and X-ray photoelectron spectroscopies and using a fluorimetric assay for hLF1–11 quantification. Surface antimicrobial activity was assessed through surface adhesion and viability assays using an MRSA (*S. aureus* ATCC 33591). The incorporation of hLF1–11 increased significantly bacterial adhesion to chitosan films. However, the presence of hLF1–11, namely when immobilized through a PEG spacer, decreased the viability of adherent bacteria with regard to the control surface. These results demonstrated that hLF1–11 after covalent immobilization by its cysteine can maintain activity, particularly if a spacer is applied. However, further studies, exploring the opposite orientation or the same C-terminal orientation, but non-cysteine related, can help to clarify the potential of the hLF1–11 immobilization strategy.

Keywords: Antimicrobial peptides, Surface immobilization, Surface characterization, Bacterial adhesion, Chitosan

2. Introduction

Antimicrobial peptides (AMPs) are a new class of antibiotics with very promising characteristics. They are usually composed of short sequences of amino acids (<50 residues), with simultaneous amphipathic and cationic behaviors [1]. Although the AMPs exact mechanism of action is not fully elucidated, it is generally accepted to include electrostatic interactions between the bacterium negatively charged outer layer and the positively charged AMP, which results in bacterial death [1,2]. Their most interesting features are: high activity against a broad spectrum of microorganisms (Gram-positive and –negative bacteria, yeasts), high selectivity towards microorganisms and not mammalian cells (which have zwitterionic membranes), fast killing even at low concentrations and, most importantly, they do not have the tendency to induce resistance [1,3]. This last feature differentiates them from the classical antibiotics presently used. However, AMP application has some associated challenges, namely (i) proteolytic degradation, (ii) peptide co-precipitation with plasma carrier proteins and (iii) peptide self-aggregation. Also, if higher titers are applied to circumvent such problems, cytotoxic effects become apparent. One current strategy to overcome these challenges is its covalent immobilization onto a surface [4].

In the present work we have chosen hLF1–11, which is a 11-mer derived from human Lactoferrin. This amphipathic peptide, with an hydrophilic N-terminal and a hydrophobic C-terminal, has a wide spectrum of activity, associated with an excellent safety profile, tested both *in vitro* and *in vivo* [5–7]. Indeed, it has been tested against methicillin-resistant *Staphylococcus aureus* (MRSA) in an osteomyelitis model [8–10]. However, in this model, the delivery system consisted of hLF1–11 incorporated in calcium phosphate (Ca–P) cement, which resulted in burst peptide release only [11]. Likewise, Kazemzadeh-Narbat *et al*. [12] tested hLF1–11 on a Ca–P microporous coating and found the peptide to have a slow and incompetent release. Therefore, as the soluble hLF1–11 application has not provided sufficient activity, we decided to test whether covalent immobilization could originate an efficient antimicrobial coating against implant-related infections. To this end, we needed a polymer that would be easily functionalized, but also would have intrinsic

characteristics favorable to the product end application, as allowing osteointegration, and inhibiting bacterial adhesion and growth. Therefore, we chose chitosan, as it fulfills the characteristics mentioned above, with reported antimicrobial [13–16] and osteogenic properties [17–20]. As summarized by us [4], AMP covalent immobilization may result in activity lost, so some parameters should be addressed in order to obtain maximum activity, namely (i) orientation (N- or C-terminal immobilization) and (ii) exposition. The combination of these parameters gives rise to different immobilization profiles that can have very distinct activities. Some papers have reported that positively charged amino acids (arginine) of its N-terminal are essential for hLF1–11 antimicrobial activity [6,7,21]. Also, the natural sequence of hLF1–11 offers a free sulfhydryl group at the cysteine residue near the C-terminal, which can be used for disulfide bridge establishment with SH-modified chitosan. This is a simple, mild reaction that allows the control of peptide orientation. Therefore in this study, we immobilize hLF1–11 by its C-terminal (exposing the arginine/positive end) directly to the polymer (for a more strict and oriented exposition of the AMP) or through a spacer (for a more movable/ flexible exposition) and compare its activity against simple physical adsorption of the peptide onto the polymer.

3. Materials and methods

3.1. hLF1–11 synthesis and characterization

hLF1–11 (GRRRRSVQWCA, C-terminal amide) was produced by Fmoc/tBu solid-phase peptide synthesis methodologies assisted with microwave energy (Liberty 1 Microwave Peptide Synthesizer, CEM Corporation) [22,23]. Crude product was purified by reverse-phase liquid chromatography and confirmed by high-performance liquid chromatography (Hitachi-Merck LaChrom Elite), liquid chromatography–electrospray ionization mass spectrometry (LCQ-DecaXP LC-MS system, ThermoFinnigan) and ultraviolet spectrometry. The peptide used presented a purity level higher than 90%.

3.2. hLF1–11 surface immobilization

3.2.1. Substrate preparation

Gold production and cleaning were performed according to Martins *et al.* [29]. Briefly, chromium (5 nm) and gold (25 nm) layers were deposited by ion beam sputtering from chromium and gold targets (99.9% purity) on silicon wafers (AUREL, GmbH). Chromium was used to improve the adhesion of gold to silicon. Gold substrates were cleaned with ''piranha'' solution (7 parts of H_2SO_4 and 3 parts of 30% H_2O_2) for 5 min (caution: this solution reacts violently with many organic materials and should be handled with suitable protective measures), thoroughly rinsed with ethanol and dried with a gentle stream of argon.

3.2.2. Preparation of chitosan ultrathin films

Commercial squid pen chitosan (France Chitine) was purified by the reprecipitation method [25]. Chitosan thin films were prepared by dispensing a drop of chitosan solution (0.4% in acetic acid w/v) [26] on the center of the Au substrates (150 µl for 1 x 1 cm^2 substrates) placed in the spin coater equipment (Laurell Technologies Corporation) and spun at 9000 rpm for 1 min. Then, the newly prepared ultrathin films were neutralized with 0.1 M NaOH for 5 min and rinsed twice with MilliQ water. Each sample was dried with a gentle stream of argon and stored in sealed plastic Petri dishes saturated with argon until use.

3.3. Peptide immobilization

hLF1–11 immobilization on chitosan thin films was performed by forming a persulfate bond (disulfide bridge) between free sulfhydryl groups present in the peptides cysteine side chain and in prefunctionalized chitosan (Figure 1).

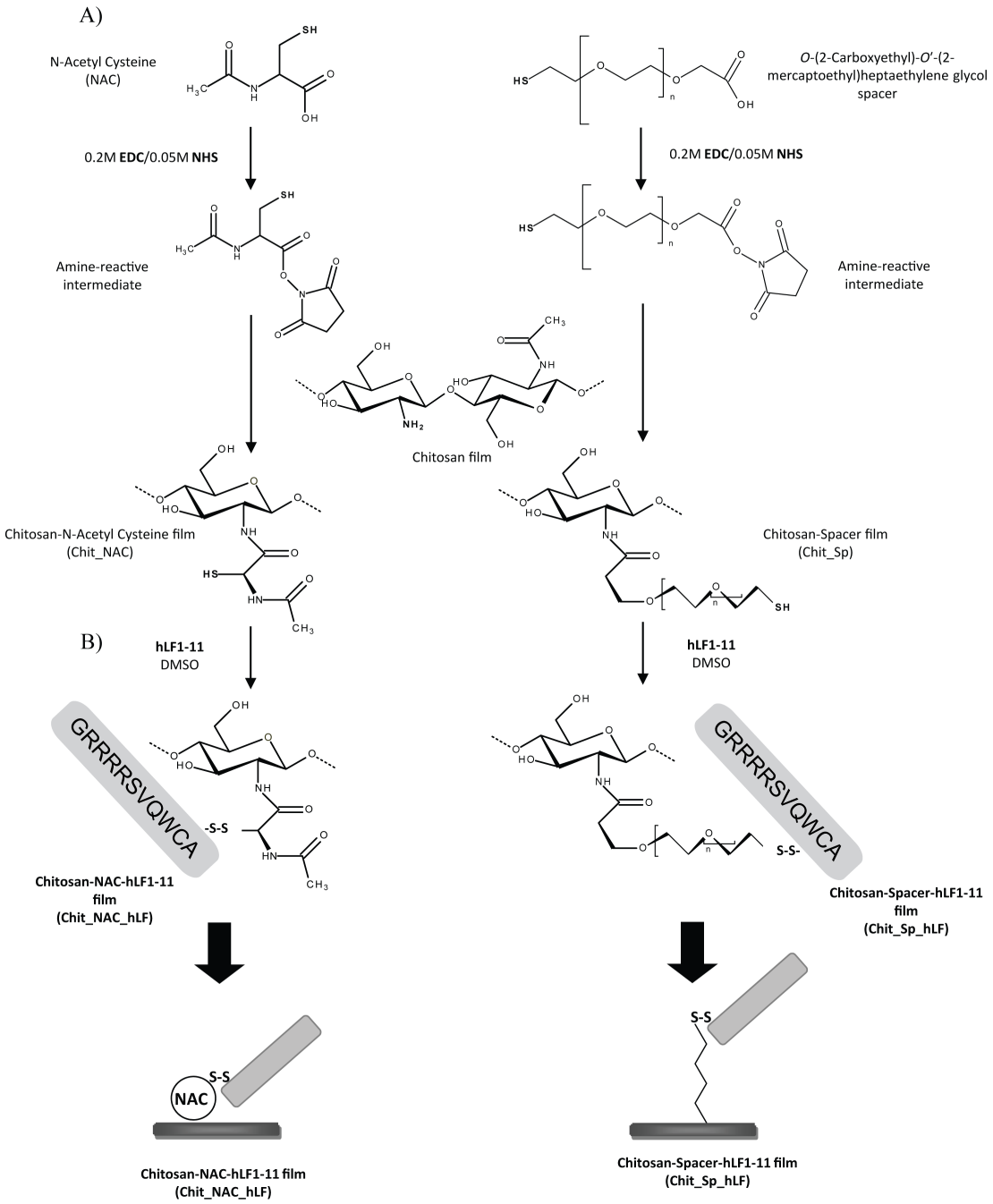

Figure 1. A) Chitosan modification with NAC or Sp; **B)** hLF1-11 immobilization by establishment of a covalent disulfide bridge.

3.3.1. Introduction of SH groups onto chitosan films

Functionalization of chitosan thin films with SH groups was obtained by the coupling of N-acetyl cysteine (NAC) (Merck), or O-(2-carboxyethyl)-o'-(2-mercaptoethyl) heptaethylene glycol (Sp) (Sigma Aldrich ≥95% purity). Chitosan thin films were treated with a solution of 0.2 M 1-ethyl-3-(3-dimethylaminopropyl)

carbodiimidehydrochloride) (EDC; Sigma–Aldrich), 0.05 M N-hydroxysulfosuccimide (NHS; Sigma–Aldrich) and 25 mM of SH agent (NAC or Sp) in 0.1 M (N-morpholino)ethanesulfonic acid (MES; Sigma–Aldrich) buffer at pH 6.5 for 1 h (NAC) or 2 h (Sp), at 37 °C and 100 rpm. Samples were then rinsed with MilliQ water, immersed for 1 min in an ultrasound bath (Bandelin Sonorex Digitec Bath 35 kHz) and rinsed again with MilliQ water.

3.3.2. Peptide chemical and physical immobilization

Non-modified (for simple physical adsoption) and modified chitosan substrates were incubated with 1 mg ml^{-1} peptide solution in 10mM TrisHCl, pH 8.0, in oxidative conditions (20% dimethyl sulfoxide (DMSO)) for 18 h, at 30 °C and 120 rpm.

3.4. Surface characterization

3.4.1. Infrared reflection absorption spectroscopy (IRRAS)

Measurements were performed on a Perkin Elmer Fourier transform infrared spectrophotometer, model 2000, coupled to a VeeMax II Accessory (PIKE) and a liquid-nitrogen-cooled mercury cadmium telluride (MCT) detector. In order to ensure that there was no water vapor adsorption, dry nitrogen was purged into the instrument for 5 min before and during the measurement of each sample. For each substrate, a similar gold surface was used as a background. Incident light was p-polarized and spectra were collected using the 80° grazing angle reflection mode. For each sample, 100 scans were collected with 4 cm^{-1} resolution.

3.4.2. Ellipsometry

Ellipsometry measurements were performed using an imaging ellipsometer, model EP3, from Nanofilm Surface Analysis. This ellipsometer was operated in a polarizer–compensator–sample–analyzer mode (null ellipsometry). The light source was a solid-state laser with a wavelength of 532 nm. The gold substrate refractive index (n = 0.6244) and extinction coefficient (k = 2.3845) were determined using a delta and

psi spectrum with a variation of angle between 65 and 71°. These measurements were made in four zones to correct for any instrument misalignment. The thickness of the chitosan films was determined using (n) chitosan = 1.54 and (k) chitosan = 0 [27]. Results are presented as the average of three measurements on each of two samples.

3.4.3. X-ray photoelectron spectroscopy (XPS)

XPS measurements were carried out on a VG Scientific Escalab 200A (UK) spectrometer using magnesium Kα (1253.6eV) as the radiation source (from CEMUP – Centro de Materiais da Universidade do Porto). The photoelectrons were analyzed at a take-off angle of 55°. Survey spectra were collected over a range of 0–1150 eV with an analyzer pass energy of 50 eV. High-resolution C1*s*, O1*s*, N1*s*, S2*p* and Au4*f* spectra were collected with an analyzer pass energy of 20 eV. The binding energy (BE) scales were referenced by setting the C1*s* BE to 285.0 eV. All the spectra were fitted using XPS peak fitting software (XPSPEAK Version 4.1). Element atomic percentages were calculated from the integrated intensities of the XPS peaks, taking into account the atomic sensitivity factors of the instrument data system. Sulfur high resolution spectra were fitted with a doublet structure with a 2:1 area ratio and splitting of 1.2 eV, as described by Castner *et al.* [28]. All sulfur spectra were fitted with a 1.7 eV full width at half maximum profile.

3.4.4. Water contact angle measurements

Contact angle measurements were performed using the sessile drop method with a contact angle measuring system from Data Physics, model optical contact angle (OCA) 15, equipped with a video CCD camera and SCA 20 software, as described by Martins *et al.* [29]. After deposition of 4 µl drops of MilliQ water, images were taken every 2 s over 300 s. Droplet profiles were fitted using different mathematical functions, to calculate the contact angle. The ellipse fitting method was used to calculate contact angles between 90° and 30°. The water contact angle of each

substrate was calculated by extrapolating the time-dependent curve to zero. Results are the average of three measurements on three independent samples.

3.4.5. Atomic force microscopy (AFM)

AFM studies were carried out using a PicoPlus scanning probe microscope interfaced with a Picoscan 2500 controller (both from Agilent Technologies, USA). Each sample was imaged with a 10 x 10 μm^2 piezo-scanner. The surface roughness was determined in 700 x 700 nm^2 scanned areas in five randomly chosen locations per sample, at room temperature. The roughness height parameter calculated was the root mean square roughness, which corresponds to the deviations from the center x–y plane (Rq). The center plane is a plane such that the volumes enclosed by the image surface above and below are equal. The control gold substrate was analyzed through Tapping® mode, with a spring constant of K = 1–5 N m^{-1} using a silicon tip. Samples were analyzed in contact mode, using a silicon nitride tip with a spring constant of K=0.58 N m^{-1}.

3.4.6. Peptide surface density

Tethered peptide quantification was performed through colorimetric reaction using 9,10-phenanthrenequinone (PHQ, Fluka) [30]. The reaction between PHQ and arginine or arginine residues forms a stable compound which fluoresces upon excitation [30]. Present protocol was adapted from Kazemzadeh-Narbat *et al.* [12] Substrates were sonicated 1 h in 0.1 M HCl in an ultrasound bath. Then, 1 ml of each sample solution was added to 3 ml of 3.5 µM PHQ in absolute ethanol. Simultaneously 0.5 ml of 2 M NaOH was added to adjust the pH. The mixture was then incubated at 30 °C for 3 h. Finally, 2.25 ml of 2.4 M HCl was added to stop the reaction. At this point, the characteristic wavelengths were determined from the excitation and emission spectra. The highest emission intensity was found at the wavelength of 380 nm. The highest peak at the excitation spectrum (256 nm) was chosen for the maximum emission output. The fluorescence emission was measured using a fluorescence microplate reader (Biotek Synergy Mx Luminometer).

The amount of hLF1–11 was calculated based on a calibration curve prepared with standard solutions of free L-arginine (Fluka) and free hLF1–11. Standard solutions of free hLF1–11 were adjusted by quantification at 280 nm in a Thermo Scientific ‘‘Nanodrop 1000’’ spectrophotometer.

3.5. Bacterial assays

3.5.1. Bacterial strains, media and growth conditions

Methicillin-resistant *S. aureus* Subsp *aureus* strains (ATCC 33591) were obtained from the American Type Culture Collection. Bacteria were grown on tryptic soya agar (TSA) (Merck) and tryptic soya broth (TSB) (Merck). Bacterial suspensions were adjusted by measuring optical density (600 nm). Bacterial numbers were confirmed by a colony forming units (CFUs) count.

3.5.2. Minimal inhibitory concentration determination

Minimal inhibitory concentration (MIC) was established with a modified broth microdilution method in Mueller Hinton broth (MHB) [31].

3.5.3. Bacterial–surface interaction

3.5.3.1. Sample preparation

Test surfaces were washed successively in 70% ethanol and sterile water, and then dried in sterile environment. Samples were then transferred to a 24-well, flat-bottom cellular suspension plates (Sarstedt, Ltd, Newton, USA).

3.5.3.2. Sample incubation with bacteria

500 µl of 3 x 10^7 CFU ml^{-1} bacterial solution (*S. aureus* ATCC 33591) was then added to each well and incubated at 37 °C for 4 h. Surrounding wells were filled with 1 ml of sterilized deionized water, in order to avoid broth evaporation.

3.5.3.3. Non-adherent viable bacteria (supernatant) assay

After the incubation period, serial dilutions of the supernatants were performed and plated onto TSA plates. CFU counts were assessed after 18 h incubation at 37 °C.

3.5.3.4. Bacterial surface adhesion assay

After the incubation period, substrates were rinsed with phosphate buffered saline (PBS) sterile solution, and then fixed with 300 µl of paraformaldehyde 4% for 20 min. Substrates were rinsed again with sterile PBS solution and stained with VECTASHIELD® Mounting Medium with (4',6-diamidino-2-phenylindole (DAPI; Vector). DAPI binds to bacteria DNA, is excited at 360 nm and emits at 460 nm, resulting in blue fluorescence. Images were obtained with an inverted fluorescence microscope (Axiovert 200 M, Zeiss, Germany) using a magnification of 1000x, corresponding to a net surface area of 0.1181 mm^2 per sample. For quantifying the total adherent bacteria, eight fields of each sample were obtained and analyzed using ImageJ software. The image analysis results were measured as the average area of cells per field of view, and are reported as the average percentage coverage. Three replicates for each condition were used.

3.5.3.5. Viable surface adherent bacteria assay

After the incubation period, substrates were rinsed with PBS sterile solution to remove non-adherent bacteria, transferred to a new plate with 500 µl of PBS and then sonicated for 8 min in an ultrasound bath (Bandelin Sonorex Digitec Bath 35 kHz) to release all adherent bacteria. After sonication, serial dilutions of the supernatant were performed, and plated onto TSA. CFU counts were performed after 18 h of incubation at 37 °C. Three replicates for each condition were used. To control sonication efficiency, the sonicated substrates were stained with VECTASHIELD® Mounting Medium with DAPI and observed using a inverted fluorescence microscopy, to guarantee that all bacteria were removed from the

surface. Also, the initial inoculum was plated before and after sonication, to ensure that minimum death was promoted by the technique.

3.6. Statistical analysis

For statistical analysis, one-way analysis of variance followed by Tukey's post hoc testing were used. When Gaussian distribution was not confirmed (Antimicrobial activity assays) the non-parametric Kruskal-Wallis test was applied using the Graphpad Prism program. Data are expressed as the mean ± standard deviation (SD) and p values of <0.05 were considered significant.

4. Results

4.1. Surface characterization

Chitosan thin films with and without hLF1–11 were characterized using ellipsometry, water contact angle measurements, AFM, IRRAS, XPS and fluorimetric assay.

4.1.1. Ellipsometry

The thickness of the spin-coated chitosan films was 14.6 ± 1.4 nm. Films remained stable during reaction procedures, since no thickness differences were detected between freshly and buffer incubated films (data not shown). Figure 2A shows the thickness of chitosan thin films after surface modification.

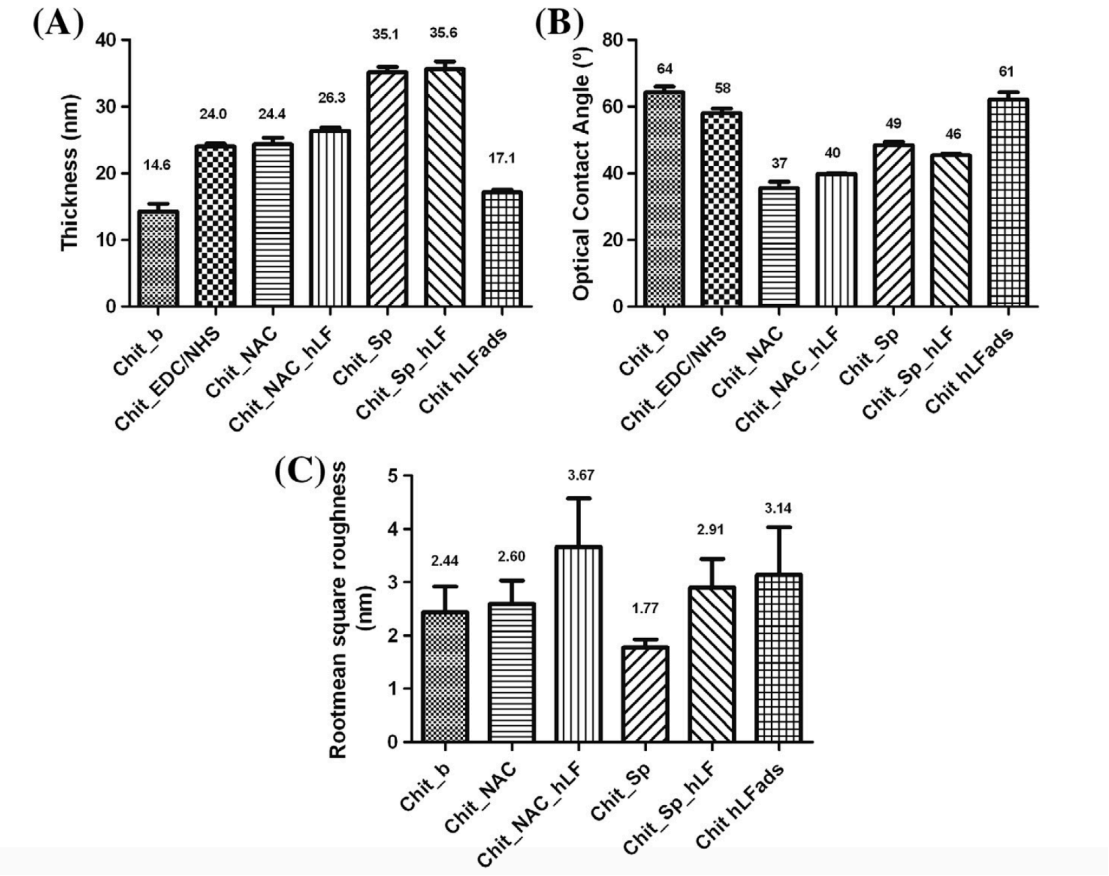

Figure 2. Surface characterization of chitosan-modified films as determined by **A)** ellipsometry (surface thickness); **B)** water optical contact angle measurements; **C)** AFM (surface roughness).

The thickness of chitosan films increased after its functionalization with NAC (+9.8 nm) or Sp (+20.5 nm) ($p < 0.05$), which is proportional to the length of the immobilized structure, suggesting the success of the functionalization. After hLF1–11 immobilization onto Chit_NAC (Chit_NAC_hLF), a 2 nm thickness increase was observed ($p < 0.05$), indicating that the peptide was successfully bond to the polymer. However, hLF1–11 immobilization onto Chit_Sp was not detected using this technique, since no significant difference was observed between the Chit_Sp film thickness before and after peptide immobilization (Chit_Sp_hLF). This can be explained by the flexibility of the spacer, which can result in a closer positioning of the peptide towards the chitosan film or due to the S-S bond formation between the SH terminal of the Sp. The small increase from 14.6 ± 1.4nm to 17.1 ± 0.4nm observed in chitosan films after immersion in the peptide solution indicates that

some hLF1–11 can be adsorbed or incorporated onto chitosan films ($p < 0.05$). No significant thickness difference was observed between chitosan solely incubated with EDC/NHS reagents and Chit_NAC. An alternative chemistry pathway can explain this situation where the absence of a carboxylic group allows a direct reaction of the carbodiimide of EDC with the free amine groups of chitosan [33] (Figure 3.).

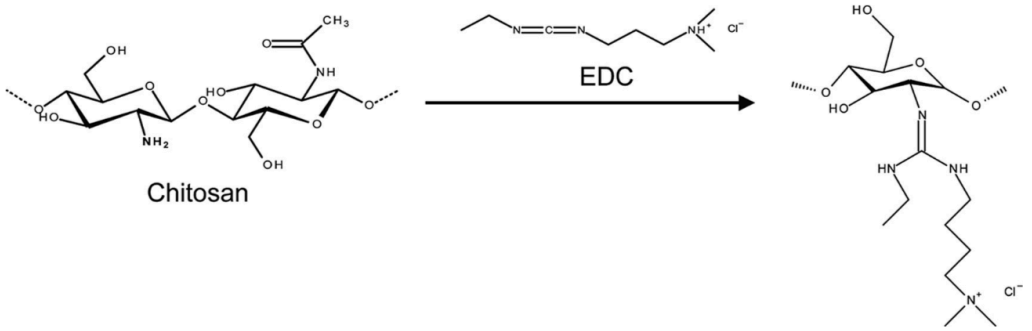

Figure 3. Reaction of carbodiimide (EDC) and NHS with chitosan free amines

4.1.2. Water contact angle measurements

Water contact angle of chitosan surfaces before and after chemical modification is shown in Figure 2B. Chitosan films ($\theta_w = 64 \pm 2°$) became more hydrophilic after NAC and Sp functionalization ($\theta_w = 37 \pm 2°$ and $49 \pm 1°$, respectively) in contrast with the EDC/NHS modification ($\theta_w = 58 \pm 1°$). After hLF1–11 direct immobilization onto Chit_NAC (Chit_NAC_hLF), the water contact angle increased to $40 \pm 0.1°$ ($p < 0.05$), suggesting peptide immobilization onto the polymer. However, surface wettability was not changed, when hLF1–11 was immobilized to Chit_Sp (Chit_Sp_hLF). hLF1– 11 adsorption onto chitosan was also not detected using this technique.

4.1.3. AFM

Alteration of surface roughness due to the successive chemical modifications on chitosan was analyzed by AFM, as presented in Figure 2C. AFM allowed the observation of peptide incorporation on both NAC- and Sp-modified chitosan, as the root mean square roughness of Chit_NAC_hLF and Chit_Sp_hLF was respectively 41% and 64% higher ($p < 0.05$) than that of the corresponding chitosan modified

substrate. No other significant differences were found between the remaining samples.

4.1.4. IRRAS

IRRAS spectra of chitosan thin films before and after covalent immobilization of NAC and Sp are shown in Figure 4.

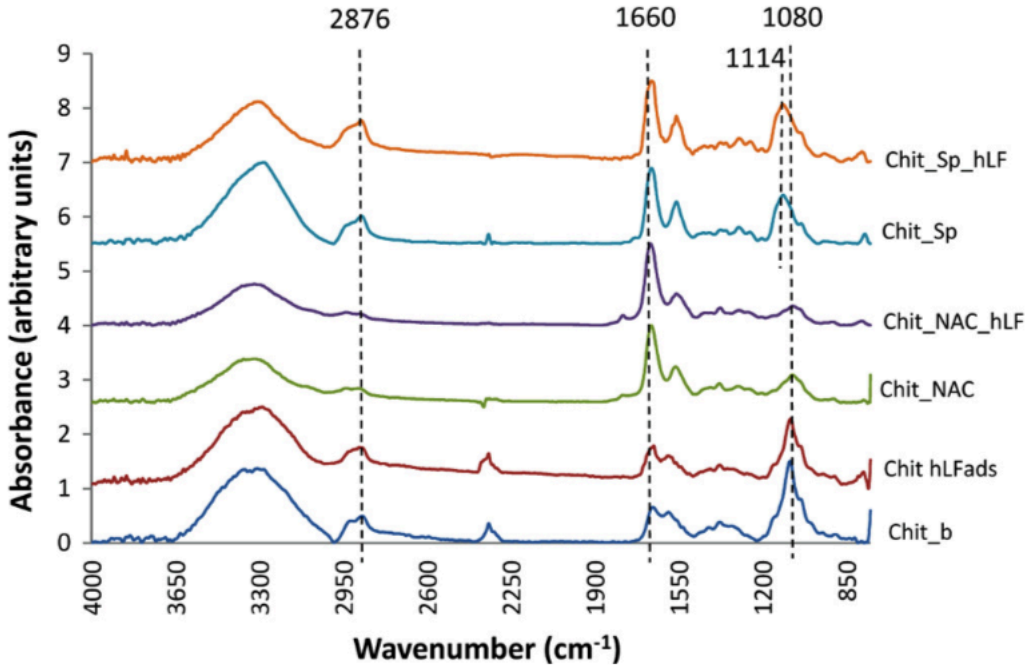

Figure 4. IRRAS spectra of chitosan modified films and hLF1–11 immobilized chitosan films.

The spectrum of chitosan immersed in buffer (Chit_b) allows the identification of the characteristic absorption bands of chitosan, as described elsewhere [25,26,34–36]. After reaction with NAC and Sp, the increase of the characteristic amide I IR absorption (1660 cm^{-1}) confirms the covalent reaction between chitosan free amine groups and the terminal carboxylic groups of NAC or Sp. Chitosan incubated with EDC/NHS reagents also presented a similar peak augmentation (data not shown) in the same region, which is consistent with the mentioned alternative chemical pathway (on Figure 3) involving the formation of an imine intermediate (C=N stretching typically ranges from 1690 to 1630 cm^{-1}) [37]. The C– H stretching peak at 2876cm^{-1} was masked on the Chit_NAC and Chit_NAC_hLF samples, but it was slightly increased in the Chit_Sp sample, as expected from the seven ethylene units

from the polyethylene (PEG) spacer. Sp-modified samples have also shown a slightly deviated peak, from 1080 cm^{-1} to 1114 cm^{-1}, attributed to C–O–C stretching vibration on a straight chain (of the spacer) instead of a glucopyranose ring (of chitosan). Spectra from chitosan thin films obtained after hLF1–11 adsorption or immobilization are shown in Figure 4. In all cases, hLF1–11 peptide could be detected through an increase of the amide I peak (1660 cm^{-1}) characteristic of peptides/proteins. However, chitosan films modified either with NAC or with Sp also display this absorption band. Therefore, to assess hLF1–11 immobilization, a peak height ratio (amide I peak height (1660 cm^{-1})/C–O–C peak height (1080 cm^{-1})) was calculated for NAC-derived samples, since Sp samples have signal overlap at the 1080 cm^{-1} band. A higher peak ratio was found on immobilized peptide samples (4.62) than on the NAC samples (2.71), suggesting peptide immobilization. The slight decrease in the C–O–C vibration peak (1080 cm^{-1}) of chitosan films (Chit_b) after immersion in the hLF1–11 solution (Chit hLFads) also demonstrated that some hLF1–11 was adsorbed or incorporated onto chitosan.

4.1.5. XPS

XPS survey spectra demonstrated the absence of contaminants on the films, since no other elements than the expected ones were detected (data not shown). The relative atomic composition of chitosan films (Chit_b) is in accordance with previous reports [26,36]. XPS *S2p* high-resolution spectra were used to detect chemical modifications, since immobilization reactions were performed using sulfur bonds. Table 1 shows the percentage of *S2p* involved in the different chemical bonds, free thiol groups (163 eV), disulfide (164–165 eV) and oxidized sulfur species (168–169 eV).

Table 1. *S2p* relative surface atomic composition of different chitosan samples.

Chitosan Samples	*S2p*(%)	*S2p* (at.%)		
		~163 eV S-H	164-165 eV S-S	168-169 eV SO_3
Chit_b	0	0	0	0
Chit_EDC/NHS	0	0	0	0
Chit_NAC	0.8	67	0	33
Chit_NAC_hLF	1.7	18	82	0
Chit_Sp	0.9	33	56	11
Chit_Sp_hLF	1.7	18	64	18
Chit hLFads	0	0	0	0

S2p was only detected on covalently modified chitosan films. Peptide immobilization was confirmed by the increase in the total sulfur percentage with regard to the controls (Chit_NAC and Chit_Sp), specifically the sulfur assigned to the establishment of the disulfide bridge (164–165 eV). However, some disulfide bonds were also observed on the Chit_Sp sample, which can be explained by the flexibility and mobility of the SH-terminated spacer chains. Adsorbed hLF was not detected using this technique, since no sulfur was observed on the Chit_hLFads sample. With the exception of Chit_NAC_hLF, some oxidized sulfur was always found, due to its exposition on the surface.

4.1.6. Peptide fluorimetric quantification

A fluorimetric technique was used to assess hLF1–11 surface density: Chit_NAC_hLF 6.4 (±1.4) ng mm^{-2}, Chit_Sp_hLF 4.9 (±0.8) ng mm^{-2} and Chit hLF ads 3.7 (±1.0) ng mm^{-2}. These results present the same tendency observed on the other characterization techniques, although no statistically significant differences were observed between samples.

4.2. Antimicrobial activity characterization

The MIC of the soluble hLF1–11 was 64 µg ml^{-1} for the tested *S. aureus* strain.

Figure 5A shows the non-adherent viable bacteria (supernatant) after contact for 4 h with the different surfaces.

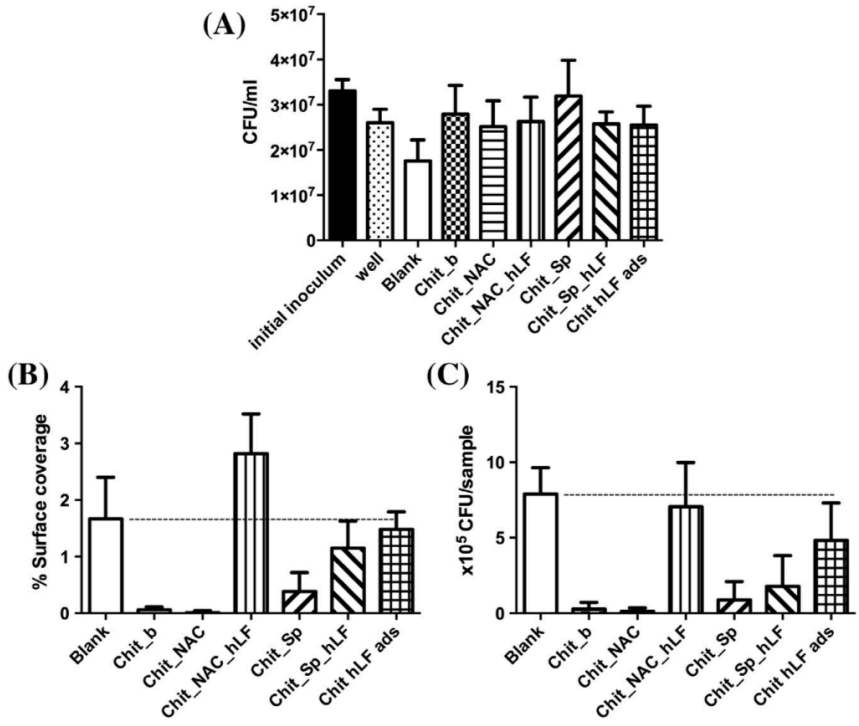

Figure 5. Antimicrobial activity characterization of chitosan-modified films by (A) non-adherent viable bacteria, (B) bacterial adhesion to different substrates in percentage of surface coverage, and (C) viable adherent bacteria on different substrates.

No significant differences were found between the CFUs of the supernatants of wells with and without samples, except for the gold surface (blank) where a decrease in the number of viable bacteria was observed. Comparing between samples, the number of CFUs on the supernatant of the gold surface was only significantly different from Chit_Sp.

Figure 5B shows that, a thin film of chitosan decreases bacterial adhesion to the gold surface (blank). In contrast, the presence of hLF1–11 induced bacterial adhesion to chitosan, particularly when the peptide was directly immobilized on chitosan (Chit_NAC_hLF) (46-fold higher ($p < 0.05$)). When analyzing the viable adhered bacteria (Figure 5C), hLF1–11 incorporation only increased significantly the number of viable bacteria onto chitosan films when the peptide was physically adsorbed onto the surface (Chit hLFads) or immobilized through NAC (Chit_NAC_hLF) ($p < 0.05$). However, although bacteria adhesion on Chit_NAC_hLF was 1.7 times

higher than on the blank surface, the number of viable adherent bacteria between these two surfaces was similar. When hLF1–11 immobilization occurred through a PEG spacer (Chit_Sp_hLF), it was possible to observe a similar surface coverage (Figure 5B) but a much lower number of viable bacteria (80%) than the blank ($p < 0.05$) (Figure 5C).

Figure 6 shows one representative image of the adherent bacteria on each sample.

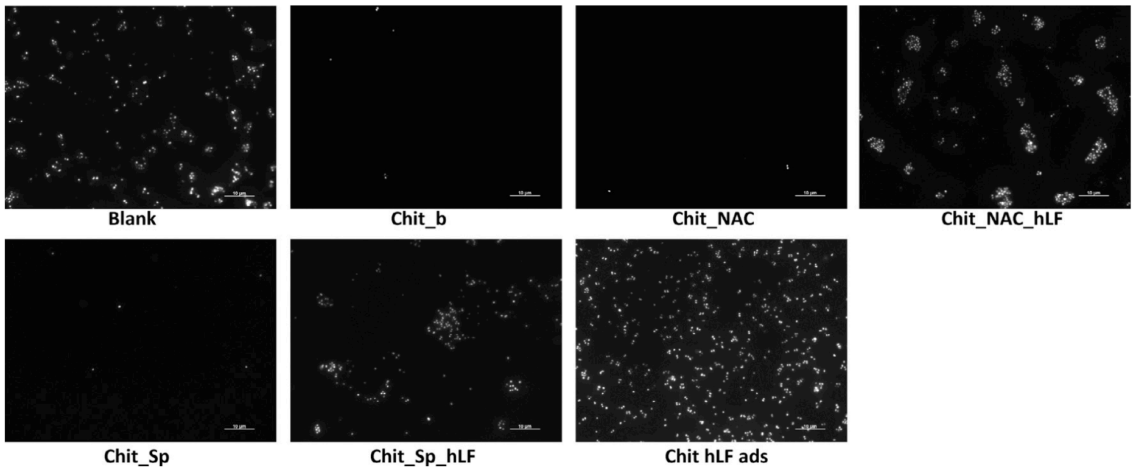

Figure 6. Representative images of the DAPI staining of the total adhered bacteria in the different chitosan-modified surfaces. An inverted fluorescence microscope was used with a magnification of 1000x. Scale bar corresponds to 10 µm.

Bacteria adhesion was uniformly distributed when hLF1–11 was physically adsorbed onto chitosan film. However, when covalently immobilized, adherent bacteria appeared clumped together. These results demonstrated that immobilization of hLF1–11 by its cysteine residue leads to a loss of activity. However, hLF1–11 was still able to attract and bind *S. aureus* and kill about half of adherent bacteria, particularly when immobilized through a spacer.

5. Discussion

In this study, different immobilization parameters (orientation and exposition) were assessed in the covalent immobilization of the hLF1–11 peptide onto chitosan

ultrathin films. *C*-terminal immobilization was chosen to orient the arginine-rich portion of the peptide (associated with the antimicrobial activity [6,7,21]) towards the exterior. Also, two exposition levels (direct link and through a spacer) were tested, in order to assess the best immobilization profile for this particular AMP. Surface characterization using a number of different techniques – ellipsometry, IRRAS, XPS, water contact angle measurements, AFM and fluorimetric peptide quantification – demonstrated that stable chitosan thin films with and without hLF1–11 were successfully produced. Fluorimetric peptide quantification demonstrated that different chemical approaches allowed the modification of chitosan films with similar amounts of peptide (ranging from 3.7 to 6.4 ng mm^{-2}) with different exposure strategies. The covalent immobilization of hLF1–11, either directly or through a spacer, was confirmed by XPS analysis, where the relative content of the *S2p* peak assigned to the disulfide bridge (164–165 eV) was clearly increased. Moreover, ellipsometry, AFM and contact angle measurements offered further support to peptide immobilization. Higher thickness and roughness were consistently observed on surfaces with peptide covalently immobilized, as well as an altered wettability congruent with the chemical modification promoted. Direct hLF1–11 immobilization (Chit_NAC_hLF) was also confirmed by IRRAS due to the rise of the characteristic infrared absorption bands of proteins, in particular, the amide I band. hLF1–11 physical adsorption onto chitosan films was not detected by water contact angle measurements or XPS analysis (no *S2p*). However, a slightly thicker film (17.1 nm) was observed when compared to control chitosan film (14.6 nm) and the slight decrease on the chitosan C–O–C vibration peak at 1080 cm^{-1}, determined by IRRAS, confirms some peptide adsorption.

Antimicrobial activity of soluble hLF1–11 was firstly tested against ATCC 33591 *S. aureus* strain, as this species is the most prevalent in implant-related infections [8,38]. This *S. aureus* strain presented a minimum inhibitory concentration of 64 μg ml^{-1}. This value is higher than that reported elsewhere [5,7,21,39]. However, since MIC values determined by different authors were performed under different conditions, namely different incubation times and initial inoculum, MIC values are mostly difficult to compare. During this work, MICs were calculated using the standard conditions described by Wiegand *et al.* [31].

The non-adherent viable bacteria assay revealed a uniform bacteria concentration over the different surfaces. The exceptions seen were the blank gold surface, and Chit_Sp. The former lower CFU value may be associated with a higher bacterial adhesion onto the surface, and the later higher CFU value may be explained by the non-fouling properties of the PEGylated surface [40,41]. Considering the bacteria adhered to the surfaces, and congruent to previous reports [13,15], bacterial adhesion to chitosan is very low. After chitosan functionalization with NAC and Sp, the values of adhered bacteria remained low. The low bacterial adhesion on Chit_NAC samples can be explained by some oxidation of the cysteine SH group in SO_3^{4-} that, due to its negative behavior, can be responsible for repulsive forces towards the negatively charged bacterial membranes. It was also reported that NAC has an inhibitory effect on the slime formation by *Staphylococcus epidermis* during biofilm formation [42]. Further studies regarding the effect of NAC functionalized chitosan films on bacterial biofilm formation are currently being performed in our laboratory. Chit_Sp has a PEGylated surface, which is well known for its non-fouling properties (i.e. it prevents cell (bacterial or mammalian) adhesion) [40,41]. The incorporation of hLF1–11 onto chitosan films was able to attract and bind bacteria, as expected by the orientation chosen for covalent immobilization (exposing the arginine/positive end). The highest value of adherent bacteria on surfaces where hLF1– 11 was directly immobilized could be related to a more rigid exposition of the arginine portion of the peptide. In the particular cases of Chit_Sp_hLF and Chit hLF ads, the enhancement of bacterial adherence is less pronounced, which may be associated with a more flexible (chit_Sp_hLF) or more random (Chit hLF ads) exposition/orientation of the peptide. Nevertheless, when comparing the bacterial surface coverage with the adhered viable bacteria, it is possible to observe that, besides attracting bacteria, the peptide maintains some antimicrobial activity, which is more evident in the spacer modified sample (similar surface coverage with regard to blank but a much lower number of viable bacteria (80%) ($p < 0.05$)). It remains to elucidate whether a *C*-terminal immobilization without compromising the cysteine residue would have a more significant activity. A number of other studies with immobilized AMPs have approached the issue of AMP exposure [43–49]. For example, Gabriel *et al.* [44] demonstrated that the LL37 peptide bound to titanium

was capable of killing *Escherichia coli* on contact, only when a PEGylated spacer was used. The authors suggested that the use of a long, flexible PEG spacer provided a parallel peptide orientation and lateral mobility that were required for bactericidal activity. Therefore, considering the parameters analyzed, the immobilization of hLF1–11 through a spacer renders the best profile, as it simultaneously attracts and kills bacteria.

Recently, Hilpert *et al.* [50] reported that, in opposition to what was expected, immobilized AMPs that expose their hydrophobic termini exhibit higher antimicrobial activity. It was suggested that the hydrophobic residues could interact with the lipophilic portion of the bacterial membrane, becoming embedded into its surface and destabilizing the packing of the phospholipids. It was also described that tryptophan (W) residues in AMPs could be important for their antimicrobial activity [51], as the aromatic hydrocarbon residues are able to position themselves deeper into the lipid portion of the phospholipid bilayer, making the peptide more efficient in disrupting/destabilizing the bacterial cell membrane [6]. Although the exact mechanism of action of hLF1–11 is still not elucidated, the membrane-induced peptide conformation [52] and high speed of action [53] suggest direct membrane disruption. Therefore, considering an *N*-terminal immobilization of hLF1–11, the hydrophobic end of the peptide would be exposed, which could result on enhanced activity. So the hLF1–11 immobilization chapter is not closed and further studies will allow conclusions to be drawn about the hLF1–11 application in its immobilized form. In view of the above, future work will include new immobilization comparing non-cysteine related *C*-terminal with *N*-terminal orientation through a chemistry that allows a higher yield of immobilized AMP.

6. Conclusion

hLF1–11 covalent immobilization was successfully performed using specific orientation through its *C*-terminal cysteine, with and without a PEG spacer in similar amounts. Chitosan thin films by themselves decreased bacterial adhesion. The functionalization with hLF1–11 increases significantly bacterial adhesion to chitosan

films, particularly when the peptide was covalently coupled without a PEG spacer. However, when a PEG spacer is used, hLF1–11 maintained part of its activity.

Acknowledgements

This work was financed by FEDER funds through the Programa Operacional Factores de Competitividade (COMPETE) and by Portu- guese funds through FCT (Fundação para a Ciência e a Tecnologia) in the framework of the projects: PTDC/CTM/101484/2008; PEst-C/ SAU/LA0002/2013. Fabíola Costa acknowledges FCT, for the PhD grant SFRH/BD/72471/2010. We acknowledge Manuela Brás from SUIM (INEB) for the AFM studies.

References

[1] Zasloff M. Antimicrobial peptides of multicellular organisms. Nature 2002;415:389–95.
[2] Seo MD, Won HS, Kim JH, Mishig-Ochir T, Lee BJ. Antimicrobial peptides for therapeutic applications: a review. Molecules 2012;17:12276–86.
[3] Perron GG, Zasloff M, Bell G. Experimental evolution of resistance to an antimicrobial peptide. Proc Biol Sci 2006;273:251–6.
[4] Costa F, Carvalho IF, Montelaro RC, Gomes P, Martins MC. Covalent immobilization of antimicrobial peptides (AMPs) onto biomaterial surfaces. Acta Biomater 2011;7:1431–40.
[5] Stallmann HP, Faber C, Bronckers AL, de Blieck-Hogervorst JM, Brouwer CP, Amerongen AV, et al. Histatin and lactoferrin derived peptides: antimicrobial properties and effects on mammalian cells. Peptides 2005;26:2355–9.
[6] Gifford JL, Hunter HN, Vogel HJ. Lactoferricin: a lactoferrin-derived peptide with antimicrobial, antiviral, antitumor and immunological properties. Cell Mol Life Sci 2005;62:2588–98.
[7] Lupetti A, Paulusma-Annema A, Welling MM, Senesi S, van Dissel JT, Nibbering PH. Candidacidal activities of human lactoferrin peptides derived from the *N* terminus. Antimicrob Agents Chemother 2000;44:3257–63.
[8] Faber C, Stallmann HP, Lyaruu DM, Joosten U, von Eiff C, van Nieuw Amerongen A *et al.* Comparable efficacies of the antimicrobial peptide human lactoferrin 1–11 and gentamicin in a chronic methicillin-resistant *Staphylococcus aureus* osteomyelitis model. Antimicrob Agents Chemother 2005;49:2438–44.
[9] van der Does AM, Bogaards SJ, Ravensbergen B, Beekhuizen H, van Dissel JT, Nibbering PH. Antimicrobial peptide hLF1–11 directs granulocyte-macrophage

colony-stimulating factor-driven monocyte differentiation toward macrophages with enhanced recognition and clearance of pathogens. Antimicrob. Agents Chemother. 2010;54:811–6.
[10] van der Does AM, Hensbergen PJ, Bogaards SJ, Cansoy M, Deelder AM, van Leeuwen HC, et al. The human lactoferrin-derived peptide hLF1–11 exerts immunomodulatory effects by specific inhibition of myeloperoxidase activity. J Immunol 2012;188:5012–9.
[11] Stallmann HP, de Roo R, Faber C, Amerongen AV, Wuisman PI. In vivo release of the antimicrobial peptide hLF1–11 from calcium phosphate cement. J Orthop Res 2008;26:531–8.
[12] Kazemzadeh-Narbat M, Kindrachuk J, Duan K, Jenssen H, Hancock RE, Wang R. Antimicrobial peptides on calcium phosphate-coated titanium for the prevention of implant-associated infections. Biomaterials 2010;31:9519–26.
[13] Kong M, Chen XG, Xing K, Park HJ. Antimicrobial properties of chitosan and mode of action: a state of the art review. Int J Food Microbiol 2010;144:51–63.
[14] Shi Z, Neoh KG, Kang ET, Poh C, Wang W. Bacterial adhesion and osteoblast function on titanium with surface-grafted chitosan and immobilized RGD peptide. J Biomed Mater Res A 2008;86:865–72.
[15] Carlson RP, Taffs R, Davison WM, Stewart PS. Anti-biofilm properties of chitosan-coated surfaces. J Biomater Sci Polym Ed 2008;19:1035–46.
[16] Hu X, Neoh KG, Shi Z, Kang ET, Poh C, Wang W. An in vitro assessment of titanium functionalized with polysaccharides conjugated with vascular endothelial growth factor for enhanced osseointegration and inhibition of bacterial adhesion. Biomaterials 2010;31:8854–63.
[17] Moutzouri AG, Athanassiou GM. Attachment, spreading, and adhesion strength of human bone marrow cells on chitosan. Ann Biomed Eng 2011;39:730–41.
[18] Kawai T, Yamada T, Yasukawa A, Koyama Y, Muneta T, Takakuda K. Biological fixation of fibrous materials to bone using chitin/chitosan as a bone formation accelerator. J Biomed Mater Res B Appl Biomater 2009;88:264–70.
[19] Lieder R, Darai M, Thor MB, Ng CH, Einarsson JM, Gudmundsson S, et al. In vitro bioactivity of different degree of deacetylation chitosan, a potential coating material for titanium implants. J Biomed Mater Res A 2012;100:3392–9.
[20] Bumgardner JD, Chesnutt BM, Yuan Y, Yang Y, Appleford M, Oh S, et al. The integration of chitosan-coated titanium in bone: an in vivo study in rabbits. Implant Dent 2007;16:66–79.
[21] Nibbering PH, Ravensbergen E, Welling MM, van Berkel LA, van Berkel PH, Pauwels EK, *et al.* Human lactoferrin and peptides derived from its *N* terminus are highly effective against infections with antibiotic-resistant bacteria. Infect Immun 2001;69:1469–76.
[22] Fields GB, Noble RL. Solid phase peptide synthesis utilizing 9-fluorenylmethoxycarbonyl amino acids. Int J Pept Protein Res 1990;35: 161–214.

[23] Collins JM, Leadbeater NE. Microwave energy: a versatile tool for the biosciences. Org Biomol Chem 2007;5:1141–50.
[25] Oliveira JR, Martins MCL, Mafra L, Comes P. Synthesis of an O-alkynyl-chitosan and its chemoselective conjugation with a PEG-like amino-azide through click chemistry. Carbohydr Polym 2012;87:240–9.
[26] Nogueira F, Goncalves IC, Martins MC. Effect of gastric environment on Helicobacter pylori adhesion to a mucoadhesive polymer. Acta Biomater 2013;9(2):5208–15.
[27] Lundin M, Macakova L, Dedinaite A, Claesson P. Interactions between chitosan and SDS at a low-charged silica substrate compared to interactions in the bulk – the effect of ionic strength. Langmuir 2008;24:3814–27.
[28] Castner DG, Hinds K, Grainger DW. X-ray photoelectron spectroscopy sulfur *2p* study of organic thiol and disulfide binding interactions with gold surfaces. Langmuir 1996;12:5083–6.
[29] Martins MC, Ratner BD, Barbosa MA. Protein adsorption on mixtures of hydroxyl- and methyl-terminated alkanethiols self-assembled monolayers. J Biomed Mater Res A 2003;67:158–71.
[30] Smith RE, MacQuarrie R. A sensitive fluorometric method for the determination of arginine using 9,10-phenanthrenequinone. Anal Biochem 1978;90:246–55.
[31] Wiegand I, Hilpert K, Hancock REW. Agar and broth dilution methods to determine the minimal inhibitory concentration (MIC) of antimicrobial substances. Nat Protoc 2008;3:163–75.
[33] Dent A, Aslam M. The preparation of protein-small molecule conjugates. In: Dent A, Aslam M, editors. Bioconjugation: protein coupling techniques for the biomedical sciences. London: Macmillan Reference; 1998. p. 368–75.
[34] Osman Z, Arof AK. FTIR studies of chitosan acetate based polymer electrolytes. Electrochim Acta 2003;48:993–9.
[35] Lawrie G, Keen I, Drew B, Chandler-Temple A, Rintoul L, Fredericks P, *et al.* Interactions between alginate and chitosan biopolymers characterized using FTIR and XPS. Biomacromolecules 2007;8:2533–41.
[36] Amaral IF, Granja PL, Barbosa MA. Chemical modification of chitosan by phosphorylation: an XPS, FT-IR and SEM study. J Biomater Sci Polym Ed 2005;16:1575–93.
[37] Socrates G. Infrared and Raman characteristic group frequencies: tables and charts. 3rd ed. Chichester: John Wiley & Sons Ltd; 2001.
[38] Toms AD, Davidson D, Masri BA, Duncan CP. The management of peri-prosthetic infection in total joint arthroplasty. J Bone Joint Surg Br 2006;88:149–55.
[39] Brouwer CP, Rahman M, Welling MM. Discovery and development of a synthetic peptide derived from lactoferrin for clinical use. Peptides 2011;32:1953–63.

[40] Tsai WB, Chen YH, Chien HW. Collaborative cell-resistant properties of polyelectrolyte multilayer films and surface PEGylation on reducing cell adhesion to cytophilic surfaces. J Biomater Sci Polym Ed 2009;20:1611–28.
[41] Lee Y, Park KM, Bae JW, Park KD. Facile surface PEGylation via tyrosinase-catalyzed oxidative reaction for the preparation of non-fouling surfaces. Colloids Surf B Biointerfaces 2013;102:585–9.
[42] Perez-Giraldo C, Rodriguez-Benito A, Moran FJ, Hurtado C, Blanco MT, Gomez-Garcia AC. Influence of N-acetylcysteine on the formation of biofilm by *Staphylococcus epidermidis*. J Antimicrob Chemother 1997;39:643–6.
[43] Haynie SL, Crum GA, Doele BA. Antimicrobial activities of amphiphilic peptides covalently bonded to a water-insoluble resin. Antimicrob Agents Chemother 1995;39:301–7.
[44] Gabriel M, Nazmi K, Veerman EC, Nieuw Amerongen AV, Zentner A. Preparation of LL-37-grafted titanium surfaces with bactericidal activity. Bioconjug Chem 2006;17:548–50.
[45] Steven MD, Hotchkiss JH. Covalent immobilization of an antimicrobial peptide on poly(ethylene) film. J Appl Polym Sci 2008;110:2665–70.
[46] Bagheri M, Beyermann M, Dathe M. Immobilization reduces the activity of surface-bound cationic antimicrobial peptides with no influence upon the activity spectrum. Antimicrob Agents Chemother 2009;53:1132–41.
[47] Gao GZ, Lange D, Hilpert K, Kindrachuk J, Zou YQ, Cheng JTJ, *et al.* The biocompatibility and biofilm resistance of implant coatings based on hydrophilic polymer brushes conjugated with antimicrobial peptides. Biomaterials 2011;32:3899–909.
[48] Glinel K, Jonas AM, Jouenne T, Leprince J, Galas L, Huck WT. Antibacterial and antifouling polymer brushes incorporating antimicrobial peptide. Bioconjug Chem 2009;20:71–7.
[49] Peyre J, Humblot V, Methivier C, Berjeaud JM, Pradier CM. Co-grafting of amino-poly(ethylene glycol) and Magainin I on a TiO2 surface: tests of antifouling and antibacterial activities. J Phys Chem B 2012;116:13839–47.
[50] Hilpert K, Elliott M, Jenssen H, Kindrachuk J, Fjell CD, Korner J, *et al.* Screening and characterization of surface-tethered cationic peptides for antimicrobial activity. Chem Biol 2009;16:58–69.
[51] Lizzi AR, Carnicelli V, Clarkson MM, Di Giulio A, Oratore A. Lactoferrin derived peptides: mechanisms of action and their perspectives as antimicrobial and antitumoral agents. Mini Rev Med Chem 2009;9:687–95.
[52] Fornili SL, Pizzi R, Rebeccani D. Conformational analysis of a synthetic antimicrobial peptide in water and membrane-mimicking solvents: a molecular dynamics simulation study. Int J Pept Res Ther 2010;16:223–31.
[53] Dijkshoorn L, Brouwer CP, Bogaards SJ, Nemec A, van den Broek PJ, Nibbering PH. The synthetic *N*-terminal peptide of human lactoferrin, hLF(1–11), is highly

effective against experimental infection caused by multidrug-resistant Acinetobacter baumannii. Antimicrob Agents Chemother 2004;48:4919–21.

CHAPTER VI

Dhvar5 antimicrobial peptide (AMP) chemoselective covalent immobilization results on higher antiadherence effect than simple physical adsorption

---

Fabíola M.T.A. Costa [a, b, c], Sílvia R. Maia [d], Paula A.C. Gomes [d, 1], M. Cristina L. Martins [a, b, e]

Biomaterials 2015 52: 531-538

[a] I3S, Instituto de Investigação e Inovação em Saúde, Universidade do Porto, Portugal

[b] INEB, Instituto de Engenharia Biomédica, Universidade do Porto, Rua do Campo Alegre, 823, 4150-180 Porto, Portugal

[c] Universidade do Porto, Faculdade de Engenharia, Porto, Portugal

[d] CIQ-UP, Centro de Investigação em Química da Universidade do Porto, Departamento de Química e Bioquímica, Faculdade de Ciências, Universidade do Porto, Porto, Portugal

[e] Universidade do Porto, Instituto de Ciências Biomédicas Abel Salazar, Porto, Portugal

1. Abstract

Bacterial colonization and subsequent biofilm formation is still one of the major problems associated with medical devices. Antimicrobial peptides (AMP) immobilization onto biomaterials surface is a promising strategy to avoid bacterial colonization. However, a correct peptide orientation and exposure from the surface is essential to maintain AMP antimicrobial activity.

This work aims to evaluate the effect of the immobilization on antibacterial activity of Dhvar5 (LLLFLLKKRKKRKY), an AMP with a head-to-tail amphipathicity. Dhvar5 was linked to thin chitosan coatings in i) a controlled orientation and exposure, testing covalent immobilization of its *N*- or *C*-terminus and using spacers with different lengths and flexibilities or in ii) a random orientation by physical adsorption. Chitosan coating was chosen due to its antimicrobial properties and readiness to be functionalized.

Surface characterization demonstrated the chemoselective immobilization of the peptide with different spacers in a similar concentration (~2 ng/mm^2).

Efficacy assays demonstrated that covalent immobilization of Dhvar5 exposing its cationic end, improves the chitosan coating antimicrobial effect by decreasing Methicillin-resistant *Staphylococcus aureus* (MRSA) colonization. This effect was enhanced when longer spacers were used independently of their flexibility. In opposite, immobilized Dhvar5 exposing its hydrophobic end has no effect on bacterial adhesion to chitosan, and when adsorbed in a random orientation even induces bacterial adhesion to chitosan coating.

Keywords: Antimicrobial peptides, Surface immobilization, Surface characterization, Bacterial adhesion, Chitosan

2. Introduction

Prevention of bacterial adhesion and biofilm formation on the surface of biomaterials remains a serious clinical issue yet unsolved. A number of different coating strategies, either for exposure or release of bactericidal substances (e.g., silver, quaternary ammonium compounds, and classic antibiotics) have been tested along the past years [1-4]. However, the application of such coatings has been limited by associated side-effects, as cytotoxicity, hypersensitivity or the progressive alarming emergence of multi-resistant pathogens.

Antimicrobial peptides (AMP) are a class of promising antibiotic compounds with the major advantages being broad spectrum of activity, high efficiency at low concentrations, fast killing, good cytotoxic profile, and importantly, they rarely promote the rise of bacterial resistance [5,6]. For the majority of these peptides, the mode of action suggested is peptide insertion into bacterial membranes with subsequent cell death induction by, in some cases, cell lysis. Dhvar5 is a synthetic peptide, derived from the histatins family, which are produced by the salivary glands. Dhvar5 is a variant of Dh-5 (histatin 5 active domain, amino acids 11-24) with an *N*- to *C*-terminal amphipathicity. It was firstly described as strongly active against *Candida albicans*, but has also a potent and broad antibacterial activity, even against methicillin-resistant *Staphylococcus aureus* (MRSA) [7-9]. The exact mechanism of action of soluble Dhvar5 is still not fully elucidated. Some cues emerged from the work by Amerongen and co-workers [10,11], where it was demonstrated that Dhvar5 binds to the membrane of yeast cells and induces leakage of intracellular content, but without permanent pore formation. The broad spectrum of Dhvar5, together with its safe cytotoxic profile, prompted its application on osteomyelitis prevention models. However, although the peptide revealed *in vivo* activity, it did not achieve the same treatment levels than gentamicin [12]. This situation may be associated with the pharmacokinetics challenges posed by AMP, as these are prone to undergo proteolytic degradation, self-aggregation and aggregation with plasma proteins. As previously summarized by us [13], covalent immobilization of AMP may offer the answer to such difficulties. Moreover, this strategy prevents the formation of a peptide concentration gradient from the implant surface, avoiding the side-

effects associated with releasing therapies. Still, peptide immobilization is not a straightforward issue, as a number of different parameters should be taken into account, such as proper orientation (*N*- vs. *C*-terminal immobilization) and selection of an adequate spacer/linker (length and flexibility) for an optimal exposure.

3. Materials and methods

3.1. Dhvar5 synthesis and characterization

Peptide Dhvar5 (LLLFLLKKRKKRKY *C*-terminal amide) and its derivatives (Table 1) were produced by Fmoc/tBu solid-phase peptide synthesis methodologies assisted with microwave (MW) energy (Liberty 1 Microwave Peptide Synthesizer, CEM Corporation) [14,15].

Table 1. Dhvar5 derived-peptides for immobilization.

Peptide	Sequence
Dhvar5	LLLFLLKKRKKRKY
Dhvar5-Ct_AHA_C	Dhvar5-(6-amino-hexanoyl)-Cys
C_AHA_Nt-Dhvar5	Cys-(6-amino-hexanoyl)-Dhvar5
C_ABA_Nt-Dhvar5	Cys-(4-aminobutanoyl)-Dhvar5
C_GG_Nt-Dhvar5	Cys-GlyGly-Dhvar5

Dhvar5-derived peptides were produced in order to introduce a terminal cysteine for subsequent immobilization. Different spacers were placed between the additional Cys and the bioactive sequence: 4-aminobutanoic (ABA) and 6-aminohexanoic (AHA) acids were used as flexible spacers of different length, whereas the dipeptide GlyGly (GG) was used as a spacer with comparable length to that of AHA, but lower flexibility, as peptide bonds do not allow the same conformational freedom as that of alkyl chains.

The crude peptides were purified by reverse-phase liquid chromatography and confirmed by High Performance Liquid Chromatography (HPLC) (Hitachi-Merck LaChrom Elite), Liquid Chromatography-Electrospray Ionization/Ion Trap Mass

Spectrometry (LC-ESI/IT MS) (LCQ-DecaXP LC-MS system, ThermoFinnigan). Purified peptides used presented a purity level higher than 90%.

3.2. Dhvar5 surface immobilization

3.2.1. Substrates preparation

Titanium substrates (Ti) were used to represent prosthesis surface and gold substrates (Au) were used due to their higher suitability for some of the surface characterization techniques used, such as ellipsometry and Infrared Reflection-Absorption Spectroscopy Analysis (IRRAS). Ti and Au (1x1 cm^2) were produced, cleaned and characterized according to references [16] and [17], respectively. Briefly, TiO_2 films (50 nm) were deposited on silicon wafers (polished/etched, crystal orientation <100>, from AUREL Gmbh) by ion beam sputtering from a Ti cp target, in the presence of a mixed Ar-O_2 beam coming from the assist gun (15.02% O_2 in Ar). For the Au substrates, chromium (5 nm) and gold (25 nm) layers were deposited by ion beam sputtering from chromium and gold targets (99.9% purity) on silicon wafers (AUREL, Gmbh). Chromium was used to improve gold adhesion to silicon. Both substrates were cleaned with "piranha" solution (7 parts of H_2SO_4 and 3 parts of 30% H_2O_2) for 90 s (Ti) and 5 min (Au) (caution: this solution reacts violently with many organic materials and should be handled with extreme care) and successively rinsed with ethanol, MilliQ water, ethanol and dried with a gentle stream of argon.

3.2.2. Preparation of chitosan ultrathin films

Chitosan ultrathin films were produced as previously described [18]. Briefly, commercial squid pen chitosan (France Chitine) was purified by the re-precipitation method [19] resulting on a molecular weight of 283,000-472,000 with a deacetylation degree (DD%) of ~85%. Chitosan ultrathin films (Ch) were prepared by spin coating (9000 rpm during 1 min; Laurell Technologies Corporation, North Wales) a chitosan solution (0.4% in acetic acid w/v) [20] on the center of the Au substrates. The ultrathin films produced were then neutralized with 0.1 M NaOH and rinsed with

MilliQ water. Each sample was dried with a gentle stream of argon and stored in plastic Petri dishes saturated with argon.

3.2.3. Introduction of SH groups onto chitosan films

Functionalization of chitosan thin films with N-acetyl cysteine (NAC), for introduction of SH groups, was previously optimized by Costa *et al.* [18], through employment of carbodiimide chemistry. Briefly, chitosan thin films were treated with a solution of 0.2 m1-Ethyl-3-[3-dimethylaminopropyl] carbodiimide hydrochloride) (EDC; Sigma-Aldrich), 0.05 m N-hydroxysulfosuccimide (NHS; Sigma-Aldrich) and 25 mM NAC (Merck), in 0.1 m (N-morpholino)ethanesulfonic acid (MES; SigmaeAldrich) buffer at pH 1⁄4 6.5, for 1 h, at 37 C and 100 rpm. The modified films were then rinsed with MilliQ water and immersed 1 min on an ultrasound bath (Bandelin Sonorex Digitec Bath 35 kHz) and rinsed again with MilliQ water.

3.2.4. Peptide immobilization

Dhvar5 immobilization on chitosan thin films was obtained through disulfide bridge formation between the side chain thiol of the terminal cysteine of the peptide and sulfhydryl groups (SH) on pre-functionalized chitosan (Figure 1).

Functionalized chitosan substrates were incubated with 1.5 mg/ml peptide solutions in 10 mM TrisHCl pH=8.0, under oxidative conditions (20% dimethyl sulfoxide (DMSO)) for 18 h at 37ºC and 120 rpm. A control Dhvar5-adsorbed sample was prepared by incubation with a non-functionalized chitosan film in the same reaction conditions.

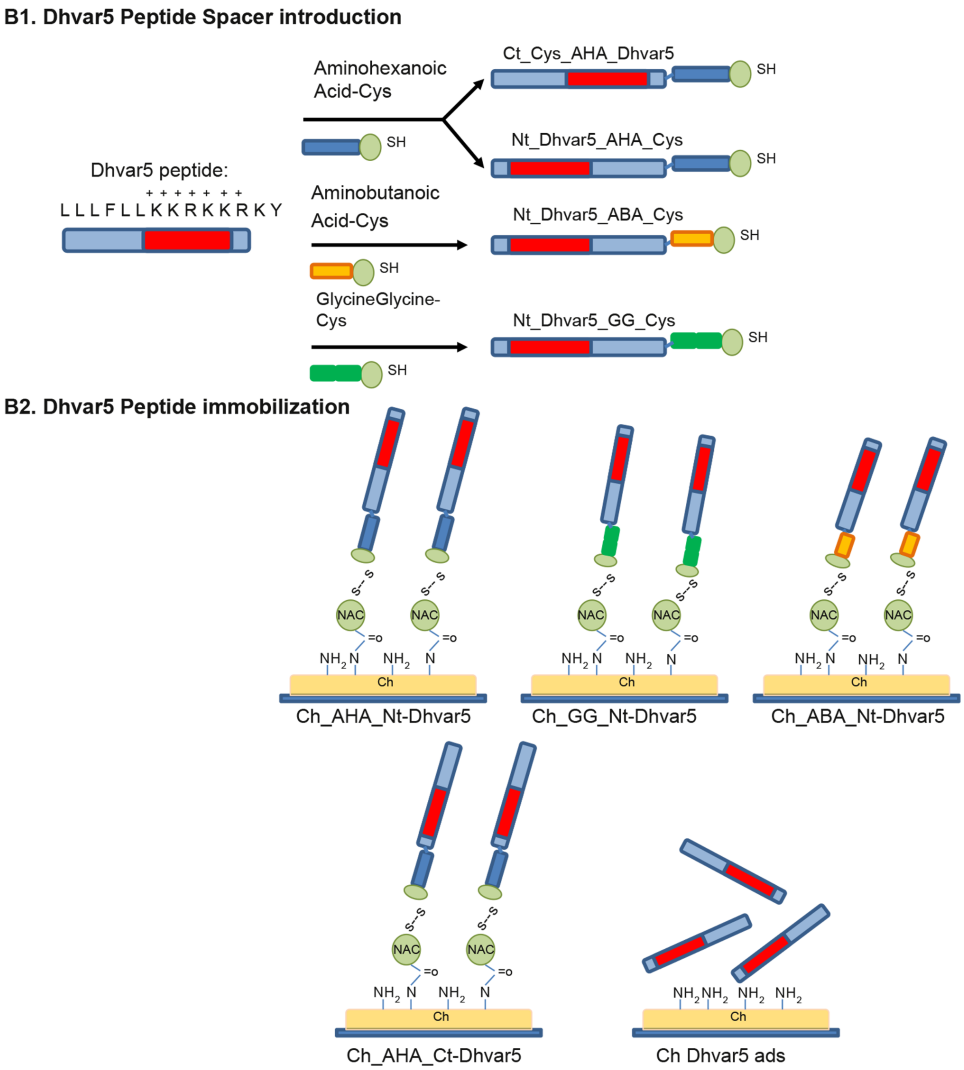

Figure 1. A) Chitosan modification with N-acetyl cysteine (NAC); B1) Dhvar5 peptide spacer introduction; B2) Immobilization of Dhvar5-derived peptides by disulfide bridge formation (a control surface, Ch Dhvar5 ads, was used where peptide was only adsorbed, not covalently bond).

3.3. Surface characterization

3.3.1. FT-IRRAS

Measurements were performed on a Perkin Elmer FTIR spectrophotometer, model 2000, coupled with a VeeMax II Accessory (PIKE) and a liquid-nitrogen-cooled MCT detector. In order to ensure that there was no water vapor adsorption, dry nitrogen was purged into the instrument for 5 min before and during measurement of each sample. For each substrate, a similar gold surface was used as a background.

Incident light was p-polarized and spectra were collected using the 80° grazing angle reflection mode. For each sample, 100 scans were collected with 4 cm^{-1} resolution.

3.3.2. Ellipsometry

Ellipsometry measurements were performed using an imaging ellipsometer, model EP3, from Nanofilm Surface Analysis. This ellipsometer was operated in a polarizer-compensator-sample-analyzer (PCSA) mode (null ellipsometry). The light source was a solid-state laser with a wavelength of 532 nm. The gold substrate refractive index (n=0.5837) and extinction coefficient (k=2.5113) were determined by using a delta and psi spectrum with an angle variation between 65° and 71°. These measurements were made in four zones to correct for any instrument misalignment. The thickness of the chitosan films was determined considering n=1.54 and k=0, for the chitosan film [21]. Results are presented as the average of three measurements on each of two samples.

3.3.3. Water contact angle measurements

Water contact angle measurements were performed using the sessile drop method with a contact angle measuring system from Data Physics, model OCA 15, equipped with a video CCD-camera and SCA 20 software, as described at [17]. After deposition of 4 µl drops of MilliQ water, images were taken every 2 s over 300 s. Droplet profiles were fitted using Younge Laplace formula, to calculate the contact angle. The water contact angle of each substrate was calculated by extrapolating the time dependent curve to zero. Results are the average of three measurements on three independent samples.

3.3.4. Peptide surface density determination

The quantification of the immobilized peptides was performed through colorimetric reaction using 9,10-phenanthrenequinone (PHQ, Fluka), that reacts with arginine

forming a stable compound which gives out fluorescence upon excitation [22]. The protocol used was adapted from Ref. [23]. Substrates were sonicated 1 h in 0.1 M HCl (1 ml) in an ultrasound bath to dissolve the modified chitosan films. Then, 1 ml of each sample solution was added to 3 ml of 3.5 mM PHQ in absolute ethanol, followed by the addition of 0.5 ml of 2 M NaOH. The mixture was then incubated at 30°C for 3 h. Finally, 2.25 ml of 2.4 M HCl was added to stop the reaction. The fluorescence emission was measured using a fluorescence microplate reader (Biotek Synergy Mx Luminometer) using an excitation wavelength of 256 nm, and detecting the emission at 380 nm. The amount of Dhvar5 was calculated based on a calibration curve prepared with standard solutions of free L-arginine (Fluka) and free Dhvar5. Standard solutions of free Dhvar5 were adjusted by quantification at 280 nm in a Thermo Scientific NanoDrop® 1000 spectrophotometer.

3.4. Bacterial assays

3.4.1. Bacterial strains, media and growth conditions

An MRSA strain of *S. aureus* was obtained from the American Type Culture Collection (ATCC 33591). Bacteria were firstly grown on Tryptic Soya Agar (TSA) (Merck) and then overnight on Tryptic Soya Broth (TSB) (Merck) at 37°C, 150 rpm. Bacterial suspensions were adjusted by measuring Optical Density (600 nm). Bacterial numbers were confirmed by a retrospective viable count.

3.4.2. MIC

Minimal Inhibitory Concentration (MIC) was established with a modified broth microdilution method in Mueller Hinton Broth (MHB) [24].

3.4.3. Surface antimicrobial activity characterization

3.4.3.1. Sample preparation

All substrates were washed successively in 70% ethanol and sterile water, and then dried in sterile environment. Samples were then tape glued onto flat-bottomed 24-well cell suspension culture plates (Sarstedt, Ldt, Newton, USA).

3.4.3.2. Surface viability assay

Bacterial solution (10^7 CFU/ml) was added to each well and incubated at 37°C and 150 rpm for 2 h in MHB. Surrounding wells were filled with sterilized deionized water, in order to avoid medium evaporation. Substrates were rinsed with 0.9% NaCl sterile solution, and then stained with a combination dye of the LIVE/DEAD® Bacterial Viability Kit (Baclight™) for 15 min in the dark. Briefly, the kit contains two fluorescent dyes, Syto9 which stains all bacteria in green, and propidium iodide (PI) which can only crossover damaged cells membranes and gives red stained cells. Thus, because PI quenches the fluorescent emission of Syto9, it is assumed that green cells are alive whereas red cells are dead. Images were obtained with an inverted fluorescence microscope (Axiovert 200M, Zeiss, Germany). For quantifying the viability of adherent bacteria, eight fields on each of triplicate replicates were obtained with a 1000x magnification, corresponding to a net area of about 0.1181 mm^2/sample. The bacteria count was performed using the manual counting software included in ImageJ software.

3.4.3.3. Long-term surface adhesion assay

Bacterial solution (10^7 CFU/ml) in MHB was added to each well containing the substrates. Cells were allowed to adhere for 2 h at 37°C and 120 rpm. Non-adherent bacteria were removed by washing three times with PBS at 120 rpm for 5 min. Thereafter, samples were placed on a new 24-well plate and incubated with fresh MHB for 24 h at 37°C and 120 rpm. Again, all unused wells were filled with sterilized deionized water, in order to avoid medium evaporation. At this point samples were rinsed with PBS, and fixed with 4% (w/v) paraformaldehyde solution (Merck) for 20 min. Samples were rinsed again with PBS and stained with VECTASHIELD® Mounting Medium with DAPI (40,6-diamidino-2-phenylindole; Vector). DAPI bound to bacterial

DNA is excited at about 360 nm and emits at about 460 nm, resulting on blue fluorescence. Images were obtained with an inverted fluorescence microscope (Axiovert 200M, Zeiss, Germany). The quantification of adhered bacteria was performed as previously explained.

3.4.3.3.1. Growth inhibition assay

After the 24 h incubation period, supernatants were successively diluted and plated in triplicate on TSA. Before counting the colonies, plates were incubated at 37°C for 18 h.

3.5. Statistical analysis

Statistical analysis was performed using One-way ANOVA with Bonferroni multiple comparison post-hoc test. When Gaussian distribution was not confirmed, non-parametric test Kruskal-Wallis was applied using the Graphpad Prism pro- gram. Data is expressed as the mean ± standard deviation (SD) and p values of <0.05 were considered significant.

4. Results

4.1. Surface characterization

Control and Dhvar5-modified surfaces were analyzed by ellipsometry, water contact angle measurement, FT-IRRAS and fluorimetric assays.

4.1.1. Ellipsometry

The spin-coating process resulted on chitosan ultrathin films of 9.3 ± 1.0 nm, which remained stable even after the reaction protocols, as there were no thickness changes between freshly made films and buffer-incubated films (Ch_b) (data not shown). Figure 2A presents chitosan films thickness before and after surface modification.

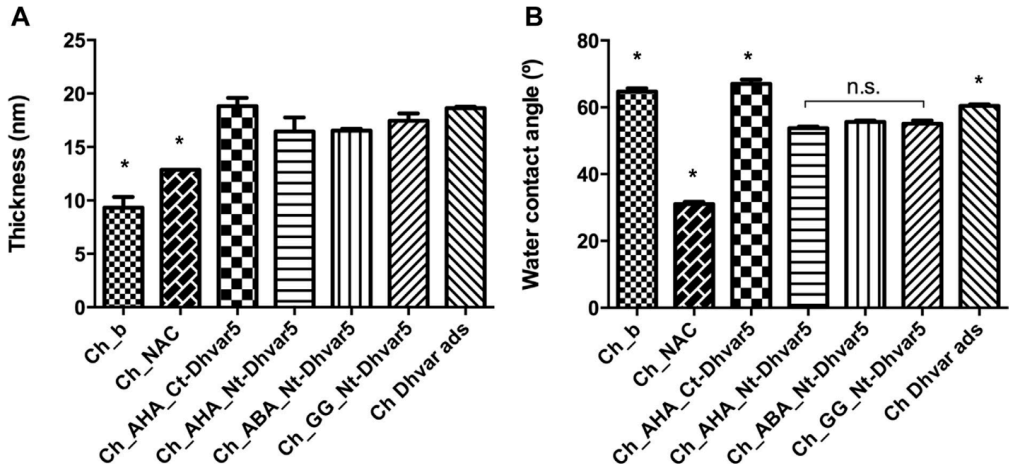

Figure 2. A) Ellipsometry analysis of the chitosan and chitosan-functionalized films; B) Water optical contact angles of chitosan and chitosan-functionalized films.
* Statistically different from all other samples ($p < 0.05$) (non-parametric Kruskal-Wallis test).

The thickness of the chitosan films (Ch_b) was augmented after functionalization with NAC (Ch_NAC). The significant increase of the Ch_NAC film thickness after incubation with Dhvar5, supports the success of peptide attachment. Also, a similar increase was observed on Ch film after its incubation with Dhvar5 solution (Ch_Dhvar5_ads), suggesting peptide adsorption to the film. No significant difference was observed between the distinct orientations and spacers applied.

4.1.2. Water optical contact angle (OCA) analysis

Water optical contact angles of the control and modified Ch films are presented on Figure 2B. The incorporation of NAC on Ch films increased significantly the hydrophilicity of the film decreasing the water contact angle from 65° to 31°. After Dhvar5 binding by its C-terminus (exposition of the more hydrophobic portion of the peptide) the water contact angle increases (θ_w=67°). On the other hand, all Nt-Dhvar5 immobilized samples showed a more hydrophilic behavior (θ_w=54-56°) than Ch_b, consistent with the immobilization of the peptide exposing its positively charged amino acids. No significant difference was observed between the samples with peptide immobilized by its N-terminus. Ch_Dhvar5_ads presented a water contact angle lower than Ch_b. Its value (θ_w=60°) is between the surfaces with

peptide immobilized by its N-terminus and its C-terminus, suggesting some adsorbed peptide in a random orientation.

4.1.3. FT-IRRAS

FT-IRRAS results of the chitosan thin films, before and after immersion on buffer solution, showed that the films remained stable even after chemical procedures (Data not shown). FT-IRRAS analysis of Dhvar5 immobilized onto chitosan showed very similar spectra, therefore Figure 3A depicts spectra of control Ch (Ch_b), and a representative spectrum of Dhvar5 immobilized onto Ch films.

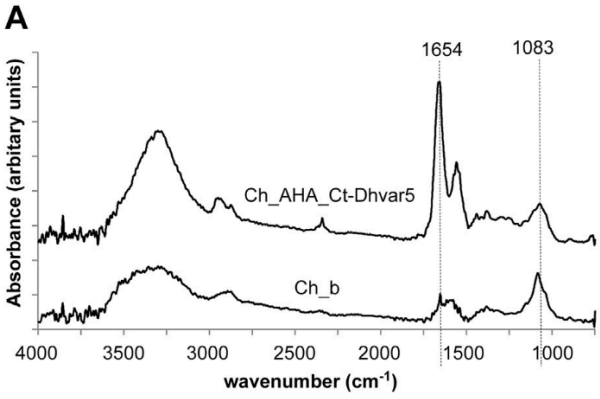

B

Ch modified films	Peak height ratio
Ch Dhvar5 ads	1.7
Ch_NAC	3.8
Ch_AHA_Ct-Dhvar5	5.2
Ch_AHA_Nt-Dhvar5	5.4
Ch_ABA_Nt-Dhvar5	5.4
Ch_GG_Nt-Dhvar5	5.9
Ch_b	0.62

Figure 3. A) FT-IRRAS spectra of Ch and a representative spectrum of Dhvar5 covalently immobilized onto Ch film (Ch_AHA_Ct-Dhvar5); B) Peak height ratio (amide I peak (1654 cm^{-1})/C-O-C peak (1083 cm^{-1})) of modified Ch films.

Ch_b spectrum allowed the identification of characteristic absorption bands of chitosan, as previously described [19,20,25-27]. After Ch functionalization with NAC, an increase of amide I absorption band (1654 cm^{-1}) was observed. This is consistent with the carbodiimide-mediated coupling reaction applied, leading to formation of an amide bond between free amine groups in Ch and the carboxylic groups of NAC. Subsequent covalent immobilization of Dhvar5-derived peptides also implies an increase of amide I band, characteristic of peptides/proteins. To assess Dhvar5 immobilization, a peak height ratio (amide I peak height (1654 cm^{-1})/C-O-C glucopyranose peak height (1083 cm^{-1})) was calculated (Figure 3B). As expected, the aforementioned ratio increased in the following order: Ch_b < Ch_NAC < Ch films

with covalently bound Dhvar5. All samples with covalently immobilized peptide presented a nearly identical ratio that was around 1.5 fold higher than Ch_NAC and about 3 fold higher than Ch_Dhvar5_ads. Altogether, FT-IRRAS results clearly support the success of the covalent immobilization chemistry applied.

4.1.4. Peptide quantification

The average surface peptide density is presented on Table 2.

Table 2. Dhvar5 surface density evaluation, based on fluorescent intensities.

Ch modified films	Dhvar5 surface density (ng/mm^2)
Ch_AHA_Ct-Dhvar5	2.4 ± 0.7
Ch_AHA_Nt-Dhvar5	1.5 ± 0.0[a]
Ch_ABA_Nt-Dhvar5	2.1 ± 0.4
Ch_GG_Nt-Dhvar5	1.8 ± 0.2
Ch Dhvar5 ads	4.0 ± 0.9[a]

[a] Statistically different from each other ($p<0.05$) (non-parametric Kruskal-Wallis test)

The average surface density was similar between all Ch films with covalently bound Dhvar5 (~2.0 ng/mm^2). The film with adsorbed Dhvar5 (Ch_Dhvar5_ads), although with a higher density (4.0 ng/mm^2), was not significantly different from the covalently immobilized samples, with the exception of Ch_AHA_Nt-Dhvar5.

4.2. Antimicrobial activity characterization

Dhvar5 antimicrobial activity was firstly assessed in solution, by an adaptation of the microtiter broth dilution method proposed elsewhere [24,28]. *S. aureus* strain used presented a MIC of 0.5 μg/ ml.

4.2.1. Viability assays

Viability of bacteria attached to the surfaces was evaluated using LIVE/DEAD® Bacterial Viability Kit (Baclight™). Figure 4A presents the average number of bacteria per mm^2 of each surface sample, after 2 h incubation at 37ºC.

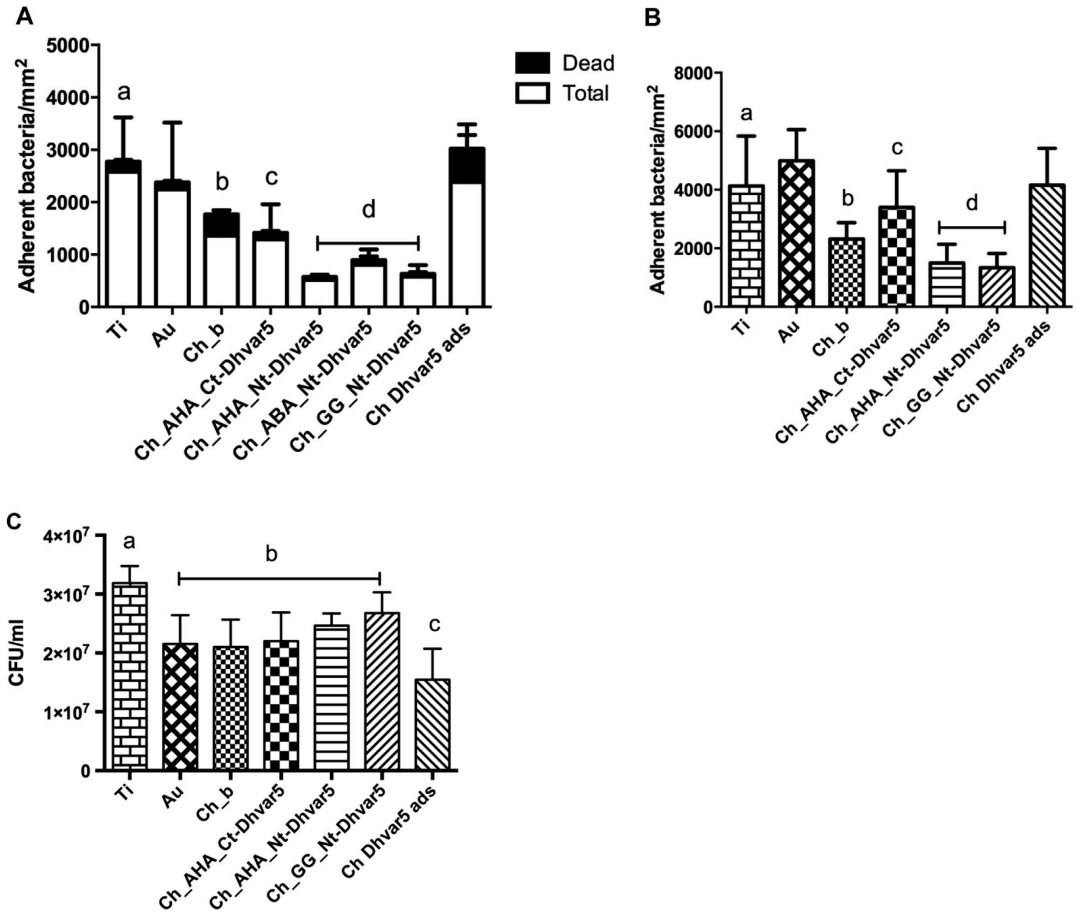

Figure 4. A) Viability of adhered *S. aureus* incubated at 37ºC for 2 h a) statistically different from all Ch samples with the exception of Ch Dhvar5 ads ($p<0.05$); b) statistically different from Ch_AHA_Nt-Dhvar5, Ch_GG_Nt-Dhvar5 and Ch_Dhvar5_ads ($p<0.05$); c) statistically different from Ch_AHA_Nt-Dhvar5, Ch_GG_Nt-Dhvar5 and Ch Dhvar5 ads ($p<0.05$); d) not statistically different; B) Total *S. aureus* adherence to surfaces after 24 h incubation period of pre-adhered inoculum. a) statistically different from Ch_b, Ch_AHA_Nt-Dhvar5, Ch_GG_Nt-Dhvar5 ($p<0.05$); b) statistically different from Ch_AHA_Ct-Dhvar5, Ch_GG_Nt-Dhvar5 and Ch Dhvar5 ads ($p<0.05$); c) statistically different from Nt-immobilized Dhvar5 ($p<0.05$); d) not statistically different; C) Number of CFU/ml found on the supernatants after a 24 h period of incubation. a) statistically different from all surfaces with the exception of Ch_GG_Nt-Dhvar5 and Ch_NAC ($p < 0.05$); b) not statistically different from each other; c) statistically different from all surfaces with the exception of Au and Ch_b (One-Way ANOVA analysis).

Regarding total adhered bacteria, control samples (Ti and Au) exhibited high values, whereas Ch coating (Ch_b) promoted a reduction of around 40% (47% comparing to

Ti and 39% comparing to Au). This result was expected, since we previously demonstrated the antimicrobial properties of this chitosan ultrathin films [18]. Remarkably, films with adsorbed peptide (Ch_Dhvar5_ads) did not significantly differ from Ti neither from Au in total adhered bacteria, demonstrating that the adsorbed Dhvar5 induced bacterial adhesion to chitosan film. In opposite, samples with peptide covalently immobilized through its N-terminus exhibited a marked decrease as compared to Ti, reaching an ~80% reduction when a longer spacer was used (Ch_AHA_Nt-Dhvar5 and Ch_GG_Nt- Dhvar5) ($p < 0.05$). These two Dhvar-bearing surfaces did not significantly differ from each other and revealed an anti-adherence behavior ~62% plus effective than that of Ch_b. In turn, C-terminus immobilization of Dhvar5 did not significantly differ from control Ch_b film regarding anti-adherence properties. Hence, these results clearly show that, amongst all surfaces analyzed, those coated with Ch covalently bound to Dhvar5 through a longer spacer and exposing the more hydrophilic and cationic end of the peptide were the best suited to avoid bacterial colonization.

It was also observed that most of the adhered bacteria were not dead, in all surfaces. Still, N-terminally immobilized Dhvar5 exhibited a total number of live adhered bacteria two-fold lower than Ch_b samples and five-fold lower than Ti substrates.

4.2.2. Long-term anti-adherence assays

The objective of this assay was to verify if the live adhered bacteria would proliferate if time and proper nutritional conditions were given. For that, surfaces with the 2 h incubation resulting adherent bacteria were immersed on fresh medium for 24 h. The results are presented in Figure 4B.

Ti and Au exhibited a similar and high number of adhered bacteria that allowed an increase of the number of adherent bacteria on their surfaces regarding to the initial adherent bacteria (~2000 bacteria/mm^2). Similar results were obtained for Ch_Dhvar5_ads. Ch films with immobilized Dhvar5 by its N-terminus presented the lowest bacterial adhesion levels (~70% and ~40% reduction as compared to Ti and Ch_b, respectively). However, these surfaces were not able to completely avoid

bacterial proliferation, since there is an increase of the adherent bacteria during incubation (24 h). Ch coating and Ch_Dhvar5_ads were the surfaces that allowed the lowest proliferation. However, the number of adherent bacteria on these surfaces was very high.

Growth inhibition assays of the supernatants of the long-term incubation experiments are depicted on Figure 4C.

Ti substrates presented the highest value of CFU/ml, which adding to the high amount of adhered bacteria at the substrate (see Figure 4B), confirms its lack of antimicrobial activity. No significant difference was found between Au, Ch_b and surfaces with immobilized Dhvar5. Ch_Dhvar5_ads was the substrate that contributed to the lowest number of CFU/ml in the supernatant, which may be related to elution of the peptide into the MHB.

5. Discussion

Dhvar5 presented a promising MIC of 0.5 μg/ml against a methicillin-resistant *S. aureus* (MRSA) that is lower than the reported elsewhere [8,9,12,29,30]. However, direct comparison of such values is very difficult, as a result of the lack of universal standardized methods to assess AMP activity, besides the use of different *S. aureus* strains. We chose to use the standard conditions already proposed by Wiegand *et al*., [24].

In this study, Dhvar5 was covalently immobilized onto chitosan thin films in order to evaluate if this strategy is able to prevent bacterial adhesion in a sustainable way. Different immobilization parameters were tested, to assess the immobilization profile that would most contribute to such goal. Different surface characterization techniques - ellipsometry, FT-IRRAS, OCA and fluorimetric peptide quantification - confirmed the production of stable chitosan thin films, with a chemoselective covalent immobilization of the peptide in different orientations. The stability of chitosan films was confirmed using ellipsometry and FT-IRRAS. Ellipsometry measurements demonstrated a clear thickness increase of Dhvar5-modified chitosan films comparing to controls (Ch_b and Ch_NAC). However, such analysis alone did

not prove the covalent immobilization of the peptide, nor its proper orientation. Demonstration of the covalent immobilization of the peptide was suggested by FT-IRRAS analysis, namely through comparison of the amide I peak height (1654 cm^{-1})/C-O-C glucopiranose peak height (1083 cm^{-1}) ratio, that was clearly increased when Dhvar5 was covalently bound to chitosan, as compared to NAC-functionalized chitosan and Ch_Dhvar5_ads. The peak height ratio was also increased on Ch_Dhvar5_ads comparing to unmodified chitosan. In this case the amide I peak is related to the peptide bonds of the adsorbed peptide and not to the covalent immobilization amide bond, noticeable by a lower peak ratio increase. Regarding the specificity of the immobilization orientation, useful information was brought by OCA measurements. NAC-functionalized chitosan films became significantly more hydrophobic (2.1 fold) upon immobilization of Dhvar5 through its C-terminus (Dhvar5 hydrophobic portion exposed) and only 1.7 fold more hydrophobic when immobilization was made through the N-terminus of the peptide (cationic residues exposed). OCA also enabled the confirmation of Dhvar5 adsorption, by the small but significant contact angle shift in Ch_Dhvar5_ads comparing to Ch_b. This shift may be the result of multiple orientations of the adsorbed peptide, rather than one preferential orientation established by the covalently immobilization process, as also proposed by Chen *et al.,* [31].

Antimicrobial activity of control and peptide-bearing surfaces was assessed through two levels of stringency: adhesion and viability after 2 h of incubation, and after long-term incubation (24 h). All Dhvar5 modified surfaces presented a significant bacterial adhesion reduction when compared to Ti and chitosan with the exception of Dhvar5 adsorbed sample. Interestingly, the adsorbed strategy exhibited an amount of adhered bacteria quite similar to controls (Ti and Au). Also, Williams *et al.* [32], reported a study where contact lenses with adsorbed lactoferrin exhibited a high adherence of *Pseudomonas aeruginosa.*

Covalently immobilized Dhvar5 resulted in different profiles depending on the exposed peptide terminus. C-terminally immobilized Dhvar5 maintained the level of bacterial adhesion of Ch_b after 2 h incubation, but had a higher number of adhered bacteria on 24 h incubation. This suggests that in a long-term incubation, exposure of the hydrophobic portion of the peptide masks Ch_b intrinsic activity, resulting in

unwanted adhesion. In opposite, N-terminally immobilized Dhvar5 have the lowest bacterial adhesion in both incubation periods. However, the viability of adhered bacteria was high independent of the terminus used for immobilization, suggesting that we have a stronger anti-adherence rather than antimicrobial effect. Confronting the levels of surface-adhered bacteria with those of free bacteria at the supernatants, we came to the conclusion that, in the absence of surface coating (i.e., on the Ti control), a high number of bacteria is found both at the surface and in solution. In turn, all the chitosan-coated surfaces, with or without further modification, presented similar amounts of free bacteria at the supernatants, which do not correlate with the respective lower amount of surface-adhered bacteria. Nevertheless, the high amount of bacteria at the supernatant may be the result of the proliferation of planktonic bacteria that were never in contact with the surfaces.

The lowest CFU count found in supernatants regards the surface with adsorbed Dhvar5, presumably as the result of peptide elution to the bulk phase. However, this result loses relevance given the ~70% increase of adhered bacteria in this sample, as compared with best performing Dhvar5-grafted surfaces.

Recently, Chen *et al.* [33], reported that melimine, a 28mer peptide with an N-terminus hydrophobic domain and cationic C-terminus, presented higher antimicrobial activity with a clear anti-adherence effect when immobilized through its N-terminus, exposing the cationic domain away from the substrate. This comes in accordance with our results. In contrast to these results, Hilpert *et al.* [34], found that immobilized AMP exposing their hydrophobic termini exhibited higher bactericidal activity. They stated that the hydrophobic domain should be free to be able to interact with the lipophilic portion of the bacterial membrane. However, they used a peptide library that did not include peptides with a clear 'head-to-tail' amphipathicity, but rather a conformation-dependent amphipathicity. Indeed, they hypothesized that a concentration of cationic residues on the exposed terminus could similarly lead to high antimicrobial activity.

Within the N-terminal immobilizations, differential anti-adherence effects were obtained depending on the length of the spacer applied. It was clear that longer spacer (AHA or GG) had better results than shorter (ABA) spacers. The two longer spacers had very similar results, suggesting that, with this particular peptide, spacer

length is more important than spacer flexibility. Bagheri *et al.* [35], demonstrated the importance of a longer spacer on AMP antimicrobial activity. Nevertheless, reports diverge in their general conclusion about the specific characteristics of the applied spacer, suggesting that it may be peptide-dependent. More recently, Bagheri *et al.* [36], tried to assess whether the mechanism of action of soluble AMP could be relevant for the correct configuration of immobilization. To that end, those authors chose different AMP with distinct putative mechanisms of action, and tested them after different tethering approaches. Overall, they concluded that peptides with intracellular targets lose activity upon covalent immobilization whereas the behavior of membrane-permeabilizing peptides depend on their amphipathicity distribution. Thus, the activity of covalently immobilized peptides whose amphipathicity is conformation-dependent (as the KLAL model peptide) is not significantly affected by the orientation of immobilization. On the other hand, peptides with sequence-based amphipathicity (as melittin) should be covalently immobilized through the position farthest away from the hydrophobic domain. In other words, these authors concluded that membrane-active AMP should have their hydrophobic domain exposed in order to insert into the bacterial lipid bilayer. As reported by Ruissen *et al*., [10], Dhvar5 can cause cytoplasmic membrane depolarization suggestive of membranolytic activity, but not through permanent pore formation. This mechanism of action, in addition to the sequence-based amphipathicity of Dhvar5, would suggest that its optimal immobilization position should be through the C-terminus, as this would result on greater exposition of the hydrophobic domain. However, this does not correlate with our results, nor with the aforementioned report by Chen *et al*., in Ref. [33]. Our results demonstrated that immobilized Dhvar5 lost part of their antimicrobial effect against *S. aureus* independently of their immobilization orientation. Nevertheless, immobilization by the N-terminus, exposing the cationic part, demonstrates a high anti-adhesive effect. These apparently contradictory findings highlight the little that is known about the mechanisms of action of AMP, mostly immobilized ones, suggesting once again that soluble and immobilized AMP may not share the same mechanism of action, as recently proposed by Kizhakkedathu *et al.,* [37]. Therefore, each individual AMP must be carefully studied

regarding main parameters of immobilization towards creation of effective antifouling coatings, as herein reported for Dhvar5.

6. Conclusions

Dhvar5 covalently immobilized onto a chitosan thin coating by the N-terminus (exposing the cationic end), improves the antimicrobial effect of the coating by decreasing *S. aureus* colonization. This effect was enhanced when longer spacers were used independently of its flexibility. In opposition, Dhvar5 covalent immobilization by the C-terminus did not change bacterial adhesion to chitosan and Dhvar5 physically adsorbed even induced bacterial adhesion to chitosan coatings.

This work demonstrated that, after surface immobilization, the exposition of the cationic end of this amphipathic peptide (Dhvar5) is fundamental to create antimicrobial surfaces by avoiding bacterial colonization.

Acknowledgments

This work was financed by FEDER funds through the Programa Operacional Factores de Competitividade (COMPETE) and by Por- tuguese funds through FCT (Fundação para a Ciência e a Tecnologia) in the framework of the projects: PTDC/CTM/101484/2008; PEst-C/ SAU/LA0002/2013; Pest-C/QUI/UI0081/2013. Fabíola Costa acknowledges FCT for the PhD grant SFRH/BD/72471/2010.

References

[1] Norowski Jr PA, Bumgardner JD. Biomaterial and antibiotic strategies for peri-implantitis: a review. J Biomed Mater Res B Appl Biomater 2009;88:530-43.

[2] Bazaka K, Jacob MV, Crawford RJ, Ivanova EP. Efficient surface modification of biomaterial to prevent biofilm formation and the attachment of microorganisms. Appl Microbiol Biotechnol 2012;95:299-311.

[3] Glinel K, Thebault P, Humblot V, Pradier CM, Jouenne T. Antibacterial surfaces developed from bio-inspired approaches. Acta Biomater 2012;8:1670-84.

[4] Banerjee I, Pangule RC, Kane RS. Antifouling coatings: recent developments in the design of surfaces that prevent fouling by proteins, bacteria, and marine organisms. Adv Mater 2011;23:690-718.

[5] Zasloff M. Antimicrobial peptides of multicellular organisms. Nature 2002;415:389-95.

[6] Seo MD, Won HS, Kim JH, Mishig-Ochir T, Lee BJ. Antimicrobial peptides for therapeutic applications: a review. Molecules 2012;17:12276-86.

[7] Ruissen AL, Groenink J, Helmerhorst EJ, Walgreen-Weterings E, Van't Hof W, Veerman EC, *et al.* Effects of histatin 5 and derived peptides on *Candida albicans*. Biochem J 2001;356:361-68.

[8] Stallmann HP, Faber C, Bronckers AL, de Blieck-Hogervorst JM, Brouwer CP, Amerongen AV, *et al.* Histatin and lactoferrin derived peptides: antimicrobial properties and effects on mammalian cells. Peptides 2005;26:2355-59.

[9] Lyaruu DM, Van T, Hof W, Veerman EC, Burger EH, Amerongen AVV. Anti-bacterial activity of human saliva histatin analogues against methicillin-resistant *S. aureus* (MRSA). J Dent Res 2000;79:227.

[10] Ruissen AL, Groenink J, Van't Hof W, Walgreen-Weterings E, van Marle J, van Veen HA, *et al*. Histatin 5 and derivatives. Their localization and effects on the ultra-structural level. Peptides 2002;23:1391-99.

[11] den Hertog AL, Sang HWWF, Kraayenhof R, Bolscher JGM, Van't Hof W, Veerman ECI, *et al.* Interactions of histatin 5 and histatin 5-derived peptides with liposome membranes: surface effects, translocation and permeabilization. Biochem J 2004;379:665-72.

[12] Faber C, Hoogendoorn RJ, Stallmann HP, Lyaruu DM, Van Nieuw Amerongen A, Wuisman PI, *et al. In vivo* comparison of Dhvar-5 and gentamicin in an MRSA osteomyelitis prevention model. J Antimicrob Chemother 2004;54:1078-84.

[13] Costa F, Carvalho IF, Montelaro RC, Gomes P, Martins MC. Covalent immobilization of antimicrobial peptides (AMPs) onto biomaterial surfaces. Acta Biomater 2011;7:1431-40.

[14] Fields GB, Noble RL. Solid phase peptide synthesis utilizing 9-fluorenylmethoxycarbonyl amino acids. Int J Pept Protein Res 1990;35: 161-214.

[15] Collins JM, Leadbeater NE. Microwave energy: a versatile tool for the bio-sciences. Org Biomol Chem 2007;5:1141-50.

[16] Sousa SR, Moradas-Ferreira P, Saramago B, Melo LV, Barbosa MA. Human serum albumin adsorption on TiO_2 from single protein solutions and from plasma. Langmuir 2004;20:9745-54.

[17] Martins MC, Ratner BD, Barbosa MA. Protein adsorption on mixtures of hydroxyl- and methyl-terminated alkanethiols self-assembled monolayers. J Biomed Mater Res A 2003;67:158-71.

[18] Costa F, Maia S, Gomes J, Gomes P, Martins MC. Characterization of hLF1-11 immobilization onto chitosan ultrathin films, and its effects on antimicrobial activity. Acta Biomater 2014;10:3513-21.

[19] Oliveira JR, Martins MCL, Mafra L, Gomes P.Synthesis of an O-alkynyl-chitosan and its chemoselective conjugation with a PEG-like amino-azide through click chemistry. Carbohyd Polym 2012;87:240-49.

[20] Nogueira F, Goncalves IC, Martins MC. Effect of gastric environment on *helicobacter pylori* adhesion to a mucoadhesive polymer. Acta Biomater 2013;9: 5208-15.

[21] Lundin M, Macakova L, Dedinaite A, Claesson P. Interactions between chitosan and SDS at a low-charged silica substrate compared to interactions in the bulk - the effect of ionic strength. Langmuir 2008;24:3814-27.

[22] Smith RE, MacQuarrie R. A sensitive fluorometric method for the determination of arginine using 9,10-phenanthrenequinone. Anal Biochem 1978;90: 246-55.

[23] Kazemzadeh-Narbat M, Kindrachuk J, Duan K, Jenssen H, Hancock RE, Wang R. Antimicrobial peptides on calcium phosphate-coated titanium for the prevention of implant-associated infections. Biomaterials 2010;31: 9519-26.

[24] Wiegand I, Hilpert K, Hancock RE. Agar and broth dilution methods to determine the minimal inhibitory concentration (MIC) of antimicrobial substances. Nat Protoc 2008;3:163-75.

[25] Osman Z, Arof AK. FTIR studies of chitosan acetate based polymer electrolytes. Electrochim Acta 2003;48:993-99.

[26] Lawrie G, Keen I, Drew B, Chandler-Temple A, Rintoul L, Fredericks P, *et al.* Interactions between alginate and chitosan biopolymers characterized using FTIR and XPS. Biomacromolecules 2007;8:2533-41.

[27] Amaral IF, Granja PL, Barbosa MA. Chemical modification of chitosan by phosphorylation: an XPS, FT-IR and SEM study. J Biomat SciPolym E 2005;16: 1575-93.

[28] Bradbury T, Fehring TK, Taunton M, Hanssen A, Azzam K, Parvizi J, *et al.* The fate of acute methicillin-resistant *Staphylococcus aureus* periprosthetic knee infections treated by open debridement and retention of components. J Arthroplasty 2009;24:101-4.

[29] Welling MM, Brouwer CP, van'tHof W, Veerman EC, Amerongen AV. Histatin-derived monomeric and dimeric synthetic peptides show strong bactericidal activity towards multidrug-resistant *Staphylococcus aureus in vivo*. Antimicrob Agents Chemother 2007;51:3416-19.

[30] Elving GJ, van der Mei HC, Busscher HJ, van Nieuw Amerongen A, Veerman EC, van Weissenbruch R, *et al.* Antimicrobial activity of synthetic salivary peptides against voice prosthetic microorganisms. Laryngoscope 2000;110:321-24.

[31] Han X, Soblosky L, Slutsky M, Mello CM, Chen Z. Solvent effect and time-dependent behavior of C-terminus-cysteine-modified cecropin P1 chemically immobilized on a polymer surface. Langmuir 2011;27:7042-51.

[32] Williams TJ, Schneider RP, Willcox MD. The effect of protein-coated contact lenses on the adhesion and viability of gram-negative bacteria. Curr Eye Res 2003;27:227-35.

[33] Chen RX, Willcox MDP, Cole N, Ho KKK, Rasul R, Denman JA, *et al.* Characterization of chemoselective surface attachment of the cationic peptide melimine and its effects on antimicrobial activity. Acta Biomater 2012;8: 4371-79.

[34] Hilpert K, Elliott M, Jenssen H, Kindrachuk J, Fjell CD, Korner J, *et al.* Screening and characterization of surface-tethered cationic peptides for antimicrobial activity. Chem Biol 2009;16:58-69.

[35] Bagheri M, Beyermann M, Dathe M. Immobilization reduces the activity of surface-bound cationic antimicrobial peptides with no influence upon the activity spectrum. Antimicrob Agents Chemother 2009;53:1132-41.

[36] Bagheri M, Beyermann M, Dathe M. Mode of action of cationic antimicrobial peptides defines the tethering position and the efficacy of biocidal surfaces. Bioconjugate Chem 2012;23:66-74.

[37] Gao G, Cheng JTJ, Kindrachuk J, Hancock REW, Straus SK, Kizhakkedathu JN. Biomembrane interactions reveal the mechanism of action of surface-immobilized host defense IDR-1010 peptide. Chem Biol 2012;19:199-209.

CHAPTER VII

N-acetyl cysteine-immobilized coating avoids bacteria adhesion/biofilm formation without impairing osteoblast adhesion and proliferation

---

Fabíola Costa [a,b,c] , Daniela M. Sousa [a,b], Meriem Lamghari [a,b] , Paula Gomes [d], M. Cristina L. Martins [a,b,e*]

Biomaterials (under review)

[a] i3S, Instituto de Investigação e Inovação em Saúde, Universidade do Porto, Portugal

[b] INEB - Instituto de Engenharia Biomédica, Universidade do Porto, Rua do Campo Alegre, 823, 4150-180 Porto, Portugal

[c] Universidade do Porto, Faculdade de Engenharia, Porto, Portugal

[d] UCIBIO-REQUIMTE, Departamento de Química e Bioquímica, Faculdade de Ciências, Universidade do Porto, Porto, Portugal

[e] Universidade do Porto, Instituto de Ciências Biomédicas Abel Salazar, Porto, Portugal

1. Abstract

N-acetylcysteine (NAC) is a well known drug frequently used as a mucolytic agent and in the treatment of acetaminophen overdose. Presently, research has been focused on NAC antimicrobial activity. However, the success of some of these strategies was impaired by NAC short half-life, stressing the importance of a high long lasting local NAC concentration. Here, we hypothesized the application of covalently immobilized NAC onto a polymer, in order to develop an antimicrobial coating able to prevent implant-related osteomyelitis. Chitosan was the polymer of choice as it is reported to have osteoconductive properties, as well as some antimicrobial activity. Therefore, the main goal of the present work was to study if NAC-immobilized onto chitosan would improve chitosan antimicrobial and antibiofilm activity, without impairing bone cell adhesion and proliferation. For that, we optimized chitosan films with increasing NAC concentrations, assessed film stability, and evaluated its biological impact on (i) Methicillin-resistant *Staphylococcus aureus* (MRSA) adherence, proliferation and biofilm production and (ii) on Osteoblasts (MC3T3-E1 cell line) metabolic activity and morphology.

NAC-functionalized chitosan coatings avoid bacterial adhesion, impairing biofilm formation, while allowing osteoblast adhesion and proliferation in a concentration dependent way. Therefore, NAC-functionalized chitosan coating is a promising non-antibiotic alternative for the prevention of implants biofilm-associated infections.

Keywords N-acetylcysteine, Antimicrobial surfaces, surface functionalization, biomaterials, Biofilm, covalent immobilization

2. Introduction

N-acetylcysteine (NAC) is a widely used drug in medical practice for more than three decades. Although it is most frequently used as a mucolytic in chronic bronchitis, and as a detox and antioxidant agent in the treatment of acetaminophen overdose, it has been used on a number of other clinical applications such as chemotherapy-induced toxicity, HIV/AIDS and psychiatric disorders [1]. Adding to this broad activity, NAC has also been reported as having an excellent safety profile [2]. In tissue regeneration, NAC application has been investigated mostly in orthopedic and dental implants, namely (i) mixed with bone cement to reduce poly(methyl metacrylate) cytotoxicity and to improve osteointegration of the biomaterial [3], (ii) mixed with dental restorative materials (resin-modified glass ionomers) for similar purposes [4], (iii) loaded in titanium nanotubes in dental implants for osteointegration enhancement [5], among others. In addition, NAC has antimicrobial properties against both Gram-positive and Gram-negative bacteria [6-10]. Although its antimicrobial mechanism is unclear, it is known that the sulfhydryl moiety of NAC acts as an antioxidant, playing a role in free radical scavenging, therefore helping the immune system in destroying intermolecular or intramolecular disulfide bonds of bacterial proteins, and in competitively inhibiting cysteine utilization by bacteria [1, 11, 12]. Furthermore, its was also reported that NAC can disrupt mature biofilms, by reducing extracellular polysaccharides with consequent decrease of bacterial adhesion [6, 8, 13]. Therefore, NAC seems a promising non-antibiotic alternative for the treatment/prevention of implants biofilm-associated infections, and has been (i) adsorbed on polyethylene and titanium [14], (ii) incorporated on collagen scaffolds [12], and (iii) applied as catheter lock solution [15]. Although having variable success rates, all these approaches stressed the importance of a long-lasting high local NAC concentration towards an optimal performance. Taking all of these findings in consideration, we hypothesized a new strategy based on the application of covalently immobilized NAC onto a polymer for the development of an antimicrobial implant coating that would prevent implant-related osteomyelitis infection. To that end, we chose chitosan, a natural cationic polysaccharide with recognized antimicrobial [16-19] and osteoconductive properties [20-22]. Therefore, the main

goal of the present work was to study if a NAC-functionalized chitosan film coating would improve chitosan antimicrobial and antibiofilm activity, without impairing bone cell adhesion and proliferation.

2. Materials & Methods

2.1. Preparation of Chitosan Ultrathin Films

A re-precipitation method [23] was used to purify commercial squid pen chitosan (France Chitine), resulting on a molecular weight of 283000-472000 with a degree of acetylation (DA) of ~15%. Chitosan ultrathin films (Ch) were prepared as previously described by us [18] [24] by deposition of a drop of chitosan solution (0.4% in acetic acid w/v) onto gold substrates (1x1 cm^2) using a spin coater (9000 rpm, 1 min). Ch were then neutralized with 0.1 M NaOH, rinsed with MilliQ water, dried with a gentle stream of Argon and stored under Argon atmosphere.

Gold substrates, produced and prepared as previously described by us [25], were chosen due to their higher suitability for some of the surface characterization techniques used, such as ellipsometry and Infrared Reflection Absorption Spectroscopy (IRRAS).

2.2. Functionalization with NAC

Functionalization of Ch with NAC was performed as described in [18]. Further optimization was developed using different NAC concentrations, namely 0.4, 4, 6 and 8 mg/ml. Ch were treated with a solution of 0.2 M 1-Ethyl-3-[3-dimethylaminopropyl] carbodiimidehydrochloride) (EDC; Sigma-Aldrich), 0.05 M *N*-hydroxysulfosuccimide (NHS; Sigma-Aldrich) and different NAC concentrations (Merck), in 0.1 M (*N*-morpholino)ethanesulfonic acid (MES; Sigma-Aldrich) buffer at pH 6.5, for 1 h, at 37°C and 100 rpm. A control NAC-adsorbed sample was prepared by incubating Ch with a 4 mg/ml NAC solution in 0.1 MES using the same incubation parameters. The modified films were then rinsed with MilliQ water in an ultrasound

bath (1 min; Bandelin Sonorex Digitec Bath 35 kHz) and rinsed twice with MilliQ water.

2.3. Surface Characterization

Prior to surface characterization, samples were dried on a Vacuum Oven (Raypa, EV 50) for 1 h at 40°C.

2.3.1 IRRAS

IRRAS spectra were obtained on a Perkin Elmer FTIR spectrophotometer, model 2000, coupled with a VeeMax II Accessory (PIKE) and a liquid-nitrogen-cooled MTC detector. In order to avoid water vapor adsorption, dry nitrogen was purged into the instrument for 5 min before and during each sample analysis. For each sample, a similar gold surface was used as a background. Incident light was p-polarised and spectra were collected using the 80° grazing angle reflection mode. For each sample, 100 scans were performed with 4 cm^{-1} resolution.

2.3.2 Ellipsometry

Film thickness was measured with an imaging ellipsometer, model EP^3, from Nanofilm Surface Analysis. This ellipsometer was used in a polarizer-compensator-sample-analyzer (PCSA) mode (null ellipsometry). The light source was a solid-state laser (532 nm). The gold substrate refractive index (n) and extinction coefficient (k) were determined by using a delta and psi spectrum with a variation of angle between 65° and 71°. A refractive index (n) of 0.6244 and extinction coefficient (k) of 2.3845 was obtained for the gold substrate. Measurements were performed in four region-of-interest to correct for any instrument misalignment. The thickness of the chitosan films was determined considering n=1.54 and k=0, for the chitosan film [26]. For each type of substrates, the results presented are the average of three measurements on each of three samples.

2.3.3 X-ray Photoelectron Spectroscopy (XPS)

The XPS measurements were performed using an ESCALAB 200A, VG Scientific (UK) with PISCES software for data acquisition and analysis (from CEMUP – Centro de Materiais da Universidade do Porto). For analysis, an achromatic Al (Kα) X-ray source (1486.6 eV) operating at 15kV (300 W) was used, and the spectrometer, calibrated with reference to Ag $3d_{5/2}$ (368.27 eV), was operated in CAE mode. Data acquisition was ran with a pressure lower them 1.E-6 Pa. Survey spectra over a range of 0–1150 eV was collected with analyzer pass energy of 50 eV. High resolution C(1s), O(1s), N(1s), S(2p) and Au(4f) spectra were collected with analyzer pass energy of 20 eV. The photoelectrons were analyzed at a take-off angle of 55°. The binding energy (BE) scales were referenced by setting the C(1s) BE to 285.0 eV. All the spectra were fitted using XPS peak fitting software (XPSPEAK Version 4.1). All the carbon spectra were fitted using asymmetrical 70% Gaussian/30% Lorentzian profiles.

2.3.4 Water Contact Angle

Measurements were performed using the sessile drop method with a contact angle measuring system from Data Physics, model OCA 15, equipped with a video CCD-camera and SCA 20 software, as described at [25]. Drops of MilliQ water (4 µl) were deposited onto the samples surfaces and images were taken every 2 s over 300 s. Droplet profiles were fitted using Young-Laplace formula, to calculate the contact angle. The water contact angle of each sample was calculated by extrapolating the time dependent curve to zero. Results are the average of two measurements on three independent samples.

2.3.5 Functionalization stability

Stability of immobilized NAC was assessed as previously described on [27] by soaking NAC-modified films in deionized water for 14 days at room temperature. Water contact angles were measured before (Day 0) and after 7 and 14 days soaking. Samples were dried overnight in the vacuum oven prior to measurements. Results are the average of two measurements on three independent replicates.

2.4 Bacterial assays

2.4.1 Bacterial Strains, Media and Growth Conditions

Methicillin-resistant *Staphylococcus aureus* strain (MRSA) was bought from the American Type Culture Collection (ATCC 33591), and streak onto Tryptic Soya Agar (TSA) (Merck). Five colonies were then cultured in 5 ml of Tryptic Soya Broth (TSB) (Merck) overnight at 37°C, 150 rpm. The bacterial suspension concentration was adjusted by Optical Density (600nm) and confirmed by retrospective viable count.

2.4.2 Surfaces sterilization

Test surfaces were incubated successively in 70% ethanol and sterile water, and then dried in sterile environment. These samples were then placed on 24-well flat bottom cellular suspension plates (Sarstedt, Ldt, Newton, USA).

2.4.3 Adherence assay

Previous to bacteria adhesion assays, samples were placed at the wells and stabilized in Mueller-Hinton Broth (MHB) for 30 min. Adjusted bacterial solution was then added to the wells to a final concentration of 10^7 CFU/ml, and incubated at 37°C for 2h. After incubation, substrates were rinsed with sterile phosphate-buffered saline (PBS) solution and fixed with 4% (w/v) paraformaldehyde (PFA) (Sigma–Aldrich) for 20 min. Substrates were rinsed again with sterile PBS and stained with VECTASHIELD® Mounting Medium with 40,6-diamidino-2-phenylindole (DAPI; Vector). Images were obtained with an inverted fluorescence microscope (Axiovert 200M, Zeiss, Germany). For quantifying the adherent bacteria, eight fields on each of triplicate replicates were obtained with a 1000x magnification, corresponding to a net area of about 0.1181 mm^2/sample. Bacterial counts were performed using the manual counting software included in ImageJ software. Also, supernatants were successively diluted, plated in triplicate on TSA and incubated at 37°C for 18 h for colony forming units (CFU) counting.

2.4.4 Proliferation assay

For proliferation assays, samples that were incubated during 2 h with bacterial solution (as described in 2.4.3.) were rinsed with sterile PBS, and immersed in fresh MHB in a new 24-well plate for 4 h at 37°C and 100 rpm. At the end of this period, surfaces were rinsed with sterile PBS, fixed and visualized as described above (2.4.3). Supernatants were also plated for CFU counting.

2.4.5 Biofilm assay

S. aureus overnight culture in TSB (100 mL) was added to 5 ml of TSB-0.25% glucose and incubated for 4 h at 37°C, 150 rpm. Then, 100 µl of this suspension was added to each well containing test surfaces already immersed in 900 µl of TSB-0.25% glucose. After a 2 h incubation period at 37°C, surfaces were gently rinsed three times with sterile PBS and re-incubated with 1000 µl of TSB-0.25% glucose for 24 h. Finally, surfaces were rinsed with sterile PBS and left to dry. At this point, surfaces were stained with crystal violet 1% for 5 min and then washed with deionized H_20. Crystal violet was solubilized in dimethyl sulfoxide (DMSO) and absorbance was read at 570 nm. Results are the average of three independent samples of two independent assays.

2.5 Cellular Biocompatibility

2.5.1 Cell culture

MC3T3-E1 *calvaria* pre-osteoblast cells (purchased from the European Collection of Cell Cultures - ECACC) were cultured in complete α-modified minimal essential medium (α-MEM, Gibco) supplemented with 10% (v/v) heat-inactivated foetal bovine serum (FBS; Gibco) and 1% (v/v) Penicilin/Streptomycin (P/S; Gibco). The cells were maintained at 37°C in humidified atmosphere of 5% CO_2, and media were refreshed every 2 to 3 days. At pre-confluence, MC3T3-E1 cells were harvested using trypsin solution (0.25% w/v trypsin, 0.1% w/v glucose and 0.05% w/v ethyldiaminetetracetic acid in PBS) and were plated on top of chitosan and

chitosan-modified films (n=5) at a density of 2.0 x 10^4 cells, under osteogenic conditions (complete α-MEM supplemented with 50 µg/ml ascorbic acid and 10 mM ß-glycerophosphate). Multiwells culture plates were previously coated with pHEMA at a final density of 0.8 mg/cm^2 to avoid adhesion of the cells to the bottom and walls of the well. Tissue culture coverslips and Au substrates were used as positive controls. All experiments were performed using cells until passage 13.

2.5.2 Cytotoxicity assays

Cell metabolic activity and morphology were evaluated at 3, 7 and 14 days of culture. Cell metabolic activity was analysed by the Resazurin assay. Briefly, cells were incubated with 10% (v/v) Resazurin solution (0.1 mg/ml; Sigma–Aldrich) for 4 h at 37 ºC. After incubation, three 150 µL/well samples were transferred to a 96-well black plate and fluorescence was measured (530 nm Ex/590 nm Em) in a microplate reader (BioTek Synergy Mx, Molecular Devices). Cell morphology was assessed by staining the filamentous actin cytoskeleton of the cells, through immunocytochemistry. For that, medium was removed from the wells, and cells were washed twice with PBS at room temperature and fixed in 4% (w/v) PFA (Sigma–Aldrich) for 10 min. Cells were then washed with PBS and permeabilized for 5 min with ice-cold 0.1% (v/v) Triton X-100 in PBS. After one PBS rinse, samples were incubated with 1% (w/v) bovine serum albumin (BSA) (Gibco, Alfagene) for 30 min at 37 ºC. Afterwards, samples were incubated with Alexa Fluor® 594 phalloidin antibody (1:100; Molecular Probes, Invitrogen) in PBS for 20 min in the dark at room temperature. Samples were washed twice with PBS to remove unbound antibody, and mounted with VECTASHIELD® with DAPI. Samples were protected from light and kept at -20 ºC until further analysis by inverted fluorescence microscopy (Zeiss AxioVision Microscope).

2.6 Statistical analysis

For statistical analysis, one-way analyses of variance followed by Tukey's post hoc testing were used. The non-parametric Kruskal–Wallis test was applied when Gaussian distribution was not confirmed. Analyses were performed using the

GraphPad Prism program. Data are expressed as the mean ± standard deviation (SD), and p values of <0.05 were considered significant.

3. Results

3.1 Surface Characterization

Control (Ch_buffer), Ch with adsorbed NAC (Ch NAC ads) and Ch functionalized with NAC at concentrations ranging from 0.4 (Ch_NAC0.4) to 8 mg/ml (Ch_NAC8) were analyzed by IRRAS, ellipsometry, water contact angle measurements and XPS.

3.1.1 IRRAS

IRRAS analyses of chitosan thin films, before and after immersion on buffer solution, showed that the films remained stable even after chemical procedures undertaken (data not shown). IRRAS spectra of control and NAC- modified chitosan are shown in Figure 1A.

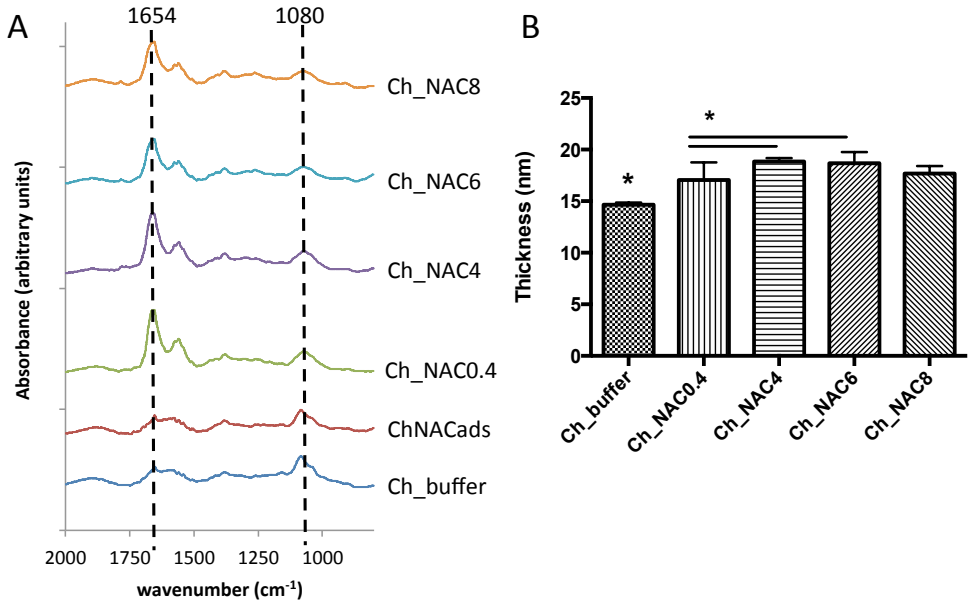

Figure 1. Surface characterization of Ch and Ch modified ultrathin films by A) IRRAS; B) Ellipsometry.

The Ch_buffer spectrum allowed the identification of characteristic absorption bands of chitosan, namely, 1655 cm^{-1} (amide I band, C=O axial stretching of acetyl groups), 1595 cm^{-1} (amide II band), 1330 cm^{-1} (amide III band, C-N axial stretching), and 1375 cm^{-1} due to CH3 symmetric deformation and 1085 cm^{-1} (skeletal vibration involving the C-O bridge stretching) as previously described [23, 24, 28-30]. The increase of the amide I absorption band (1654 cm^{-1}) observed after functionalization of Ch with NAC strongly suggests that covalent immobilization of NAC was successful, as the carbodiimide-mediated coupling between free amine groups of Ch and carboxylic groups of NAC produces amide bonds. In addition, no difference was observed between the spectra of Ch_buffer before and after NAC adsorption (Ch NAC ads), which further supports the success of NAC immobilization upon carbodiimide-mediated coupling. However, no difference was observed among spectra of Ch modified with different NAC concentrations.

3.1.2 Ellipsometry

The spin coating process resulted on uniformly distributed Ch with 14.7 ± 0.2 nm thickness, which remained stable even after the reaction protocols used, as there were no thickness changes between freshly made films and buffer-incubated films (data not shown). Figure 1B presents thickness of Ch before and after surface modification with different NAC concentrations, ranging from 0.4 to 8 mg/ml.

The Ch_buffer thickness was augmented after NAC functionalization until a maximum of 18.9 ± 0.3 nm was reached, when using NAC at 4 mg/ml concentration. No difference was observed in film thickness using NAC concentrations between 4 and 8 mg/ml. Therefore, further assays were conducted using samples functionalized with NAC at 0.4 and 4 mg/ml.

3.1.3 XPS analysis

XPS survey spectra demonstrated the absence of surface contaminants, since no other elements than those expected were detected (data not shown). The relative

atomic composition of all surfaces is described at Table 1. Ch_buffer was in accordance with our previous reports [24, 30].

Table 1. Surface atomic composition (%) calculated from high-resolution XPS spectra of different chitosan samples.

	Atomic composition (%)				C_{1s} composition (%)		
Surface	C (1s)	O (1s)	N (1s)	S (2p)	C-C/C-H 285 eV	C-OH/C-O-C 286.4 eV	O-C-O/N-C=O 288.1 eV
Ch_buffer	59.2	33.3	7.5	0	25	60	15
Ch_NAC0.4	61.9	25.2	12.9	0	27	51	22
Ch_NAC4	61.5	26.1	11.6	0.8	36	37	27
Ch NAC ads	57.7	34.6	7.7	0	25	58	17

The presence of NAC on the surface can be demonstrated by the increase of the nitrogen (N1s). N1s increase was observed onto Ch_NAC0.4 and on Ch_NAC4. However, no differences was observed between surfaces.

NAC immobilization onto Ch can be detected by the increase of the *C1s* peak at 288.1 eV assigned to amide bond formation, which was poorly observed when NAC was only adsorbed on the surface. This increase was concentration-dependent, reinforcing the success of covalent immobilization of NAC onto Ch. High-resolution *S2p* XPS spectra only allowed the detection of the NAC free thiol group (~163 eV) on the sample where the higher amount of NAC was applied, underpinning the different concentrations of NAC used to prepare the two NAC-modified surfaces analyzed. Neither Ch_Buffer, nor Ch NAC ads showed any traces of sulfur by XPS, indicating that probably NAC adsorption happened at a low yield.

3.1.4 Water optical contact angle (OCA) analysis

Water optical contact angles of the control and NAC-modified Ch films are presented on Figure 2 (black bars).

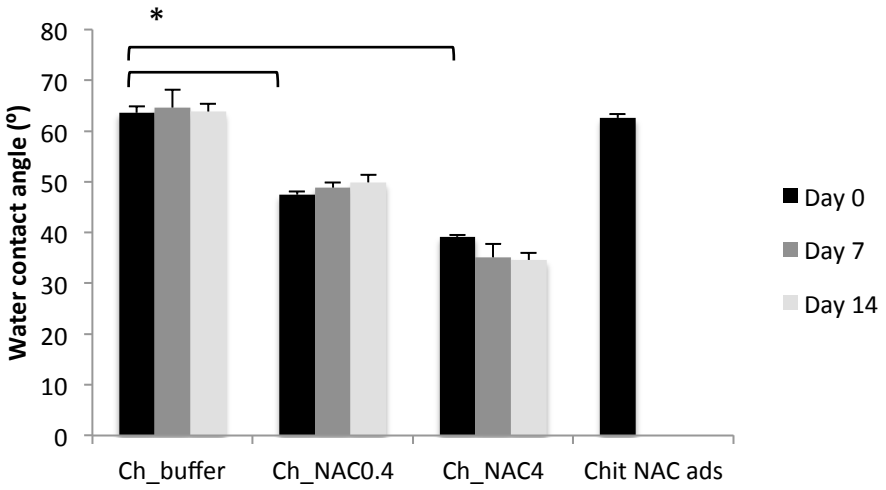

Figure 2. Water contact angle measurements over time. *Statistically different ($p<0.05$) (non-parametric Kruskal-Wallis test).

Chitosan functionalization with NAC increased significantly the hydrophilicity of the films, decreasing the water contact angle from 64 ± 1° to 47 ± 2° or to 39 ± 1° depending on the concentration used (0.4 or 4 mg/ml, respectively) as seen on black bars of Figure 2. Also, no significant difference was observed between contact angles of Ch_buffer (64 ± 1°) and Ch NAC ads (63 ± 1°).

3.1.5 Functionalization stability

To determine whether NAC covalently bound to Ch remained stable over time, a soak test was performed in deionized water for 14 days at room temperature. Results, depicted on Figure 2, demonstrated that no significant difference was observed between the contact angles at different time points, suggesting that, as expected, the amide bonds formed between Ch and NAC were stable throughout the 14 days period.

3.2 Antimicrobial Activity Characterization

The antimicrobial properties of NAC-functionalized Ch was evaluated by the assessment of their capacity to avoid bacterial adhesion, proliferation and biofilm formation.

3.2.1 Adhesion assays

The effect of developed thin films on *S. aureus* adhesion is demonstrated on Figure 3A.

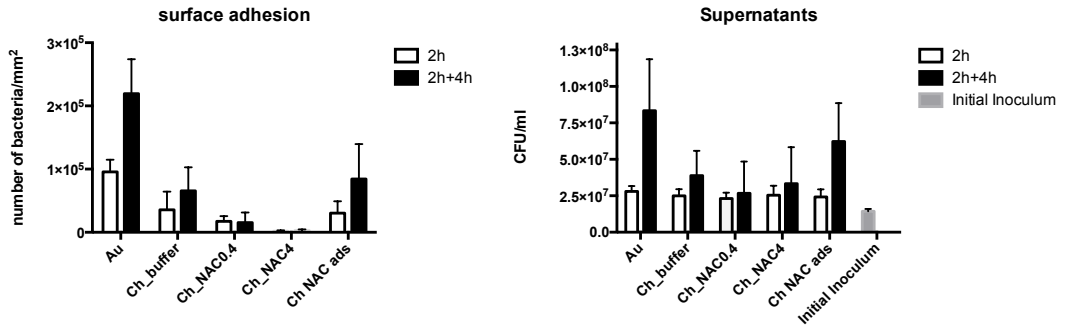

Figure 3.A) Bacterial adhesion on Au, Ch and NAC-modified Ch films after 2 h incubation in MHB (white bars) and 4 h re-incubation on fresh medium MHB after the 2 h pre-incubation period (black bars); B) CFU counts of the supernatants after 2 h incubation period (white bars) and after 4 h re-incubation in fresh medium (black bars) (one-way ANOVA $p<0.05$).

As seen on Figure 3A, after the 2 h incubation period (white bars), bacteria adhered preferably to the Au substrates used as control. Ch film coating promoted a 2.6-fold decrease in bacterial adhesion compared to Au, as previously described by us [18]. Covalent immobilization of NAC clearly decreased bacterial adhesion to Ch films by 2-fold and 21-fold when using NAC at, respectively, 0.4 and 4 mg/ml, demonstrating the anti-adhesive capacity of Ch_NAC films. Moreover, Ch film modified with the highest NAC concentration (4 mg/ml) decreased bacterial adhesion by 56-fold regarding Au. On the other hand, physically adsorbed NAC onto Ch films did not present significant differences regarding control Ch films, reinforcing the key role of covalent immobilization.

Figure 3B represents bacterial behavior at the supernatants, which shows that bulk phase bacteria were able to duplicate in number during the 2 h incubation period in MHB (white bars), as compared to the initial inoculum (grey bar). No significant difference was found between the amount of bacteria in different samples. This can be explained by the high initial inoculum that was free to proliferate on this bulk phase.

3.2.2 Proliferation assays

To assess the degree of proliferation of surface adherent bacteria in the 2 h incubation assay (white bars of Figure 3A), surfaces were re-incubated in fresh MHB medium for 4 h. Results obtained are depicted by the black bars of Figures 3A and 3B.

Adherent bacteria on Au, Ch_buffer and Ch NAC ads surfaces were able to proliferate, since the number of surface adherent bacteria duplicated regarding the respective values obtained on the previous 2 h adherence assay (white bars). Also, at the supernatants of these samples (black bars of Figure 3B), high CFUs were observed, suggesting that bacteria were further able to detach and proliferate in bulk phase.

In contrast, surfaces with covalently immobilized NAC maintained the low amount of adherent bacteria throughout the extended 4 h incubation period, demonstrating that adherent bacteria could not proliferate on the surface (black bars of figure 3A). In addition, although some adherent bacteria could be detached from the surface and proliferate in solution (black bars of Figure 3B), they were not able to adhere on NAC-surfaces since, as described above, the number of adherent bacteria did not increase on these surfaces.

The above observations provide undeniable evidence of the bacterial anti-adhesive effects brought by covalent immobilization of NAC onto Ch. Such is further reinforced by visualization of adherent bacteria on the different surfaces by SEM, as depicted on Figure 4.

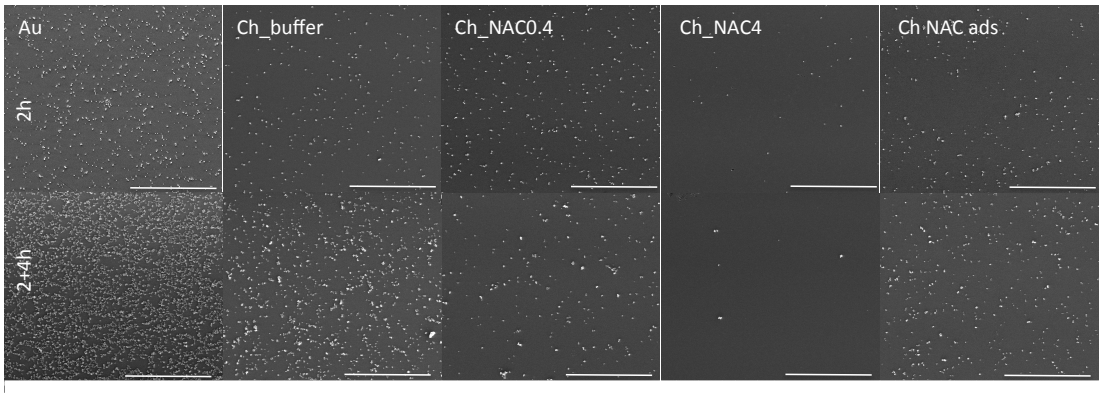

Figure 4. SEM images of *S. aureus* adherent to Ch and NAC-modified Ch films after 2 h and 2+4 h incubation periods. Au were used as controls. Scale bar: 100 µm.

SEM images correlate with what was previously found on the adhesion assays (Figure 3A). Neither frequent cell damage, nor exopolysaccharides (EPS) were seen on any sample.

3.2.3 Biofilm assay

In order to evaluate surface activity during long-term bacteria interaction, biofilm assays were performed. Crystal violet (CV) staining was used as an indicator of total biofilm biomass. Results, presented in Figure 5, clearly demonstrate that covalent immobilization of NAC at the higher concentration (4 mg/mL) provides anti-biofilm properties to the chitosan thin film. Ch_NAC4 presented the lowest value of biofilm biomass that was ~3-fold lower than that of control Ch_buffer. No difference was observed between the controls Au and Ch_buffer and Ch modified with the lower concentration of NAC. Interestingly, physically adsorbed NAC onto Ch induced an increase of the total biofilm mass that was ~2-fold higher than that of Ch_buffer.

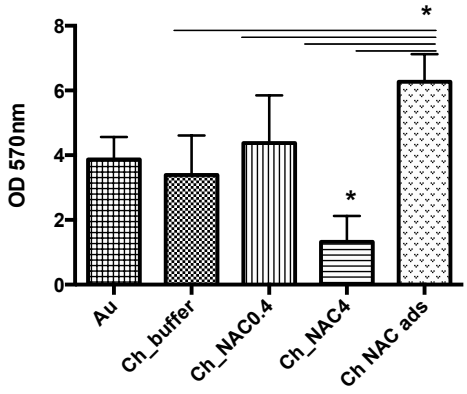

Figure 5. Effect of Ch and NAC-modified Ch surfaces on *S. aureus* total biofilm biomass formation (Kruskal-Wallis analysis *p<0.05).

3.3 NAC-modified surfaces influence on osteoblastic cells

In order to evaluate possible cytotoxic effects of the modified surfaces on cell interaction/adhesion, osteoblastic MC3T3-E1 cells (a pre-osteoblast cell line) were cultured on top of Ch and Ch_NAC surfaces for 14 days under osteogenic conditions. Cell metabolic activity, cell adhesion, integrity and morphology were assessed at days 3, 7 and 14 of culture.

As depicted in Figure 6A, no significant differences were found in MC3T3-E1 metabolic activity for all three modified surfaces tested (Ch_NAC0.4, Ch_NAC4 and Ch NAC ads), when compared with the Ch_buffer control. Additionally, the metabolic activity has not been reduced to less than 70% when comparing to the same control, demonstrating that NAC-modified surfaces have no cytotoxic potential, according to ISO 10993-5:2009(E). These data suggest that MC3T3-E1 cells plated on top of NAC surfaces were viable and able to proliferate and differentiate along the time of incubation.

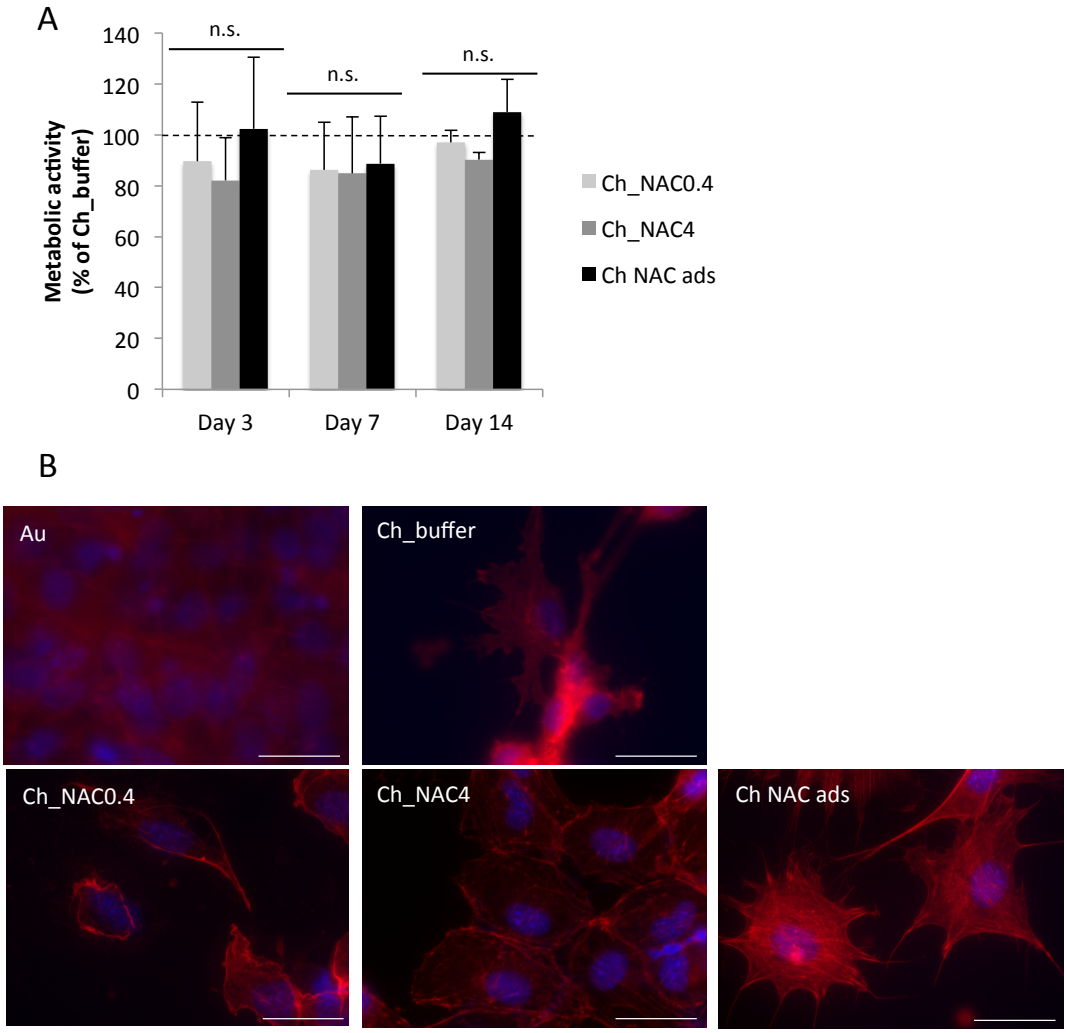

Figure 6. A) MC3T3-E1 cell metabolic activity after 3, 7 and 14 days in contact with Ch and Ch_NAC modified surfaces. Data are expressed as percentage in relation to Ch_buffer (100%) and represent mean ± SD (n=5). (one-way ANOVA $p<0.05$; n.s.-non-significant); B) Osteoblast morphology following 14 days of culture on top of Ch and Ch_NAC modified surfaces. Scale bar 50 µm. (magnification 630x) The images are representative of three independent experiments. F-actin filaments are stained in red and nuclei are stained in blue.

Regarding MC3T3-E1 proliferation, cells became confluent on Au control sample at day 3 and continued to proliferate on the followings days, covering the whole surface at day 14 of culture. On Ch_buffer, MC3T3-E1 cells tended to agglomerate and grow forming big clusters spread throughout the Ch film surface, as previously described for other osteoblast-like cells [31]. On Ch_NAC0.4 surface, a very low cell adhesion was observed on the initial time points, with cells being more round shaped rather than presenting a fibroblastic-like morphology. Nevertheless, as time

progressed, cells were able to proliferate and establish cell-cell contacts. On the Ch_NAC4 sample, a low number of adhered cells was also observed at the initial time point (day 3), and cells were dispersed but elongated. As time progressed, cells were able to proliferate to cover most of the sample surface at day 14, as shown in figure 6B. Similarly, on the Ch NAC ads sample, a low number of cells was observed on the initial time point (day 3), and cells were well elongated and dispersed. Also in this case, and as time progressed, cells were able to proliferate and cover a considerable part of the sample surface at day 14. In all cases, cells were well spread with a typical osteoblast-like morphology.

4. Discussion

NAC is an FDA-approved drug clinically applied on a broad range of pathologies [1]. Moreover, NAC has been reported as exhibiting antimicrobial activity against a variety of microorganisms, including the clinically relevant MRSA [6, 13, 32, 33]. However, since NAC serum levels obtained with intravenous infusions (about 0.035 mg/ml)[34] are much lower than the antimicrobial concentration reported in most studies (between 4 and 80 mg/ml) [13, 14, 33, 35], strategies that accomplish high local concentrations would be beneficial [10, 15].

In this study, covalent immobilization of NAC was performed, in order to obtain long-lasting high local concentration of the drug onto a chitosan-derived implant-related coating. Chitosan, a natural cationic polysaccharide, was chosen as the implant coating due to its recognized antimicrobial [16-19] and osteoconductive properties [20-22]. For that, we functionalized chitosan films with increasing NAC concentrations, assessed film stability, and evaluated their antiadhesive and anti-biofilm effect on (i) methicillin-resistant *Staphylococcus aureus* (MRSA), the most clinically relevant bacterium in osteomyelitis [36, 37], and their impact on ii) osteoblasts adherence and proliferation, since some antimicrobial coatings may impair tissue integration.

The production of NAC-functionalized chitosan films was optimized and characterized by a number of different techniques (IRRAS, ellipsometry, water contact angle measurements, and XPS). Strong evidence on successful covalent

tethering was brought by the sum of different contributions. IRRAS analysis demonstrated an increase of the amide I peak (assignment to peptide bonds) on NAC-functionalized surfaces that was not observed when NAC was simply adsorbed. Similar results had already been reported by us [18]. This technique, however, did not offer distinction between the different NAC concentrations applied. Ellipsometry analysis suggests surface saturation at a NAC concentration of 4 mg/ml, as no further thickness increase was observed above this concentration. Surfaces prepared with the two lowest NAC concentrations (0.4 and 4 mg/ml) where therefore well distinguished using i) OCA measurements, by the increase of surface hydrophylicity and by ii) XPS, by the increase of carbon at 288.1 eV (amide bond), with increase of NAC concentration. Moreover sulfur at ~163eV (thiol group) was only detected on Ch_NAC4, probably because the amount of NAC on both Ch_NAC0.4 and Ch NAC ads is below the limit of detection of the XPS equipment used.

Regarding stability of NAC functionalization, NAC-chitosan films were proved to be stable for 14 days, as no significant change was observed on surface wettability. These results differ from those reported by Harris *et al* [27], where NAC covalently immobilized onto poly(dimethyl)siloxane presented low yield and stability. This might be explained by the well-known high stability of amide bonds, as those formed between primary amines of chitosan and carboxyl groups of NAC, herein reported.

Regarding bacterial adhesion assays, surfaces were challenged with a very high initial inoculum over 2 h, to assess the NAC-immobilized response to harsh conditions. As already reported in some studies, chitosan films were able to reduce bacterial adhesion in about 2.6-fold [18, 38]. Furthermore, NAC immobilization significantly reduced adhered bacteria to chitosan in a concentration dependent way. Such anti-adhesive properties could be explained simply by physical-chemical interactions, as less hydrophobic surfaces (Ch_NAC0.4 and Ch_NAC4) have been correlated with lower cellular adhesion [39], but it can also be related to the antimicrobial activity attributed to NAC, putatively due to NAC-mediated destruction of disulfide bonds in proteins [11], impairing bacteria adhesion and production of exopolysaccharides precursors of biofilm matrix [6, 14, 40]. On proliferation assay, the capacity of surface adherent bacteria (from the 2h adhesion assay) to proliferate/detach from the surface was evaluated. Results demonstrated that NAC-functionalized samples

had no increased number of adhered bacteria after incubation in a fresh medium, although some of adherent bacteria were able to detach from the surface and proliferate in solution (Figure 3A and 3B). This is indicative that some of adherent bacteria were not killed by the surface. However, the anti-adhesive effect of the NAC-functionalized surface avoided the planktonic bacteria adhesion to the surface. Although some authors defend a bactericidal effect for NAC, the reported minimal bactericidal concentrations (MBC) are very high [33, 35, 40]. Therefore, the effect observed may be a result of bacteriostatic effects combined with non-adherent detach of bacteria from the surface, as suggested by others [12]. SEM images corroborated these findings, as only an anti-adhesion effect was observed without any visualization of frequent bacterial membrane damage. Regarding the control Ch film, bacteria were able to overcome the initial antimicrobial effect, as a growing value of adhered and planktonic bacteria was observed. Remains to elucidate if the increased amount of bacteria on this control surface was a result of direct surface proliferation or of deposition and adherence of the growing number of planktonic bacteria. Nevertheless, the results of both assays suggest some bactericidal activity of Ch_buffer when compared with Au. On the Au surface, no *S. aureus* proliferation interference was observed, with high bacterial numbers both at the surface and bulk phase.

Ch_NAC4 anti-adherence properties were further highlighted on the biofilm total biomass quantification, as this was the only sample that efficiently reduced the amount of biofilm, evidencing once again a concentration-dependent effect. The Ch_buffer surface had its antimicrobial activity overwhelmed by the extended incubation period, presenting a biofilm total biomass similar to the one found on the control Au sample. The Ch_NAC4 anti-biofilm activity may be explained by lower bacterial adhesion, possibly by adhesins degradation, summed to lower EPS production, and even detachment of pre-formed initial biofilm, as already reported for soluble/adsorbed NAC in a number of different studies [6, 7, 13, 40].

The NAC effect towards eukaryotic cells in its soluble form has been described as non-cytotoxic and even cell stimulating [3, 5, 41, 42]. However, our most promising antimicrobial surface is hydrophilic, which is usually related with poor cell adhesion and proliferation. Indeed, Harris *et al*. [27] proposed the use of NAC-immobilized

poly(dimethyl)siloxane to develop a hydrocephalus shunt free from astrocyte and macrophage adhesion, and found their material to have some efficacy. In the present study, NAC was immobilized on chitosan, a polymer known for its osteogenic properties [20-22, 43]. Results show a lower, yet growing, metabolic activity on cells adhered to NAC-modified samples, ending up by reaching values similar to those of control Ch_buffer. Hence, over time, NAC samples did not impair cellular proliferation.

5. Conclusion

Ch_NAC4 is a promising material as it avoids bacterial adhesion, impairing biofilm formation, while allowing osteoblast adhesion and proliferation. This is particularly interesting towards further developments, and future perspectives include the assessment of this coating on an *in vivo* setting, as a prevention coating and as coadjuvant in systemic antibiotic therapies.

Acknowledgements

This work was financed by FEDER funds through Programa Operacional Factores de Competitividade – COMPETE and by Portuguese funds through FCT –Fundação para a Ciência e a Tecnologia in the framework of project PTDC/CTM/101484/2008; PEst-C/SAU/LA0002/2013; UID/Multi/04378/2013 and the grants: SFRH/BD/72471/2010 (Fabíola Costa).

References

[1] Samuni Y, Goldstein S, Dean OM, Berk M. The chemistry and biological activities of N-acetylcysteine. Biochimica et biophysica acta. 2013;1830:4117-29.

[2] Kao LW, Kirk MA, Furbee RB, Mehta NH, Skinner JR, Brizendine EJ. What is the rate of adverse events after oral N-acetylcysteine administered by the intravenous route to patients with suspected acetaminophen poisoning? Annals of emergency medicine. 2003;42:741-50.

[3] Tsukimura N, Yamada M, Aita H, Hori N, Yoshino F, Chang-Il Lee M, *et al.* N-acetyl cysteine (NAC)-mediated detoxification and functionalization of poly(methyl methacrylate) bone cement. Biomaterials. 2009;30:3378-89.

[4] Minamikawa H, Yamada M, Iwasa F, Ueno T, Deyama Y, Suzuki K, *et al.* Amino acid derivative-mediated detoxification and functionalization of dual cure dental restorative material for dental pulp cell mineralization. Biomaterials. 2010;31:7213-25.

[5] Lee YH, Bhattarai G, Park IS, Kim GR, Kim GE, Lee MH, *et al.* Bone regeneration around N-acetyl cysteine-loaded nanotube titanium dental implant in rat mandible. Biomaterials. 2013;34:10199-208.

[6] Olofsson AC, Hermansson M, Elwing H. N-acetyl-L-cysteine affects growth, extracellular polysaccharide production, and bacterial biofilm formation on solid surfaces. Applied and environmental microbiology. 2003;69:4814-22.

[7] Marchese A, Bozzolasco M, Gualco L, Debbia EA, Schito GC, Schito AM. Effect of fosfomycin alone and in combination with N-acetylcysteine on *E. coli* biofilms. International journal of antimicrobial agents. 2003;22 Suppl 2:95-100.

[8] Perez-Giraldo C, Rodriguez-Benito A, Moran FJ, Hurtado C, Blanco MT, Gomez-Garcia AC. Influence of N-acetylcysteine on the formation of biofilm by *Staphylococcus epidermidis*. The Journal of antimicrobial chemotherapy. 1997;39:643-6.

[9] del Prado G, Ruiz V, Naves P, Rodriguez-Cerrato V, Soriano F, del Carmen Ponte M. Biofilm formation by *Streptococcus pneumoniae* strains and effects of human serum albumin, ibuprofen, N-acetyl-l-cysteine, amoxicillin, erythromycin, and levofloxacin. Diagnostic microbiology and infectious disease. 2010;67:311-8.

[10] Zhao T, Liu Y. N-acetylcysteine inhibit biofilms produced by *Pseudomonas aeruginosa*. BMC microbiology. 2010;10:140.

[11] Sevier CS, Kaiser CA. Formation and transfer of disulphide bonds in living cells. Nature reviews Molecular cell biology. 2002;3:836-47.

[12] Yamada M, Ishihara K, Ogawa T, Sakurai K. The inhibition of infection by wound pathogens on scaffold in tissue-forming process using N-acetyl cysteine. Biomaterials. 2011;32:8474-85.

[13] Oosterhof JJ, Elving GJ, Stokroos I, van Nieuw Amerongen A, van der Mei HC, Busscher HJ, *et al.* The influence of antimicrobial peptides and mucolytics on the integrity of biofilms consisting of bacteria and yeasts as affecting voice prosthetic air flow resistances. Biofouling. 2003;19:347-53.

[14] Drago L, De Vecchi E, Mattina R, Romano CL. Activity of N-acetyl-L-cysteine against biofilm of *Staphylococcus aureus* and *Pseudomonas aeruginosa* on orthopedic prosthetic materials. The International journal of artificial organs. 2013;36:39-46.

[15] Aslam S, Jenne K, Reed S, Ghannoum M, Mehta R, Darouiche R. N-acetylcysteine lock solution prevents catheter-associated bacteremia in rabbits. The International journal of artificial organs. 2012;35:893-7.

[16] Kong M, Chen XG, Xing K, Park HJ. Antimicrobial properties of chitosan and mode of action: a state of the art review. International journal of food microbiology. 2010;144:51-63.

[17] Carlson RP, Taffs R, Davison WM, Stewart PS. Anti-biofilm properties of chitosan-coated surfaces. Journal of biomaterials science Polymer edition. 2008;19:1035-46.

[18] Costa F, Maia S, Gomes J, Gomes P, Martins MC. Characterization of hLF1-11 immobilization onto chitosan ultrathin films, and its effects on antimicrobial activity. Acta biomaterialia. 2014;10:3513-21.

[19] Hu X, Neoh KG, Shi Z, Kang ET, Poh C, Wang W. An *in vitro* assessment of titanium functionalized with polysaccharides conjugated with vascular endothelial growth factor for enhanced osseointegration and inhibition of bacterial adhesion. Biomaterials. 2010;31:8854-63.

[20] Moutzouri AG, Athanassiou GM. Attachment, spreading, and adhesion strength of human bone marrow cells on chitosan. Annals of biomedical engineering. 2011;39:730-41.

[21] Kawai T, Yamada T, Yasukawa A, Koyama Y, Muneta T, Takakuda K. Biological fixation of fibrous materials to bone using chitin/chitosan as a bone formation accelerator. Journal of Biomedical Materials Research Part B: Applied Biomaterials. 2009;88:264-70.

[22] Bumgardner JD, Chesnutt BM, Yuan Y, Yang Y, Appleford M, Oh S, *et al*. The integration of chitosan-coated titanium in bone: an in vivo study in rabbits. Implant dentistry. 2007;16:66-79.

[23] Oliveira JR, Martins MCL, Mafra L, Comes P. Synthesis of an O-alkynyl-chitosan and its chemoselective conjugation with a PEG-like amino-azide through click chemistry. Carbohydrate Polymers. 2012;87:240-9.

[24] Nogueira F, Goncalves IC, Martins MC. Effect of gastric environment on *Helicobacter pylori* adhesion to a mucoadhesive polymer. Acta biomaterialia. 2013;9:5208-15.

[25] Martins MC, Ratner BD, Barbosa MA. Protein adsorption on mixtures of hydroxyl- and methyl-terminated alkanethiols self-assembled monolayers. Journal of Biomedical Materials Research Part A. 2003;67:158-71.

[26] Lundin M, Macakova L, Dedinaite A, Claesson P. Interactions between chitosan and SDS at a low-charged silica substrate compared to interactions in the bulk-the effect of ionic strength. Langmuir. 2008;24:3814-27.

[27] Harris CA, Resau JH, Hudson EA, West RA, Moon C, Black AD, *et al.* Reduction of protein adsorption and macrophage and astrocyte adhesion on ventricular catheters by polyethylene glycol and N-acetyl-L-cysteine. Journal of Biomedical Materials Research Part A. 2011;98:425-33.

[28] Osman Z, Arof AK. FTIR studies of chitosan acetate based polymer electrolytes. Electrochimica Acta. 2003;48:993-9.

[29] Lawrie G, Keen I, Drew B, Chandler-Temple A, Rintoul L, Fredericks P, *et al.* Interactions between alginate and chitosan biopolymers characterized using FTIR and XPS. Biomacromolecules. 2007;8:2533-41.

[30] Amaral IF, Granja PL, Barbosa MA. Chemical modification of chitosan by phosphorylation: an XPS, FT-IR and SEM study. Journal of Biomaterials Science, Polymer Edition. 2005;16:1575-93.

[31] Chua PH, Neoh KG, Kang ET, Wang W. Surface functionalization of titanium with hyaluronic acid/chitosan polyelectrolyte multilayers and RGD for promoting osteoblast functions and inhibiting bacterial adhesion. Biomaterials. 2008;29:1412-21.

[32] El-Feky MA, El-Rehewy MS, Hassan MA, Abolella HA, Abd El-Baky RM, Gad GF. Effect of ciprofloxacin and N-acetylcysteine on bacterial adherence and biofilm formation on ureteral stent surfaces. Polish journal of microbiology / Polskie Towarzystwo Mikrobiologow = The Polish Society of Microbiologists. 2009;58:261-7.

[33] Aslam S, Darouiche RO. Role of antibiofilm-antimicrobial agents in controlling device-related infections. The International journal of artificial organs. 2011;34:752-8.

[34] Prescott LF, Donovan JW, Jarvie DR, Proudfoot AT. The disposition and kinetics of intravenous N-acetylcysteine in patients with paracetamol overdosage. European journal of clinical pharmacology. 1989;37:501-6.

[35] Leite B, Gomes F, Teixeira P, Souza C, Pizzolitto E, Oliveira R. Combined effect of linezolid and N-acetylcysteine against *Staphylococcus epidermidis* biofilms. Enfermedades infecciosas y microbiologia clinica. 2013;31:655-9.

[36] Toms AD, Davidson D, Masri BA, Duncan CP. The management of peri-prosthetic infection in total joint arthroplasty. The Journal of bone and joint surgery British volume. 2006;88:149-55.

[37] Faber C, Stallmann HP, Lyaruu DM, Joosten U, von Eiff C, van Nieuw Amerongen A, *et al.* Comparable efficacies of the antimicrobial peptide human lactoferrin 1-11 and gentamicin in a chronic methicillin-resistant *Staphylococcus aureus* osteomyelitis model. Antimicrobial agents and chemotherapy. 2005;49:2438-44.

[38] Costa FM, Maia SR, Gomes PA, Martins MC. Dhvar5 antimicrobial peptide (AMP) chemoselective covalent immobilization results on higher antiadherence effect than simple physical adsorption. Biomaterials. 2015;52:531-8.

[39] Barbosa JN, Martins MC, Freitas SC, Goncalves IC, Aguas AP, Barbosa MA. Adhesion of human leukocytes on mixtures of hydroxyl- and methyl-terminated self-assembled monolayers: effect of blood protein adsorption. Journal of Biomedical Materials Research Part A. 2010;93:12-9.

[40] Quah SY, Wu S, Lui JN, Sum CP, Tan KS. N-acetylcysteine inhibits growth and eradicates biofilm of *Enterococcus faecalis*. Journal of endodontics. 2012;38:81-5.

[41] Ueno T, Yamada M, Igarashi Y, Ogawa T. N-acetyl cysteine protects osteoblastic function from oxidative stress. Journal of Biomedical Materials Research Part A. 2011;99:523-31.

[42] Yamada M, Ueno T, Minamikawa H, Sato N, Iwasa F, Hori N, *et al*. N-acetyl cysteine alleviates cytotoxicity of bone substitute. Journal of Dental Research. 2010;89:411-6.

[43] Lieder R, Darai M, Thor MB, Ng CH, Einarsson JM, Gudmundsson S, *et al. In vitro* bioactivity of different degree of deacetylation chitosan, a potential coating material for titanium implants. Journal of Biomedical Materials Research Part A. 2012;100:3392-9.

CHAPTER VIII

General Discussion and Future Work

Implant-related infection prevention continues as a challenging problem, without significant improvement in the last decades. Efforts have united researchers towards developing an implant coating that is biocompatible and that protects against infection establishment. The uprising of antibiotic resistance a few years from its implementation has prompted the search for alternative measures. AMP appears as an alternative, and covalent immobilization as a preferred strategy to obtain a long-lasting, highly effective coating. Indeed, the work herein discussed [1, 2], demonstrated a better antimicrobial performance of covalently immobilized rather than adsorbed AMP. This finding is corroborated with the reported by [3-5]. Since the beginning of this thesis (and highlighted in blue in Table 3 of chapter II) an increasingly higher number of reports have been published using the covalent immobilization strategy. It is clear a shift from fundamental studies to more applied research, as the solid supports used were mainly titanium (in 42% of the reports) and silicone (23% of reports). Therefore, the immobilization chemistries have also diversified, with most frequent being silanization [3, 4, 6-8], dopamine immersion [9-11], UV-treated Allyl Glycidyl Ether [12-14] frequently combined with CuAAC click [15-17] and carbodiimide [10, 17-20] chemistry. Also, more challenging assays have been employed with antibiofilm [4, 10, 12, 13, 21, 22], cytocompatibility [3, 4, 9, 12, 13, 15, 16, 18, 22, 23] and film stability [4-6, 8, 12, 18, 23, 24] studies being frequent throughout publications. Regarding the cytocompatibility assays, cell line testing is preferred over the past simple haemolytic assays, in an attempt to have a deeper knowledge of AMP-surfaces implications on tissue environment. Within film stability studies, the most frequent are leaching assays [5, 12, 23]. Also resilience against 2h ultrasonication [4, 6, 7], resilience through autoclaving process [18] and resilience to varying pHs [24], were tested. More interestingly Chen *et al*.[8] assessed, the influence of proteolytic enzymes on the immobilized AMP. They reported that the surfaces with covalently immobilized GL13K after incubation in saliva for 11 days, showed only 2% of peptide release, whether the adsorbed peptide surface had a release up to 9%. This suggests that covalent immobilization may protect against degradation by proteolytic enzymes.

Nevertheless, despite some promising results the key profile of immobilization has not been fully disclosure yet, and parameters such as spacer application, peptide

orientation and surface density need further reflection. One important aspect highlighted in Chapters V and VI is the inclusion of a spacer for better antimicrobial performance. Indeed, an elevated number of the recently published studies chose to include a spacer or to apply a polymer brush coating, resulting in better antimicrobial activity [3, 5-7, 10, 12-14, 17, 21, 22, 24]. Exception is found in the work of Chen *et al*., [8], Tan *et a*l.,[9, 11] and willcox *et al*.,[18, 25], where direct immobilization did not impair surface antimicrobial activity.

Regarding orientation, many of the recently published studies have decided to apply a simpler chemistry, resulting in randomly oriented immobilized AMP [4, 9-11, 18, 19, 21, 23]. Although, in some of these studies a high bactericidal effect was observed, in fact, this bactericidal effect was associated with increased adherence of dead bacteria [4, 9, 21], which may compromise long-term performance. Therefore, a chemoselective tethering could help to have a bigger control of the coating performance. Chemoselective immobilization has been reported both throught Nt-immobilization [5, 14, 15, 17, 22, 26], and Ct-immobilization [3, 6, 7, 12, 16, 19, 24]. Like chapter VI a few studies tried to compare Nt- to Ct- immobilization [20, 25] in order to obtain the most active immobilization profile. Indeed, a few studies tried to correlate AMPs mode of action with preferred orientation at immobilization [27][28]. Hipert *et al.* [27] suggested an extrapolation of the peptide membrane insertion model to an universal tethering profile, where hydrophobic exposition of immobilized AMPs should result on higher antimicrobial activity. Bagheri *et al.* [28] also defended that peptides with a head-to-tail amphipathicity should be immobilized exposing the hydrophobic end. However, results from both tested AMPs (hLF1-11 and Dhvar5) showed that the proposed correlations may be still a bit further from reality. Both tested peptides (hLF1-11 and Dhvar5) have a head-to-tail amphipathicity. However, the exposition of the cationic end revealed different outcomes. In the case of hLF1-11 a moderate bactericidal effect was observed accompanied with a relevant number of bacterial adhesion. The recently published work by Godoy-Gallardo *et al.*, [3, 6, 7] showed that hLF1-11 when immobilized preferentially by its Nt (exposing its hydrophobic end) appeared to have a higher antimicrobial effect against *S. sanguinis* than what we found for MRSA. Nevertheless, remains to clarify if the observed differences are not the consequence

of insufficient hLF1-11 density or bacteria species tested. Regarding Dhvar5, the cationic end exposition comprised the most promising surface, with a very low bacterial adhesion. Similarly, besides the already mentioned Chen *et al*. work [25], also Lim *et al*. [12] and Lin *et al.* [26] studied head-to-tail amphipathic AMPs, and found promising results with the cationic end exposition. Therefore, the most effective immobilization profile does not seem to be linked to a specific structure or proposed model of action. Nevertheless, as highlighted by Raspch *et al*. [23] and Bagheri *et al.* [28], only peptides with strong membrane interference abilities as main mode of action are capable of acting as potential functional molecules for an antimicrobial surface coating by covalent attachment. In Raspch *et al.* [23] work, different immobilization chemistries (preactivated reactive surfaces with epoxy, aldehyde, NHS, and p-Phenylene diisothiocyanate (PDITC) functionalities to conjugate with AMPs free amines) with AMPs with different putative mechanisms of action were tested. They found that different immobilization moieties could strongly influence the antimicrobial surface performance. Moreover, they emphasized the importance of spacer inclusion and high peptide surface density, proposing a minimal concentration threshold to obtain significant antimicrobial activity. They also suggested that the inclusion of a spacer and peptide surface density are more important than peptide orientation. However, they did not test specific immobilization orientation, as the AMPs free amines were unspecifically used for immobilization.

Another point still needing further investigation is peptide surface density. Initially, as discussed in Chapter II, surface peptide density appeared to be as important as other immobilization parameters, such as orientation and spacer application. Moreover, many studies fail to report a quantification assay. Consequently, comparisons and correlations between studies became very difficult to establish. Indeed, researchers struggled to find a proper way to quantify immobilized peptides, therefore, quantification relays in indirect approximations [3-5, 8, 11-13, 16, 21-23, 26, 29, 30]. The two most used methods are: estimation from film thickness [3, 16, 22, 26] and fluorescence reading of fluorescence-labeled immobilized AMPs [11, 15, 24]. Other methods include HPLC measurements of the remained peptide at reaction supernatant whose concentration that is latter on subtracted from the initial

concentration [13, 21], free amines quantification [12, 23], arginine colorimetric quantification [1, 2], phenyl alanine fluorescence measurement [30], and XPS estimation [4]. Even though the use of fluorescent-labeled peptides appears to be the most direct way to quantify immobilized AMPs, one cannot be really assure that the chemical yield is the same using a simple AMP and a fluorescent-labeled AMP. Nevertheless, it is possible to suggest that the real influence of peptide density is peptide-specific and may be linked to a minimal concentration threshold as proposed by Raspch *et al.* [23].

Gathering the information of all published studies with the work herein exposed, it is possible to conclude that a general immobilization profile may not be attainable, as the specificities of each AMP most be taken in consideration. For sequence-based amphipathic AMPs as the ones herein tested, it seems that spacer inclusion, and chemoselective exposition are parameters of paramount importance to develop an effective antimicrobial surface.

Nevertheless, the ideal antimicrobial coating should comprise killing capacity, but more importantly should avoid bacteria adhesion, in order to maintain long lasting activity. Therefore, the antiadhesive performance observed in chapter VII through the immobilization of NAC is very promising, as it impairs the bacterial adhesion to such low levels that it is less probable infection establishment.

The use of chitosan as a coating material also contributed to the observed antimicrobial outcome. In opposition to the reported by Foster *et al.* [31], chitosan films may have significant antimicrobial activity. As seen in Chapters V, VI and VII, ultrathin chitosan films may reduce bacterial adhesion up to ~80%. The observed antimicrobial activity may be related to the small thickness of the film, the absence of a crosslinking step, which allows for a high level of free amine groups that can act by either of the proposed mechanism-of-action (bacterial membrane disturbance or divalent cations chelation). Furthermore, the ethanol 70°-related sterilization step did not impair chitosan antimicrobial activity. Regarding the cytocompatibility of the ultrathin chitosan films, towards an osteoblast cell line, results showed that cells were able to adhere and proliferate, with a gathered adhesion profile similar to what was previously reported (see Chapter III).

Future work comprises further development of the two most promising surfaces (Ch_AHA_Nt-Dhvar5 and Ch_NAC4) for *in vivo* proof-of-concept. To this end, a number of optimizations need to be performed: (i) immobilization of the Ch films onto titanium surfaces, which comprises covalent linking between Ch film and Ti, and possibly an extra crosslinking step, (ii) stability assays of the obtained coatings (both proteolytic-based and harsh processing assays), (iv) *in vitro* cytocompatibility assays, using fibroblast and pre-osteoblast cell lines through metabolic and differentiation assays and finally (iv) *in vivo* assays. Some of these optimizations are already being performed namely, immobilized AMP cytocompatibility assays, and *in vivo* model establishment. Regarding the Ch_AHA_Nt-Dhvar5 cytocompatibility assay, a HFF-1 fibroblast cell line was used. Both morphology and metabolic activity (through a resazurin assay) was assessed during a 7 days period. Preliminary assay is depicted in Figure 1.

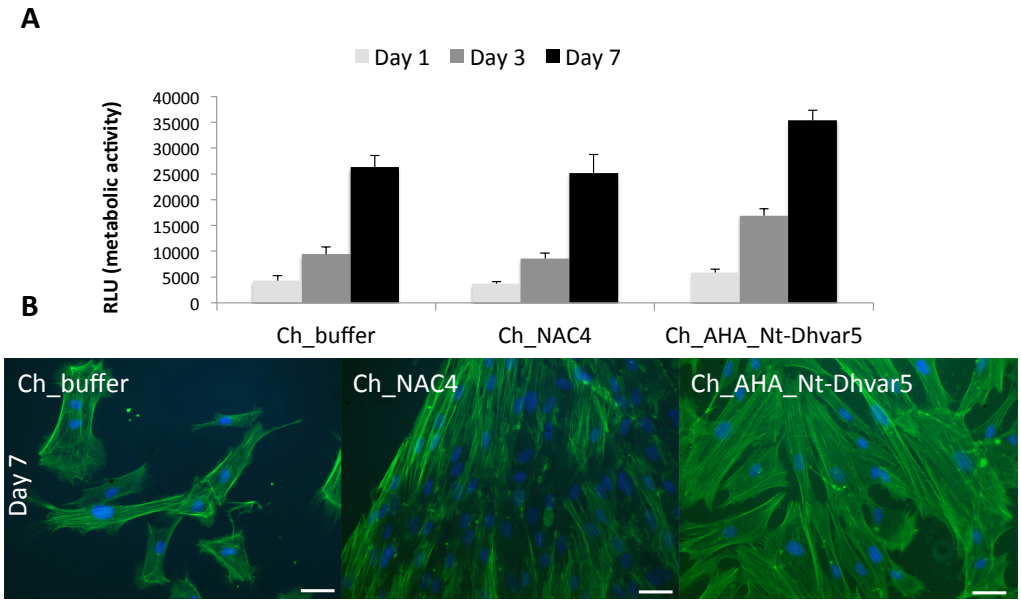

Figure 1. A) HFF-1 cell metabolic activity after 1, 3 and 7 days in contact with Ch_B, Ch_NAC and Ch_AHA_Nt-Dhvar5 surfaces. Data represent mean ± SD (n = 5); B) Fibroblast morphology following 7 days of culture on top of modified surfaces. Scale bar 50 µm. (Magnification 630x). F-actin filaments are stained in green (Phalloidin) and nuclei are stained in blue (Dapi).

As seen on Figure 1, HFF-1 cells were able to adhere and proliferate over the 7 days period. HFF-1 metabolic activity increased over time, being even higher than the control (Ch_buffer) (see Figure 1A), suggesting that the presence of Dhvar5 did not negatively influenced cells. Moreover, at day 7 cells were well spread with a

fibroblast-like morphology, establishing numerous cell-to-cell contacts (see Figure 1B).

Regarding the *in vivo* assays, a rat osteomyelitis model is currently being established at our lab, which is an adaptation of [29]. Briefly, male wister han rats with an average weight of 375g are used. A cavity is created at the left tibia lumen, with a needle and a high inoculum of a high slime-producing *S. aureus* strain is inoculated in the presence of a titanium rod "implant". The implanted rods can be naked or coated (with Ch_buffer, Ch_NAC4 or Ch_AHA_Nt-Dhvar5). At the end of surgical procedures, X-ray imaging allows to verify the correct positioning of the implant. Animals are followed during 26 days, monitoring weight, temperature and overall aspect. At end of the 26 days period, X-ray allows the assessment of bone damage. Both tibias are collected, as well as the implant. Also, blood, liver and spleen samples are recovered to assess possible infection dissemination. These samples are processed in order to assess the amount of CFUs present. Some tibia (infected and control) are prepared for histological analysis. After some optimizations of surgical procedures, a pilot assay was performed to assess infection establishment and infection reproducibility in a time frame of 15 days, using two groups of 6 animals: one group received a non-inoculated implant, the other group received an inoculated implant. At end of this period, x-rays (Figure 2) and CFU counts were performed on the obtained samples.

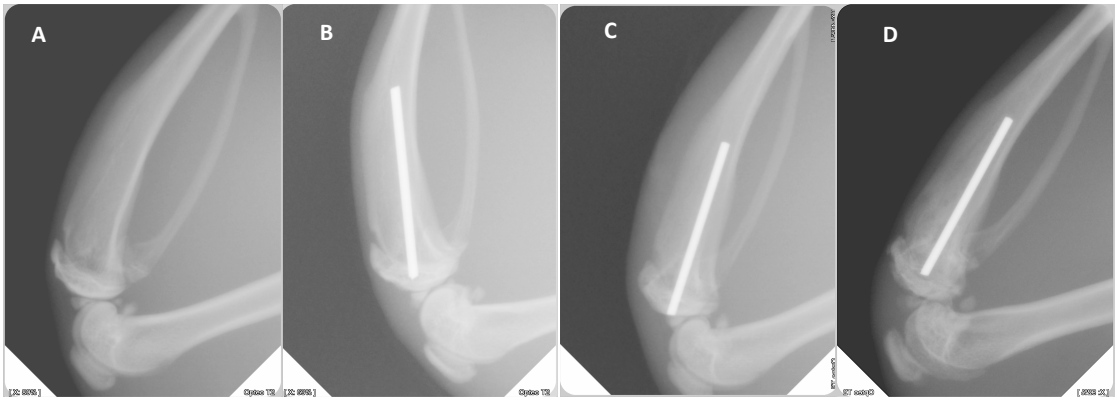

Figure 2. X-rays obtained from A) non-operated tibia; B) non-inoculated implant inserted tibia Day 15; C) inoculated implant inserted tibia Day 0; D) inoculated implant inserted Day 15.

As is possible to observe in Figure 2 at the end of 15 days infected tibia (Figure 2D) reveals lighter round shades with lower bone density, not observed at day 0 (Figure 2C). The bone CFU counts corroborated the infection establishment in all inoculated rats (Data not shown).

At this point, the tethering of the modified chitosan films (Ch_AHA_Nt-Dhvar5 and Ch_NAC4) onto titanium rods needs to be further optimized, in order to develop a stable coating eligible to the *in vivo* assays.

[1] Costa F, Maia S, Gomes J, Gomes P, Martins MC. Characterization of hLF1-11 immobilization onto chitosan ultrathin films, and its effects on antimicrobial activity. Acta biomaterialia. 2014;10:3513-21.

[2] Costa FM, Maia SR, Gomes PA, Martins MC. Dhvar5 antimicrobial peptide (AMP) chemoselective covalent immobilization results on higher antiadherence effect than simple physical adsorption. Biomaterials. 2015;52:531-8.

[3] Godoy-Gallardo M, Mas-Moruno C, Fernandez-Calderon MC, Perez-Giraldo C, Manero JM, Albericio F, et al. Covalent immobilization of hLf1-11 peptide on a titanium surface reduces bacterial adhesion and biofilm formation. Acta biomaterialia. 2014;10:3522-34.

[4] Holmberg KV, Abdolhosseini M, Li Y, Chen X, Gorr SU, Aparicio C. Bio-inspired stable antimicrobial peptide coatings for dental applications. Acta biomaterialia. 2013;9:8224-31.

[5] Ivanov IE, Morrison AE, Cobb JE, Fahey CA, Camesano TA. Creating antibacterial surfaces with the peptide chrysophsin-1. ACS applied materials & interfaces. 2012;4:5891-7.

[6] Godoy-Gallardo M, Mas-Moruno C, Yu K, Manero JM, Gil FJ, Kizhakkedathu JN*, et al.* Antibacterial properties of hLf1-11 peptide onto titanium surfaces: a comparison study between silanization and surface initiated polymerization. Biomacromolecules. 2015;16:483-96.

[7] Godoy-Gallardo M, Wang Z, Shen Y, Manero JM, Gil FJ, Rodriguez D, *et al.* Antibacterial coatings on titanium surfaces: a comparison study between *in vitro*

single-species and multispecies biofilm. ACS applied materials & interfaces. 2015;7:5992-6001.

[8] Chen X, Hirt H, Li Y, Gorr SU, Aparicio C. Antimicrobial GL13K peptide coatings killed and ruptured the wall of *Streptococcus gordonii* and prevented formation and growth of biofilms. PloS one. 2014;9:e111579.

[9] Tan XW, Lakshminarayanan R, Liu SP, Goh E, Tan D, Beuerman RW, *et al.* Dual functionalization of titanium with vascular endothelial growth factor and beta-defensin analog for potential application in keratoprosthesis. Journal of Biomedical Materials Research Part B Applied Biomaterials. 2012;100:2090-100.

[10] Peyre J, Humblot V, Methivier C, Berjeaud JM, Pradier CM. Co-grafting of amino-poly(ethylene glycol) and Magainin I on a TiO2 surface: tests of antifouling and antibacterial activities. The journal of physical chemistry B. 2012;116:13839-47.

[11] Tan XW, Goh TW, Saraswathi P, Nyein CL, Setiawan M, Riau A, *et al.* Effectiveness of antimicrobial peptide immobilization for preventing perioperative cornea implant-associated bacterial infection. Antimicrobial agents and chemotherapy. 2014;58:5229-38.

[12] Lim K, Chua RR, Saravanan R, Basu A, Mishra B, Tambyah PA, *et al.* Immobilization studies of an engineered arginine-tryptophan-rich peptide on a silicone surface with antimicrobial and antibiofilm activity. ACS applied materials & interfaces. 2013;5:6412-22.

[13] Li X, Li P, Saravanan R, Basu A, Mishra B, Lim SH, *et al.* Antimicrobial functionalization of silicone surfaces with engineered short peptides having broad spectrum antimicrobial and salt-resistant properties. Acta biomaterialia. 2014;10:258-66.

[14] Mishra B, Basu A., Yuan Chua R.R., Saravanan R., Tambyah P.A., Ho B., Chang M.W., Jan Leong S.S. Site specific immobilization of a potent antimicrobial peptide onto silicone catheters: evaluation against urinary tract infection pathogensJournal of Materials Chemistry B. 2014:1706-16.

[15] Wang L, Chen J, Shi L, Shi Z, Ren L, Wang Y. The promotion of antimicrobial activity on silicon substrates using a "click" immobilized short peptide. Chemical communications. 2014;50:975-7.

[16] Li Y, Santos CM, Kumar A, Zhao M, Lopez AI, Qin G, *et al.* "Click" immobilization on alkylated silicon substrates: model for the study of surface bound antimicrobial peptides. Chemistry. 2011;17:2656-65.

[17] Santos CM, Kumar A, Kolar SS, Contreras-Caceres R, McDermott A, Cai C. Immobilization of antimicrobial peptide IG-25 onto fluoropolymers via fluorous interactions and click chemistry. ACS applied materials & interfaces. 2013;5:12789-93.

[18] Dutta D, Cole N, Kumar N, Willcox MD. Broad spectrum antimicrobial activity of melimine covalently bound to contact lenses. Investigative ophthalmology & visual science. 2013;54:175-82.

[19] Lombana A, Raja Z, Casale S, Pradier CM, Foulon T, Ladram A, *et al.* Temporin-SHa peptides grafted on gold surfaces display antibacterial activity. Journal of peptide science: an official publication of the European Peptide Society. 2014;20:563-9.

[20] Etayash H, Norman L, Thundat T, Stiles M, Kaur K. Surface-conjugated antimicrobial peptide leucocin a displays high binding to pathogenic gram-positive bacteria. ACS applied materials & interfaces. 2014;6:1131-8.

[21] Qi X, Poernomo G, Wang K, Chen Y, Chan-Park MB, Xu R, *et al.* Covalent immobilization of nisin on multi-walled carbon nanotubes: superior antimicrobial and anti-biofilm properties. Nanoscale. 2011;3:1874-80.

[22] Gao G, Lange D, Hilpert K, Kindrachuk J, Zou Y, Cheng JT, *et al.* The biocompatibility and biofilm resistance of implant coatings based on hydrophilic polymer brushes conjugated with antimicrobial peptides. Biomaterials. 2011;32:3899-909.

[23] Rapsch K, Bier FF, Tadros M, von Nickisch-Rosenegk M. Identification of antimicrobial peptides and immobilization strategy suitable for a covalent surface coating with biocompatible properties. Bioconjugate Chemistry. 2014;25:308-19.

[24] Cleophas RT, Sjollema J, Busscher HJ, Kruijtzer JA, Liskamp RM. Characterization and activity of an immobilized antimicrobial peptide containing bactericidal PEG-hydrogel. Biomacromolecules. 2014;15:3390-5.

[25] Chen R, Willcox MD, Cole N, Ho KK, Rasul R, Denman JA, *et al.* Characterization of chemoselective surface attachment of the cationic peptide melimine and its effects on antimicrobial activity. Acta biomaterialia. 2012;8:4371-9.

[26] Lin W, Junjian, C., Chenzhi, C., Lin, S., Sa, L., Li, R., Yingjun, W. Multi-biofunctionalization of a titanium surface with a mixture of peptides to achieve excellent antimicrobial activity and biocompatibilty. Journal of Materials Chemistry B. 2015:30-3.

[27] Hilpert K, Elliott M, Jenssen H, Kindrachuk J, Fjell CD, Korner J, *et al*. Screening and Characterization of Surface-Tethered Cationic Peptides for Antimicrobial Activity. Chemistry & Biology. 2009;16:58-69.

[28] Bagheri M, Beyermann M, Dathe M. Mode of Action of Cationic Antimicrobial Peptides Defines the Tethering Position and the Efficacy of Biocidal Surfaces. Bioconjugate Chemistry. 2012;23:66-74.

[29] Yuksel E, Karakecili A. Antibacterial activity on electrospun poly(lactide-co-glycolide) based membranes via Magainin II grafting. Materials science & engineering C, Materials for biological applications. 2014;45:510-8.

[30] Foster LJ, Butt J. Chitosan films are NOT antimicrobial. Biotechnology letters. 2011;33:417-21.

[31] Monzon M, Garcia-Alvarez F, Lacleriga A, Amorena B. Evaluation of four experimental osteomyelitis infection models by using precolonized implants and bacterial suspensions. Acta orthopaedica Scandinavica. 2002;73:11-9.

Appendix I

Acta Biomaterialia 7 (2011) 1431–1440

Contents lists available at ScienceDirect

Acta Biomaterialia

journal homepage: www.elsevier.com/locate/actabiomat

Review

Covalent immobilization of antimicrobial peptides (AMPs) onto biomaterial surfaces

Fabíola Costa [a], Isabel F. Carvalho [b], Ronald C. Montelaro [c], P. Gomes [d], M. Cristina L. Martins [a,*]

[a] INEB – Instituto de Engenharia Biomédica, Divisão de Biomateriais, Universidade do Porto, Rua do Campo Alegre 823, 4150-180 Porto, Portugal
[b] IBMC – Instituto Biologia Celular e Molecular, Universidade do Porto, Rua do Campo Alegre 823, 4150-180 Porto, Portugal
[c] Microbiology and Molecular Genetics, University of Pittsburgh School of Medicine, Pittsburgh, PA, USA
[d] CIQ-UP, Departamento de Química e Bioquímica, Faculdade de Ciências, Universidade do Porto, Rua do Campo Alegre 687, 4169-007 Porto, Portugal

ARTICLE INFO

Article history:
Received 6 July 2010
Received in revised form 5 October 2010
Accepted 1 November 2010
Available online 5 November 2010

Keywords:
Antimicrobial peptides
Bacterial adhesion
Biofilms
Surface functionalization
Nanostructured surfaces

ABSTRACT

Bacterial adhesion to biomaterials remains a major problem in the medical devices field. Antimicrobial peptides (AMPs) are well-known components of the innate immune system that can be applied to overcome biofilm-associated infections. Their relevance has been increasing as a practical alternative to conventional antibiotics, which are declining in effectiveness. The recent interest focused on these peptides can be explained by a group of special features, including a wide spectrum of activity, high efficacy at very low concentrations, target specificity, anti-endotoxin activity, synergistic action with classical antibiotics, and low propensity for developing resistance. Therefore, the development of an antimicrobial coating with such properties would be worthwhile. The immobilization of AMPs onto a biomaterial surface has further advantages as it also helps to circumvent AMPs' potential limitations, such as short half-life and cytotoxicity associated with higher concentrations of soluble peptides. The studies discussed in the current review report on the impact of covalent immobilization of AMPs onto surfaces through different chemical coupling strategies, length of spacers, and peptide orientation and concentration. The overall results suggest that immobilized AMPs may be effective in the prevention of biofilm formation by reduction of microorganism survival post-contact with the coated biomaterial. Minimal cytotoxicity and long-term stability profiles were obtained by optimizing immobilization parameters, indicating a promising potential for the use of immobilized AMPs in clinical applications. On the other hand, the effects of tethering on mechanisms of action of AMPs have not yet been fully elucidated. Therefore, further studies are recommended to explore the real potential of immobilized AMPs in health applications as antimicrobial coatings of medical devices.

Introduction

The use of biomaterial implants and medical devices such as catheters, heart valves, stents, shunts, arthoprostheses and fracture fixation devices is an increasingly common and often life-saving procedure. Although infection incidence has been reduced by aseptic surgical techniques and prophylactic systemic antibiotic therapy, bacterial colonization of medical devices or implants still represents a serious hazard [1–3]. Mortality attributable to such infections is highest among patients with cardiovascular implants, particularly prosthetic heart valves and aortic grafts. However, infections associated with orthopaedic devices often result in serious disabilities [4]. These infections may cause implant failure, complex revision processes and implant removal, all leading to patient suffering, prolonged hospitalization and even death [5].

Implant-associated infections are classified in three ways: superficial immediate infections, deep immediate infections and deep late infections. Superficial immediate infections are caused by bacteria that normally populate the skin and start to colonize the medical device (e.g. infected sutures). Deep immediate infections become apparent shortly after invasive surgeries and may be due to inadvertent relocation of skin bacteria into the body, i.e. non-sterile implantation procedures. Finally, deep late infections appear months or years after surgery and may be a delayed display of contamination that was seeded during surgery or resulted from bacteria that migrated from another anatomic site [6].

Implant surface susceptibility to infection is dependent on the immune system performance and on the activity and virulence of the involved microorganisms [2,7]. Immune system performance can be compromised by direct surgical trauma, implant presence, low availability of blood vessels in the implant vicinity and inflammatory escalation, frequently resulting in peri-implant tissue damage. The activity and virulence of microorganisms are correlated with their capacity for biofilm formation [8]. Biofilms can colonize almost every kind of material (metals, ceramics and polymers) and therefore medical devices [9]. Biofilms are a differentiated, high-density population of microorganisms that are surrounded by a

* Corresponding author. Tel.: +351 226074982.
E-mail address: cmartins@ineb.up.pt (M. Cristina L. Martins).

1742-7061/$ - see front matter © 2010 Acta Materialia Inc. Published by Elsevier Ltd. All rights reserved.
doi:10.1016/j.actbio.2010.11.005

three-dimensional, well-organized exopolymeric matrix composed of polysaccharides, proteins, nucleic acids and lipids produced simultaneously by the microorganisms in the biofilm [3] and by proximal host cells [10,11]. This biofilm matrix is characterized by its resistance to stressful environmental conditions such as UV radiation, pH variation, osmotic shock, desiccation and flow conditions, and additionally by prevention of the entrance of antibiotics and biocidal substances [9]. Furthermore, the biofilm structure facilitates horizontal gene transfer between resistant and non-resistant microbial strains [9]. The overall result is an antibiotic resistance that is typically 10–1000 higher in biofilms than in the planktonic form of the same bacterial species [9,12,13]. Moreover recent research data have demonstrated that sub-therapeutic doses of both classical and recent antibiotics may induce specific gene expression, resulting in the paradoxical effect of exarcebating biofilm formation [14–17].

Biofilm establishment results from a specific sequence of events: microbial adherence, microcolony formation and proliferation, matrix production, biofilm maturation and, finally, cell detachment with propagation of infection [2,3]. Therefore, biofilms may represent reservoirs for the development of pathogenic infections [2,3]. When a biomaterial is implanted, a conditioning layer primarily composed of proteins (fibronectin, vitronectin, fibrinogen, albumin and immunoglobulins) adheres to its surface, favouring surface–microorganism interactions [5,13]. The interaction between bacteria and surface proteins results initially from weak attraction forces such as Van der Waals and electrostatic charges, which are later reinforced by specific interactions involving bacterial adhesion proteins [9]. Further, cell adhesion is facilitated by bacterial signalling and matrix production, yielding a mature biofilm [2,13]. After formation, a biofilm cannot be easily eliminated by standard clinical procedures, and the infection often can only be eradicated by the removal of the infected implant. In order to solve this problem, research has been conducted on the development of antimicrobial surface coatings that can prevent the initial bacterial colonization and/or actively reduce bacterial titres, minimizing the potential for biofilm formation [2,10].

2. Antimicrobial coatings

In order to avoid implant-associated infections, several strategies have been reported with the aim of creating antimicrobial surfaces, such as the development of (i) non-fouling surfaces (surfaces that avoid protein adsorption and cell adhesion) [1,18–20], (ii) surfaces previously colonized with non-pathogenic bacteria [9], (iii) surfaces combined with biocidal substances [21–23] and (iv) surfaces combined with antibiotics [24–26].

The physicochemical properties of the implant surface, such as surface roughness energy and potential, are fundamental issues in the initial adhesion and subsequent growth of bacteria. Non-fouling surfaces combine one or more approaches in order to influence the amount and/or conformation of adsorbed proteins, preventing bacterial adhesion and biofilm formation. Some examples are UV radiation of titanium surfaces to augment wettability [27], use of anti-adherent agents bearing negative charges [28], polymer coatings such as poly(ethylene glycol) (PEG), poly(hydroxyethylmethacrylate) (PHEMA) [18,29], poly(methacrylic acid) [30], polyurethanes [31] or even bioactive polymers such as chitosan, which possess the ability to inhibit bacterial adhesion and/or to kill adherent bacteria [32]. Unfortunately, the effectiveness of non-fouling coatings for reducing bacterial adhesion is limited and varies greatly depending on bacterial species.

Another approach involves the simultaneous use of an antimicrobial agent and a non-pathogenic bacterial coating layer. The non-pathogenic bacteria, resistant to a specific antimicrobial is used to populate the ecological space, preventing adherence of pathogenic bacteria to the surface [9].

Surfaces combined with antibiotics or other biocidal substances have the advantage of delivering drugs directly to the implant site, resulting in locally high drug doses without exceeding the systemic toxicity level of the drug, thus preventing harmful side effects [3]. Several antimicrobial surfaces have been described in the literature, including non-antibiotic antimicrobial agents such as silver, salicylic acid, quaternary ammonium compounds, phenol derivatives, chlorhexidine and nitric oxide [3,5,13,33]. However, many of these compounds are associated with anaphylaxis, cytotoxicity or low efficiency [5,13]. These limiting aspects prompt the use of true antibiotics such as vancomycin, tobramycin, cefalozin, teicoplanin, carbenicillin, amoxicillin, penicillin, ampicillin and gentamicin [3,34–37], through two different strategies: substance-releasing coating and substance covalent immobilization. The release strategy offers the potential for extended activity, but has to date failed to achieve delivery of a sustained and effective dosage over a relatively prolonged period of time. To address this issue, there has been an increased interest in covalent attachment of drugs to the implant surface to achieve long-lasting antibacterial activity. For example, vancomycin has been successfully attached to titanium and proven to be bactericidal to *Staphylococcus aureus* and *Staphylococcus epidermidis* [5,7]. In addition, Aumsuwan et al. [34,37] reported the covalent attachment of penicillin and ampicillin to expanded polytetrafluoroethylene (ePTFE). When these drugs were immobilized through a PEG-spacer, the surfaces displayed high antimicrobial efficiency among their spectrum of activity, indicating that antibiotic mobility is essential to activity. The advantages of covalent attachment to the implant surface are long-lasting antimicrobial activity, low incidence of side effects and non-accumulation in tissues (brain, liver and spleen) [5]. However, the effectiveness of coatings with classical antibiotics is strongly dependent on the spectrum of activity of the chosen drug, and the possibility of development of antimicrobial resistance in a relatively short time period [38]. Therefore, alternative answers must be developed. There is a clear need for a broad-spectrum antimicrobial that prevents colonization of biomaterials, minimizes the development of bacterial resistance, displays long-term stability, even through the sterilization process, and has a low cytotoxic profile. Antimicrobial peptides have the potential to meet these criteria [39–42] and therefore represent a promise for the new generation of antimicrobial surfaces.

3. Antimicrobial peptides

In the past 50 years, resistance to new antibiotics has appeared in microbial populations within a few years of the introduction of a new therapeutic drug [38]. The decline in the effectiveness of current therapies has led to a search for new kinds of agents, including antibiotics based on antimicrobial peptides (AMPs), which are part of the innate immune system of all multicellular organisms [39–43]. So far, more than 750 different AMPs have been isolated from a wide variety of animals, plants, bacteria, fungi and viruses [39–42,44]. The AMPs comprise a chemically and structurally heterogeneous family. Nevertheless, three characteristics that are shared by almost all known AMPs can be distinguished: (i) small size (10–25 amino acids), with molecular weights (MW) between 1 and 5 kDa; (ii) highly cationic character, though with large variations in the net positive charge; (iii) tendency to adopt amphipathic structures, i.e. structures with separate hydrophobic and hydrophilic domains, in non-polar media. Because of these physicochemical characteristics, AMPs have the tendency to associate with negatively charged microbial surfaces and membranes [45]. These peptides offer several attractive advantages: they exhibit

bactericidal, fungicidal, viricidal and tumoricidal properties, they act at a very low concentration, and they are less likely to promote bacterial resistance. These properties make AMPs promising candidates for therapeutic drugs [44]. Unlike conventional antibiotics such as penicillin, which microbes readily deceive, acquisition of resistance by a sensitive microbial strain against AMPs is less probable. Because the target of AMPs is the bacterial membrane, a microorganism would have to redesign its membrane, changing the composition and/or organization of its lipids, which represent an expensive solution for most microbial species.

However, some resistance mechanisms have been reported in Gram-positive and Gram-negative bacteria. For instance, some Gram-positive bacteria (e.g. *S. epidermidis*, *S. aureus*) can express an AMP sensor system that has been proposed to regulate selected resistance genes when the bacteria come into contact with AMPs [46–48]. These resistance genes include dlt-operon, which is responsible for D-alanylation of teichoic acid; mprF, which mediates the incorporation of lysyl-phosphatidylglycerol in the cytoplasmic membrane (both of these genes decrease the negative net charge of the cell envelope); and the vraFG genes of a transport system [46,47,49–51]. Other reported resistance mechanisms include protease inhibitors, such *S. aureus* IsdA surface protein [52], and biofilm stabilizers such exopolysaccharide intercellular adhesin (PIA) [53]. Nevertheless, bacterial resistance mechanisms to AMPs differ with regard to efficiency, specificity and distribution among species [46], and natural AMPs have evolved to avoid some of these resistance mechanisms. Moreover, synthetic AMPs can be rationally engineered to circumvent specific bacterial resistance mechanisms based on the specific application (target bacteria, environment, etc.).

Most peptides are created from nondescript sequences of amino acids lacking unique motifs that could serve as the recognition site of a protease required for selective destruction of the antibiotic in the presence of cellular protein constituents [54]. Furthermore, some cationic peptides bind to lipopolysaccharide (LPS) and lipoteichoic acid (LTA) with high affinity (competitively displacing membrane-stabilizing bivalent cations Ca^{2+} or Mg^{2+}), disrupting these sites and leading to enhanced uptake of cationic peptides across the outer membrane. Disruption of outer membranes can also lead to promotion of uptake of conventional antibiotics across the outer membrane, leading to an "enhancement" effect. This self-promoted uptake process is responsible for two additional advantages: anti-endotoxin activity, in contrast to other antibiotics, which induce endotoxinaemia, and "enhancer" activity (i.e. synergy with classical antibiotics) [45,55,56]. The more resistant an isolate is to a given antibiotic, the more profound is the "enhancement" effect by an appropriate cationic peptide. Thus cationic peptides also have the ability to serve as anti-resistance compounds [45,55].

The properties of natural AMPs have prompted research towards *de novo* AMPs, i.e. fully synthetic peptides. These are distinct from those in nature, with simpler but rationally engineered composition, obtained by varying the amino acid content and sequence and overall peptide length to achieve enhanced activity and very low cytotoxic properties [57]. For example, Mietzner and co-workers [58–61] have developed a series of *de novo* peptides based on structure–function properties observed in natural AMPs. They engineered the peptide composition to achieve enhanced potency, selectivity and stability. They performed extensive *in vitro* and *in vivo* (intravenous murine infection model and intraperitoneal mouse infection model) studies in order to evaluate the antimicrobial activity (against *Pseudomonas aeruginosa, S. aureus, Streptococcus gordonii, Fusobacterium nucleatum* and *Porphyromonas gingivalis*), cytotoxicity (towards red blood cells, white blood cells, human skin fibroblasts), and salt resistance (towards NaCl, Mg^{2+} and Ca^{2+}). The engineered peptide derivative WLBU2 (RRWVRRVRRWVRRVVRVV RRWVRR) was identified as a promising prophylactic and therapeutic molecule. The *in vitro* studies revealed good selectivity, and potency at physiological conditions (salt resistance), which was reinforced by *in vivo* efficacy in the intravenous and intraperitoneal *P. aeruginosa* infection models.

Finally, the potential of future AMP-based drugs is underlined by the number of clinical trials with various AMP species for treatment of skin and soft tissue infections, oral mucositis and paediatric sepsis [44,62,63].

3.1. Mode of antibacterial action

AMPs target the fundamental difference in the membrane structures of microorganisms and multicellular animals. Bacterial membranes are organized in such a way that the outermost leaflet of the bilayer is heavily occupied by lipids with negatively charged phospholipid headgroups. In contrast, the outer leaflet of the membranes of plants and animals is composed principally of lipids with no net charge. Here most of the lipids with negatively charged headgroups are segregated into the inner leaflet, facing the cytoplasm [54].

Although the exact mechanism of action of AMPs remains a matter of controversy, there is a consensus that the following sequence occurs: (i) cationic, i.e. positively charged, peptides are electrostatically attracted to the negatively charged microbial cell membranes, and (ii) upon binding to the phospholipid membrane, the AMP adopts an amphipathic structure, adapting to the specific conditions at the membrane–water interface. Most AMPs only assume their amphipathic structure upon interaction with the membrane, as it is not the most favoured structure in water. This interaction is generally believed to lead to a lethal increase in the permeability of the cell membrane [45]. How this interaction ends in fatal outcome still remains to be determined. Many hypotheses have been presented, which include: fatal depolarization of the normally energized bacterial membrane; creation of physical holes resulting in leakage of cellular contents; activation of deadly processes such as induction of hydrolases that degrade the cell wall; alteration of the usual distribution of lipids between the leaflets of the bilayer that results in disturbance of membrane functions; and damage to the critical intracellular targets after internalization of the peptide [54]. Recently, it has been shown that peptide reorientation together with membrane destabilization happens after a certain peptide threshold concentration is achieved. This can be ascribed to a first step of membrane surface coverage by the AMP until charge neutralization is reached. Thereafter, peptide orientation changes from parallel to perpendicular to the membrane surface, followed by pore formation and eventually membrane disruption [64–66].

Based on the available data, three models explaining the mode of action of AMPs have been proposed (Fig. 1).

(i) *The carpet model:* After the microbial cell membrane is fully covered by a carpet-like cluster of peptides, a saturation point is reached that results in extensive wormhole formation, causing the abrupt lysis of the microbial cell. Cell lysis is believed to result as the lipid layer bends back on itself, with lateral expansions in the polar head-group region, providing the gaps that will be filled up by individual peptide molecules.

(ii) *The toroidal pore model:* After binding to the phospholipid head groups, the peptides insert into the membrane and then cluster into unstructured bundles that span the membrane. These bundles, in association with water molecules, are believed to create channels responsible for leakage of ions and possibly larger molecules throughout the membrane. This last model differs from the other two in that only

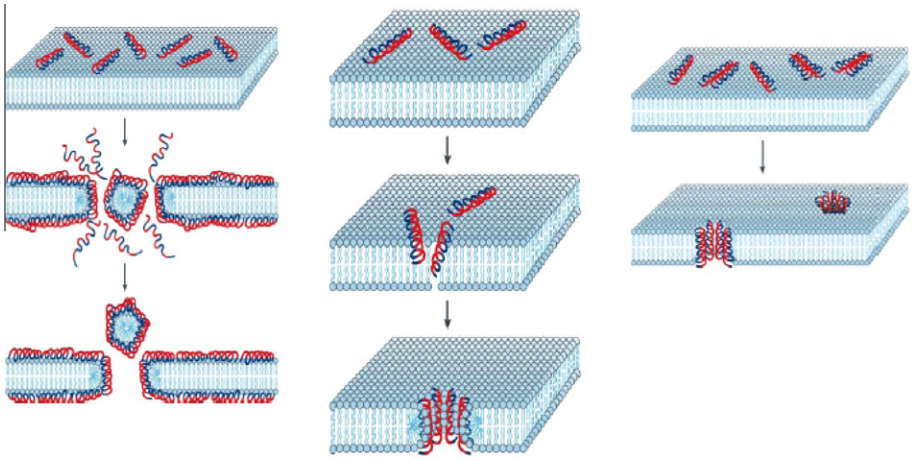

Fig. 1. Current models of the mechanism of action of membrane-active antimicrobial peptides (AMPs): (A) carpet model; (B) toroidal pore model; (C) barrel-stave model. Adapted with permission from Ref. [64].

short-lived transmembrane clusters of an undefined nature are formed, which allows the peptides to cross the membrane without causing significant membrane depolarization. Once inside, the peptides home on their intracellular targets to exert their killing activities [45].

(iii) *The barrel-stave model:* After initial electrostatic binding to the outer leaflet of the bacterial membrane, α-helical amphipathic peptides group together into barrel-like bundles that line amphipathic transmembrane pores. The non-polar side chains associate with the hydrophobic fatty acid tails at the inside of the phospholipid bilayer, and the hydrophilic side-chains are oriented inward into the water-filled pore.

Taking into consideration the proposed theories for soluble AMPs, one could expect that immobilized AMPs would lose their antimicrobial activity completely or to a large extent. However, the research reviewed herein proves differently, and even provides some insights into the specific mechanisms underlying this activity. Haynie et al. [67] was able to demonstrate that immobilized magainin that is attached through very short linkers (2 or 6 carbon atoms) displays antimicrobial activity, meaning that outer membrane interaction by magainin is sufficient for lethal activity. Humblot et al. [68] reported that the immobilized AMPs had a bacteriostatic rather that bactericidal effect, perhaps due to the low peptide concentration or short contact time. Other research has performed the immobilization through long linkers in an attempt to permit sufficient flexibility to penetrate target cell membranes [1,69,70], as the directly attached AMPs lost their antimicrobial activity. Hilpert et al. [71], in their screening and characterization of surface-tethered cationic peptides studies, reported that the immobilization of peptides to a surface should result in constraints on the peptide mobility and on the capacity of peptides to enter or even transpose the cellular membranes. Scanning electron microscopy (SEM), ATP release and depolarization assays performed with short peptides indicated that, although their length was insufficient to stretch across the membrane, the immobilized peptides could destabilize the cell membrane. The high local concentration of immobilized peptides was presumed to lead to the displacement of positively charged counterions attached to the outer surface layers. This could promote a dramatic change in bacterial surface electrostatics, which could trigger the activation of autolytic enzymes or the disruption of the ionic balance of more internal layers. Hilpert et al. [71] also demonstrated that hydrophobic residues at the exposed end of immobilized AMPs can have a major influence on the antimicrobial activity. They suggested that these residues are responsible for the triggering connection between AMPs and the bacteria cell wall.

4. Covalent immobilization of an antimicrobial peptide

The toxicity sometimes associated with AMPs is usually related to the high concentrations used to compensate for the relatively short half-life of AMPs due to a rapid protease digestion [67], or to peptide aggregation [11]. These characteristics have limited the use of AMPs in applications that require systemic distribution of the antimicrobial. However, AMPs are designed to work at local surfaces in most of their natural applications. Thus, stable immobilization of AMPs onto a biomaterial could be the pathway to overcome these difficulties [72]. Covalent immobilization of AMP can increase their long-term stability while decreasing their toxicity, as compared to incorporation approaches on leach- or release-based systems [11,35,36,69,72–75]. Furthermore, the proper orientation of the peptide may result in enhanced activity [34]. Towards this goal, the effect of AMP chemical immobilization on antimicrobial activity has been studied by several investigators [3,4,6,25–27,29,48,49,71] (Table 1). In the current review, different AMP surface covalent immobilization strategies are discussed, focusing on the importance of solid supports and chemical coupling strategies, spacer specificities (type, length and flexibility), surface density and exposure/orientation as determinants of immobilized peptide biocidal and cytotoxic activity. As summarized in Table 1, the various studies of immobilized AMPs differ in important aspects, including the immobilization method applied, the peptide sequence, mode of action of the AMPs used, and the bacteria tested. These experimental variations make it difficult to achieve a straightforward comparison. Nevertheless, important lessons can be derived from these diverse studies.

In 1995, Haynie et al. [67] demonstrated that some AMPs (natural occurring magainin 2 and several idealized synthetic amphipathic peptides) immobilized onto a polyamide resin (pepsin K) retained lethal activity against several Gram-positive and Gram-negative bacteria. As already mentioned, these results demonstrated that the interaction of magainin with the outer membrane of the bacteria is sufficient for their lethal activity, since the potential peptide penetration depth is very low due to the short spacer (short 2 or 6 carbon chain linkers) used.

Willcox et al. [11] compared the antimicrobial activity of the synthetic peptide melimine that was adsorbed or covalently immobilized onto commercial contact lenses (Etafilcon A). Covalent

Table 1
Overview of the reported AMP immobilization strategies.

	AMP	Substrate	AMP immobilization strategy	Microorganisms assessed
[67]	Magainin 2 and Related synthetic amphiphilic peptides	Polyamide resin (pepsin K)	Directly synthesized on polyamide resin, after immobilization through their *C*-terminal amino acids • AMP orientation was controlled • Short spacer, with 2- or 6-carbon chains, was used • Stability to heat was studied • no AMP release was observed	*Escherichia coli* ATCC 35695; and ATCC 25922, *Staphylococcus aureus* ATCC 25923 and ATCC 6538, *Klebsiella pneumoniae* ATCC 4352, *Bacillus subtilis* ATCC 6051, *Candida albicans* ATCC 10231, *Aspergillus niger* ATCC 6275, and *Pseudomonas aeruginosa* ATCC 27853.
[1]	Magainin I	Non-fouling copolymer brushes based on different percentages of:2-(2-methoxyethoxy)ethyl methacrylate (MEO_2MA)/hydroxyl-terminated oligo(ethylene glycol) methacrylate (HOEGMA)	Peptide immobilized by its *C*-terminal amino acid The process consisted of a previous incorporation of a cysteine residue on the *C*-terminal of magainin, to be reacted with the polymeric brushes via PMPI (*N*-(*p*-maleimidophenyl)isocyanate) • AMP orientation was controlled • Brushes were used as spacers • Different AMPs densities was tested	*Listeria ivanovii*, *Bacillus cereus*
[68]	Magainin I	Mixed OH/COOH-terminated self-assembled monolayers (SAMs)	Immobilization by the free AMP amines after activation of the COOH groups of the SAM with NHS/EDC • AMP orientation was not controlled • No spacers • No AMP release was observed	*L. ivanovii*, *Enterococcus faecalis* and *S. aureus*
[69]	Magainin-derived MK5E and KLAL	PEGylated TentaGel S, HypoGel 400 and HypoGel 200 resin beads	C-terminally immobilized peptides were achieved by standard solid-phase peptide synthesis and Fmoc (9-fluorenylmethoxycarbonyl)-chemistry N-terminal and side-chain immobilization were achieved by thioalkylation and oxime formation • AMP orientation was controlled • Different AMPs densities were tested • Effect of PEGylated spacers was tested • The haemolytic effect was assayed	*E. coli* strain DH5α, *B. subtilis* strain DSM 347
[11]	Melimine	Commercial contact lenses (etafilcon A)	Immobilization by the free AMP amines using 1-ethyl-3-(3-dimethylaminopropyl)carbodiimide • AMP orientation was not controlled • No spacers	*P. aeruginosa* 6294, *P. aeruginosa* ATCC 15442, *S. aureus* Saur31, *S. aureus* CK5, *S. pneumoniae* 010
[76]	Melimine	Glass coverslips	Immobilization through the free AMP amines using two different strategies: • Using EDC after previous activation of the OH groups of the glass surface with 4-azidobenzoic acid (ABA) and irradiation with UV-light (320 nm) • As above but using 4-fluoro-3-nitrophenyl azide (FNA) instead of ABA • AMP orientation was not controlled • No spacers • Different AMP densities were tested	*S. aureus* strain 38, *P. aeruginosa* PA01
[70]	Cathelin LL37	Silanized titanium surfaces: Using glycidyloxypropyl triethoxysilane (epoxy silane) 3-aminopropyl triethoxysilane(amino silane)	• *N*-maleimidopropionic acid succinimide ester • *R*-*N*-hydroxysuccinimidyl-ö-maleimidyl-PEG • Effect of AMP orientation was tested • Effect of PEGylated spacers was tested • Different AMPs densities were tested	*E. coli* strain K12
[77]	E14LKK	Oxidized polyethylene films (ox-PE)	Immobilization by the terminal AMP amine (using protected E14LKK side chains amines) with and without PEGylated spacer onto ox-PE using 1-ethyl-3-(3-aminopropyl)-carbodiimide • AMP orientation was controlled • Effect of PEGylated spacers was tested	*E. coli* ATCC 25922
[56]	FKVKFKVKFK	PEG-PS Resin beads	Peptide–resin conjugates were synthesized by using Fmoc (9-fluorenylmethoxycarbonyl)-chemistry. To investigate the effect of the resin on the activity, the β-sheet peptide was conjugated with MBHA–resin	*S. aureus* ATCC 6538, *Micrococcus luteus* ATCC 9341, *P. aeruginosa* ATCC9027, *E. coli* ATCC 25922
[78]	6K8L	PEG-PS resin beads	The peptide was synthesized by solid-phase peptide synthesis on a PEG-modified polystyrene resin (PEG-PS) using Fmoc (9-fluorenylmethoxycarbonyl)-chemistry. The antimicrobial activity of the peptide–resin conjugate was evaluated against different microorganisms.	*B. subtilis* (wild-type PB2, 168 Marburg strain27), *E. coli* O157: H7 ATCC 33150, *Kluyveromyces marxianus*, *L. monocytogenes* ATCC 689426, *P. fluorescence*, *Salmonella typhimurium* H 3380 phage type DT 104, *Serratia liquefasciens* and *S. aureus* ATCC 13566.
[71]	122 variant peptides of 2 starting sequences: Bac2A and Indolicidin	Cellulose bifunctional resin TGS (1–6-dichloro-1- Beta-dideoxy-Beta-fructofuranosM-chloro-4-deoxy-galactopyranoside) NH_2/RAM (*p*-[(R,S)-a-[1-(9H-fluren-9-yl)-methoxyformamido]-2,4-dimethoxybenzyl]-phen-oxyacetic acid) Microtiter plate	Peptides were: • directly synthesized on a cellulose support using a cellulose-amino-hydroxypropyl ether (CAPE) linker chemistry or; • directly synthesized onto a bifunctional resin or; • directly bound to the microtiter plate via biotin–streptavidin interaction. • AMP orientation was controlled • No spacers	Mini-Tn5-luxfliC::lux CDABE strain H1001 of *P. aeruginosa* PAO1, *S. aureus* ATCC 25923, *C. albicans* (lab isolate).

immobilization was performed directly through the free peptide amines (the *N*-terminal amino acid or the lysine side chain) without a specific control on the orientation of the peptide onto the surface. An apparent increase in efficacy was observed when the peptide was covalently attached to the surface, which was ascribed to a possibly higher relative surface availability of the peptide, in contrast to the adsorption process where peptide aggregation could produce uneven peptide distribution.

The effect of α-helix secondary structure of immobilized AMP was also studied by Haynie et al. [67]. They demonstrated that only those immobilized peptides still retaining their ability to form amphipathic α-helices had antibacterial activity. Likewise, in the work of Cho et al. [56], the secondary β-sheet structure was essential for antibacterial activity. Thus, these studies indicate that the biocidal activity of immobilized AMPs is dependent on the presence of a well-established secondary structure.

Other important activity-modulating parameters include the length, flexibility and kind of spacer between the active sequences and the solid matrices [67,69,70], the AMP surface density [1,68,69], and orientation after immobilization [1,11,67–70,76–78]. These parameters are discussed below.

4.1. Solid supports and chemical coupling strategies

A wide variety of solid supports has been assessed for production of surfaces with immobilized AMPs, including polymeric brushes and resins [1,56,67,69,71,77,78], metal (e.g. silanized titanium) [70], glass coverslips [76], model surfaces (e.g. self-assembled monolayers) [68], microtitre plates [71] and even commercial contact lenses [11].

As shown in Table 1, the chemical strategies behind covalent immobilization of peptides differ depending on the sequence, orientation and position of the specific AMP, the presence/absence of a spacer, or the spacer properties such as length and flexibility.

Peptide immobilization may be carried out in a relatively random manner, e.g. through formation of amide bonds between amine groups from the pre-synthesized peptide and surface carboxyls (or the other way around, i.e. carboxyls from the peptide reacting with surface amines), as in Refs. [10,43,44] (Table 1). Alternatively, peptide immobilization can be controlled through peptide construction (or immobilization) on the surface by chemoselective formation of a peptide–surface covalent bond, enabling tethering in a predictable and defined fashion.

Controlled immobilization is obviously preferred over random tethering, as the former can be designed (i) to maintain peptide structural motifs known to be relevant for activity, and (ii) to allow exposure and flexibility that more closely mimic the behaviour of soluble AMPs. Uncontrolled immobilization can be especially detrimental when involving peptide amine groups, as these amine groups are normally provided by lysines which are key amino acids in the majority of cationic amphipathic AMPs [39–42].

The best way to control orientation of immobilized peptides is to synthesize them directly onto the solid support (e.g. polyamide resins, PEG-modified polystyrene resins, cellulose), as done in Refs. [28,35,39] or [46] (Table 1). To this end, standard solid-phase peptide synthesis (SPPS) methods may be used, such as the well-established Fmoc/^{t}Bu strategy [79]. In this strategy selectively protected amino acids are incorporated stepwise into the growing peptide chain that is built from its *C*- to its *N*-terminal residue. Once the peptide sequence is assembled, convenient treatment to cleave off the amino acid side-chain-protecting groups is performed.

An alternative to building the peptide directly onto the surface is to pre-synthesize a peptide chain with a specific building block incorporated in a selected position. This peptide chain can subsequently be chemoselectively attached to an adequately functionalized surface. The most common approaches involve incorporation of an additional cysteine into the peptide chain (e.g. [1]) or exploiting a cysteine already available in the native sequence (if not crucial for AMP activity), taking advantage of chemical reactions specific to the thiol group. These reactions may include, as depicted in Fig. 2, (i) disulfide bond formation between peptide and surface thiols, as well as specific reactions of the peptide Cys thiol with (ii) surface-bound maleimide groups [1,42], or (iii) surface-bound epoxides (though these are generally reactive towards any nucleophiles, including lysine amines, and hence are not truly chemoselective).

Other chemoselective approaches not involving Cys or other thiol donors have been proposed more recently, namely those involving Huisgen 1,3-dipolar cycloadditions, the so-called click-reactions [80]. Here, the peptide can bear an additional azide (e.g. from incorporation of 6-azidohexanoic acid) or an alkyne donor (e.g. from incorporation of propynoic acid) to be "clicked on" surface-bound alkyne or azide groups, respectively.

Both epoxide and click-based approaches have been used to immobilize peptides and proteins onto surfaces (e.g. [81–83]), but examples of their application to AMP tethering are still scarce.

Irrespective of alternatives available for peptide tethering onto surfaces, careful comparative investigation of different strategies must be carried out, in which the influence of peptide-surface spacers, coupling chemistries and support materials on antimicrobial activity should be thoroughly analyzed. Only Hilpert et al. [71] have assessed the effect of different support materials on the antimicrobial activity, and found that, at least for their specific systems, the supports did not affect the activity of the tested peptides.

4.2. Influence of the spacer

Although some studies demonstrated that immobilized AMPs have antimicrobial activity without incorporation of a spacer [11,68,71,76], most protocols presented a spacer attachment step [1,56,67,69,70,77,78], particularly with a PEG spacer with a MW ranging from 3000 to 5400 [56,69,70,77,78]. The utilization of PEG as a spacer presents several advantages. This polymer can create non-adhesive surfaces due to its non-fouling characteristics, thus preventing non-specific peptide binding to the surface and shielding the peptides from the hydrophobic nature of a particular biomaterial [56,77]. Studies comparing AMP immobilization with and without PEGylated spacers demonstrated that some immobilized AMPs are only bactericidal when a PEGylated spacer was used [56,69,70,77]. For example, Gabriel et al. [70] demonstrated that the LL37 peptide bound to titanium through a PEGylated spacer was capable of killing *Escherichia coli* on contact. In marked contrast, LL37 peptide attached directly to the titanium surface displayed no antibacterial activity. The authors suggest that the use of a long, flexible PEG spacer provided a parallel peptide orientation and lateral mobility that were required for bactericidal activity. Bagheri et al. [69] also analyzed the influence of PEGylated spacer length (3000, 400 and 200 Da) on bactericidal activity of an amphipathic model KLAL peptide and magainin-derived MK5E. They demonstrated that the antimicrobial activity of these peptides distinctly decreased with reduction in the spacer length, suggesting that the increased flexibility associated with longer spacers maximizes the antimicrobial activity of immobilized peptides [69].

However, these results contradict those of Haynie et al. [67] whose experiments indicated no difference in bactericidal activity whether peptides were conjugated to the support with a two-carbon or a six-carbon chain linker [67]. In addition, Hilpert et al. [71] reported that short 9-mers covalently linked without spacer have bactericidal activity. They suggested an electrostatic interference and destabilization rather than a penetrating mechanism.

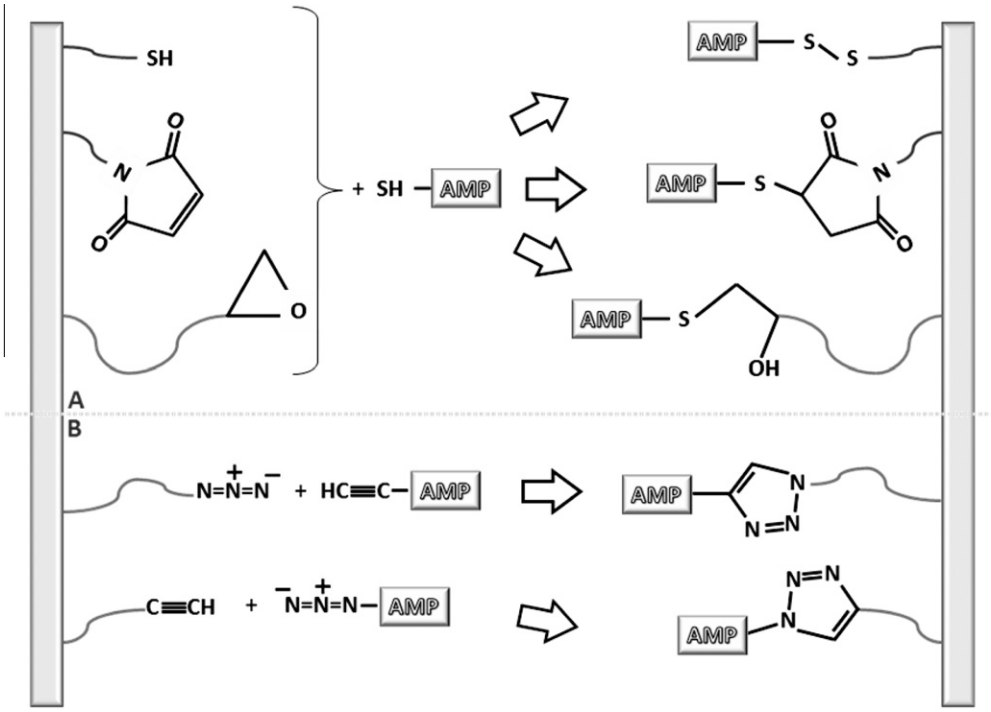

Fig. 2. Examples of chemical strategies for controlled covalent attachment of AMPs on surfaces: (A) use of thiol-bearing peptides (Cys usually as thiol donor) for covalent immobilization onto thiol-, maleimide- or epoxide-modified surfaces; (B) use of the Huisgen 1,3-dipolar cycloaddition for immobilization of either alkyne-bearing peptides onto azide-modified surfaces or azide-bearing peptides onto alkyne-modified surfaces.

Comparison of these studies is difficult, since AMPs, support materials, coupling chemistry and peptide orientations differ from study to study. However, one can speculate that the requirement for a spacer is directly associated with the mode of action of the specific AMP.

4.3. Peptide concentration

Peptide surface concentration depends on the immobilization strategy used, as limited accessibility of the peptide reactive groups and different coupling procedures can affect the efficiency of peptide immobilization. Most studies indicate that peptide concentrations, albeit important, do not appear to be the most critical parameter for antimicrobial activity [1,69,70,76]. Gabriel et al. [70] observed that the bactericidal activity of LL37 immobilized onto titanium surfaces was independent of the peptide concentration [70]. Glinel et al. [1] demonstrated that the biocidal activity of magainin I was not substantially reduced as the concentration of immobilized peptide was reduced. Bagheri et al. [69] reported a study aimed to determine the effect on bactericidal activity of different surface peptide densities and spacer lengths. These studies demonstrated that an increase in the loading capacity of the resin was not sufficient to compensate for the decrease in activity due to reduction of the spacer length. Based on these observations, they concluded that spacer length has a more profound impact on activity than peptide concentration. Further, the maximum peptide loading concentration was obtained with the *C*-terminal coupling strategy, which correlated with higher Minimal Inhibitory Concentration (MICs), suggesting that immobilization orientation can compensate for low peptide loading [69].

Despite these reports, which strongly support the concept that peptide surface loading levels are not a key factor in the antimicrobial activity of immobilized AMP, other studies have provided evidence that the effects of peptide surface concentration cannot be disregarded. For instance, Chen et al. [76] evaluated the effect of melimine concentration after immobilization by two different bifunctional azides (4-fluoro-3-nitrophenyl azide (FNA) and 4-azidobenzoic acid (ABA)) as crosslinking reagents. In this study, the higher concentration of the peptide via ABA immobilization correlated with a more profound antibacterial activity. Humblot et al. [68] correlated low peptide concentrations with bacteriostatic rather than bacteriocidal effect of immobilized magainin I, explaining that the low peptide concentration precludes the possibility of multiple peptide entries into the cell membrane. In addition, Hilpert et al. [71] studied the effect of immobilized peptide density on antimicrobial activity by utilizing different concentrations of biotinylated peptide solutions with streptavidin-coated plates. Antimicrobial activity was clearly concentration dependent, decreasing sigmoidally as a function of decreasing peptide concentration.

4.4. Peptide orientation after immobilization

Different strategies for surface binding of peptides have been conducted on different chain positions, such as *C*-terminal, *N*-terminal and/or *N*-side-chain peptide attachment. As a result, different peptide orientations and flexibility were obtained, which could be correlated with differential antimicrobial activities. The chain position was determined based upon (i) previous knowledge of peptide robustness to changes in given positions, i.e. on its ability to retain or lose antimicrobial activity upon deletion of *N*-terminal or *C*-terminal amino acids or amino acid segments; (ii) the availability of functional groups suitable for a particular coupling chemistry; or (iii) the promotion of parallel alignment of peptide chains [56,67,68,70]. The studies of Gabriel et al. [70] and Steven et al. [77] compared the antimicrobial efficiency of *N*-terminally and *N*-side-chain immobilized peptides. They performed site-specific activation and coupling by blocking the

undesired functional groups. Even though the experimental AMPs were different in the respective studies, only *N*-terminally attached peptides displayed antimicrobial activity. Gabriel et al. [70] concluded that only *N*-terminal conjugation permitted the appropriate parallel orientation of the peptide helices, which is required for interaction among the peptide molecules and between the peptides and the lipid double layer during membrane pore formation. These results are supported by the reported key role of basic lysine side-chains (and of those from other basic amino acids, as arginine or histidine) in the bioactivity of cationic AMP [39–42], which could explain the deleterious effect of AMP immobilization through Lys ε-amino groups towards antimicrobial activity. The possibility of *C*-terminal peptide immobilization should be considered as this orientation may achieve similar specific activity as *N*-terminal conjugation. Bagheri et al. [69] compared the activity profile of *C*-terminal, *N*-terminal and *N*-side-chain immobilized AMP sequences. Slightly different results were obtained depending on the specific peptide sequence and bacteria tested. *C*-terminally attached AMPs displayed higher MICs, compared to *N*-terminal and *N*-side-chain immobilization. The *N*-immobilization orientations presented similar results, suggesting that the blockage of the cationic Lys side chains was of minor importance to the overall antimicrobial activity. However, it is possible that the observed reactivity pattern may be specific to the systems used by these authors, where the AMP orientation appeared to be less relevant when peptides were immobilized using long and flexible spacers [69]. Hilpert et al. [71] used a different strategy to screen the efficiency of immobilized AMPs. They rearranged the sequence of a known active peptide and *C*-terminally immobilized the different variants. They concluded that the placement of cationic residues close to the linker site correlated with increased antimicrobial activity as compared with peptides with cationic residues localized to the *N*-terminus or within the middle portion of the peptide. The positioning of hydrophobic residues proximal to the *N*-terminus was critical to the activity of their immobilized AMPs.

4.5. Activity efficiency of immobilized AMPs

Only a few studies have described an experimental comparison of soluble and immobilized AMPs [56,67,69,71]. However, a straightforward comparison between MICs of soluble and immobilized AMPs is very difficult because precise quantification of immobilized AMP can be problematic. In most cases the immobilized AMPs displayed an increase in their MIC value compared to the soluble peptide. In studies by Haynie et al. [67] the immobilized AMPs presented a 50-fold higher MIC compared to soluble peptides. These investigators suggested that the coupling chemistry may have resulted in more covalently bound peptide in the resin interior than on the surface, which could explain the higher concentration needed for activity. Cho et al. [56] found an extensive variation range in the observed MIC values which were augmented 8- or 64-fold depending on the bacteria evaluated (*E. coli*, *Micrococcus luteus* and *S. aureus* more sensitive; *P. aeruginosa* less susceptible). In the Bagheri et al. [69] studies, the active concentrations increased about 100-fold from the micromolar MICs of the soluble peptides to the milimolar range of the immobilized-AMPs. All these studies reported MIC increases that varied with peptide and bacteria specificity.

However, Hilpert et al. [71] compared soluble MICs and inhibition of luminescence by immobilized AMPs. No correlation of antimicrobial activity was observed between soluble and immobilized AMPs, as inactive soluble AMPs presented activity when immobilized, and some active soluble AMPs lost activity when immobilized.

4.6. Cytotoxicity

KLAL and MK5E are examples of immobilized AMPs for which haemolytic activity has been assessed. The KLAL- and MK5E-soluble haemolytic concentrations (EC25) were at least 16-fold higher than the respective MIC. Moreover, the haemolytic activity levels of the immobilized-peptide beads and the bare beads were indistinguishable from each other. This observation leads to the conclusion that both immobilized peptides at their MICs are inactive toward red blood cells [69]. Hilpert et al. [71] assessed cytotoxicity of a battery of immobilized peptides through human red blood cell haemolysis. They reported that the immobilization of AMPs had a reduced haemolytic activity when compared with the soluble counterpart. Thus, these initial studies indicate that peptide immobilization does not enhance the haemolytic properties of the peptides, and may actually reduce potential haemolysis when compared to soluble peptides.

4.7. Long-term stability

In order to check the activity persistence of immobilized peptides, investigators have subjected the modified surfaces to various harsh procedures, such as washing operations, heat treatments, pH variations and long-term activity assessment [11,67,68,78]. In the washing influence study, two different AMP-modified resin beads were extensively washed without loss of antimicrobial activity [67,78]. The heat stability experiment was conducted to evaluate whether exposure of AMP to autoclaving (121 °C for 20 min) or to a dry oven (200 °C for 30 min) would alter the ability of the peptide to inhibit bacterial growth. The bactericidal efficacy of the heat-treated 6K8L was maintained under both heating conditions [78]. In addition, the antimicrobial efficacy of melimine was maintained during autoclaving [11]. Cole et al. [84] verified that the levels of melimine in lenses after removal, cleaning and sterilization did not differ from those determined before 24 h of use. The effect of pH on the modified surface was assessed. The peptide 6K8L immobilized on PEG-poly(styrene) resin beads retained its antimicrobial activity over a pH range of 3.5–7 in citrate buffer, although bacterial killing was significantly greater at pH 3.5 than at pH 7 [78], possibly due to the higher positive charge at the lower pH. Humblot et al. [68] assayed the stability of antimicrobial activity of immobilized peptide at various times over a 6 month period. Samples were cleaned, dried and stored at 4 °C, between each antibacterial activity assay. The results showed that the peptide remained active over the 6 month period, even though the activity of the immobilized peptide was reduced at the 6 month time point.

All these studies, although limited, point to remarkably high long-term stability and resistance of immobilized AMP to environmental conditions.

5. Conclusions

Infections associated with the use of biomaterials remain one of the major barriers to the long-term use of medical devices in patients. Colonization of biomedical surfaces is considered the basis for biofilm formation and infection. The establishment of a biofilm results in lower antibiotic activity, and higher antibiotic resistance, which in turn can demand implant removal. There is a clear need for a broad-spectrum antimicrobial that prevents colonization of biomaterials, without damaging mammalian cells, that minimizes the potential for bacterial resistance, and that is stable throughout the sterilization process. AMPs have enormous potential to fulfil all these requirements and are therefore suitable for the generation of antimicrobial surfaces. Different approaches may be applied to improve surfaces with such antimicrobial agents. Covalent

immobilization of AMPs to surfaces can offer important advantages, including long-term stability and lower toxicity when compared to leach- or release-methodologies. The implications of the studies reviewed herein suggest that immobilized AMPs may be effective in the prevention of biofilm formation by reduction of microorganism survival post-contact with the coated material. The mechanisms of action behind each antimicrobial coating vary according to the specific AMP, chemistry and support used. Moreover, the overall comparison of results suggests that free and immobilized AMPs may act through different mechanisms. Further studies may clarify the mechanisms of action underlying immobilized AMPs and their potential use in health applications as antimicrobial coatings of medical devices.

Acknowledgements

The authors would like to thank the Portuguese Foundation for Science and Technology (FCT) (Ref. PTDC/CTM/101484/2008) and FEDER (Ref. FCOMP-01-0124-FEDER-009400) for co-funding the research project.

Appendix A. Figures with essential colour discrimination

Certain figures in this article, particularly Figure 1, is difficult to interpret in black and white. The full colour image can be found in the on-line version, at doi:10.1016/j.actbio.2010.11.005.

Appendix B. Supplementary data

Supplementary data associated with this article can be found, in the online version, at doi:10.1016/j.actbio.2010.11.005.

References

[1] Glinel K, Jonas AM, Jouenne T, Leprince J, Galas L, Huck WT. Antibacterial and antifouling polymer brushes incorporating antimicrobial peptide. Bioconj Chem 2009;20(1):71–7.
[2] Vila J, Soriano A, Mensa J. Molecular basis of microbial adherence to prosthetic materials. Role of biofilms in prosthesis-associated infection. Enferm Infecc Microbiol Clin 2008;26(1):48–54. quiz 55.
[3] Hetrick EM, Schoenfisch MH. Reducing implant-related infections: active release strategies. Chem Soc Rev 2006;35(9):780–9.
[4] Darouiche RO. Treatment of infections associated with surgical implants. N Engl J Med 2004;350(14):1422–9.
[5] Zhao L, Chu PK, Zhang Y, Wu Z. Antibacterial coatings on titanium implants. J Biomed Mater Res B Appl Biomater 2009;91(1):470–80.
[6] Dee KC, Puleo DA, Bizios R. An introduction to tissue-biomaterial interactions. New York: Wiley-Liss; 2002.
[7] Subramani K, Jung RE, Molenberg A, Hammerle CH. Biofilm on dental implants: a review of the literature. Int J Oral Maxillofac Implants 2009;24(4):616–26.
[8] Fey PD, Olson ME. Current concepts in biofilm formation of *Staphylococcus epidermidis*. Future Microbiol 2010;5(6):917–33.
[9] de Carvalho CC. Biofilms: recent developments on an old battle. Recent Pat Biotechnol 2007;1(1):49–57.
[10] Costerton JW, Stewart PS, Greenberg EP. Bacterial biofilms: a common cause of persistent infections. Science 1999;284(5418):1318–22.
[11] Willcox MD, Hume EB, Aliwarga Y, Kumar N, Cole N. A novel cationic-peptide coating for the prevention of microbial colonization on contact lenses. J Appl Microbiol 2008;105(6):1817–25.
[12] Lewis K. Riddle of biofilm resistance. Antimicrob Agents Chemother 2001;45(4):999–1007.
[13] Monteiro DR, Gorup LF, Takamiya AS, Ruvollo-Filho AC, de Camargo ER, Barbosa DB. The growing importance of materials that prevent microbial adhesion: antimicrobial effect of medical devices containing silver. Int J Antimicrob Agents 2009;34(2):103–10.
[14] Gooderham WJ, Bains M, McPhee JB, Wiegand I, Hancock RE. Induction by cationic antimicrobial peptides and involvement in intrinsic polymyxin and antimicrobial peptide resistance, biofilm formation, and swarming motility of PsrA in *Pseudomonas aeruginosa*. J Bacteriol 2008;190(16):5624–34.
[15] Bagge N, Schuster M, Hentzer M, Ciofu O, Givskov M, Greenberg EP, et al. *Pseudomonas aeruginosa* biofilms exposed to imipenem exhibit changes in global gene expression and beta-lactamase and alginate production. Antimicrob Agents Chemother 2004;48(4):1175–87.
[16] Ahmed NA, Petersen FC, Scheie AA. AI-2/LuxS is involved in increased biofilm formation by Streptococcus intermedius in the presence of antibiotics. Antimicrob Agents Chemother 2009;53(10):4258–63.
[17] Hoffman LR, D'Argenio DA, MacCoss MJ, Zhang Z, Jones RA, Miller SI. Aminoglycoside antibiotics induce bacterial biofilm formation. Nature 2005;436(7054):1171–5.
[18] Harbers GM, Emoto K, Greef C, Metzger SW, Woodward HN, Mascali JJ, et al. A functionalized poly(ethylene glycol)-based bioassay surface chemistry that facilitates bio-immobilization and inhibits non-specific protein, bacterial, and mammalian cell adhesion. Chem Mater 2007;19(18):4405–14.
[19] Chapman RG, Ostuni E, Liang MN, Meluleni G, Kim E, Yan L, et al. Polymeric thin films that resist the adsorption of proteins and the adhesion of bacteria. Langmuir 2001;17(4):1225–33.
[20] Goncalves IC, Martins MC, Barbosa MA, Naeemi E, Ratner BD. Selective protein adsorption modulates platelet adhesion and activation to oligo(ethylene glycol)-terminated self-assembled monolayers with C18 ligands. J Biomed Mater Res A 2009;89(3):642–53.
[21] Chung DW, Papadakis SE, Yam KL. Evaluation of a polymer coating containing triclosan as the antimicrobial layer for packaging materials. Int J Food Sci Technol 2003;38(2):165–9.
[22] Leung D, Spratt DA, Pratten J, Gulabivala K, Mordan NJ, Young AM. Chlorhexidine-releasing methacrylate dental composite materials. Biomaterials 2005;26(34):7145–53.
[23] Ravikumar T, Murata H, Koepsel RR, Russell AJ. Surface-active antifungal polyquaternary amine. Biomacromolecules 2006;7(10):2762–9.
[24] Bach A, Darby D, Bottiger B, Bohrer H, Motsch J, Martin E. Retention of the antibiotic teicoplanin on a hydromer-coated central venous catheter to prevent bacterial colonization in postoperative surgical patients. Intensive Care Med 1996;22(10):1066–9.
[25] Jose B, Antoci Jr V, Zeiger AR, Wickstrom E, Hickok NJ. Vancomycin covalently bonded to titanium beads kills Staphylococcus aureus. Chem Biol 2005;12(9):1041–8.
[26] Kilic D, Agalar C, Ozturk E, Denkbas EB, Cime A, Agalar F. Antimicrobial activity of cefazolin-impregnated mesh grafts. ANZ J Surg 2007;77(4):256–60.
[27] Gallardo-Moreno AM, Pacha-Olivenza MA, Saldana L, Perez-Giraldo C, Bruque JM, Vilaboa N, et al. In vitro biocompatibility and bacterial adhesion of physico-chemically modified Ti6Al4V surface by means of UV irradiation. Acta Biomater 2009;5(1):181–92.
[28] Jansen B, Kohnen W. Prevention of biofilm formation by polymer modification. J Ind Microbiol 1995;15(4):391–6.
[29] Martins MC, Wang D, Ji J, Feng L, Barbosa MA. Albumin and fibrinogen adsorption on cibacron blue F3G-A immobilised onto PU-PHEMA (polyurethane-poly(hydroxyethylmethacrylate)) surfaces. J Biomater Sci Polym Ed 2003;14(5):439–55.
[30] Zhang F, Zhang Z, Zhu X, Kang ET, Neoh KG. Silk-functionalized titanium surfaces for enhancing osteoblast functions and reducing bacterial adhesion. Biomaterials 2008;29(36):4751–9.
[31] Flemming RG, Capelli CC, Cooper SL, Proctor RA. Bacterial colonization of functionalized polyurethanes. Biomaterials 2000;21(3):273–81.
[32] Singla AK, Chawla M. Chitosan: some pharmaceutical and biological aspects—an update. J Pharm Pharmacol 2001;53(8):1047–67.
[33] Murata H, Koepsel RR, Matyjaszewski K, Russell AJ. Permanent, non-leaching antibacterial surface—2: how high density cationic surfaces kill bacterial cells. Biomaterials 2007;28(32):4870–9.
[34] Aumsuwan N, Danyus RC, Heinhorst S, Urban MW. Attachment of ampicillin to expanded poly(tetrafluoroethylene): surface reactions leading to inhibition of microbial growth. Biomacromolecules 2008;9(7):1712–8.
[35] Cevher E, Orhan Z, Mulazimoglu L, Sensoy D, Alper M, Yildiz A, et al. Characterization of biodegradable chitosan microspheres containing vancomycin and treatment of experimental osteomyelitis caused by methicillin-resistant *Staphylococcus aureus* with prepared microspheres. Int J Pharm 2006;317(2):127–35.
[36] Faber C, Stallmann HP, Lyaruu DM, Joosten U, von Eiff C, van Nieuw Amerongen A, et al. Comparable efficacies of the antimicrobial peptide human lactoferrin 1–11 and gentamicin in a chronic methicillin-resistant *Staphylococcus aureus* osteomyelitis model. Antimicrob Agents Chemother 2005;49(6):2438–44.
[37] Aumsuwan N, Heinhorst S, Urban MW. Antibacterial surfaces on expanded polytetrafluoroethylene; penicillin attachment. Biomacromolecules 2007;8(2):713–8.
[38] Palumbi SR. Humans as the world's greatest evolutionary force. Science 2001;293(5536):1786–90.
[39] Andreu D, Rivas L. Animal antimicrobial peptides: an overview. Biopolymers 1998;47(6):415–33.
[40] Rivas L, Luque-Ortega JR, Andreu D. Amphibian antimicrobial peptides and Protozoa: lessons from parasites. Biochim Biophys Acta 2009;1788(8):1570–81.
[41] Gordon YJ, Romanowski EG, McDermott AM. A review of antimicrobial peptides and their therapeutic potential as anti-infective drugs. Curr Eye Res 2005;30(7):505–15.
[42] Guani-Guerra E, Santos-Mendoza T, Lugo-Reyes SO, Teran LM. Antimicrobial peptides: general overview and clinical implications in human health and disease. Clin Immunol 2010;135(1):1–11.
[43] Perron GG, Zasloff M, Bell G. Experimental evolution of resistance to an antimicrobial peptide. Proc Biol Sci 2006;273(1583):251–6.
[44] Reddy KV, Yedery RD, Aranha C. Antimicrobial peptides: premises and promises. Int J Antimicrob Agents 2004;24(6):536–47.

[45] van't Hof W, Veerman EC, Helmerhorst EJ, Amerongen AV. Antimicrobial peptides: properties and applicability. Biol Chem 2001;382(4):597–619.
[46] Li M, Cha DJ, Lai Y, Villaruz AE, Sturdevant DE, Otto M. The antimicrobial peptide-sensing system aps of *Staphylococcus aureus*. Mol Microbiol 2007;66(5):1136–47.
[47] Li M, Lai Y, Villaruz AE, Cha DJ, Sturdevant DE, Otto M. Gram-positive three-component antimicrobial peptide-sensing system. Proc Natl Acad Sci USA 2007;104(22):9469–74.
[48] Otto M. Bacterial sensing of antimicrobial peptides. Contrib Microbiol 2009;16:136–49.
[49] Peschel A, Collins LV. Staphylococcal resistance to antimicrobial peptides of mammalian and bacterial origin. Peptides 2001;22(10):1651–9.
[50] Peschel A, Jack RW, Otto M, Collins LV, Staubitz P, Nicholson G, et al. Staphylococcus aureus resistance to human defensins and evasion of neutrophil killing via the novel virulence factor MprF is based on modification of membrane lipids with l-lysine. J Exp Med 2001;193(9): 1067–76.
[51] Cao M, Helmann JD. The *Bacillus subtilis* extracytoplasmic-function sigmaX factor regulates modification of the cell envelope and resistance to cationic antimicrobial peptides. J Bacteriol 2004;186(4):1136–46.
[52] Clarke SR, Foster SJ. IsdA protects Staphylococcus aureus against the bactericidal protease activity of apolactoferrin. Infect Immun 2008;76(4): 1518–26.
[53] Vuong C, Voyich JM, Fischer ER, Braughton KR, Whitney AR, DeLeo FR, et al. Polysaccharide intercellular adhesin (PIA) protects *Staphylococcus epidermidis* against major components of the human innate immune system. Cell Microbiol 2004;6(3):269–75.
[54] Zasloff M. Antimicrobial peptides of multicellular organisms. Nature 2002;415(6870):389–95.
[55] Hancock RE. Peptide antibiotics. Lancet 1997;349(9049):418–22.
[56] Cho WM, Joshi BP, Cho H, Lee KH. Design and synthesis of novel antibacterial peptide–resin conjugates. Bioorg Med Chem Lett 2007;17(21):5772–6.
[57] Statz AR, Park JP, Chongsiriwatana NP, Barron AE, Messersmith PB. Surface-immobilised antimicrobial peptoids. Biofouling 2008;24(6):439–48.
[58] Deslouches B, Gonzalez IA, DeAlmeida D, Islam K, Steele C, Montelaro RC, et al. De novo-derived cationic antimicrobial peptide activity in a murine model of *Pseudomonas aeruginosa* bacteraemia. J Antimicrob Chemother 2007;60(3): 669–72.
[59] Novak KF, Diamond WJ, Kirakodu S, Peyyala R, Anderson KW, Montelaro RC, et al. Efficacy of the de novo-derived antimicrobial peptide WLBU2 against oral bacteria. Antimicrob Agents Chemother 2007;51(5):1837–9.
[60] Deslouches B, Islam K, Craigo JK, Paranjape SM, Montelaro RC, Mietzner TA. Activity of the de novo engineered antimicrobial peptide WLBU2 against *Pseudomonas aeruginosa* in human serum and whole blood: implications for systemic applications. Antimicrob Agents Chemother 2005;49(8):3208–16.
[61] Deslouches B, Phadke SM, Lazarevic V, Cascio M, Islam K, Montelaro RC, et al. De novo generation of cationic antimicrobial peptides: influence of length and tryptophan substitution on antimicrobial activity. Antimicrob Agents Chemother 2005;49(1):316–22.
[62] Levin M, Quint PA, Goldstein B, Barton P, Bradley JS, Shemie SD, et al. Recombinant bactericidal/permeability-increasing protein (rBPI21) as adjunctive treatment for children with severe meningococcal sepsis: a randomised trial. rBPI21 Meningococcal Sepsis Study Group. Lancet 2000;356(9234):961–7.
[63] Giroir BP, Scannon PJ, Levin M. Bactericidal/permeability-increasing protein–lessons learned from the phase III, randomized, clinical trial of rBPI21 for adjunctive treatment of children with severe meningococcemia. Crit Care Med 2001;29(7 Suppl):S130–135.
[64] Brogden KA. Antimicrobial peptides: pore formers or metabolic inhibitors in bacteria? Nat Rev Microbiol 2005;3(3):238–50.
[65] Bastos M, Bai G, Gomes P, Andreu D, Goormaghtigh E, Prieto M. Energetics and partition of two cecropin–melittin hybrid peptides to model membranes of different composition. Biophys J 2008;94(6):2128–41.
[66] Melo MN, Ferre R, Castanho MA. Antimicrobial peptides: linking partition, activity and high membrane-bound concentrations. Nat Rev Microbiol 2009;7(3):245–50.
[67] Haynie SL, Crum GA, Doele BA. Antimicrobial activities of amphiphilic peptides covalently bonded to a water-insoluble resin. Antimicrob Agents Chemother 1995;39(2):301–7.
[68] Humblot V, Yala JF, Thebault P, Boukerma K, Hequet A, Berjeaud JM, et al. The antibacterial activity of Magainin I immobilized onto mixed thiols self-assembled monolayers. Biomaterials 2009;30(21):3503–12.
[69] Bagheri M, Beyermann M, Dathe M. Immobilization reduces the activity of surface-bound cationic antimicrobial peptides with no influence upon the activity spectrum. Antimicrob Agents Chemother 2009;53(3):1132–41.
[70] Gabriel M, Nazmi K, Veerman EC, Nieuw Amerongen AV, Zentner A. Preparation of LL-37-grafted titanium surfaces with bactericidal activity. Bioconj Chem 2006;17(2):548–50.
[71] Hilpert K, Elliott M, Jenssen H, Kindrachuk J, Fjell CD, Korner J, et al. Screening and characterization of surface-tethered cationic peptides for antimicrobial activity. Chem Biol 2009;16(1):58–69.
[72] Batista MKS, Gallemi M, Adeva A, Gomes CAR, Gomes P. Facile regioselective synthesis of a novel chitosan–pexiganan conjugate with potential interest for the treatment of infected skin lesions. Synthetic Commun 2009;39(7): 1228–40.
[73] Venter JC. Immobilized and insolubilized drugs, hormones, and neurotransmitters: properties, mechanisms of action and applications. Pharmacol Rev 1982;34(2): 153–87.
[74] Endo Y, Tani T, Kodama M. Antimicrobial activity of tertiary amine covalently bonded to a polystyrene fiber. Appl Environ Microbiol 1987;53(9):2050–5.
[75] Chuang HF, Shukla A, Loose CR, Hammond-Cunningham PT, Stephanopoulos, G. Structures including antimicrobial peptides. United States; 2009.
[76] Chen R, Cole N, Willcox MD, Park J, Rasul R, Carter E, et al. Synthesis, characterization and in vitro activity of a surface-attached antimicrobial cationic peptide. Biofouling 2009;25(6):517–24.
[77] Steven MD, Hotchkiss JH. Covalent immobilization of an antimicrobial peptide on poly(ethylene) film. J Appl Polym Sci 2008;110(5):2665–70.
[78] Appendini P, Hotchkiss JH. Surface modification of poly(styrene) by the attachment of an antimicrobial peptide. J Appl Polym Sci 2001;81(3):609–16.
[79] Fields GB, Noble RL. Solid phase peptide synthesis utilizing 9-fluorenyl-methoxycarbonyl amino acids. Int J Pept Protein Res 1990;35(3): 161–214.
[80] Rostovtsev VV, Green LG, Fokin VV, Sharpless KB. A stepwise huisgen cycloaddition process: copper(I)-catalyzed regioselective "ligation" of azides and terminal alkynes. Angew Chem Int Ed Engl 2002;41(14):2596–9.
[81] Abad JM, Velez M, Santamaria C, Guisan JM, Matheus PR, Vazquez L, et al. Immobilization of peroxidase glycoprotein on gold electrodes modified with mixed epoxy-boronic acid monolayers. J Am Chem Soc 2002;124(43): 12845–53.
[82] Lee MR, Shin I. Fabrication of chemical microarrays by efficient immobilization of hydrazide-linked substances on epoxide-coated glass surfaces. Angew Chem Int Ed Engl 2005;44(19):2881–4.
[83] Hudalla GA, Murphy WL. Immobilization of peptides with distinct biological activities onto stem cell culture substrates using orthogonal chemistries. Langmuir 2010;26(9):6449–56.
[84] Cole N, Hume EB, Vijay AK, Sankaridurg P, Kumar N, Willcox MD. In vivo performance of melimine as an antimicrobial coating for contact lenses in models of CLARE and CLPU. Invest Ophthalmol Vis Sci 2010;51(1):390–5.